The copyright of this thesis vests in the author. No quotation from it or information derived from it is to be published without full acknowledgement of the source. The thesis is to be used for private study or non-commercial research purposes only.

Published by the University of Cape Town (UCT) in terms of the non-exclusive license granted to UCT by the author.

University of Cape Town

SYNTHESIS OF MIXED LIGAND, WATER SOLUBLE SQUARE PLANAR PLATINUM (II) COMPLEXES AND AN INVESTIGATION OF THEIR ASSOCIATION WITH HAEMATIN AND POTENTIAL TO INHIBIT THE FORMATION OF SYNTHETIC MALARIA PIGMENT

University of Cape Town

A dissertation submitted to the

UNIVERSITY OF CAPE TOWN

in fulfilment of the requirements for the degree of

MASTER OF SCIENCE

By

PAUL LOMBARD SWAN

B.Sc. (Hons.) (University of Cape Town)

Department of Chemistry

University of Cape Town
Rondebosch
7700
South Africa

March 2002

Abstract

To establish their potential as a template for novel anti-malarial drugs, a series of platinum (II) complexes were synthesised, their association with haematin determined in 40% aqueous DMSO, pH 7.4 at 25 °C and their ability to inhibit the formation of β-haematin (synthetic malaria pigment) was investigated.

The compounds synthesised and investigated contained a platinum(II) ion coordinated to acylthiourea and diimine ligands. The diimines used include both substituted and unsubstituted 2,2'-bipyridines and 1,10-phenanthrolines. 2-phenyl pyridine was also utilised as a ligand. It has been shown that the uncoordinated planar ligands interact weakly with haematin with a log K in the range of 1.9 to 3.3 while the twisted or more sterically hindered ligands show no observable association with the porphyrin. A series of complexes having platinum coordinated to a 2,2-bipyridine and acylthiourea ligand showed an appreciable interaction with haematin which was reflected in association constant log K values in the range of 4.8 to 5.8. Using a 1,10-phenanthroline ligand in place of a 2,2-bipyridine ligand increased the association constant of the platinum complex, resulting in this series of complexes having log K values in the range of 5.8 to 6.2. It has been shown that when platinum(II) is coordinated to diimines, it is the electron withdrawing properties of the metal which result in the strong association between the diimine containing complex and haematin. Finally both the complex containing platinum *cis* to two acylthiourea ligands as well as a platinum complex containing 2-phenyl pyridine were shown to have no observable interaction with haematin.

All charged platinum complexes in this study were shown to inhibit the formation of β-haematin. All complexes containing a 1,10 phenanthroline ligand showed a level of inhibition of β-haematin formation comparable to that of chloroquine while some of the complexes containing 2,2'-bypiridine ligands were shown to be less effective. None of the ligands nor the neutral platinum complexes demonstrated the ability to inhibit the formation of β-haematin.

The geometry of association of (*N*-benzoyl-*N'*,*N'*-di-2-hydroxyethylthioureato-S,O)(2,2'-bipyridyl) platinum(II) chloride and (*N*-benzoyl-*N'*,*N'*-di-2-hydroxyethylthioureato-*S*,*O*)(4,4'-dimethyl-2,2'-bipyridyl) platinum(II) chloride with zinc(II)protoporphyrin IX was investigated in 80% deutero-dimethylsulfoxide / 20% deuterium oxide using ^{1}H NMR spectroscopy. The

University of Cape Town

diimines of these platinum complexes were found to directly interact with the aromatic ring system of the porphyrin with π-π or π-cation face to face stacking interactions dominating the association. (N-benzoyl-*N'*,*N'*-di-2-hydroxyethylthioureato-*S*,*O*)(2,2'-bipyridyl) platinum(II) chloride was found to probably adopt a smaller range of conformations with zinc(II)protoporphyrin as the dimethylated complex. This probably gives rise to the difference observed between these two complexes regarding their ability to inhibit the formation of β-haematin.

The major finding of this work is that platinum complexes of the type [Pt(diimine)acylthiourea]Cl both associate strongly with haematin and inhibit the formation of β-haematin. This suggests that these complexes are likely to be good templates in the search for novel anti-malarial drugs.

The major finding of this work is that platinum complexes of the type [Pt(diimine)acylthiourea]Cl both associate strongly with haematin and inhibit the formation of β-haematin. This suggests that these complexes are likely to be good templates in the search for novel anti-malarial drugs.

University of Cape Town

Acknowledgements

- The Lord Jesus Christ for His creation which gives rise to what we call chemistry and His encouragement of my inmost being despite the frustrations that are involved in studying His creation

- Dr Timothy Egan for his continual oversight of this work, many discussions of results and help in shaping me as a chemist

- Prof. Klaus Koch for the initial dream of this project and help with both the synthetic and NMR aspects of the work as well as his many and interesting discussions

- My parents for their moral and financial support, even when the details of what I was doing remained somewhat of a mystery

- My colleagues and fellow students (Winile Mavuso, Catherine Kaschula, Kanyile Nkosi, Yu Shan Wu, Claire Lawrence, Oren Hallale and Jörn Miller) for their great companionship and for being sounding boards for my various hypotheses with a particular thank you to Claire for proof reading this dissertation

- Pete Roberts, Noel Hendricks and Elizna Maree for all the NMR work

- Dr. Thinus van der Merwe for running all my mass spectra

- Piero Benincasa for many elemental analyses

- The National Foundation for Research for partial funding of this work

University of Cape Town

Abbreviations

Å	angstrom
CD_3CN	deutero-acetonitrile
COSY	homonuclear correlated spectroscopy
CQ	chloroquine
d	doublet
dd	doublet of doublets
D_2O	deuterium oxide
DMF	dimethylformamide
DMSO	dimethyl sulfoxide
DNA	deoxyribonucleic acid
dtbbipy	4,4'-ditertiarybutyl-2,2'-bipyridyl
Fe(III)PPIX	ferriprotoporphyrin IX
Ga(III)PPIX	gallium(III)protoporphyrin IX
HEPES	N-[2-hydroxyethyl]piperazine-N'-[2-ethane sulphonate]
HL	*N*-benzoyl-*N',N'*-di-2-hydroxyethylthiourea
HL'	*N*-benzoyl-*N',N'*-bisdiethylaminoethylthiourea
HSQC	heteronuclear single quantum coherence
Hz	hertz
K	association constant
m	multiplet
Me	methyl

University of Cape Town

NMR	nuclear magnetic resonance
NOESY	nuclear overhauser effect spectroscopy
$(Pt(ppy)Cl)_2$	di-μ-chlorobis[2-(2-pyridinyl)phenyl-(*C,N*)]di-platinum
[Pt(3,4,7,8-tetraMe phen)L]Cl	(*N*-benzoyl-*N'*,*N'*-di-2-hydroxyethylthioureato-*S,O*) (3,4,7,8-tetramethyl-1,10-phenanthroline) platinum(II) chloride
[Pt(4-Me phen)L]Cl	(*N*-benzoyl-*N'*,*N'*-di-2-hydroxyethylthioureato-*S,O*)(4-methyl-1,10-phenanthroline) platinum(II) chloride
[Pt(5-Cl phen)L]Cl	(*N*-benzoyl-*N'*,*N'*-di-2-hydroxyethylthioureato-*S,O*)(5-chloro-1,10-phenanthroline) platinum(II) chloride
[Pt(5-Me phen)L]Cl	(*N*-benzoyl-*N'*,*N'*-di-2-hydroxyethylthioureato-*S,O*)(5-methyl-1,10-phenanthroline) platinum(II) chloride
[Pt(5-NO_2 phen)L]Cl	(*N*-benzoyl-*N'*,*N'*-di-2-hydroxyethylthioureato-*S,O*)(5-nitro-1,10-phenanthroline) platinum(II) chloride
[Pt(bipy)L']Cl	(*N*-benzoyl-*N'*,*N'*-bisdiethylaminoethylthioureato-*S,O*)(2,2'-bipyridyl)- platinum(II) chloride
[Pt(bipy)L]Cl	(*N*-benzoyl-*N'*,*N'*-di-2-hydroxyethylthioureato-*S,O*)(2,2'-bipyridyl) platinum(II) chloride
[Pt(diMebipy)L]Cl	(*N*-benzoyl-*N'*,*N'*-di-2-hydroxyethylthioureato-*S,O*)(4,4'-dimethyl-2,2'-bipyridyl) platinum(II) chloride
[Pt(dtbbipy)L]Cl	(*N*-benzoyl-*N'*,*N'*-di-2-hydroxyethylthioureato-*S,O*)(4,4'-ditertiarybutyl-2,2'-bipyridyl)platinum(II) chloride
[Pt(phen)L]Cl	(*N*-benzoyl-*N'*,*N'*-di-2-hydroxyethylthioureato-*S,O*)(1,10-phenanthroline) platinum(II) chloride
Pt(3,4,7,8-tetraMe phen)Cl_2	3,4,7,8-tetramethyl-1,10-phenanthrolinedichloroplatinum(II)
Pt(4-Me phen)Cl_2	4-methyl-1,10-phenanthrolinedichloroplatinum(II)
Pt(5-Cl phen)Cl_2	5-chloro-1,10-phenanthrolinedichloroplatinum(II)
Pt(5-Me phen)Cl_2	5-methyl-1,10-phenanthrolinedichloroplatinum(II)
Pt(5-NO2 phen)Cl_2	5-nitro-1,10-phenanthrolinedichloroplatinum(II)
Pt(bipy)Cl_2	2,2'-bipyridyldichloroplatinum(II)
Pt(diMebipy)Cl_2	4,4'-dimethyl-2,2'-bipyridyldichloroplatinum(II)
Pt(dtbbipy)Cl_2	4,4'-ditertiarybutyl-2,2'-bipyridyldichloroplatinum(II)
cis-[PtL_2]	*cis*-bis(N-benzoyl-N',N'-di-2-hydroxyethylthioureato) platinum (II)

University of Cape Town

$Pt(phen)Cl_2$	1,10-phenanthrolinedichloroplatinum(II)
[Pt(ppy)L']	(*N*-benzoyl-*N'*,*N'*-bisdiethylaminoethylthioureato-*O*,*S*)(2-phenyl pyridine) platinum(II) chloride
RNA	ribonucleic acid
s	singlet
$SiMe_4$	tetramethylsilane
t	triplet
TLC	thin layer chromatography
unres.	unresolved
UV	ultraviolet
Zn(II)PPIX	zinc(II)protoporphyrin IX
ΔG	changes in Gibbs free energy
$\Delta\delta$	change in chemical shift

University of Cape Town

Table of contents

		Page
	Abstract	1
	Acknowledgements	iii
	Abbreviations	iv
	Table of contents	vii
1	**Introduction**	
1.1	Significance and occurrence of malaria	1
1.2	The life cycle and mode of action of *Plasmodium* parasites	1
1.3	Structure of haemozoin and its mechanism of formation	3
1.4	Current antimalarial drugs and their proposed mode of action	5
1.5	Haematin – drug interactions	11
1.6	Metals in antimalarial drugs	15
1.7	*N*-Benzoyl-*N'*,*N'*-dialkylthioureato-diimine platinum (II) complexes as a starting point in the search for a novel platinum containing antimalarial drug	19
1.8	Objectives	20
2	**Synthesis and characterisation**	
2.1	Overview of synthesis	23
2.2	*N*-benzoyl-*N'*,*N'*-dialkylthiourea ligands	24
2.3	4,4'-ditertiarybutyl-2,2'-bipyridyl	29
2.4	Pt(diimine)Cl_2 complexes	30
2.5	[Pt(diimine)acylthiourea]Cl complexes	31
2.6	*cis*-bis(*N*-benzoyl-*N'*,*N'*-di-2-hydroxyethylthioureato) platinum (II)	43
2.7	Di-μ-chlorobis[2-(2-pyridinyl)phenyl-(*C*,*N*)]di-platinum	44
2.8	(*N*-benzoyl-*N'*-*N'*-bisdiethylaminoethylthioureato-*O*,*S*)(2-phenylpyridine) platinum(II)	45
2.9	Gallium(III)protoporphyrin IX chloride	46
3	**Association of haematin with ligands and platinum complexes**	
3.1	A solvent system for spectrophotometric titrations	50
3.2	The UV-visible spectrum of haematin	50
3.3	Changes in the spectrum of haematin due to interaction with the platinum complexes	53

University of Cape Town

3.4	Titrations	56
3.5	Discussion of titration results	59
3.6	Conclusion	62
4	**Inhibition of β-Haematin formation and preliminary biological study**	
4.1	Introduction	64
4.2	Characterisation of β-haematin	64
4.3	Results of the inhibition of β-haematin formation experiments	66
4.4	Discussion of results from the inhibition of β-haematin formation experiments	69
4.5	Preliminary biological study	72
4.6	Conclusion	74
5	**Geometry of platinum complex – Zn(II)PPIX interactions**	
5.1	Objectives	76
5.2	Methodology	76
5.3	Assignment of the Zn(II)PPIX proton NMR spectrum	78
5.4	Interaction of platinum complexes with Zn(II)PPIX	82
5.5	Conclusion	91
6	**Conclusion**	93
7	**Experimental**	
7.1	Materials for synthesis	97
7.2	Instrumentation for synthetic characterisation	97
7.3	Preparation of compounds	97
7.4	Spectrophotometric titrations	108
7.5	β-Haematin synthesis and inhibition	109
8	**References**	111
9	**Appendices**	
9.1	Appendix 1: Tables of data from spectrophotometric titrations	118
9.2	Appendix 2: Infra red spectra from the inhibition of β-haematin formation experiments	124
9.3	Appendix 3: NMR titration curves from the addition of Zn(II)PPIX to platinum complexes	129

University of Cape Town

1 Introduction

The aim of this work was to investigate the interactions between platinum complexes and their ligands with haematin and its analogue, zinc(II) protoporphyrin IX, as well as their ability to inhibit the formation of a synthetic form of malaria pigment (haemozoin) known as β-haematin. These types of interactions are of interest as they probably play an important role in the mode of action of anti-malarial drugs such as chloroquine. The purpose of this dissertation is to provide insights into the basis of these interactions and evaluate these complexes as templates for potential future novel antimalarial drugs.

1.1 Significance and occurrence of malaria

The most serious parasitic disease and fifth most lethal infectious disease world wide is malaria. World Health Organisation (WHO) statistics[1] indicate that there are in excess of 1 million deaths annually and 200-300 million cases of infection, with a further 2 billion people at risk of infection. The disease is most prevalent in Sub-Saharan Africa where children under 5 years of age contribute to the majority of mortality statistics[2]. The disease also leads to extensive morbidity and impacts significantly upon the economy of the continent. Other impacted regions include parts of South America and South and Southeast Asia[2].

University of Cape Town

1.2 The life cycle and mode of action of *Plasmodium* parasites

Malaria is caused by parasites of the genus *Plasmodium*, of which there are four species that are pathogenic to humans, *P. falciparum*, *P. vivax*, *P. ovale*, and *P. malariae*. The biology of *P. falciparum* is best understood, and it is this species which is responsible for the vast majority of fatalities[1]. *P. falciparum* has three major stages in its life cycle in which it resides in two hosts, the female Anopheles mosquito which is the vector and humans, the blood of which provides a source of nutrition (Figure 1.1)[3]. The first stage takes place with the injection of sporozoites from the mosquito into the human host where they enter the blood stream, travel to the liver and infect hepatocytes. In a period of about 10 days, the parasites multiply asexually and then simultaneously rupture the hepatocytes and re-enter the blood stream as merozoites which invade erythrocytes. This begins the second stage in the life cycle. Once in red blood cells, the parasites mature from a ring stage to a trophozoite stage and then finally transform into a blood

schizont stage. Further asexual reproduction in the blood stage leads to increasing numbers of parasites producing greater symptoms of the disease in the host. Some merozoites form sexual gametocytes which await to be sucked up by a feeding mosquito and hence start the third stage of the life cycle. Once in the gut of the mosquito the parasites reproduce sexually resulting in zygotes which penetrate the gut wall becoming ookinetes, which develop to form oocytes. Some time passes as the oocyst grows releasing sporozoites which move to the salivary glands of the mosquito to complete the cycle[3].

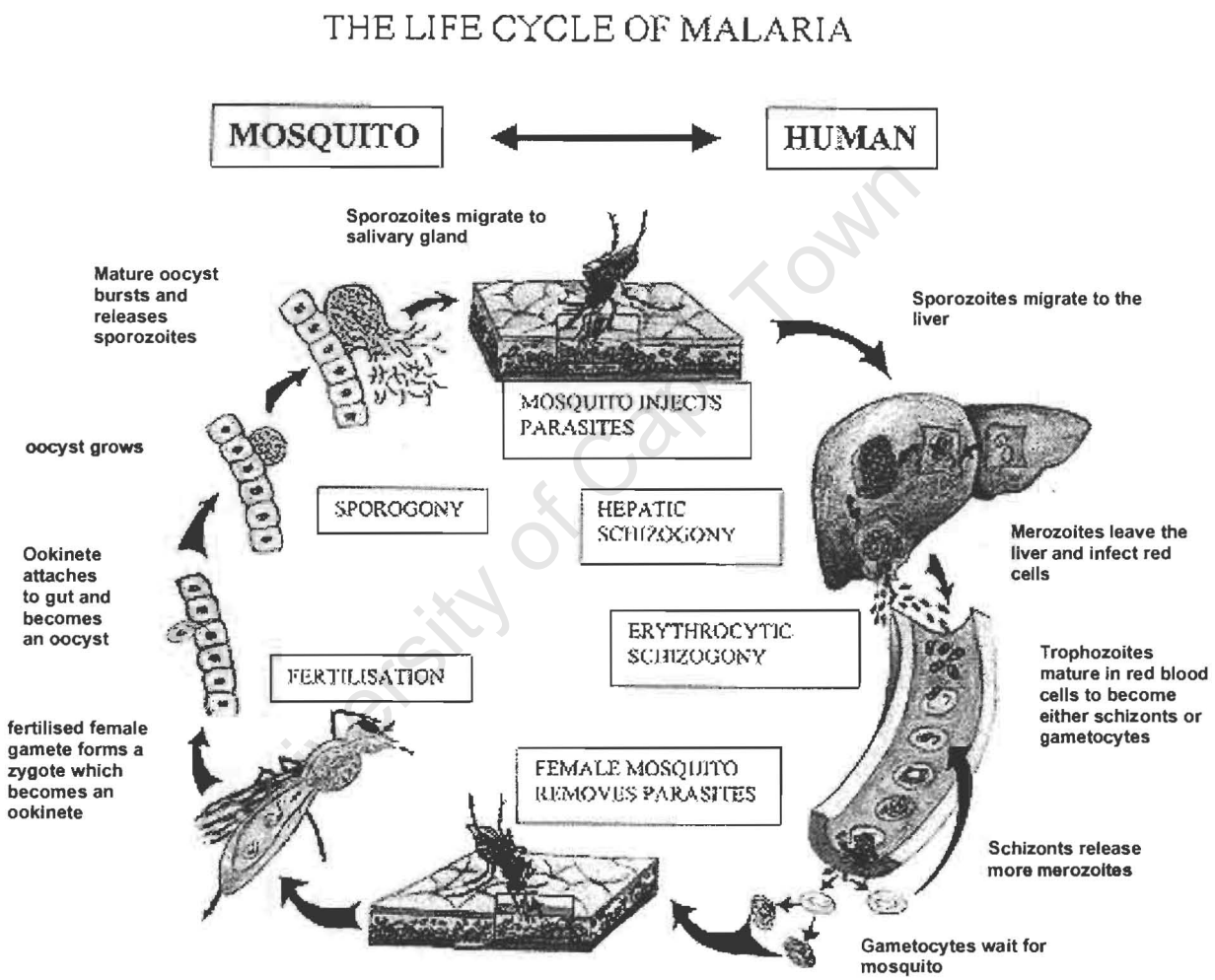

Figure 1.1 Life cycle of *Plasmodium falciparum*[4]

During the blood stage of malaria, symptoms of the disease manifest themselves[3] and it is this stage that many antimalarial drugs are thought to be effective against. Inside the infected erythrocyte the parasite ingests host haemoglobin which passes into an acidic compartment called the food vacuole with a pH range of 5.2-5.6[5, 6]. Here haemoglobin is degraded by proteinase enzymes, plasmepsins I[7] and II[8], falcilysin[9] and a cystein proteinase enzyme, falcipain[10] yielding amino acids as a food source for *P. falciparum*. Haemoglobin also contains

4 haem units which are released as ferroprotoporphyrin IX and autoxidised to haematin (aquaferriprotoporphyrin IX or H_2O-Fe(III)PPIX). This could theoretically reach concentrations of about 0.4 M should it all be released simultaneously and remain in solution in the food vacuole[11]. Haematin exhibits toxicity[12, 13] possibly due to free radical or osmotically mediated lysis of membranes[12, 14, 15, 16] and hence must be detoxified by the parasite. In higher eukaryotes detoxification is mediated by haem oxygenase yielding biliverdin, carbon monoxide and a ferric ion[17] but in *Plasmodium* this enzyme is absent and detoxification takes place at least in part by formation of haemozoin from haematin[18] (Figure 1.2). If the detoxification pathway to haemozoin formation can be blocked, the concentration of haematin will increase leading to parasite death.

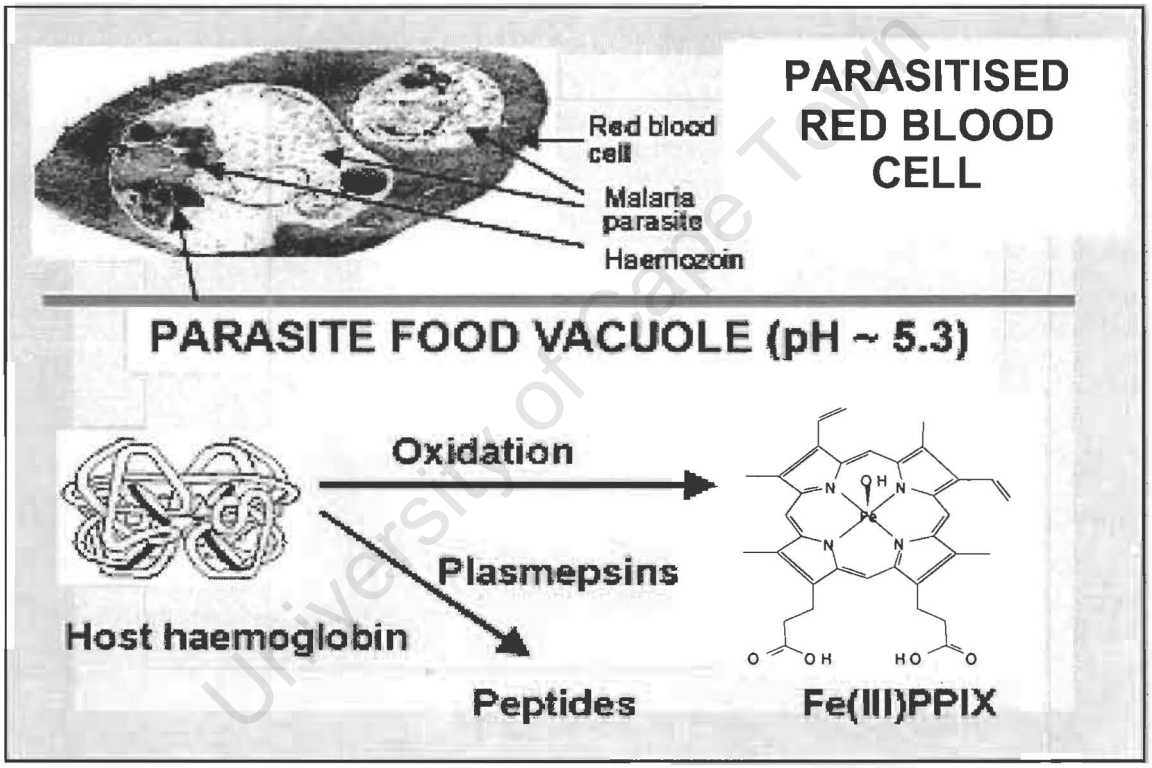

Figure 1.2 Breakdown of haemoglobin in the food vacuole of *Plasmodium* [19]

1.3 Structure of haemozoin and its mechanism of formation

Haemozoin is an insoluble, microcrystalline substance, which has a dimeric structure where a propionate side chain of one Fe(III)PPIX molecule bonds to the iron centre of another Fe(III)PPIX molecule which in turn bonds to the iron of the first molecule with its propionate side chain completing the dimer as is shown in the crystal structure in Figure 1.3.

University of Cape Town

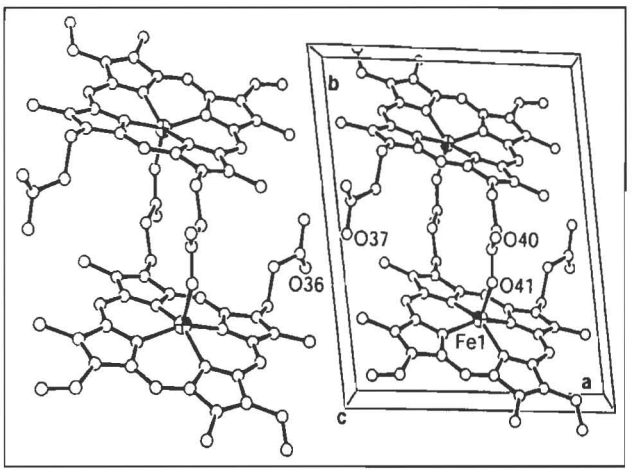

Figure 1.3. Crystal structure of haemozoin[11]

Two propionate side chains from the dimer become available for hydrogen bonding to other dimers as can be seen by the proximity of oxygen 36 and 37 in Figure 1.3[11]. β-haematin is synthetically produced haemozoin and has been proven to be chemically identical to haemozoin by Bohle *et al.*[18] by means of x-ray powder diffraction.

The mechanism of formation of haemozoin *in vivo* is, at present, unclear but its elucidation may well help with future drug design. Initial work by Slater and Cerami[20] based upon the harsh conditions required to form β-haematin synthetically[21], as well as an observation that an extract obtained from plasmodial membranes apparently catalysed β-haematin formation, suggested that the involvement of enzymes was required. However Dorn *et al.*[22] found that β-haematin formation is independent of proteins. Bendrat *et al.*[23] then discovered that an extract of trophozoite lysate using acetonitrile, probably a lipid, acts as a catalyst for β-haematin formation. This result has been further supported by Dorn *et al.*[24, 25] who report that certain purified lipids also catalyse formation of β-haematin. Sullivan *et al.*[26] have reported that histidine rich proteins secreted by *Plasmodium* either initiate, or catalyse the formation of haemozoin *in vivo*. This finding complements the work of Ziegler *et al.*[27] who, having synthesised peptide dendrimers of the repeat motif of histidine rich protein II have demonstrated these peptide dendrimers to both bind Fe(III)PPIX as well as promote the formation of β-haematin. Egan *et al.*[28] have shown that the formation of β-haematin closely parallels many mineralization processes and suggest that haemozoin formation may be a unique biomineralization process, a view supported by Wright *et al.*[29] who have proposed that it is histidine rich protein II in *Plasmodium* which acts as a biomineralization template for the formation of haemozoin. More research is clearly required to bring greater clarity to the complex mechanism of haemozoin formation *in vivo* although much progress has been made[19].

University of Cape Town

1.4 Current antimalarial drugs and their proposed mode of action

Several compounds are presently being used commercially as antimalarial agents either in prophylactic or curative roles. This dissertation is primarily concerned with those substances which exhibit specific activity against the blood stage of the disease and these are summarised in Figure 1.4.

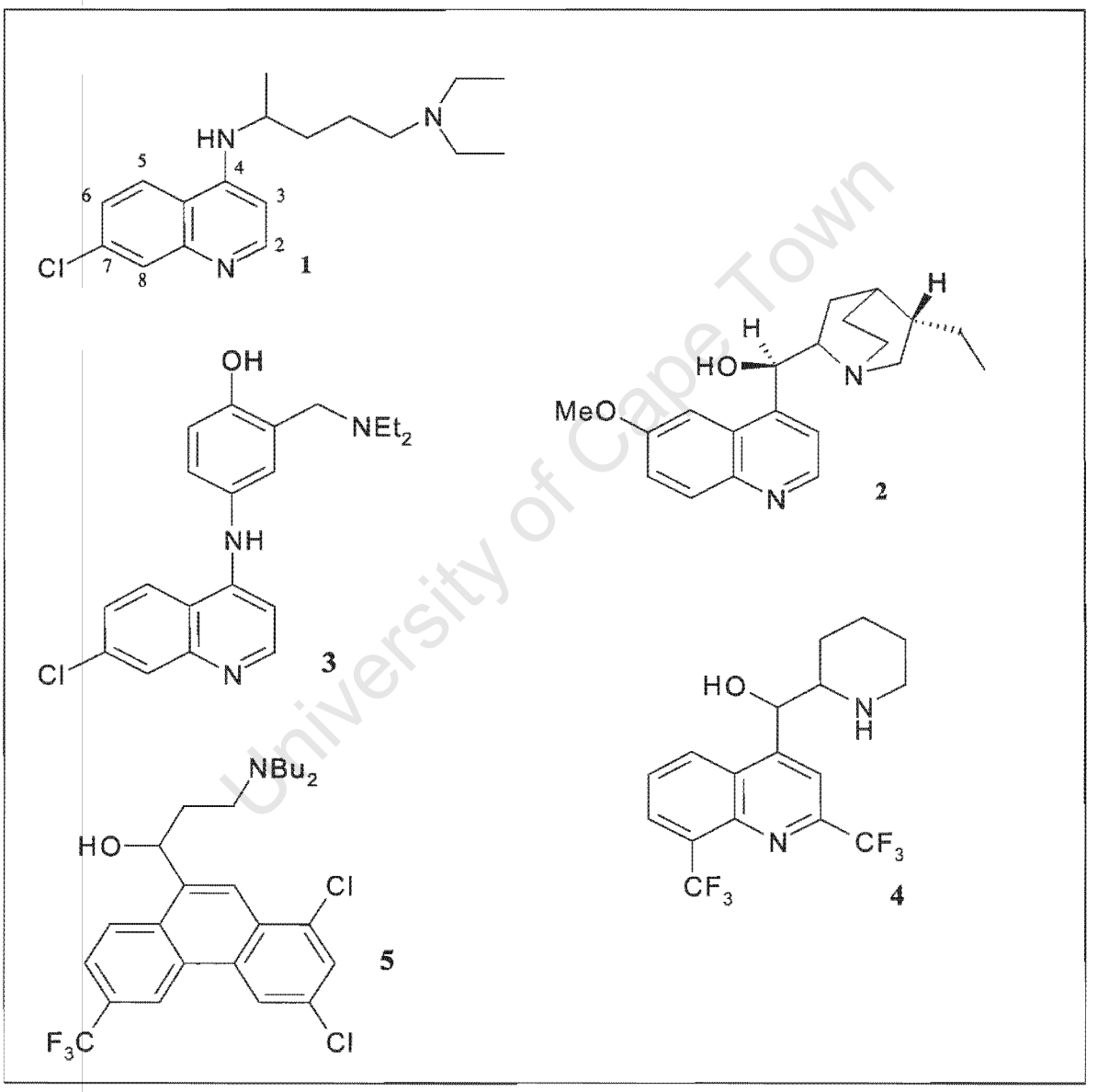

University of Cape Town

Figure 1.4. Drugs effective against the blood stage of malaria: **1** chloroquine, **2** quinine, **3** amodiaquine, **4** mefloquine, **5** halofantrine (not used clinically at present)

The literature reports several hypotheses regarding the mode of action of antimalarial drugs that are effective against the blood stage of the disease. There are two main categories of hypotheses based whether their proposed site of action is extravacuolar or intravacuolar.

Extravacuolar mechanisms

These mechanisms are describing events which take place outside of the acidic food vacuole of the malaria parasite and include the general cytoplasm as well as the nucleus of the parasite.

- DNA binding (intercalation)

  Evidence in favour of the mechanism:-

  Chloroquine **1,** and quinine **2,** have been shown to bind to DNA and chloroquine does exhibit antibacterial activity by inhibiting DNA and RNA synthesis[30, 31, 32, 33].

  Evidence against the mechanism:-

  Concentration of chloroquine that is required to bind to DNA is 1000 times higher than its IC_{50} and mefloquine which is active against the blood stage of malaria does not bind DNA[34, 35].

- Inhibition of protein synthesis

  Evidence in favour of the mechanism:-

  Chloroquine is reported to inhibit protein synthesis in *P. falciparum* at 3 μM concentrations[36].

  Evidence against the mechanism:-

  Not confirmed by several other studies [37, 38, 39] and requires concentrations greater than the IC_{50} of chloroquine (~30 nM)[34].

- Inhibition of polyamine metabolism

  Evidence in favour of the mechanism:-

  Chloroquine and mefloquine **4**, inhibit ornithine decarboxylase activity in trophozoite extracts[40].

  Evidence against the mechanism:-

  It does not explain why chloroquine is only active against the blood stage of the parasite[34].

University of Cape Town

Intravacuolar mechanisms

The food vacuole is likely to be the site of action of chloroquine and related drugs due to their accumulation by "pH trapping" and other effects in this compartment. The aminoalkyl chain of these drugs result in weak base properties. The pKa's of chloroquine are 8.3 and 10.2[41]. At physiological pH (7.4) most of the drug exists as the diprotonated base. However, the concentration of free base is much greater in the general cytoplasm than at pH 5.3 in the parasite's food vacuole. The free base which is sufficiently hydrophobic to cross lipid bilayers[42], consequently accumulates in the food vacuole as a result of mass action. Once adsorbed into the food vacuole the drug is protonated due to the lower pH conditions. The protonated drug also does not easily diffuse out of the food vacuole as it is now in a protonated and charged form which inhibits its membrane crossing properties. Due to these factors, the concentration of the free base form of the drug in the food vacuole approaches the concentration found in the surrounding medium and this results in approximately an 8000 fold increase of the total drug concentration within the food vacuole. Actual accumulation appears to take place to a greater extent due to additional mechanisms[19].

- Increased pH of food vacuole

  Evidence in favour of the mechanism:-

  Chloroquine and structurally related drugs are weak bases and will accumulate in the food vacuole, altering the pH[42].

  Evidence against the mechanism:-

  Experiments indicate no change[43, 44] or a change of less than 0.25 pH units[45] which is too small to be the main origin of activity[34].

- Inhibition of vacuolar phospholipase

  Evidence in favour of the mechanism:-

  Treatment with chloroquine results in accumulation of single membrane endocytic vesicles in the food vacuole of the parasite[46] which could result from either a general breakdown in lysosomal function or the inhibition of phospholipase enzymes by chloroquine[47].

  Evidence against the mechanism:-

  This mechanism requires high concentrations of chloroquine and is not specific to the blood stage[34].

University of Cape Town

- Inhibition of vacuolar protease

  Evidence in favour of the mechanism:-

  Chloroquine shows partial inhibition of aspartic protease enzymes which degrade haemoglobin[48].

  Evidence against the mechanism:-

  Chloroquine only acts in this way at higher concentrations than those occurring in the vacuole[19].

- Degradation of haem

  In has recently been reported by Ginsburg *et al.*[49] and Loria *et al.*[50] that chloroquine and related drugs inhibit the breakdown of haem in the parasite. Both authors suggest that only 30% of haem is converted into haemozoin. Ginsburg *et al.*[49] propose that glutathione is responsible for the degradation of haem in the food vacuole of the parasite and that addition of chloroquine prevents this from taking place, resulting in the accumulation of toxic haem. Loria *et al.*[50] suggest that hydrogen peroxide which is a by-product from the oxidation of ferroprotoporphyrin IX to ferriprotoporphyrin IX, degrades haem in the parasite's cytoplasm and again, chloroquine suppresses the degradation leading to toxic levels of free haematin. Our laboratories however, using Mössbauer spectroscopy, have shown that most of the iron originating from haemoglobin is converted into haemozoin in parasitised red cells. This suggests that the mechanism of the degradation of haem is unlikely as most haem is converted into haemozoin and not predominately degraded via another mechanism.

- Inhibition of haemozoin formation

  It is this mechanism that enjoys much support in the literature at present, based on the following extensive evidence. (1) Drugs active against the blood stage have been shown to directly bind to Fe(III)PPIX in both aqueous and 40% aqueous DMSO solutions[51, 16]. These associations are significant with log K values of 4-5.5[51]. Thus Fe(III)PPIX is a potential drug target. (2) When these drugs are added to haematin in β-haematin synthesis in acetate solution, the formation of the latter is inhibited under a wide range of pH, temperature and acetate concentrations[19]. Bearing in mind that little free Fe(III)PPIX is probably required in the food vacuole to exhibit toxicity, this mechanism allows for much lower concentrations of drug compared with the other mentioned mechanisms. It would also be difficult to envisage how haemozoin would form in the parasite under mild conditions if β-haematin

University of Cape Town

formation is inhibited *in vitro* by these drugs under far harsher conditions. (3) Convincing evidence is provided by a strong correlation between drugs active against the blood stage and the inhibition of β-haematin formation while similar compounds with significantly less or no antimalarial activity do not inhibit β-haematin formation[19]. (4) A study has demonstrated that the uptake of chloroquine is significantly reduced, when no haemoglobin is degraded, by the introduction of inhibitors of plasmepsin I and falcipain[52, 53]. This finding further supports the mechanism, since chloroquine in the food vacuole would normally bind to released Fe(III)PPIX, hence lowering the "free" chloroquine concentration, resulting in more chloroquine diffusing into the food vacuole. If there is no free Fe(III)PPIX, then chloroquine uptake is expected to be reduced. (5) Another study, also utilising proteinase inhibitors, has shown that the effectiveness of chloroquine is diminished when haemoglobin degradation is inhibited [53a]. (6) Finally, this mechanism correctly predicts that chloroquine and related drugs would be active against the blood stage of the disease during the degradation of haemoglobin and indeed this fits the experimental evidence.

The available evidence weighs heavily in favour of the mechanism of drugs binding to haematin and directly preventing the formation of haemozoin and it shall be the mechanism that underpins the rationale behind the work of this dissertation.

The structure activity relationship of chloroquine

By linking the structure of chloroquine **1** (Figure 1.4) to its activity, inferences made may be useful in rational design of new drugs. Recently Egan *et al.*[54] have shown the structure activity relationships for chloroquine and its analogues. (1) An aromatic moiety (quinoline ring) is required for binding to Fe(III)PPIX. (2) The amino group must be attached to the quinoline ring in either the 2 or 4 position to cause significant interaction with Fe(III)PPIX. (3) A strongly electron withdrawing group such as a chlorine atom must be attached to the ring in the 7 position to inhibit the formation of β-haematin. Both binding to Fe(III)PPIX and inhibition of β-haematin formation are prerequisites for activity. (4) An amine containing side chain also appears necessary, presumably for the purposes of pH trapping in the parasite food vacuole.

University of Cape Town

Drug resistance

The problem of malaria is becoming more serious due to significant and widespread resistance being developed to front line drugs, particularly chloroquine[2]. The map depicted in Figure 1.5 illustrates this problem. The mode of chloroquine resistance is not well understood and will not be discussed at length here; however there is some evidence showing that the concentration of chloroquine in the food vacuole of chloroquine resistant parasites is significantly lower than in sensitive parasites[52].

Evidence shows that changing the spacing between the nitrogens in the side chain of chloroquine analogues is sufficient to overcome resistance[55]. This has lead to speculation that the parasite has developed the ability to identify chloroquine by its side chain and hence develop mechanisms to protect itself from the drug, by either preventing choloquine from entering the food vacuole, or by exporting choloquine from the vacuole. There is, however, no evidence at present to support a change in the presence or amount of the drug target, Fe(III)PPIX.

University of Cape Town

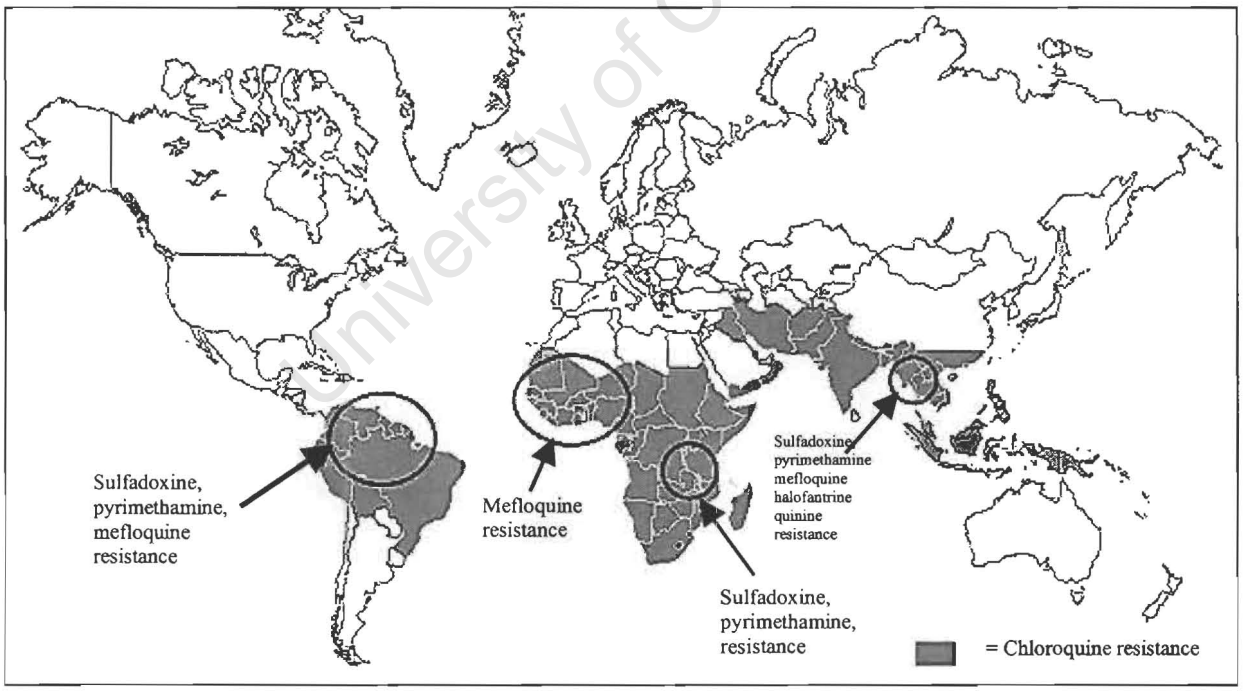

Figure 1.5. World map illustrating the extent of drug resistance

It is essential that new drugs be developed to curb the rising problem of malaria as discussed in section 1 of this chapter. Current research has focused significantly on new quinolines[56]; however, other systems are being investigated. This dissertation will focus on the potential of

new water soluble platinum(II) complexes which will be discussed in section 1.7 to act as a starting point for the discovery of novel antimalarials and as probes for the underlying process. It is the process of haemozoin formation that again will be the focus as this remains an ideal target as it is unique to the parasite with the host having other mechanisms available to deal with toxic haematin.

1.5 Haematin – drug interactions

Based on the proposed intravacuolar mechanism of action involving the inhibition of haemozoin formation, the interactions between chloroquine and related drugs with Fe(III)PPIX are clearly important when considering the development of potentially new antimalarial drugs. There is strong evidence to suggest that drug-Fe(III)PPIX associations are based on so-called π-π interactions[57]. In cases such as quinine there may be additional interactions where the side chain hydroxyl group is also able to bind to the iron centre of the porphyrin[58]. There is however generally a poor understanding of π-π interactions with the common misconception that the two aromatic molecular orbitals attract each other. In a general context, Burley *et al.*[59, 60] have shown that π-π interactions can take 2 distinct geometries which are illustrated in Figure 1.6, with either a face to face conformation (A) or a face to edge orientation (B).

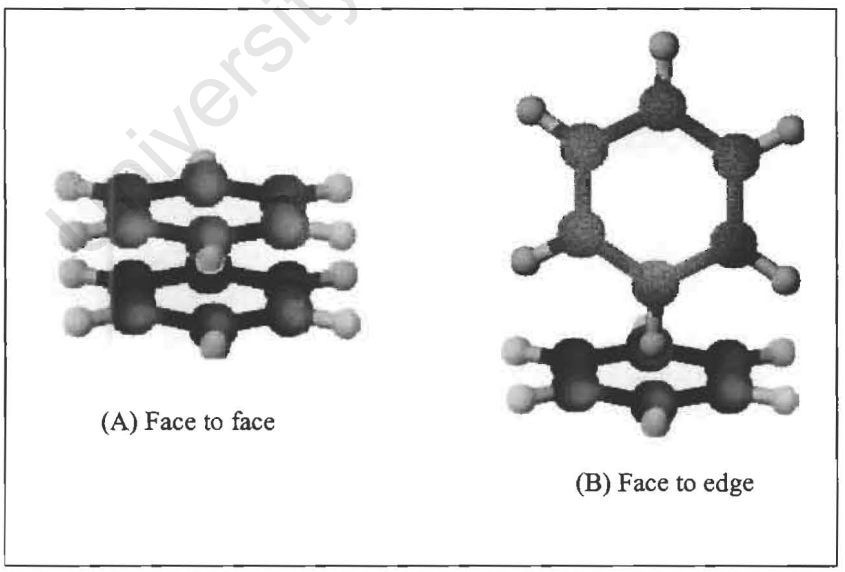

Figure 1.6. Illustration of the two modes of π-π interactions

Orientation B is preferred by smaller ring systems such as benzene where the slightly positively charged proton of one molecule interacts with the electron rich ring system of the

University of Cape Town

other molecule. In larger systems such as [18] annulene, conformation A is preferred[61]. This is also the mode of interaction that applies to porphyrins and related systems[62].

In general the energy of interaction between two molecules can described by equation 1.1.

$$E_{TOTAL} = E_{ELECTROSTATIC} + E_{INDUCTIONAL} + E_{DISPERSIVE} + E_{REPULSIVE} \qquad (1.1)^{62}$$

This equation can be simplified for π-π interactions and a simple but convincing model has been developed by Hunter and Sanders[62] which supersedes solvophobic, electron donor-acceptor and atomic charge models as it predicts not only the strength of interactions, but also the geometries of association which agree well with experimental data. Hunter and Sanders show that the interaction between two molecules is governed principally by van der Waals forces and electrostatic interactions. According to the Hunter and Sanders model, Van der Waals forces govern the strength of the interaction and are roughly proportional to the overlapped aromatic surface area of the two molecules[62].

The model also dictates that it is the electrostatic forces which govern the geometry of the association. In Figure 1.7(A) it can be seen that the net interaction between two centrosymetrically stacked systems is repulsive.

University of Cape Town

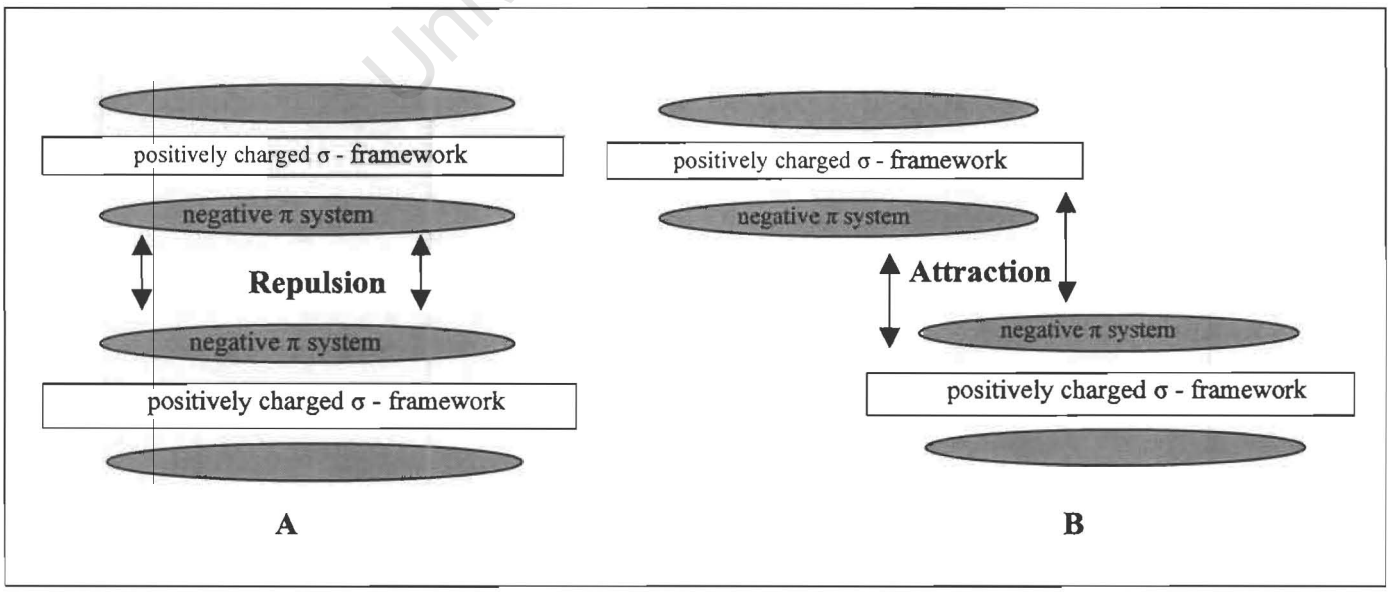

Figure 1.7. Illustration of repulsion between centrosymetrically stacked aromatic systems (A)[62] and attraction between offset molecules (B)

By offsetting the molecules along the xy plane (Figure 1.7 (B)), the overall interaction becomes attractive[62]. Van der Waals forces and solvophobic effects are maximised when molecules are centrosymetrically stacked. This however carries a significant electrostatic repulsion term resulting in an optimised conformation in which the two aromatic rings are off-set by a distance approximately equivalent to the displacement in the z direction[62].

Including strongly polarising heteroatoms rings in the aromatic framework such as nitrogen allows for electron redistribution resulting in areas of high and low electron density in the π framework. This has a marked effect on electrostatic interactions[64], and either increases association or decreases the extent of offset in the xy plane. Such a model appears to apply to both porphyrin and quinoline systems[64].

Insight into the role of the chloro atom in chloroquine can now be gained considering this model. The chloro atom could be expected to significantly influence the electrostatic component of the interaction of chloroquine with Fe(III)PPIX, and hence while not influencing the overall strength of the association significantly, it is conceivable that it could alter the geometry of the complex. This preferred geometry is possibly responsible for the ability of chloroquine to inhibit β-haematin formation.

The π-π interaction of porphyrins with aromatic molecules is a well studied phenomenon and is known to occur not only with anti-malarial drugs but also with many other aromatic hetrocycles, including phenanthrolines, particularly in aqueous media[65, 66]. Porphyrin self-association is also well documented[66,67] so that it is likely that many compounds with aromatic surfaces could express antimalarial activity, through binding to Fe(III)PPIX. Support for this idea has been obtained from other metalloprotoporphyrin IX's including Cr, Co, Mn, Cu, Mg, Zn and Sn which not only bind to Fe(III)PPIX, but also inhibit β-haematin formation[68].

It has been found that the solvent system significantly affects the strength of drug-Fe(III)PPIX interactions[19]. As one moves from an aqueous system to organic solvents the association decreases dramatically. This is especially true of coordinating solvents such as DMSO and non-polar liquids[51, 69]. It appears that the Hunter and Sanders model[62] is better suited to the gas- or solid phase when considering association strength as it does not take into account the large effect of solvent. Insight into the role of solvent can be gained by considering that the strength

University of Cape Town

of interaction can be quantified by the Gibbs function which is dependant on entropy, temperature and enthalpy as defined in equation 1.2 where a large negative ΔG represents a strong interaction.

$$\Delta G = \Delta H - T\,\Delta S \qquad (1.2)$$

It is possible to conceptually break down the formation of these complexes into the following 4 steps.

(i)	drug solvent $_n$ → drug + n solvent	$\Delta H > 0, \Delta S > 0$
(ii)	Fe(III)PPIX solvent $_m$ → Fe(III)PPIX + m solvent	$\Delta H > 0, \Delta S > 0$
(iii)	drug + Fe(III)PPIX → drug · Fe(III)PPIX	$\Delta H < 0, \Delta S < 0$
(iv)	m + n solvent + bulk solvent → bulk solvent	$\Delta H < 0, \Delta S < 0$ [65]

The Hunter and Sanders model would only appear to consider step (iii) which is solvent independent; however the remaining steps are all solvent dependant. The entropy for interaction of chloroquine with Fe(III)PPIX in 40% aqueous DMSO is 90 ± 3 $J.K^{-1}.mol^{-1}$ [51] which results in the association being largely entropically driven at 37 °C. This entropic driving force is solvent based. Thus it can be claimed that hydrophobic effects play an important role in Fe(III)PPIX-drug interactions.

Much effort has been invested in establishing thermodynamic parameters for Fe(III)PPIX-drug interactions by isothermal titration calorimetry and spectrophotometric titrations with both methods yielding similar ΔH and ΔS results[19]. Establishing accurate values for the binding constant reported as log K requires that iron in Fe(III)PPIX solutions is both high spin and monomeric. This is not easy to achieve as Fe(III)PPIX has a strong propensity to aggregate in aqueous solution as well as precipitate at lower pH values. The desired speciation of Fe(III)PPIX can be achieved for spectrophotometric titrations where concentrations are in the order of 2×10^{-6} M by using 40% aqueous DMSO solutions at an apparent pH of 7.4[51].

Finally it must be stressed that a compound binding to Fe(III)PPIX is not sufficient in itself to achieve the inhibition of β-haematin formation. An example of this is 9-epiquinine which has an association constant of 4.04 ± 0.03 log units with Fe(III)PPIX yet does not inhibit β-

University of Cape Town

haematin formation[51]. 4-aminoquinolines with a hydrogen atom in the 7 position are also reported to bind to Fe(III)PPIX but do not inhibit the formation of β-haematin unless present in a very high concentration[70].

1.6 Metals in antimalarial drugs

The majority of drug research that has been conducted up to the present has been within the realms of organic chemistry. It should not however be forgotten that metal ions play an absolutely vital role in biological systems from structural frameworks of calcium containing bones, to enzymes utilising a host of metals. Without metal containing complexes life would be impossible. More emphasis should thus be placed on developing inorganic drugs on the basis that metals potentiate biological systems and the seemingly infinite number of possible metal containing complexes.

Medicinal inorganic chemistry dates back to Ancient Egypt (3000 B.C.) when copper was used for water purification processes. 1500 years later zinc and iron were being utilised medicinally, while in Arabia and China, gold was being used in the treatment of various ailments[71, 72]. The rational development of medicinal inorganic chemistry started during the 1900's with $K[Au(CN)_2]$ being used in the treatment of tuberculosis, gold salts being exploited for antibacterial properties and antimony compounds finding application in treating leishmaniasis. Currently, inorganic chemotheraputic drugs are being used as anticancer, antibiotic, antiviral, antiarthritic drugs and as radiopharmaceuticals[73] with antimalarial applications being investigated.

Some of the most promising new anti-malarial compounds being investigated include metal ions. The most common themes have been coordinating metals to the nitrogen in the quinoline ring of chloroquine (CQ) or modifying the aminoalkyl side chain by inclusion of ferrocene. Several of these compounds are depicted in Figure 1.8. The rhodium complex Rh(1,5-cyclooctadene)(CQ)Cl **6**, shows some promising antiplasmodial activity with a similar activity to chloroquine when tested against chloroquine sensitive parasites and is twice as effective against resistant strains. The ruthenium complex $[RuCl_2(CQ)]_2$ **7**, exhibits activity 4 times greater than chloroquine against chloroquine sensitive *P. falciparum* and has a similar activity to **6** against resistant parasite strains[74]. Compound **8** $[Au(PPh_3)(CQ)]PF_6$ is significantly more

University of Cape Town

active than **6** or **7** against both chloroquine sensitive and resistant *P. falciparum*[75]. This seems to indicate that complexes need not necessarily be uncharged to cross membranes to enter the parasite food vacuole, but can be formally charged as well. 7-Chloro-4-(((2-((dimethylamino)methyl)ferrocenyl)methyl)amino)quinoline **9**, is 22 times more active than chloroquine against resistant strains of *P. falciparum*[76]. This is consistent with ideas brought up in section 1.3 where it was noted that a significant change to the aminoalkyl side chain overcomes resistance.

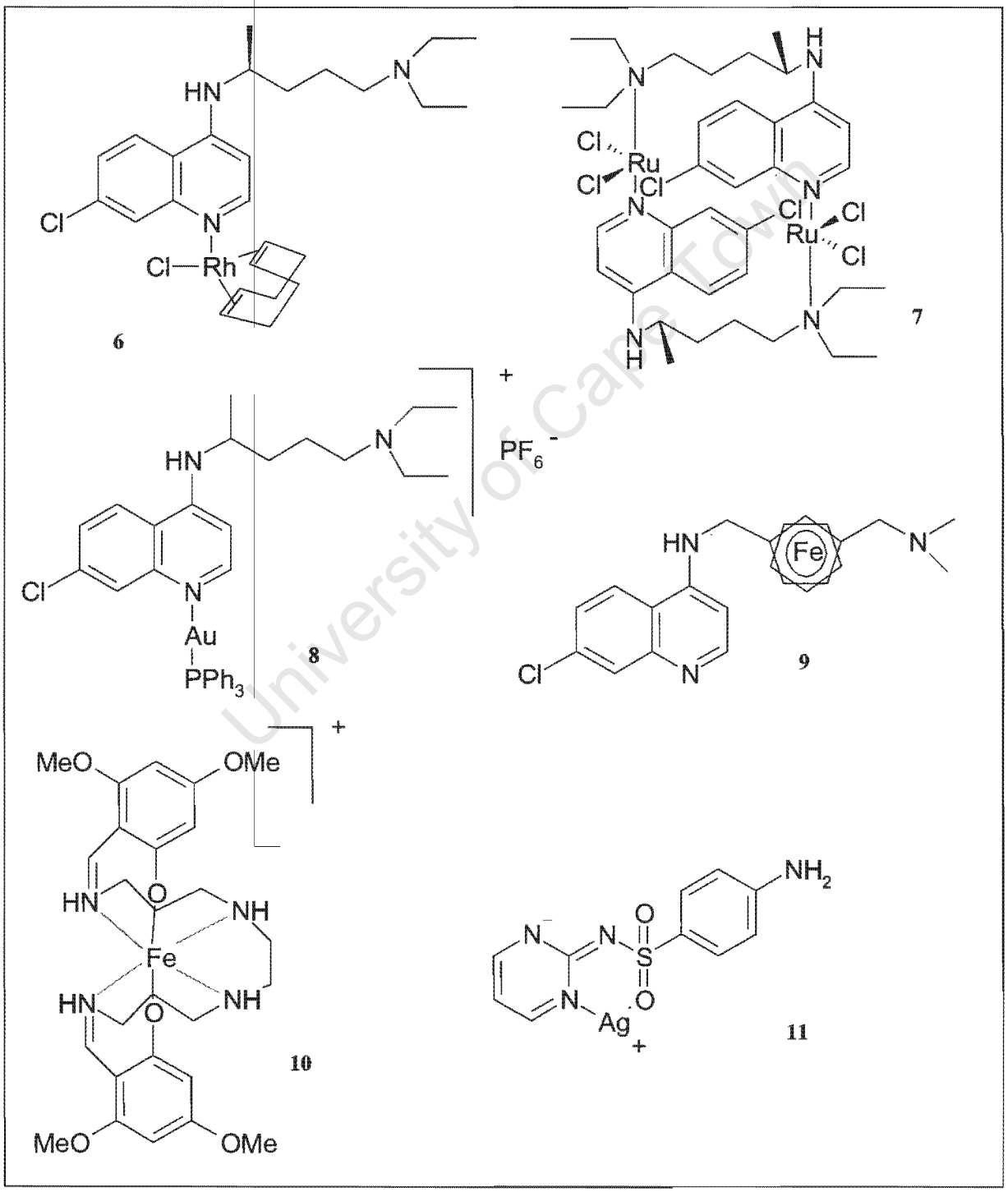

University of Cape Town

Figure 1.8 Metal containing complexes showing antimalarial activity[75, 74, 77, 78]

Complex **10** is one of a series of Schiff-base phenolate metal complexes where Al^{3+}, and Ga^{3+} have also shown stage specific activity by inhibiting haemozoin formation[77]. The 4-amino-*N*-2-pyridinyl-benzenesulfonamide silver complex **11,** showed *in vivo* activity against *Plasmodium berghei* during testing against mice and the drug exhibited activity via a different mechanism compared with purely organic sulphonamides[78].

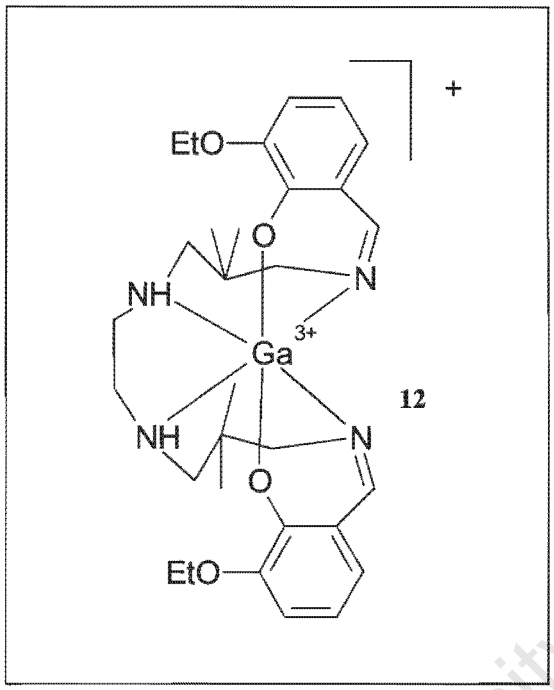

12

Figure 1.9 [{1,12-bis(2-hydroxy-3-methyoxybenzyl)-1,5,8,12-tetraazadodecane}gallium(III)]

A metalloporphyrin, magnesium(II) meso-tetrakis(4-sulfonatophenyl)porphyrin, has been recently reported to have a synergistic effect when co-administered with either artemisinin or beta-arthemether (existing antimalarials) when tested *in vitro* against *P. falciparum.* Finally, a novel gallium complex, **12** (Figure 1.9) is reported to have significant activity against chloroquine resistant strains of *P. falciparum* by inhibiting the formation of haemozoin[79].

University of Cape Town

The Role of Platinum in Inorganic Drugs

Platinum (II) complexes have played a significant role in the development of inorganic medicinal chemistry in the search for a cure for cancer. Chemotherapy using platinum complexes is one of the mainstay treatments in ovarian, testicular, head and neck cancers[80]. This started in 1964 with Rosenberg's discovery that *cis*-diamminedichloro-platinum(II) now commercially known as "cisplatin", exhibits strong activity against cancer cells[81]. Cisplatin, once absorbed into the patient's body, hydrolyses through the loss of the more labile chlorides and in this state has a high affinity to bind to DNA[80]. Crystal structures of nucleotides have shown platinum binding to adjacent guanosine base pairs through nitrogen, resulting in significant bending of 40-50° of the nucleotide and results in fraying, unwinding and shortening of the DNA strands[80, 82]. Cisplatin interestingly exhibits stage non-specific anti-

plasmodial activity according to a study by Nair *et al.*[83]. Mice infected with *P. berghei* showed cisplatin to be more active than either chloroquine or quinine. The reason for the antiplasmodial activity of cisplatin was suggested to be as a result of binding to parasite DNA.

Distortions of the double helix of DNA can also be achieved through intercalation of drugs between base pairs. Again platinum complexes have featured in these intercalation agents. These drugs intercalate due to π-π interactions between the metal complexes and the base pairs of the DNA. Early examples of these intercalates include [(2,2',2"-terpyridyl)platinum(II) chloride and 2-hydroxyethane-thiolato(2,2',2,"-terpyridine) platinum(II)[84]. X-ray crystal structures of nucleotides containing intercalators have been determined and show that the entire platinum complex, not just the triimine, is intercalated between base pairs[85, 86]. Intercalation results in increased spacing between base pairs and causes unwinding of the DNA helix strands so preventing the binding of enzymes responsible for strand repair, which leads to cell death[87, 88]. X-ray crystal structures show closer interaction between diimine-palladium complexes and base pairs compared to non-coordinated diimine ligands[89, 90] indicating an increased association. It would be reasonable to expect specific platinum complexes to enhance the interaction of aromatic ligands with DNA as well. 2,2'-bipyridyl platinum(II) complexes coordinated to various pyridines have also been shown to intercalate DNA to an extent depending on the pK_a (which reflects electron density) of the pyridine involved[91]. Metal complexes of 1,10-phenanthroline also demonstrate intercalation properties[92].

Despite the high cost of platinum (II) complexes and that, depending on the type and structure of the complex, they can exhibit toxicity in humans, they remain the metal of choice in the treatment of cancer. There are several properties that place it in a favourable position. Firstly platinum (II) is kinetically inert having a rate of exchange of co-ordinated waters of 7.1×10^{-6} M^{-1} s^{-1} [94]. This is significantly slower than other platinum group metals such as palladium (10.2 M^{-1} s^{-1} [95]). As a result, complexes of platinum (II) tend to be less labile than other metal complexes in biological systems and are able to get to the required biological site before decomposing. Secondly, platinum (II) which has a d^8 valence electron configuration is stable in aqueous solution and forms square planar complexes with many ligands. This planarity of complexes makes them ideal intercalators. Moreover the ligand 2,2'-bipyridine which has a twisted structure as an unbound ligand is forced into a planar configuration when coordinated to platinum (II)[96]. Additionally, due to platinum(II) being electropositive, it is effective in

University of Cape Town

removing electron density from π systems thus polarising the π system which may lead to stronger π-π interactions and hence better intercalation with DNA.

It is thus proposed that platinum diimine complexes should be investigated as potential antimalarial agents based on the precedent they have set as DNA intercalators and their potential to form similar π-π complexes with Fe(III)PPIX.

1.7 *N*-Benzoyl-*N'*,*N'*-dialkylthioureato-diimine platinum(II) complexes as a starting point in the search for a novel platinum containing antimalarial drug

The synthesis of mixed ligand diimine-*N*-benzoyl-*N'*,*N'*-dialkylthioureato platinum (II) complexes has been reported by Koch *et al.* [97] in a study which describes the pronounced self-association of these complexes in an acetonitrile solvent system. These complexes are presumed to associate via π-π interactions and stack with an offset geometry as predicted by the Hunter and Sanders model[62]. It was speculated that these complexes may also have potential anticancer applications as a result of DNA intercalation[97]. This suggests that they may also exhibit antimalarial activity if appropriately designed. Two of the molecules from the study are (*N*-benzoyl-*N'*,*N'*-di-*n*-butylthioureato-*S*,*O*) (1,10-phenanthroline)platinum(II) hexafluorophosphate **13** and (*N*-benzoyl-*N'*,*N'*-di-*n*-butylthioureato-*S*,*O*) (2,2'-bipyridyl) platinum(II) hexafluoro-phosphate **14** (Figure 1.10) which show dimerisation constants of 3.0 ± 0.6 M^{-1} and 23.3 ± 3.1 M^{-1} respectively in acetonitrile. These dimerisation constants are expected to be significantly larger in aqueous solvent due to hydrophobic solvent interactions. The study by Koch *et al.*[97] also demonstrated a correlation between the surface area of the diimine and the association constant and clearly showed that it was the diimines that were interacting with each other rather than the acylthiourea moieties.

University of Cape Town

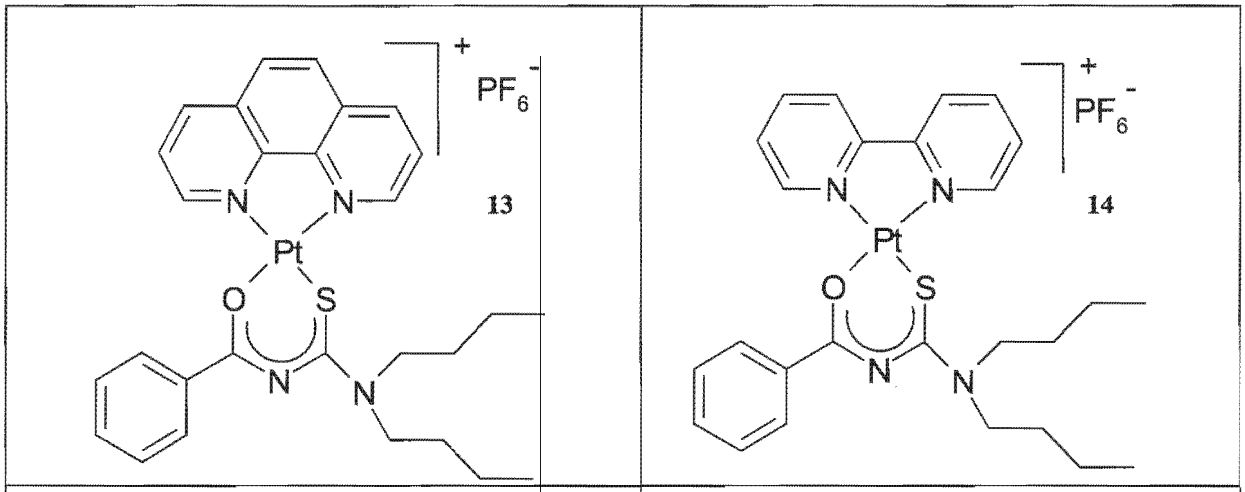

(*N*-Benzoyl-*N'*,*N'*-di-n-butylthioureato-*S*,*O*)(1,10-phenanthroline) platinum(II) hexafluorophosphate

(*N*-Benzoyl-*N'*,*N'*-di-n-butylthioureato-*S*,*O*)(2,2'-bipyridyl) platinum(II) hexafluorophosphate

Figure 1.10 Structures of 2 mixed ligand platinum(II) complexes used in the dimerisation study of Koch *et al.*[97]

University of Cape Town

While these complexes are significantly different to quinoline systems such as chloroquine there are some structural similarities including a flat hetroaromatic ring system containing nitrogen as well as side chains which could be appropriately modified.

Shelnutt[98] has demonstrated using Raman difference spectroscopy, the ability of various uncoordinated 1,10-phenanthrolines to bind to both copper and iron uroporphyrin I in basic aqueous solutions in a similar fashion. The interaction was shown to be π-π in nature rather than direct coordination to the metal centre of the porphyrin by the nitrogen of the diimine. Changing the substituents on 1,10-phenanthroline also resulted in some changes in the Gibbs free energy of association between these molecules and the metalloporphyrin. These changes exhibited a relationship with the Hammett constant of the substituents. Electron withdrawing chloro, nitro and hydroxy substituents cause stronger interactions, while electron donating methyl substitution weakens the interaction[98].

Coordination of such diimines to a metal such as platinum (II) might result in stronger associations with porphyrins due to the strong electron withdrawing effect of the metal thus polarising the π system of the diimine ligand moiety.

The choice of acylthioureas as ligands is based on the following points. Firstly, they are known to bind strongly with platinum via bidentate chelation through their oxygen and sulphur

atoms[99]. These complexes show great selectivity for platinum group metals to such an extent that they have industrial application in the purification and recovery of these metals from strongly interfering matrices[99, 100]. They first bind to platinum through the soft sulphur donor and after loss of the N' proton, coordinate through the oxygen as well, resulting in a very stable six membered ring with extensive electronic delocalisation[101]. These platinum (II) complexes are stable under acid conditions and as a result could be orally administered if they prove to be a viable drug since they would survive the low pH conditions in the stomach. Moreover, acylthioureas are easily synthesised according to a procedure by Douglass and Dains[102] involving a simple synthesis of related *N'*-monosubstituted acylthioureas. *N',N'*-substituted acylthioureas are synthesised in the same manner with dialkyl amine replacing the monoalkyl amine and these ligands were first synthesised and studied in detail by Beyer and Hoyer in 1975[103]. For this project *N*-monosubstituted thioureas were not considered as these do not always form bidentate chelates with metal ions due to an intramolecular hydrogen bond preventing appropriate isomerisation[104]. The wide range of different N and N' substituents that can be successfully incorporated into the thiourea motif makes these ligands very versatile enabling complexes to be synthesised according to the functionality required. It has been noted in section 1.4 that amines are required in the side chain of chloroquine to effect significant accumulation in the food vacuole of the parasite. Suitable amine side chains could thus simply be included in the alkyl side chains of the thiourea.

A final attribute of $[Pt(L\text{-}S,O)bipy]^+PF_6^-$ or $[Pt(L\text{-}S,O)phen]^+PF_6^-$ complexes is that they are positively charged, allowing for good solubility of complexes in aqueous media which is required for favourable bioactivity. Moreover the positive charge of these complexes might be expected to result in stronger self association, as well as interaction with uncharged π systems including metalloporphyrins. The charge could have a negative effect however, by hampering the complex in crossing cell membranes resulting in decreased bioactivity. However the precedent set by the gold chloroquine complex **8** shows that charged complexes can also exhibit excellent activity. Furthermore, charged platinum complexes used in cancer chemotherapy show outstanding activity[105]. The effect of charge could be investigated by studying the activities of both charged and formally neutral related complexes.

University of Cape Town

1.8 Objectives

The objectives of this work are to examine whether mixed ligand platinum (II) complexes of the type [Pt(L-*S,O*)bipy]Cl and [Pt(L-*S,O*)phen]Cl specifically associate with Fe(III)PPIX and to establish if they cause inhibition of β-haematin formation. This project thus involved the following steps.

- Synthesis and characterisation of a series of mixed-ligand [Pt(diimine)(*N*-benzoyl-*N'N'*-dialkylthiourea)]$^{+}$Cl^{-} complexes

- Synthesis and characterisation of a neutral Pt(2-phenylpyridine)(*N*-benzoyl-*N'N'*-dialkylthiourea) complex

- Investigation of the binding potential of these complexes to Fe(III)PPIX by means of spectrophotometric titrations

- Investigation of the binding of free diimines and acythioureas with Fe(III)PPIX

- Investigation of the geometry of interaction between these platinum complexes and a non-paramagnetic haem analogue, Zn(II)PPIX, using ^{1}H NMR spectroscopy

- Investigation of the ability of the complexes and free ligands to inhibit the formation of β-haematin

University of Cape Town

2 Synthesis and characterisation

2.1 Overview of synthesis

Three classes of molecules have been synthesised in this project, [Pt(diimine)(L-*S,O*)]Cl, Pt(2-phenylpyridine)(L-*S,O*) and Ga(III) protoporphyrin IX. Due to the long names of these complexes, abbreviations will be used both in this chapter and in the rest of the dissertation and these are defined in Table 2.1 for both final complexes as well as isolated intermediates. The synthesis and characterisation of each class of these molecules is discussed in the ensuing sub-sections.

University of Cape Town

Table 2.1 Complexes and ligands synthesised with full and abbreviated names

Complex / ligand name	**Abbreviation**	Number
4,4'-ditertiarybutyl-2,2'-bipyridine	dtbbipy	**15**
N-benzoyl-*N',N'*-bisdiethylaminoethylthiourea	HL'	**16**
N-benzoyl-*N',N'*-di-2-hydroxyethylthiourea	HL	**17**
2,2'-bipyridyldichloroplatinum(II)	Pt(bipy)Cl_2	**18**
4,4'-dimethyl-2,2'-bipyridyldichloroplatinum(II)	Pt(diMebipy)Cl_2	**19**
4,4'-ditertiarybutyl-2,2'-bipyridyldichloroplatinum(II)	Pt(dtbbipy)Cl_2	**20**
1,10-phenanthrolinedichloroplatinum(II)	Pt(phen)Cl_2	**21**
4-methyl-1,10-phenanthrolinedichloroplatinum(II)	Pt(4-Me phen)Cl_2	**22**
5-methyl-1,10-phenanthrolinedichloroplatinum(II)	Pt(5-Me phen)Cl_2	**23**
3,4,7,8-tetramethyl-1,10-phenanthrolinedichloroplatinum(II)	Pt(3,4,7,8-tetraMe phen)Cl_2	**24**
5-chloro-1,10-phenanthrolinedichloroplatinum(II)	Pt(5-Cl phen)Cl_2	**25**
5-nitro-1,10-phenanthrolinedichloroplatinum(II)	Pt(5-NO_2 phen)Cl_2	**26**
(*N*-benzoyl-*N',N'*-di-2-hydroxyethylthioureato-*S,O*)(2,2'-bipyridyl) platinum(II) chloride	[Pt(bipy)L]Cl	**27**
(*N*-benzoyl-*N',N'*-di-2-hydroxyethylthioureato-*S,O*)(4,4'-dimethyl-2,2'-bipyridyl) platinum(II) chloride	[Pt(diMebipy)L]Cl	**28**
(*N*-benzoyl-*N',N'*-di-2-hydroxyethylthioureato-*S,O*)(4,4'-ditertiarybutyl-2,2'-bipyridyl)platinum(II) chloride	[Pt(dtbbipy)L]Cl	**29**
(*N*-benzoyl-*N',N'*-di-2-hydroxyethylthioureato-*S,O*)(1,10-phenanthroline) platinum(II) chloride	[Pt(phen)L]Cl	**30**

(*N*-benzoyl-*N'*,*N'*-di-2-hydroxyethylthioureato-*S*,*O*)(4-methyl-1,10-phenanthroline) platinum(II) chloride	[Pt(4-Me phen)L]Cl	**31**
(*N*-benzoyl-*N'*,*N'*-di-2-hydroxyethylthioureato-*S*,*O*)(5-methyl-1,10-phenanthroline) platinum(II) chloride	[Pt(5-Me phen)L]Cl	**32**
(*N*-benzoyl-*N'*,*N'*-di-2-hydroxyethylthioureato-*S*,*O*) (3,4,7,8-tetramethyl-1,10-phenanthroline) platinum(II) chloride	[Pt(3,4,7,8-tetraMe phen)L]Cl	**33**
(*N*-benzoyl-*N'*,*N'*-di-2-hydroxyethylthioureato-*S*,*O*)(5-chloro-1,10-phenanthroline) platinum(II) chloride	[Pt(5-Cl phen)L]Cl	**34**
(*N*-benzoyl-*N'*,*N'*-di-2-hydroxyethylthioureato-*S*,*O*)(5-nitro-1,10-phenanthroline) platinum(II) chloride	[Pt(5-NO_2 phen)L]Cl	**35**
(*N*-benzoyl-*N'*,*N'*-bisdiethylaminoethylthioureato-*S*,*O*)(2,2'-bipyridyl)- platinum(II) chloride	[Pt(bipy)L']Cl	**36**
cis-bis(*N*-benzoyl-*N'*,*N'*-di-2-hydroxyethylthioureato) platinum (II)	*cis*-[PtL_2]	**37**
di-μ-chlorobis[2-(2-pyridinyl)phenyl-(*C*,*N*)]di-platinum	$(Pt(ppy)Cl)_2$	**38**
(*N*-benzoyl-*N'*,*N'*-bisdiethylaminoethylthioureato-*O*,*S*)(2-phenyl pyridine) platinum(II) chloride	Pt(ppy)L'	**39**
gallium(III)protoporphyrin IX	Ga(III)PPIX	**40**

2.2 *N*-benzoyl-*N'*,*N'*-dialkylthiourea ligands

Both acylthioureas, HL and HL' (Figure 2.1) were synthesised according to the general method of Douglass and Dains[102] in a one pot synthesis. KSCN was dissolved in dry refluxing acetone to which benzoyl chloride was added, followed by the amine 90 minutes to 2 hours later. HL was easily isolated from solution. Addition of cold water dissolved residual KCl contaminating the product which was recovered by filtration. Care was taken during recrystallisation not to boil the solvent containing the product to minimise decomposition. HL' was less trivial to isolate, proving soluble in most polar solvents including water. The product was initially isolated from the reaction as an oil but purification by means of two silica gel chromatography columns and recrystallisation from hot petroleum ether resulted in the precipitation of pure crystalline HL'.

University of Cape Town

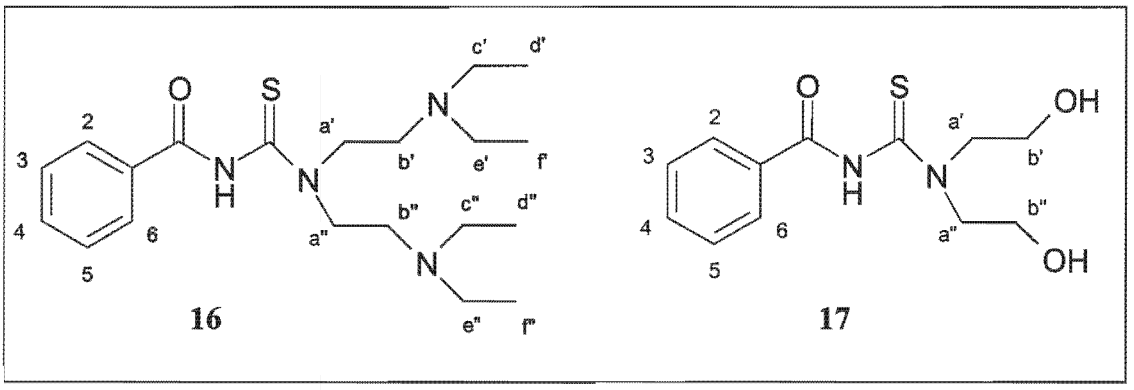

Figure 2.1 Structure and numbering schemes for the acylthiourea ligands **16** – HL' and **17** - HL

It was proposed by Takamizawa *et al.*[106] in 1963 that two mesomeric forms of thiocyanate are likely to exist in acetone (represented in Figure 2.2) and the change of form is stimulated by addition of heat.

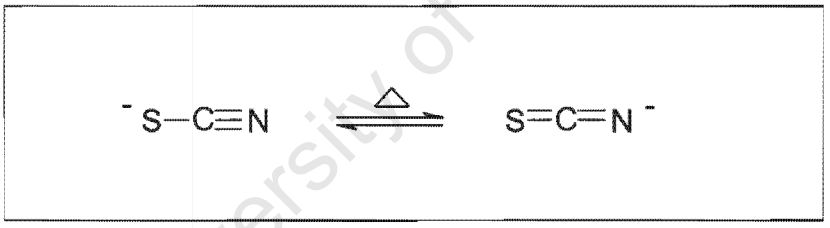

Figure 2.2 Mesomerisation of thiocyanate in acetone [106]

Upon reaction of the thiocyanate with acylchloride, two products are theoretically possible depending on which isomer of the thiocyanate is involved (Figure 2.3). In practice, only one product is formed and Takamizama *et al.*[106] have suggested that acylthiocyanate in the form of **A** is unstable and further reacts with isothiocyanate yielding a single product, **B**.

University of Cape Town

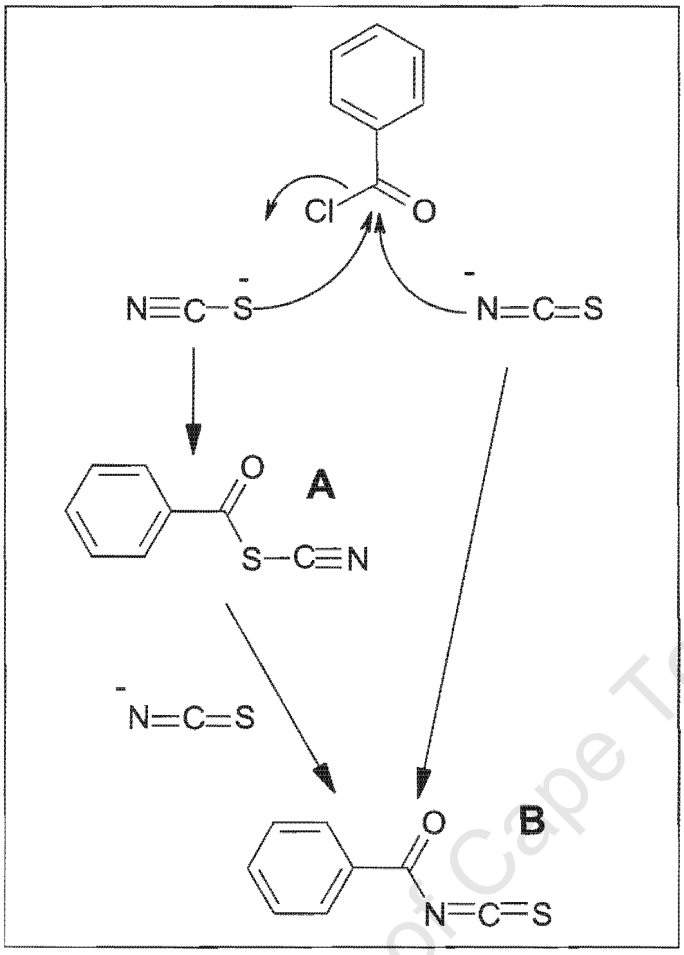

Figure 2.3 Reaction of thiocyanate with benzoyl chloride

The acylthiocyanate formed, **B**, is fairly reactive, with the acyl carbon and thiocarbonyl carbon both being susceptible to electrophilic attack. Many reactions with acylthiocyanates are hence possible and these have been explored in some detail by Elmore *et al.*[107]. Of interest to this work is the substitution of a secondary amine onto the thiocarbonyl carbon. This is achieved by the use of polar solvents. It has been suggested[107] that a donor-acceptor complex of the isothiocyanate and amine forms first and then undergoes proton transfer and double bond migration to yield the desired product as shown in Figure 2.4.

University of Cape Town

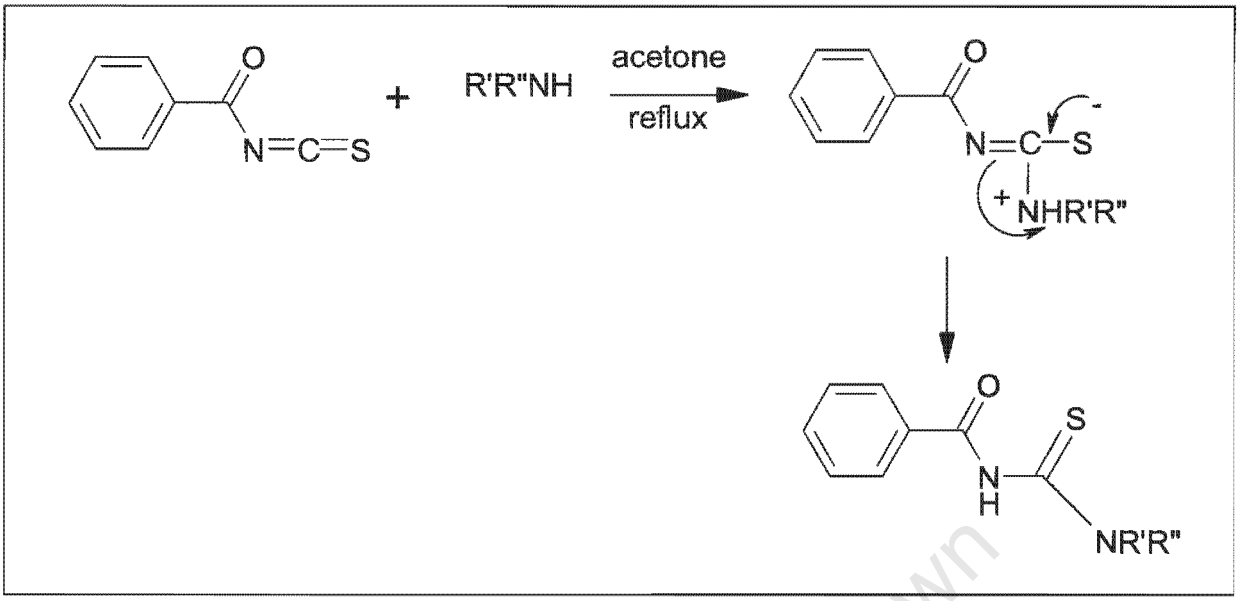

Figure 2.4 Proposed reaction mechanism of benzoylisothiocyanate with a secondary amine[107]

Characterisation of these ligands was by means of ^{1}H NMR, ^{13}C NMR, micro-analysis, mass spectrometry as well as melting point determination. The downfield aromatic resonances in the proton NMR spectra of the ligands give the expected multiplicities and integrations making assignments easy. Using a two dimensional proton-carbon correlation NMR technique known as heteronuclear single quantum coherence (HSQC) spectroscopy, the assignment of the carbon aromatic resonances is possible. In the case of HL', limited separation of the carbon resonances did not allow for unambiguous assignment of all the ring carbons. Both the proton and carbon spectra show that in HL' and HL the alkyl side chains gives rise to two sets of resonances (Figure 2.5). This can be explained by restricted rotation around the amine / thiocarbonyl bond. The thiocarbonyl and acyl carbons of HL and HL' give rise to peaks in the ^{13}C spectrum which agree well with what has previously been found for similar acylthioureas[108]. The ^{1}H shifts of HL generally compare well with that reported by Koch *et al.*[109] despite having used d_6-acetone in this study rather than d_6-DMSO as used by Koch *et al.* The only significant deviation from the literature values arises from the hydroxy protons whose shifts are very sensitive to the solvent used.

University of Cape Town

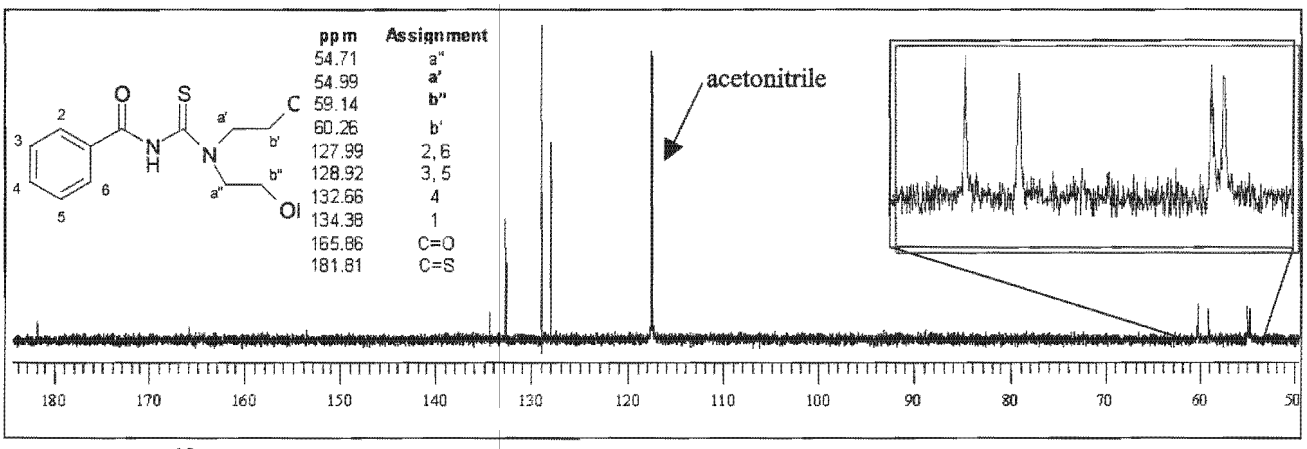

Figure 2.5 ^{13}C NMR spectrum of HL in d_3-acetonitrile showing assignments and expansion of the 55 ppm – 65 ppm region to illustrate restricted rotation of the alkyl side chain

The mass spectra of the two acylthiourea ligands shown in Figure 2.6 confirm the MH^+ ion but also indicate that, even in the mild conditions of electrospray mass spectrometry, these molecules decompose with some ease, particularly HL. At a cone voltage of 30 volts, HL' is the dominant species (m/z = 379) and upon increasing the cone voltage to 40 volts, which represents harsher conditions, a second main species, which is likely to be protonated tetraethyldiethylenetriamine (Figure 2.7 (A)), is evident (m/z = 216).

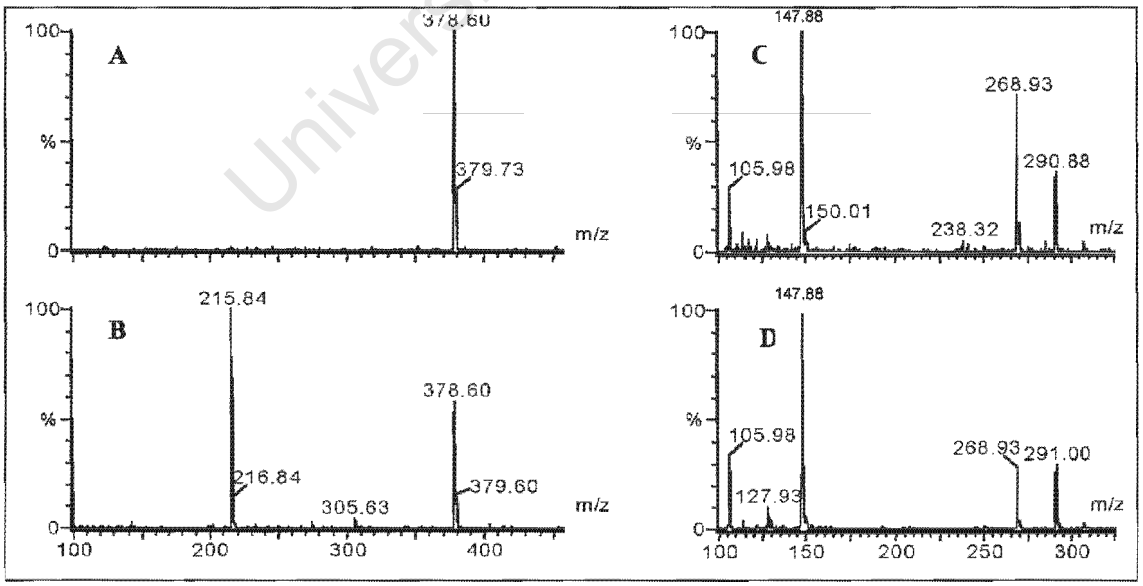

Figure 2.6 Mass spectra of (A) HL' (m/z = 379) with cone voltage = 30V; (B) HL' with cone voltage = 40V; (C) HL (m/z = 269) with cone voltage = 30 V; (D) HL with cone voltage = 40V

University of Cape Town

At a cone voltage of 30 volts, HL already shows many smaller fragments present, the dominant species with a m/z of 148, probably being a result of the cleavage of the thiocarbonyl carbon – amide bond as shown in Figure 2.7 (B). An increase of cone voltage to 40 volts resulted in greater intensities of peaks representing the fragments compared with intensity of the parent ion peak. The species represented by 291 m/z is probably due to the presence of HL Na^+.

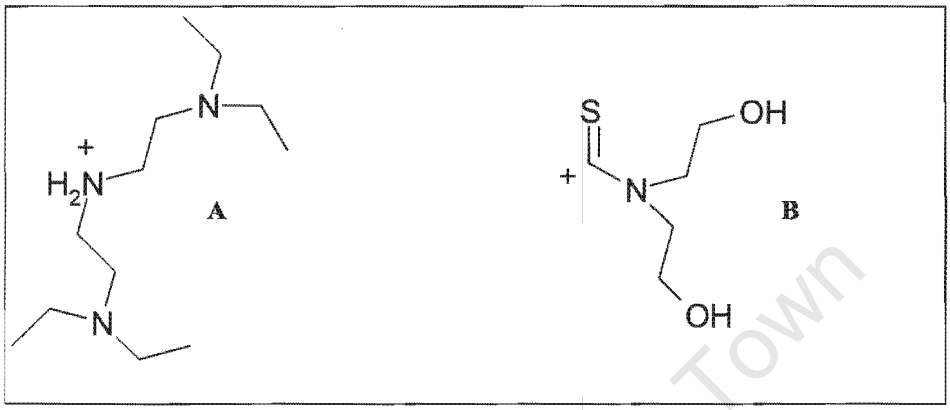

Figure 2.7 Structures of the likely decomposition fragments from (A) HL' and (B) HL

2.3 4,4'-ditertiarybutyl-2,2'-bipyridine

Of all the diimines that were required in this project, dtbbipy was the only one which was not commercially available and had to be synthesised. The synthesis was carried out in accordance with Hadda *et al.*[110] and while yielding the desired product, did so in a low yield (18%). The synthesis involved the carbon-carbon coupling of two 4-tertiarybutylpyridine molecules in the presence of a palladium catalyst suspended on charcoal (Figure 2.8).

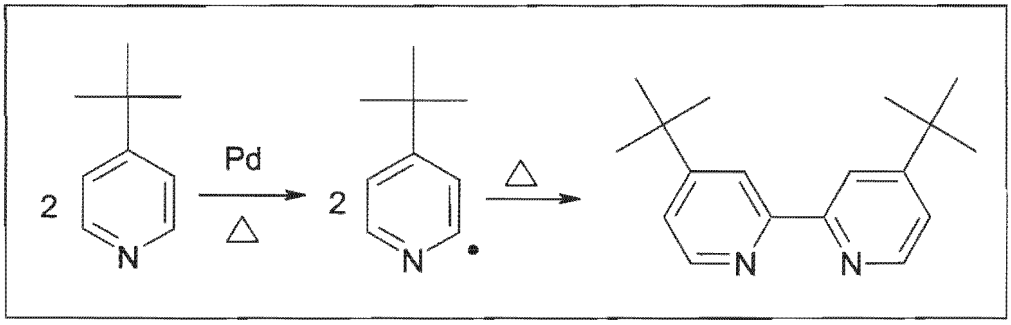

Figure 2.8 Reaction scheme of palladium mediated self condensation of 4-tertiarybutyl-2-pyridine

The catalyst was activated by degassing at 180 °C for 8 hours to remove both water and oxygen. The mixture of catalyst and reagent was then heated at 190 – 200 °C for 6 days under

University of Cape Town

nitrogen. The literature prescribed refluxing; however, this was not feasible with the equipment available and probably contributed to the low yield. The purification stages detailed in section 6.3.1 were concluded with sublimation of the product to exclude both the starting material and 4,4',4"-tritertiarybutyl-2,2',2"-tripyridine. Recrystallisation then yielded the pure ligand.

Characterisation of the diimine was by means of melting point, elemental analysis, ^{1}H and ^{13}C NMR as well as mass spectrometry. All experimental results compared well with those expected and with established values in the literature. Two dimensional carbon-proton correlation NMR (HSQC) was used in assignment of the ^{13}C NMR spectrum. The very sharp melting point of 159°C indicates excellent purity of the ligand.

2.4 Pt(diimine)Cl_2 complexes

This series of complexes was synthesised according to the general method of Morgan *et al.* [111] in which 1 mol equivalent of diimine is added to K_2PtCl_4 in acidified (HCl) aqueous solution and refluxed for two hours yielding a precipitate which was yellow in all cases except for Pt(5-Cl phen)Cl_2 which was orange. Filtration and washing with water yielded a pure product in high yields (80-97%). Figure 2.9 gives an overall scheme for the reaction as well as the structures of the various diimines utilised.

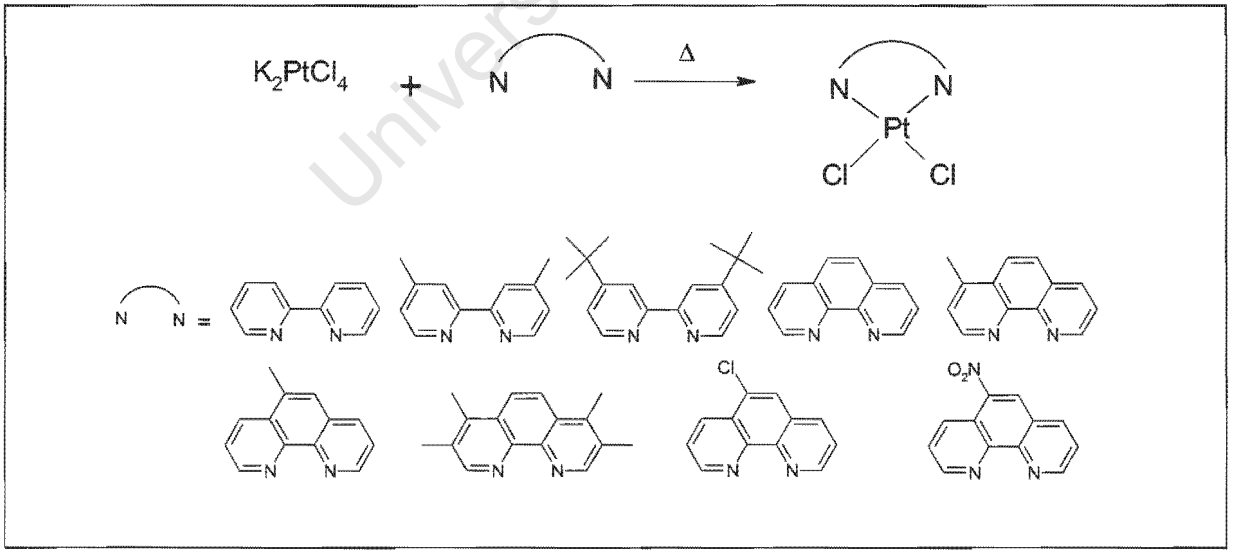

Figure 2.9 Reaction scheme for the synthesis of Pt(diimine)Cl_2 and structures of the diimines used

The insolubility of these complexes posed problems for their characterisation. Since these complexes were intermediates and their synthesis was straight forward only elemental analysis

University of Cape Town

was used to confirm that the required product had formed (Table 2.2). They all showed no visible change upon heating to 330 °C and hence no melting or decomposition temperatures are recorded.

Table 2.2: Elemental analysis (CHN) for Pt(diimine)Cl_2 complexes with experimental and calculated values reported.

Compound	%C exp.	%C calc.	%H exp.	%H calc.	%N exp.	%N calc.
Pt(bipy)Cl_2	28.37	28.44	1.70	1.90	6.39	6.64
Pt(diMebipy)Cl_2	32.36	32.00	2.59	2.69	6.11	6.22
Pt(dtbbipy)Cl_2	41.00	40.46	4.18	4.53	5.10	5.24
Pt(phen)Cl_2	32.34	32.29	1.56	1.81	6.05	6.29
Pt(4-Me phen)Cl_2	34.07	33.93	1.97	2.19	6.05	6.09
Pt(5-Me phen)Cl_2	34.30	33.93	1.98	2.19	6.00	6.09
Pt(3,4,7,8-tetraMe phen)Cl_2	38.25	38.26	3.11	3.21	5.41	5.58
Pt(5-Cl phen)Cl_2	30.31	29.99	1.27	1.47	5.71	5.83
Pt(5-NO_2 phen)Cl_2	29.82	29.34	1.16	1.44	8.33	8.55

University of Cape Town

2.5 [Pt(diimine)acylthiourea]Cl complexes

Preparation of this class of compounds has been previously published[97] using different acylthioureas and anions. The reactions proceeded smoothly with the dropwise addition of the acylthiourea dissolved in the solvent used for the reaction, to the required Pt(diimine)Cl_2 complex. The reactions were carried out between 60-80 °C without the need for an inert atmosphere. A suitable base was added after two hours to deprotonate the acylthiourea. In the case of HL', no additional base was required as the amines in the pendant side chains of the acylthiourea were found to be sufficiently basic. In the case of HL, either isopropyl amine or triethylamine gave good results except in the case of Pt(5-NO_2 phen)Cl_2 *.

* A rapid reaction between Pt(5-NO_2-phen)Cl_2 and isopropyl amine was found to take place yielding an intense purple solution. This chemistry was not further investigated as it was outside of the scope of this dissertation but this platinum complex could find application as an indicator.

In the synthesis of these complexes, acetonitrile, DMF and acetone were used as solvents, depending on the solubilities of the Pt(diimine)Cl_2 intermediates as well as the final complexes. The solvent which resulted in the best solvation of the reactants and most complete precipitation of the products was used in each case. The proposed reaction mechanism is outlined in Figure 2.10.

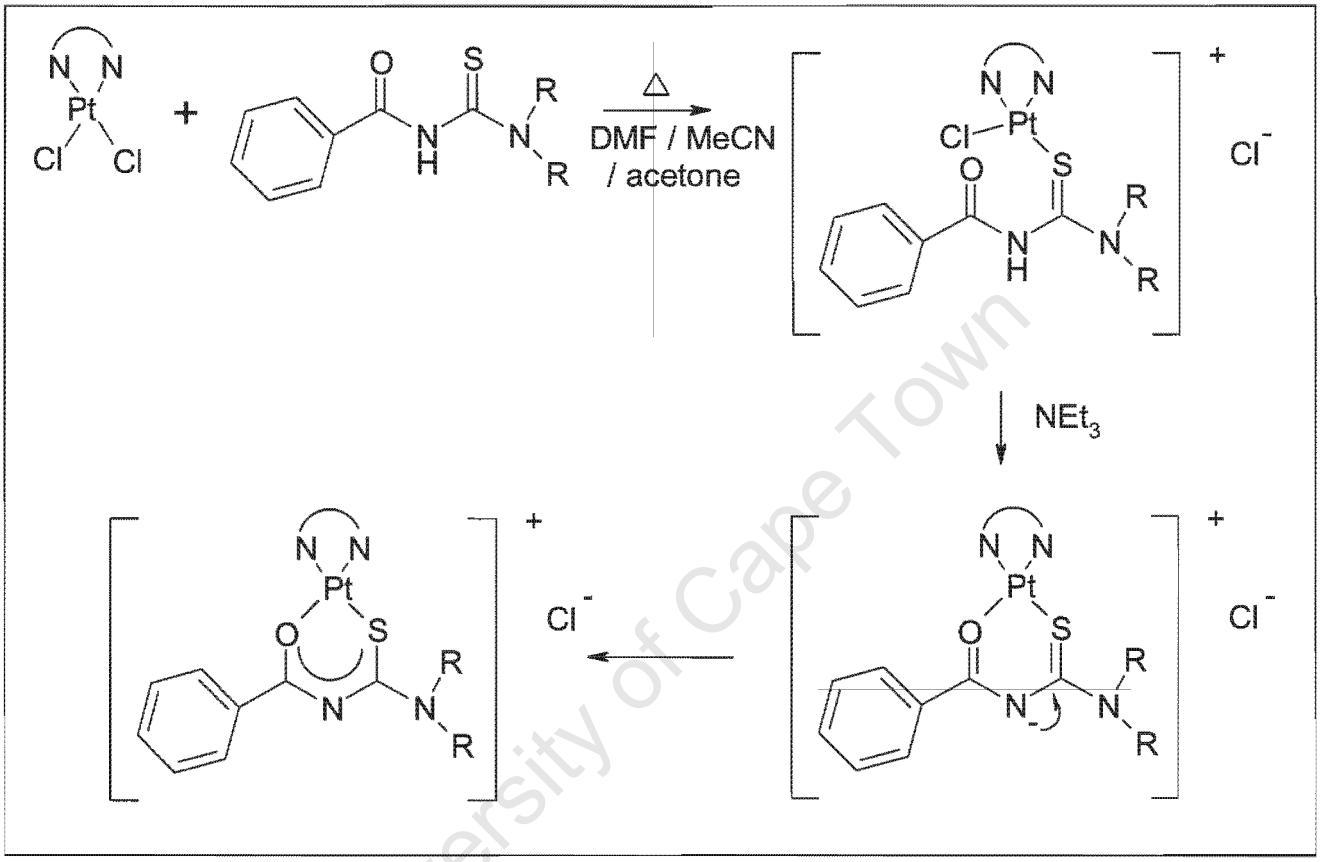

Figure 2.10 Reaction scheme for the synthesis of [Pt(diimine)acylthiourea]$^+Cl^-$ from Pt(diimine)Cl_2 and acylthiourea

University of Cape Town

The use of the asymmetrical diimines 4-methyl-1,10-phenanthroline, 5-methyl-1,10-phenanthroline, 5-chloro-1,10-phenanthroline and 5-nitro-1,10-phenanthroline gives rise to a further complexity in providing two possible isomers, either syn or anti in configuration. Figure 2.11 shows the two possible [Pt(4-Me phen)L]Cl isomers with the numbering scheme used in the NMR assignments. For a complex to be syn, the sulphur atom in the acylthiourea must be *cis* to the side of the 1,10-phenanthroline containing the methyl group.

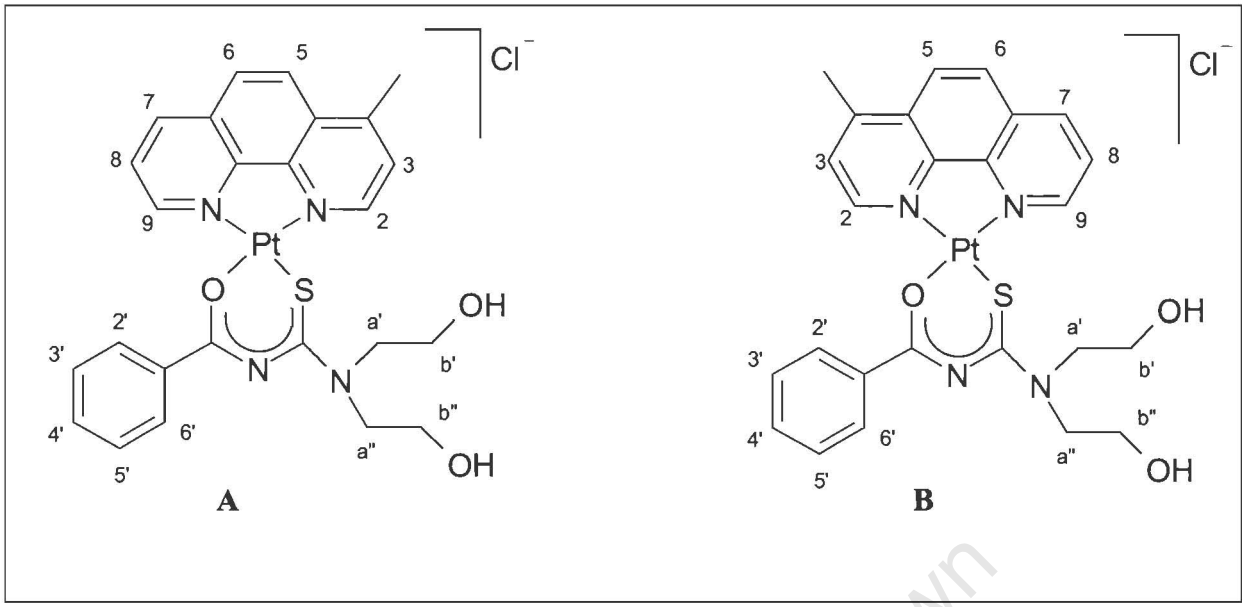

Figure 2.11 Structure and numbering of (A) syn-[Pt(4-Me phen)L]Cl and (B) anti-[Pt(4-Me phen)L]Cl

University of Cape Town

Purification of the [Pt(diimine)acylthiourea]Cl complexes was achieved by filtration of the crude product from the reaction followed by washing with acetonitrile to remove salts formed from deprotonation of the acylthiourea as well as other soluble by-products. The recovered precipitate was dissolved in methanol. Any starting material remained insoluble and was removed by centrifugation. The volume of the methanol solution was reduced under vacuum and acetonitrile was added to aid precipitation of the desired product. The volume of mixed solvent was then further reduced under vacuum with the preferential loss of methanol. The product was filtered and washed with acetonitrile followed by ether and then the yellow powder was dried under vacuum. No feasible way of separating the two isomers of the product, where these arose due to the use of asymmetrical diimines, was found. Characterisation was thus performed on the mixtures of these isomers.

Characterisation of these molecules was by means of elemental analysis, melting point / decomposition temperature determination, ^{1}H NMR and mass spectrometry. The elemental analysis of these complexes showed, particularly in the case of the various substituted phenanthroline complexes and [Pt(bipy)L']Cl, that they are hydrophilic and have waters of hydration associated with them despite attempts to dry them under vacuum over anhydrous phosphorus pentoxide for periods of up to a week.

These complexes were all observed to decompose upon melting when heated (Table 2.2). [Pt(diMebipy)L]Cl has an unusually high melting range compared to the rest of the series. This compound is also more insoluble than the rest of the series in aqueous and acetonitrile/aqueous solvent mixtures and perhaps these two phenomena are linked. It is also observed that compounds that contain mixtures of isomers have a depressed melting range. The complex, [Pt(5NO_2-phen)L]Cl, which was the most difficult to synthesise due to decomposition of the product during synthesis reflects its lower stability in the melting range. Finally, by substituting HL (m.p. 120-121 °C) with HL' (m.p. 98-99 °C) the melting range of the resulting [Pt(bipy)acylthiourea]Cl is significantly reduced.

Table 2.2 Decomposition temperatures of [Pt(diimine)acylthiourea]Cl complexes

Compound	**Decomposition temperature**
[Pt(bipy)L]Cl	206-207 °C
[Pt(diMebipy)L]Cl	223-225 °C
[Pt(dtbbipy)L]Cl	206-208 °C
[Pt(phen)L]Cl	209-210 °C
[Pt(4-Me phen)L]Cl	195-197 °C
[Pt(5-Me phen)L]Cl	194-196 °C
[Pt(3,4,7,8-tetraMe phen)L]Cl	203-205 °C
[Pt(5-Cl phen)L]Cl	192-194 °C
[Pt(5-NO_2 phen)L]Cl	182-183 °C
[Pt(bipy)L']Cl	169-171 °C

University of Cape Town

The mass spectra of these complexes gave the predicted M^+ values but also show higher aggregates including dimers and in certain cases, trimers. This is unsurprising as these [Pt(diimine)acylthiourea]Cl complexes have been shown to self aggregate in acetonitrile-water mixed solvent systems[97]. In Figure 2.12 is the mass spectrum of [Pt(diMebipy)L]Cl. The insert shows an enlargement of the 1280-1350 m/z region, showing clearly the existence of a dimer, albeit in a far lower concentration than the parent ion. The dimer peak at 1327 m/z probably arises rise from the $[Pt(diMebipy)L]_2Cl^+$ species while the peak at 1292 m/z correlates to exactly double the value of the parent ion (646 m/z). What is also evident is that the platinum complex is far more robust than HL from the very low concentration of decomposition

fragments seen in Figure 2.12 compared with Figure 2.6 of HL. This shows that the chelation of the platinum(II) stabilises this acylthiourea.

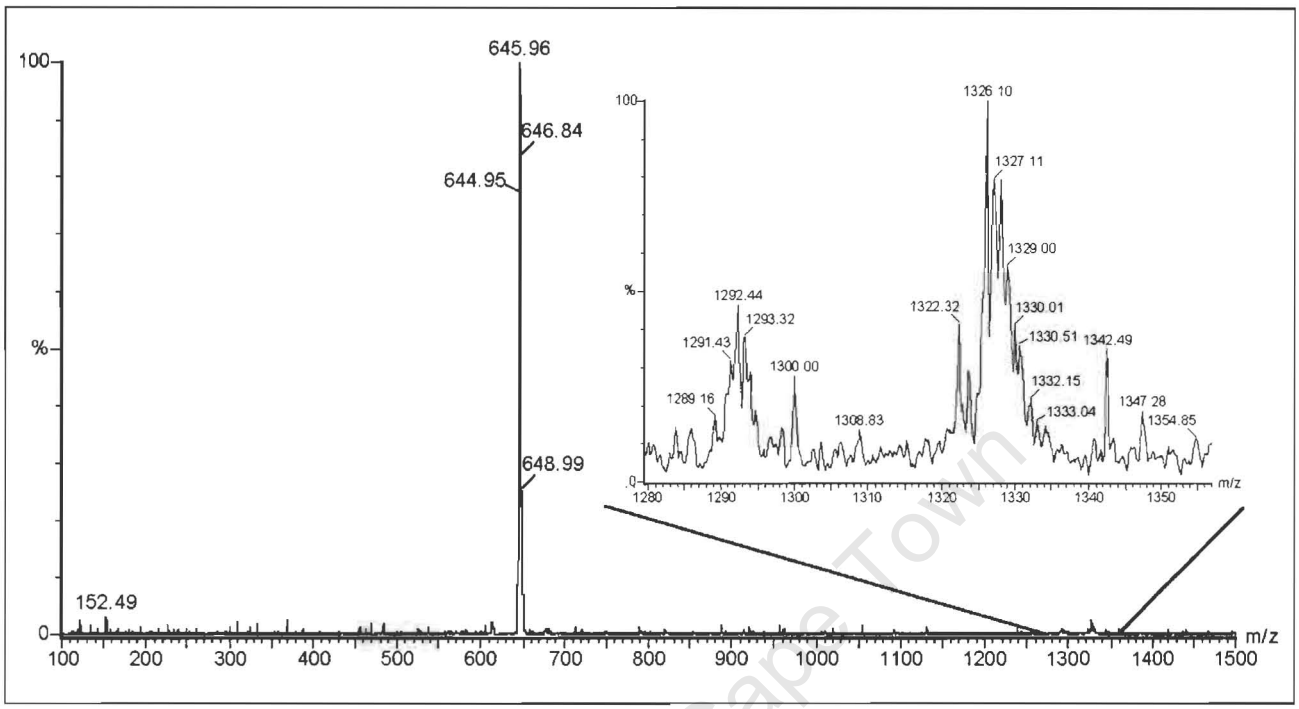

Figure 2.12 Mass spectrum of [Pt(diMebipy)L]Cl showing expansion of region 1280 – 1350 m/z

The ^{1}H NMR spectra of these [Pt(diimine)acylthiourea]Cl complexes proved the most useful but also complex to interpret. Two dimensional spectroscopy, COSY was used extensively in assignment of the protons. The chemical shifts between one dimensional NMR and COSY do not correlate well in this chapter as the reference points were not correctly set and only the one dimensional spectra could be re-referenced due to technical limitations regarding this procedure when applied to COSY spectra. The incorrect referencing of the two dimensional spectra does not otherwise affect the data.

Figure 2.13 shows 3 systems of protons, A, B and C for [Pt(phen)L]Cl which will be used as an exemplar for the [Pt(diimine)acylthiourea]Cl series. The assignments of A, B and C will be dealt with separately.

University of Cape Town

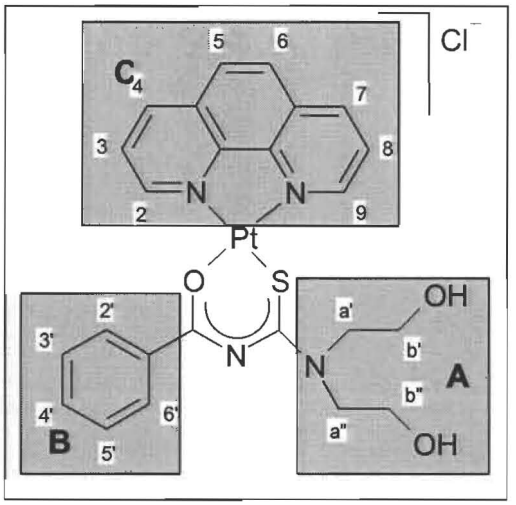

Figure 2.13 The structure of [Pt(phen)L]Cl detailing the 3 systems of protons

The most easily assigned of the three groups of protons are the acylthiourea side chains, A. In the case of HL, the side chain gives rise to four triplets from the four $-CH_2-$ groups. The hydroxy protons undergo rapid exchange, compared to the NMR time-scale, with D_2O, which comprises half the solvent and hence are not observed. In some cases the triplets overlap making the spectrum more problematic to interpret, but by using COSY, and examining peak intensity "stealing" in the 1-D spectrum they remain straight forward to assign. One assumption had to be made and that was the assignment of $H_{b"}$ as the most up-field of the four triplets. This assumption has previously been made and justified in the assignment of protons in the related complex PtL_2 [109]. Figure 2.14 shows the COSY spectrum of the region in which the protons labelled as A in Figure 2.13 of [Pt(phen)L]Cl resonate. It can be seen from this spectrum that $H_{b"}$ is coupled to one of the two protons in the 3.40–3.50 ppm region. It is not clear from this spectrum alone, with which peak it is coupled. It is however evident that $H_{b"}$ is not coupled with the peak at 3.64 ppm. Upon inspection of Figure 2.15 it can be seen that $H_{b"}$ is not coupled with the triplet closest to it at 3.54 ppm. If $H_{b"}$ were coupled to this peak, it would be evident from the right hand side of the triplet since it would have an increased magnitude. Thus it is possible to assign $H_{b"}$ and $H_{a"}$ and in the same way, also assign $H_{a'}$ and $H_{b'}$. Since there are four peaks representing the $-CH_2-$ groups, each group must be in a different electronic environment as was the case with the uncomplexed ligand, again strongly suggesting partial double bond character of the amine / thiocarbonyl bond.

The assignment of the peaks of [Pt(bipy)L'] was done in the same way. Because of water being present in the sample due to the product being highly hygroscopic, peaks close to the large

University of Cape Town

water peak were more difficult to assign as the integration was not accurate and the multiplicity was somewhat obscured.

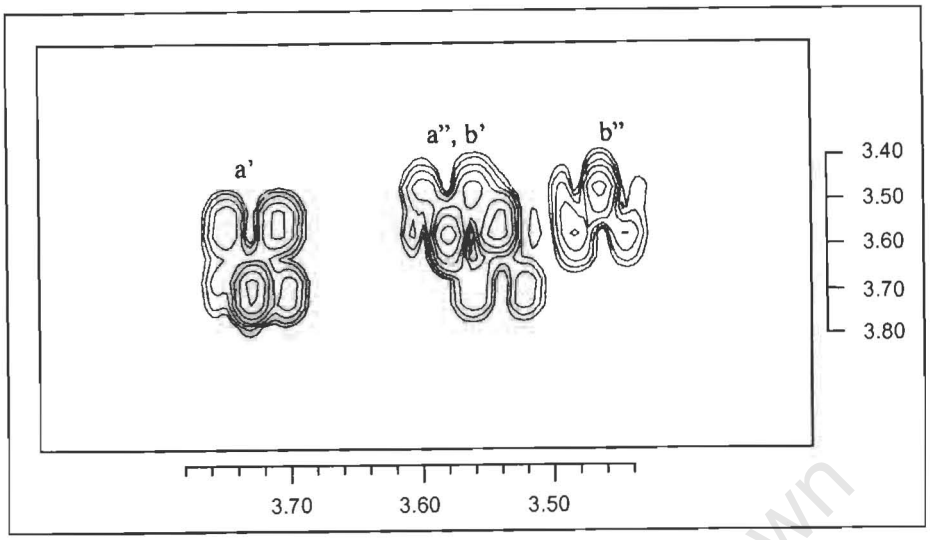

Figure 2.14 COSY spectrum of [Pt(phen)L]Cl showing peaks arising from acylthiourea pendant side chain

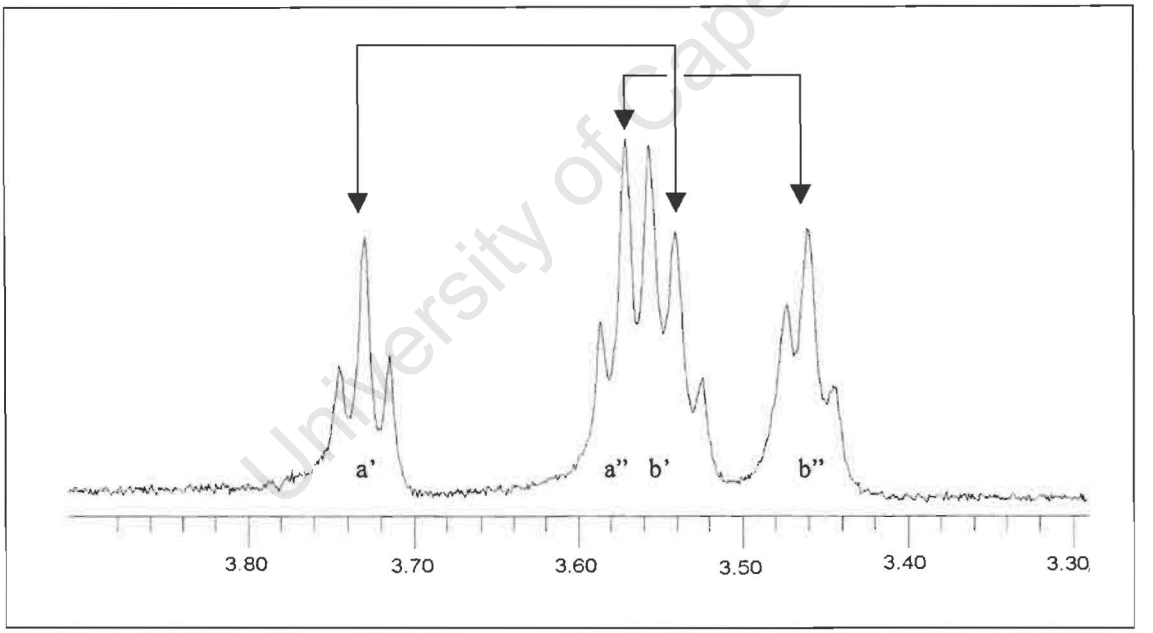

Figure 2.15 ^{1}H NMR spectrum of [Pt(phen)L]Cl showing the peaks arising from the pedant side chain of the acylthiourea.

The peaks of the protons from the B and C systems lie in the aromatic region. System B is a mono-substituted benzene ring which theoretically gives rise to a doublet of integration 2, a triplet of integration 2 and a triplet of integration 1. These peaks are all observed in Figures 2.16 and 2.17. The COSY spectrum (Figure 2.16) clearly shows the first triplet at 7.04 ppm, which arises from the equivalent protons $H_{3'}$ and $H_{5'}$, coupling to the two other peaks due to

University of Cape Town

protons $H_{2'}$ and $H_{6'}$ (6.96 ppm) and $H_{4'}$ (7.36 ppm). This coupling has been illustrated with a solid black line. The appropriate assignments are also reflected in Figure 2.17.

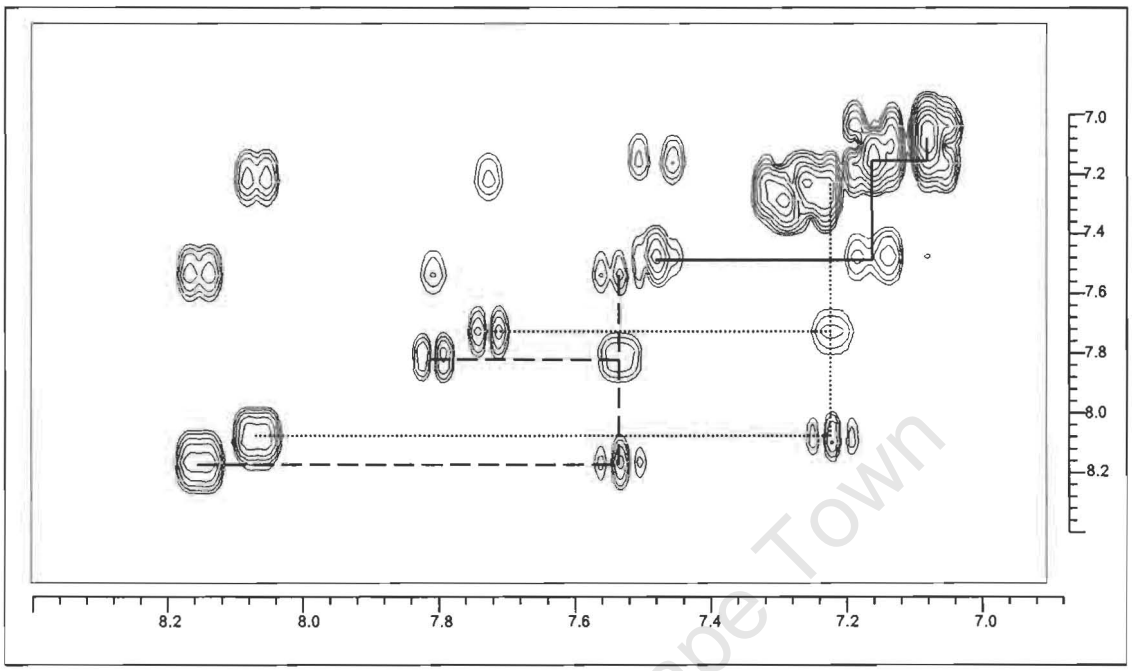

Figure 2.16 COSY spectrum of [Pt(phen)L]Cl showing the aromatic region

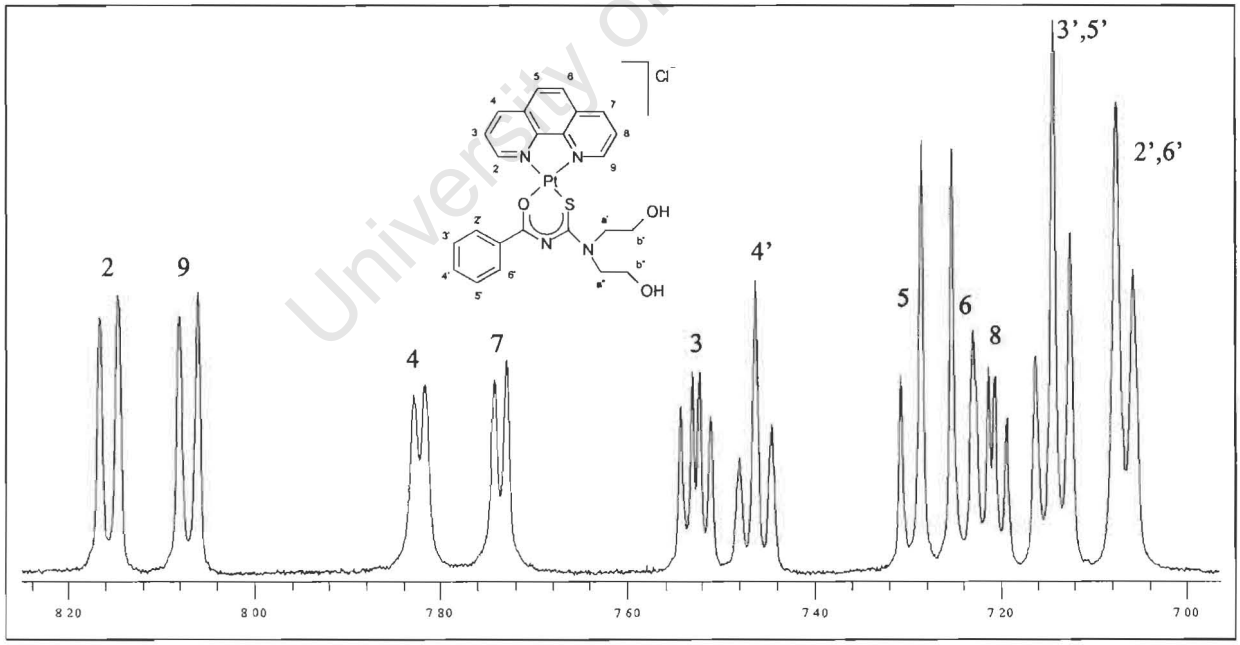

Figure 2.17 ^{1}H NMR spectrum of [Pt(phen)L]Cl showing the aromatic region with full assignments of the peaks

The assignments of the peaks in system C from 1,10-phenanthroline are based on an assumption that H_2 will be down-field of H_9. This assumption is based upon the Pt-S bond

having greater strength than the Pt-O bond as platinum is classed as a "soft" metal and sulphur, a "soft" donor. Therefore as a result of the trans-influence, the Pt-N_1 bond is weaker than the Pt-N_{10} bond resulting in more electron density being withdrawn from the ring trans to the oxygen of the acylthiourea. The reduction of electron density from this ring system will result in up-field shifts of the protons H_7, H_8 and H_9 compared with H_2, H_3, and H_4. The assignments of H_5 and H_6 are speculative and based upon a follow through of this effect. These assignments are shown in Figure 2.16 and Figure 2.17 with the COSY spectrum having illustrations added to clarify the assignments of H_3, H_4, H_7 and H_8. The ^{1}H NMR assignments of the remaining complexes of this series were made using the same reasoning and assumptions as above.

Proton NMR also allows for the assignment of configuration of isomers arising from the use of asymmetrical diimines. Looking at the peaks arising from the methyl group attached to the 1,10-phenanthroline derivatives in [Pt(4-Me phen)L]Cl and [Pt(5-Me phen)L]Cl as illustrated in Figure 2.18, allows for establishment of the ratio of isomers. From the integration of the methyl peaks, it is established that in the case of [Pt(4-Me phen)L]Cl, that the anti isomer accounts for 89% and the syn isomer, 11% of the species present. With the 5-methyl complex, a completely racemic mix is formed.

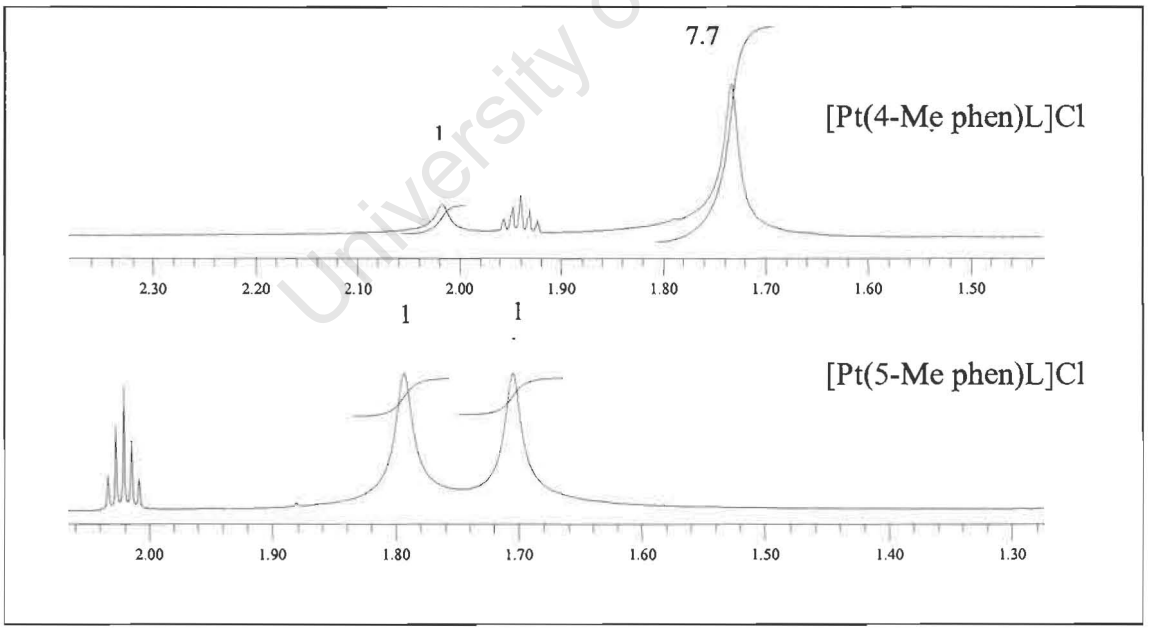

Figure 2.18 ^{1}H NMR spectra of [Pt(4-Me phen)L]Cl and [Pt(5-Me phen)L]Cl showing regions contain peaks representing methyls attached to the phenanthroline ring

Assigning each peak to its respective isomer is achieved by predictions based on the ortho/para or meta directing properties of the attached groups, which should allow assignment of the

University of Cape Town

major isomer. This is then confirmed by making predictions about the resultant peaks in the ^1H NMR and comparing these with the experimental spectra. In the case of Pt(4-Me phen)Cl_2, the methyl group increases electron density on the nitrogen that is para to it as methyl is an ortho/para director. This results in the chlorine trans to the N_1 atom being more labile due to the trans-effect causing the acylthiourea co-ordinating first to this position through the sulphur resulting in the anti isomer. This process is shown in Figure 2.19.

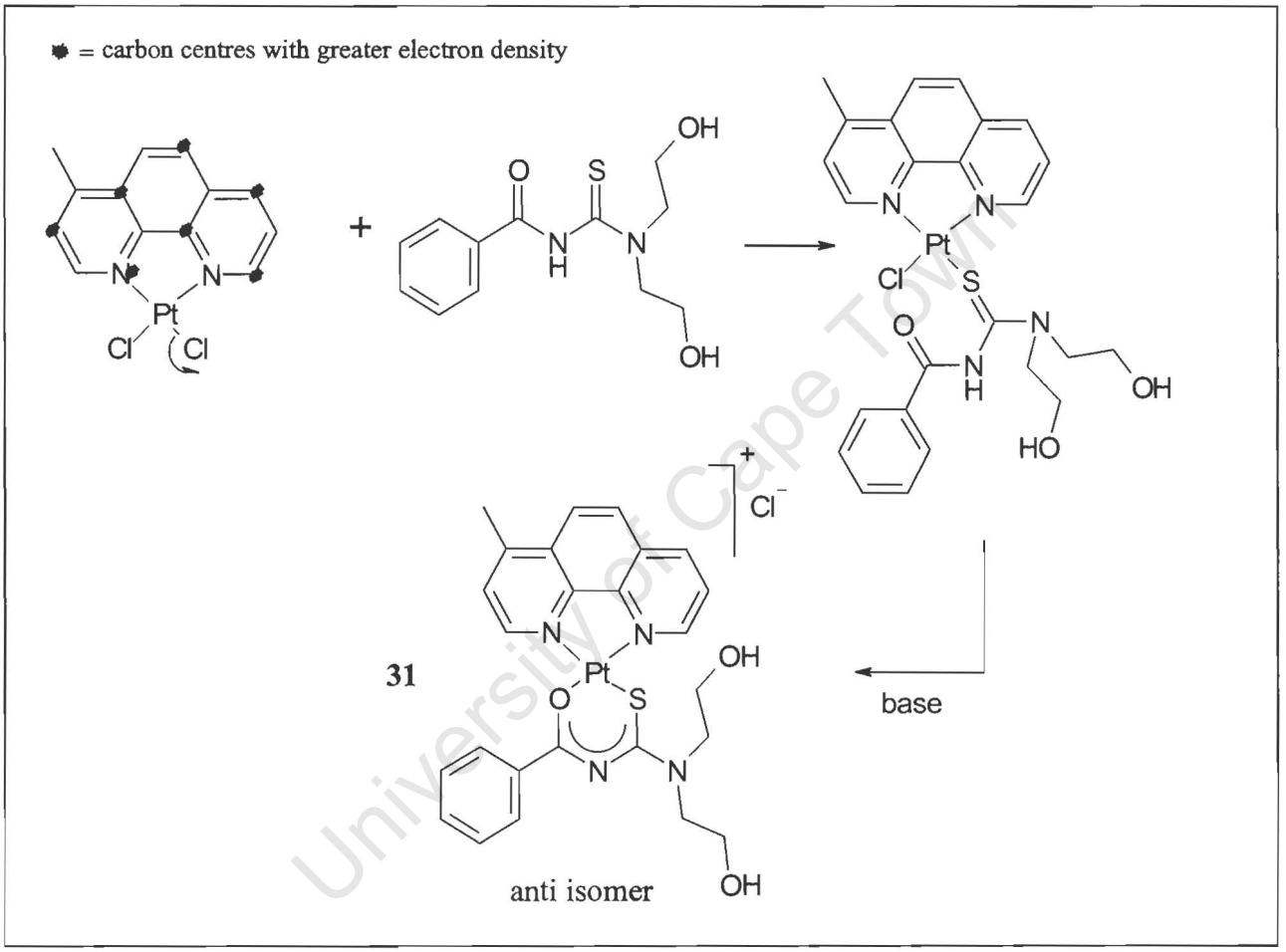

Figure 2.19 Diagram showing the electronic effect of a methyl group in the 4-methyl-1,10-phenanthroline in determining the ratio of isomers formed of [Pt(4-Me phen)L]Cl

When predicting the relative positions of peaks of protons H_2 and H_9 in the ^1H proton spectrum of the two isomers, two effects must be considered. Firstly, it has already been noted that the protons in the diimine ring trans to sulphur are shifted less up-field than the diimine ring protons *cis* to sulphur. A second effect is caused by the methyl attached to the diimine ring. From the proton spectra of *o*, *m* and *p*-methylpyridine which have been reported[112] a trend emerges that protons meta to the methyl are shifted less up-field compared to protons in the ortho or para positions[112]. When extending this rationale to the major [Pt(4-Me phen)L]Cl

University of Cape Town

isomer one would expect the H_2 proton to be shifted less up-field than the H_9 proton as the H_2 proton is meta to the methyl while the H_9 proton is effectively in a para position. Thus with these two effects combining, it is predicted that the major isomer (anti) will have a greater separation of H_2 and H_9 than in the case of the minor isomer (syn) and this indeed observed in Figure 2.20.

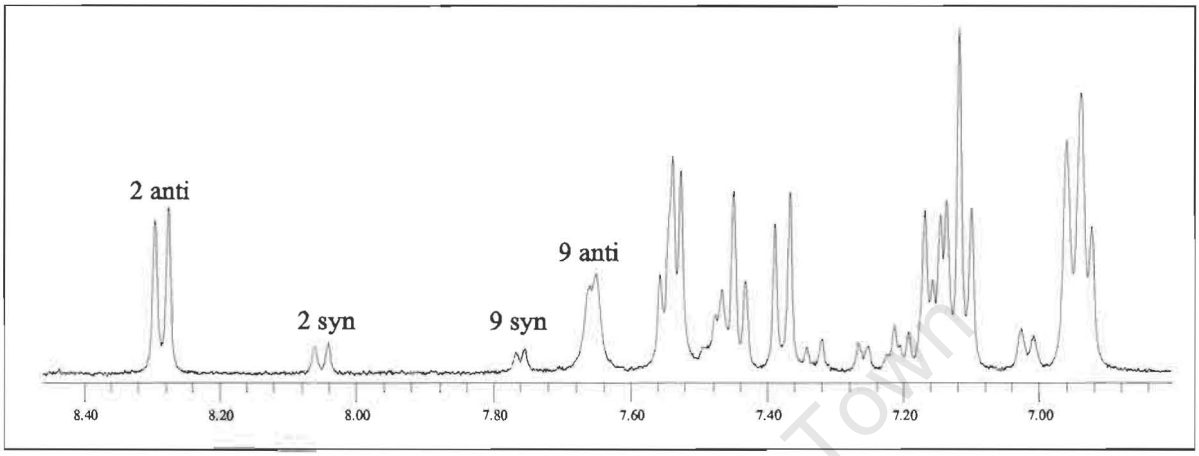

Figure 2.20 ^{1}H NMR spectrum of [Pt(4-Me phen)L]Cl showing the aromatic region and confirming the assignment of syn and anti isomers

Assigning the dominant isomer of [Pt(5-Cl phen)L]Cl and [Pt(NO_2 phen)L]Cl is done in a similar way as for the 4-methyl complex. The ortho/para directing properties of the chloro group and meta directing of the nitro group result in the anti isomer being dominant in the former and the syn isomer dominant in the latter. This gives rise to an electron density distribution as shown in Figure 2.21.

Groups that are electron withdrawing attached to 1,10-phenanthroline cause protons attached to carbons from which electrons have been withdrawn, to undergo a larger up-field shift. This is based on observations of the ^{1}H NMR spectra of 5-nitro-1,10-phenanthroline as well as o, m and p-chloropyridine[112]. This should result in the major isomer peaks of H_2 and H_9 of the 5-chloro complex and the 5-nitro complex being located closer together, with the minor isomer peaks exhibiting a greater separation. This is borne out by experimental evidence as shown by the two spectra in Figure 2.22. The numbering of the 5-nitro-1,10-phenanthroline complex now breaks with the trend for the other complexes in that H_2 is now *cis* to the sulphur of the acylthiourea as expected.

University of Cape Town

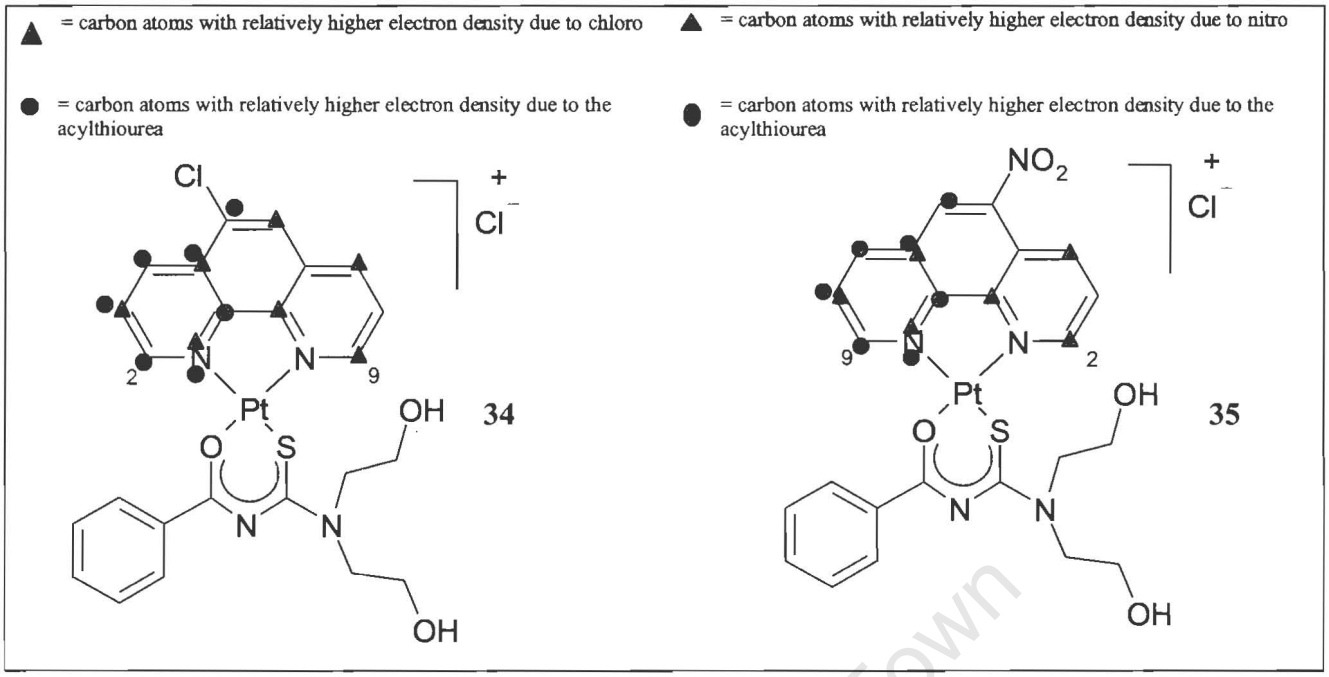

Figure 2.21 Illustration of how chloro and nitro attached to the 5 position of 1,10-phenanthroline effect the electron distribution in the diimine ring and result in formation of major isomers when complexed to Pt(II)acylthiourea.

The percentage of isomers formed for the complexes in the above figure is calculated based on the integrals of the peaks of the diimine protons of each respective isomer.

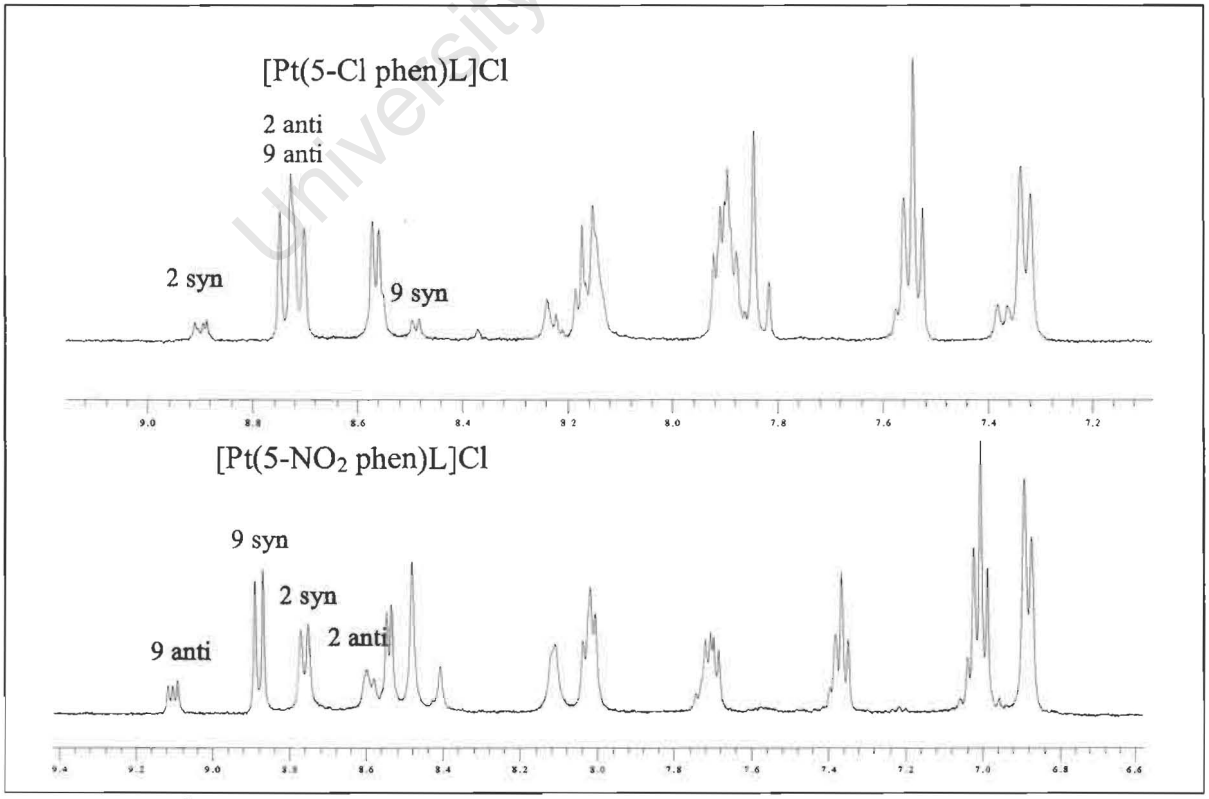

Figure 2.22 ^{1}H NMR spectra of [Pt(5-Cl phen)L]Cl and [Pt(5-NO_2 phen)L]Cl showing the aromatic region which illustrates the two isomers of each complex and confirms the assigned isomer configuration

University of Cape Town

2.6 *cis*-bis(*N*-benzoyl-*N'*,*N'*-di-2-hydroxyethylthioureato) platinum(II)

This complex was synthesised using a modification of the method of Koch *et al.*[109] where an acetonitrile-water mixture was used as a solvent system instead of a dioxane-water system. Potassium tetrachloroplatinate dissolved in water was added dropwise to 2 mol equivalents of acylthiourea and sodium acetate dissolved in acetonitrile. The reaction proceeded at 35 °C and evaporation of the acetonitrile resulted in the formation of a yellow precipitate which was centrifuged, washed and then dried at reduced pressure and ambient temperature resulting in a 78% yield. This compared favourably with the reported yield of 84% in the literature[109].

Characterisation was by means of melting point, elemental analysis, mass spectrometry and ^{1}H NMR spectroscopy. The melting point of 158-159 °C is significantly higher than the literature value of 144-146 °C. It must be noted however that the elemental analysis results reported in the literature do not correlate very closely with the calculated values whereas the elemental analysis results obtained in this dissertation are significantly better (Table 2.3). This suggests that purity of this sample is better than that of the sample used for the literature publication, and this could account for the discrepancy in melting points.

University of Cape Town

Table 2.3 Elemental analysis results for *cis*-[PtL_2]

	%C	%H	%N
Calculated values	39.50	4.14	7.68
Literature values [109]	38.8	4.1	7.0
Experimental values	39.24	3.92	7.69

The mass spectrum of *cis*-[PtL_2] using ESMS was found to be optimal in a negative ion mode with M^- at 807.34 which correlates to the complex associated with a DMSO molecule. DMSO had been added to the sample solution to assist in dissolution of the sample. The proton NMR spectrum was assigned according to the literature[109] and observed shifts compared well with those previously reported. The proton NMR spectrum clearly showed only one isomer, which has previously been shown to be in a *cis* configuration by single crystal x-ray diffraction of related complexes[109, 113]. As has been mentioned in this chapter, sulphur exhibits a *trans* influence on platinum resulting in the bond *trans* to the sulphur being weaker. By this

rationale, the thermodynamically favoured product would not have sulphur *trans* to another sulphur. The *cis* product which is the only isomer observed must then be a result of thermodynamic factors acting over kinetic factors in the overall mechanism.

2.7 Di-μ-chlorobis[2-(2-pyridinyl)phenyl-(*C,N*)]di-platinum

This intermediate product was synthesised by reacting tetrachloroplatinate with 2-phenylpyridine at 60 °C in a water-acetone solvent system for 2½ hours. The mixed solvent system allowed for solubility of both reactants. After the reaction was complete, evaporation of the acetone resulted in precipitation of the product. Although a published method was available[114], this was not followed as the starting materials required were not readily available. Figure 2.23 illustrates the overall reaction.

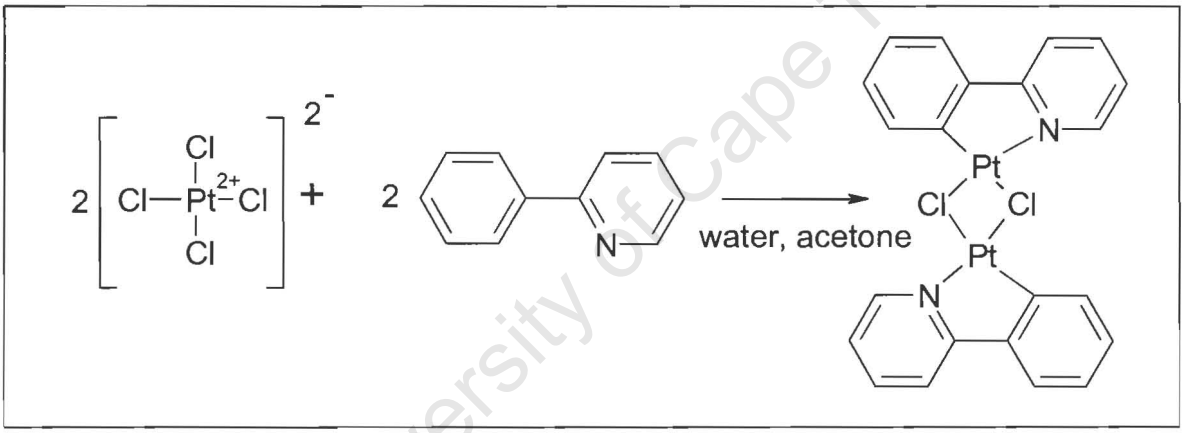

Figure 2.23 Reaction scheme for the formation of di-μ-chlorobis[2-(2-pyridinyl)phenyl-(*C,N*)]di-platinum

University of Cape Town

Characterisation was primarily by means of elemental analysis which confirmed the presence of the product. The hydrogen and nitrogen values agreed well with the calculated values while the carbon experimental value was 35.10% compared with the calculated value of 34.34% indicating a small impurity. The published method[114] reported a decomposition of the product at 275 °C. When establishing a melting point in this work it was found that the product gradually decomposed over a wide temperature range (180 – 300 °C) from yellow translucent crystals to a dark powder.

2.8 *N*-benzoyl-*N'*,*N'*-bisdiethylaminoethylthioureato-(*O*,*S*)(2-phenylpyridine) platinum(II)

Preparation of this complex was achieved by addition of two mol equivalents of acyl thiourea, HL, dissolved in acetonitrile to a solution of $(Pt(ppy)Cl)_2$ which was then heated at 60 °C for an hour. No additional base was required for formation of the product as the amines in the pendant side chain of the acylthiourea acted as a base to deprotonate the nitrogen bonded to the acyl group. The reaction was monitored using TLC and showed a spot to spot conversion after 30 minutes. The product was precipitated by addition of diethyl ether and HCl; the latter was required to protonate the side chain of the acylthiourea. The mechanism involved in the formation of the product is not known and was not investigated. Based on the proton NMR spectrum (Figure 2.24) only one isomer was formed. This isomer is most likely to be *syn* as the chloride trans to the platinum-carbon bond in $(Pt(ppy)Cl)_2$ is more labile than the chloride trans to the platinum nitrogen bond due to the trans effect. Thus the sulphur will coordinate trans to the platinum-carbon bond.

The product showed interesting behaviour in aqueous solution, first forming a clear solution and then became milky, possibly indicating extensive aggregation. Addition of acid to the solution resulted in disappearance of the fine suspended precipitate.

Characterisation of the product was by means of melting point, elemental analysis, mass spectrometry and proton NMR spectroscopy. Elemental analysis results showed that the product had been isolated in a hydrated state as the di-hydrochloride salt which is unsurprising considering HCl was added to assist precipitation of the product. Mass spectrometry confirmed the presence of the parent ion with M^+ at 727.49 m/z with the calculated value being 727 m/z. The melting (decomposition) point of 217-219 °C is significantly higher than that of the related [Pt(bipy)L']Cl complex possibly indicating greater intermolecular interactions or greater thermal stability of the complex. Finally, the proton NMR spectrum was assigned in a way analogous to the assignment of [Pt(bipy)L']Cl, with the assistance of a COSY spectrum. The proton spectrum of Pt(ppy)L' is shown in Figure 2.24. Satellites from $H_{6'}$ coupling to platinum

University of Cape Town

are now evident due to a formal covalent platinum carbon bond. This assists in the assignment of the proton spectrum by defining $H_{6'}$.

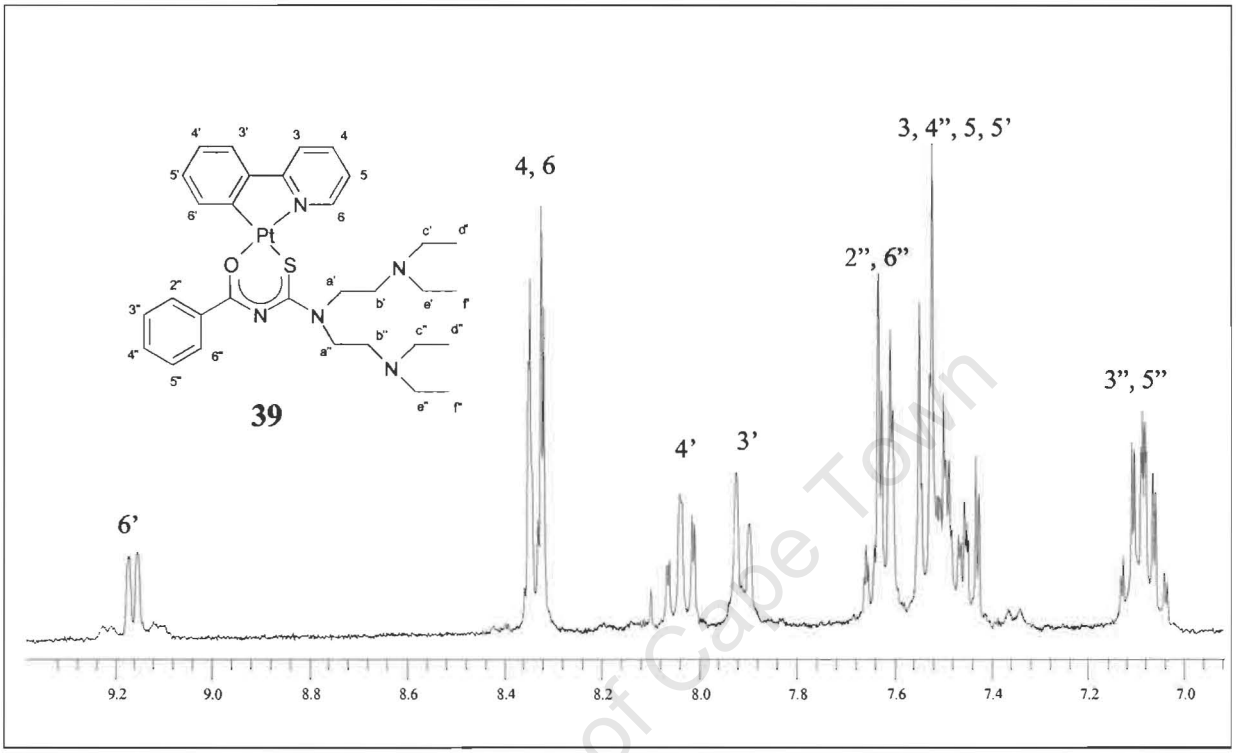

Figure 2.24 ^{1}H NMR spectrum of Pt(ppy)L' showing aromatic region with assignments

2.9 Gallium(III)protoporphyrin IX chloride

Synthesis of Ga(III)PPIX was achieved by modifying a synthesis used by Coutsolelos *et al.*[115] to synthesise chloro-(porhyrinato) gallium(III). A gallium(iii) solution was prepared by dissolving gallium chloride in 1 M hydrochloric acid and this was added to a solution of protoporphyrin IX dissolved in acetic acid. Excess sodium acetate was added to the solution followed by sufficient sodium hydroxide to neutralise the hydrochloric acid. The solution was heated under reflux and was monitored by visible spectroscopy. Figure 2.25 shows the visible spectrum at various times during the synthesis. Bands at 508nm and 630nm are shown to disappear upon formation of the product. After the reaction was quenched, the product was precipitated with addition of diethyl ether, then filtered, washed and dried.

University of Cape Town

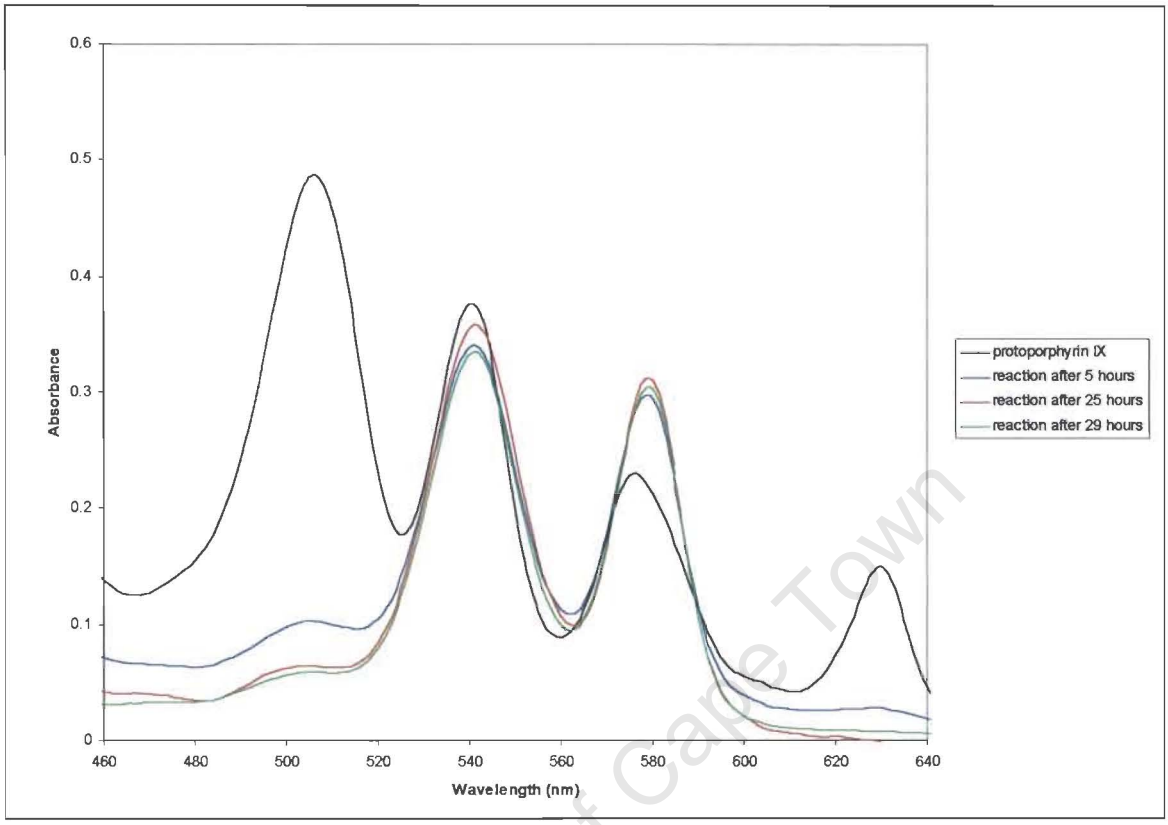

Figure 2.25 Visible spectra of reaction mixture during the synthesis of Ga(III)PPIX

Characterisation of Ga(III)PPIX was primarily by means of elemental analysis for carbon nitrogen and hydrogen which closely matched calculated values for the monohydrate. It was found that the product did not melt or visibly decompose upon heating to 330 °C. Solution based analysis revealed interesting behaviour of the product. The compound was synthesised as a model molecule for paramagnetic Fe(III)PPIX for ^{1}H NMR experiments in Chapter 5. However the ^{1}H NMR spectrum (Figure 2.26) was very broad with the solvent peak and water peak dominating the spectrum. Elevating the temperature and addition of pyridine did not improve the spectrum.

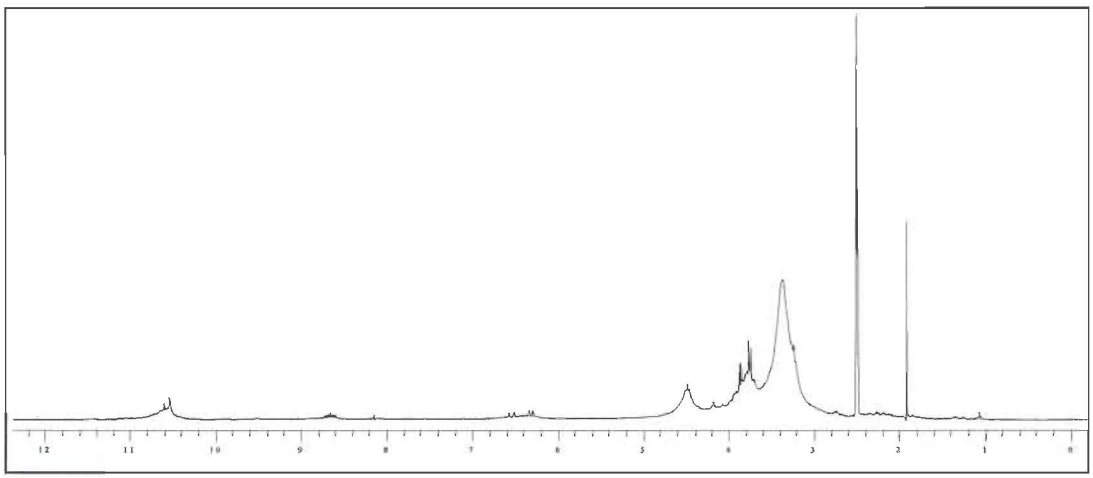

Figure 2.26 ^{1}H NMR spectrum of Ga(III)PPIX

University of Cape Town

Mass spectrometry gives added insights into the phenomenon observed in the NMR spectrum. In Figure 2.27, the mass spectra for Ga(III)PPIX, Fe(III)PPIX and Zn(II)PPIX are shown. The Fe(III)PPIX spectrum shows two main peaks representing Fe(III)PPIX and Fe(III)PPIX-DMSO with small peaks at 1232 and 1269 probably representing dimers $Fe(III)PPIX_2^+$ and $Fe(III)PPIX_2\ Cl\ H^+$. The Zn(II)PPIX spectrum shows a greater extent of aggregation, with small peaks in the region 630 to 673 m/z probably representing doubly charged dimers and possibly triply charged trimers. However, the monomer still dominates the spectrum. In the case of Ga(III)PPIX, it is clearly evident that dimers and larger aggregates dominate the spectrum. The large number of peaks confirms that in solution, Ga(III)PPIX forms many aggregates and only a small percentage of material is in the monomeric form. This large number of aggregated forms would explain the broadness experienced in the proton NMR spectrum.

University of Cape Town

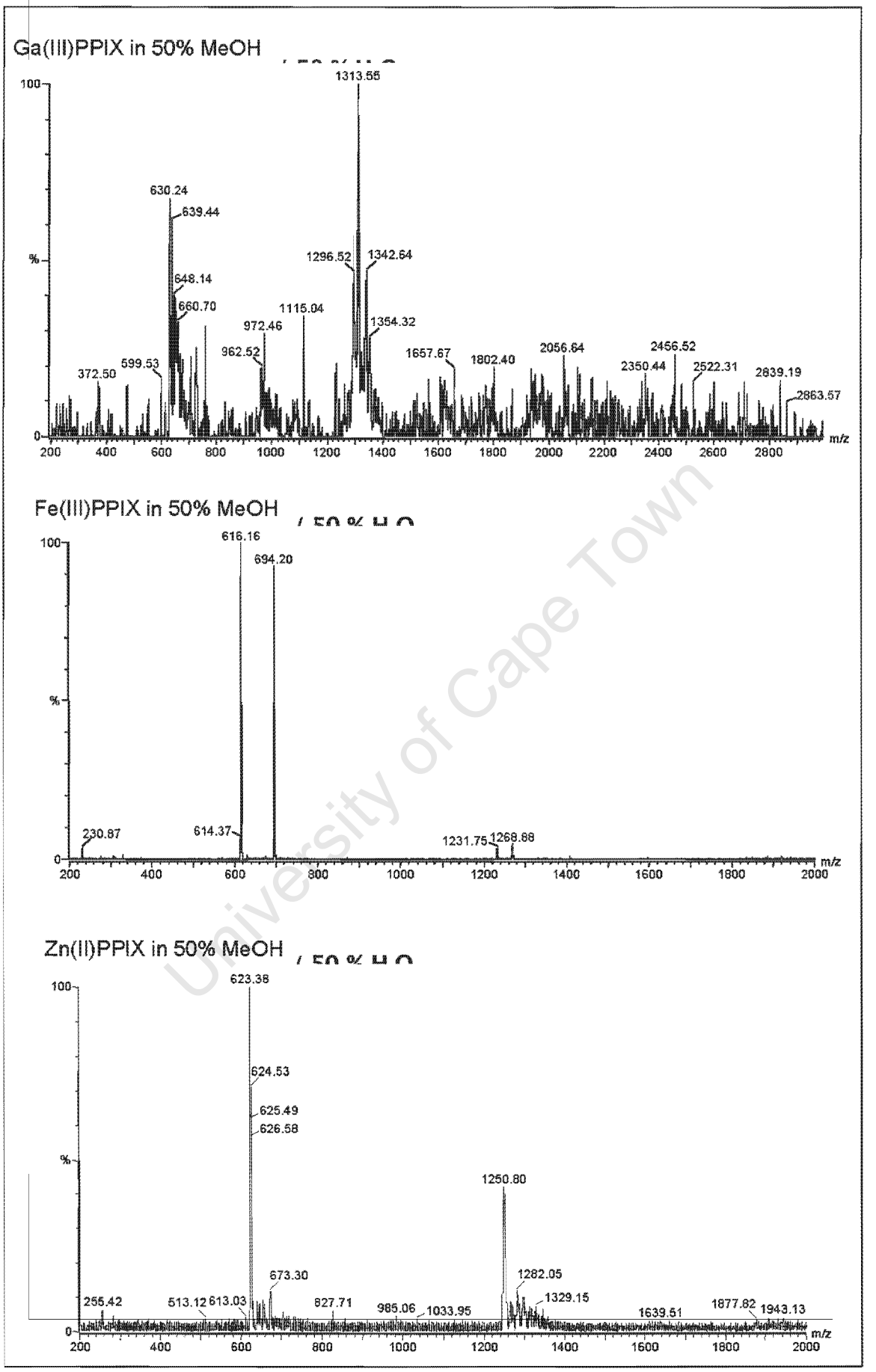

University of Cape Town

Figure 2.27 Mass spectra of Ga(III)PPIX, Fe(III)PPIX and Zn(II)PPIX illustrating extensive aggregation of the latter

3 Association of haematin with platinum complexes and corresponding ligands

3.1 A solvent system for spectrophotometric titrations

In studying the interaction of haematin with the platinum complexes described in this dissertation as well as the free ligands, a suitable solvent system must be found. One of the requirements for quantitative measurements of the interactions with haematin is that the haematin is in a monomeric form. If it were in a partially aggregated or dimeric state then energy may be required to break apart the dimer / aggregate before association with the interacting substance could take place. This obviously would lead to a change in observed ΔG of the association and hence a different log K value would result from that observed with monomeric haematin. DMSO has been found to be an excellent solvent for maintaining haematin in a monomeric state and the spectrum shown in Figure 3.1 is that of the monomeric form of Fe(III)PPIX[51]. As has been mentioned in Chapter 1.5, associations of haematin with compounds which interact with it via π-π interactions are dependent on water being present. Thus in DMSO alone only very weak associations with haematin occur and it does not mimic the environment found in the food vacuole of the malaria parasite. To use only water as a solvent is also problematic as water has been shown to cause extensive aggregation of haematin[116]. A 40% aqueous DMSO solvent system has however been found to produce essentially monomeric haematin but also allows for strong interactions of haematin with compounds which associate with it under fully aqueous conditions[51]. This system has been used extensively to study interactions of quinolines with haematin[51, 19, 117]. As acid conditions may also lead to aggregation of haematin, the system was buffered at an apparent pH of 7.5 using *N*-[2-hydroxyethyl]piperazine-*N'*-[2-ethane sulphonate] (HEPES). It has been shown that results from association studies in purely aqueous systems are comparable to those in 40% aqueous DMSO systems[19]. It must also be taken into consideration that a 40% aqueous DMSO solution represents about 10% by mol fraction. It is thus reasoned that while a 40% aqueous DMSO system may not mimic *in-vivo* conditions completely, it is none the less a good model system which has been shown to produce consistent and reasonable data.

University of Cape Town

3.2 The UV-visible spectrum of haematin

By observing changes in the UV-visible spectrum of haematin upon addition of molecules which bind to it, it is possible to quantify the interaction[51] and it is therefore important to understand the basis of the spectrum and the subsequent changes that it experiences. The uv-visible spectrum of haematin is shown in Figure 3.1 and can be seen to be rather complex with a number of bands present. The region from 450 nm to 700 nm was recorded at a higher sample concentration as the absorbances in this region are considerably weaker than in the 350 nm to 450 nm region. By deconvoluting the spectrum by fitting Gaussians to the observed spectral envelope, the individual bands giving rise to the spectrum become more obvious and these are illustrated in Figure 3.2.

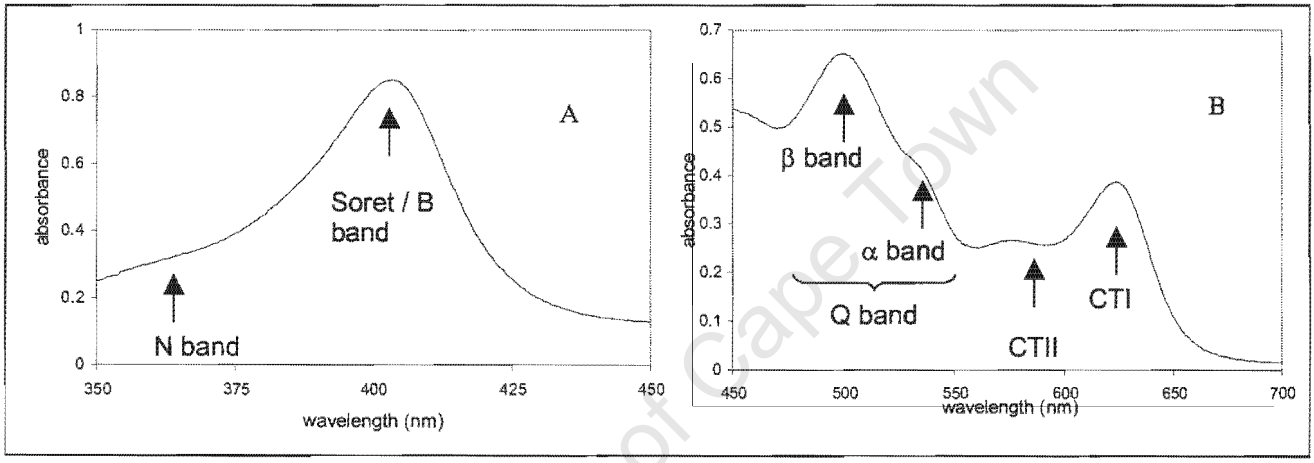

Figure 3.1 UV-visible spectrum of haematin in DMSO showing the region (A) 350 – 450 nm and (B) 450 –700 nm

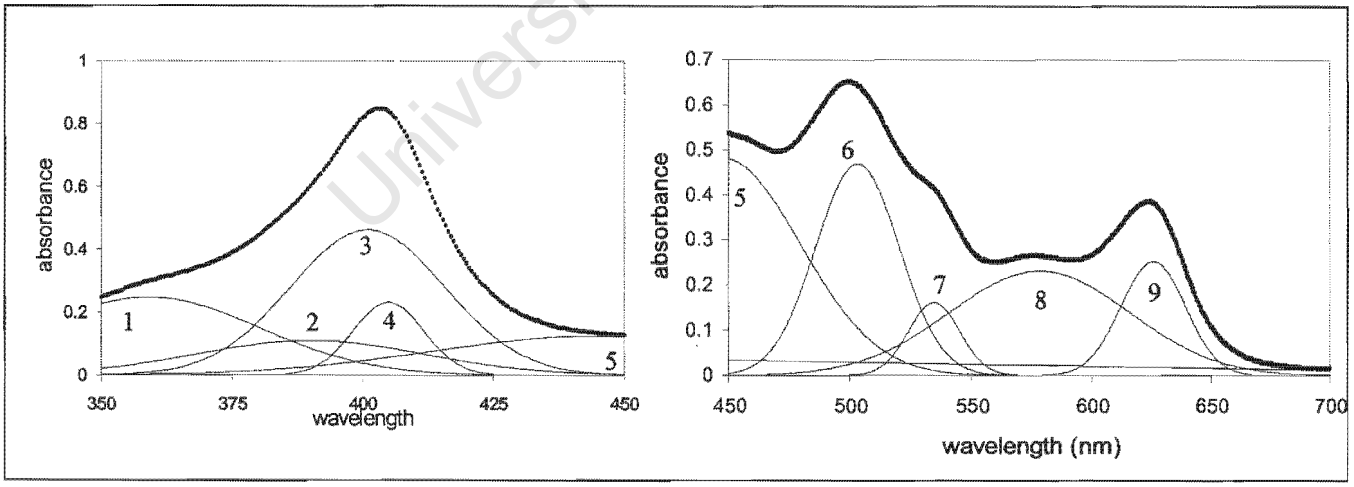

Figure 3.2 Deconvolution of the spectrum in figure 3.1 showing bands (1-9) leading to the N, Soret, Q and charge transfer bands in figure 3.1

Molecular orbital calculations on porphyrin systems have identified certain key energy levels[118]. When extended to metalloporphyrins, the energy level diagram must take into account the partially filled d orbitals of the metal. The energy level diagram for

University of Cape Town

(aqua)metmyoglobin (metMb) which contains Fe(III)PPIX is shown in Figure 3.3. It is transitions within these orbitals which give rise to peaks 1 - 9 shown in Figure 3.2 and hence to various bands in the spectrum of haematin (Figure 3.1).

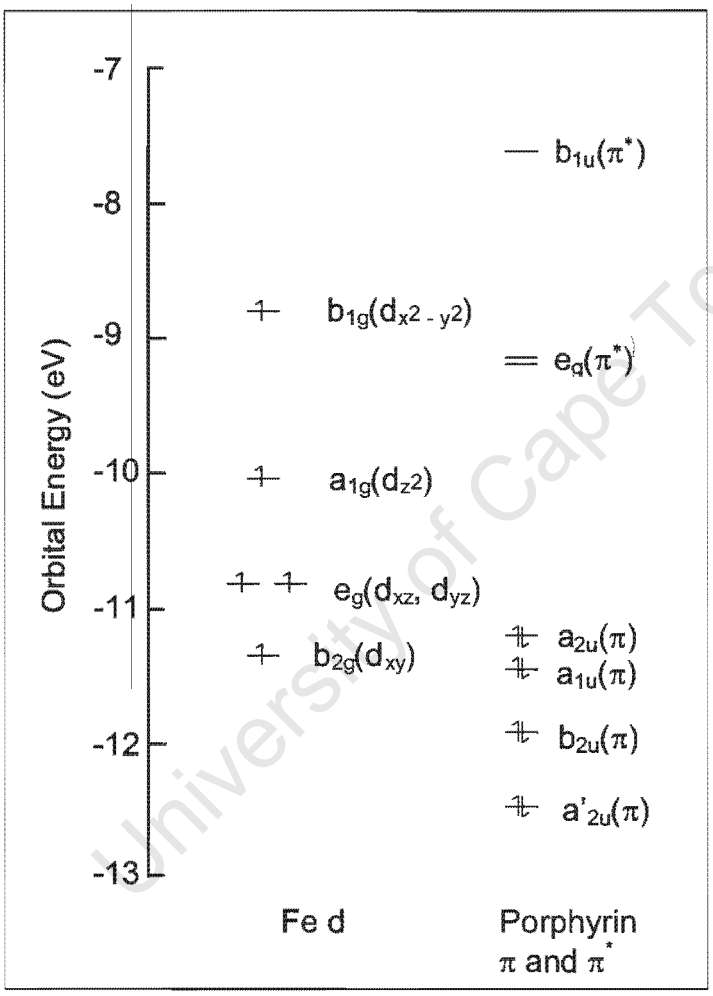

Figure 3.3 Energy levels in met(Mb) responsible for its uv-visible spectrum [119]

Table 3.1 shows which electronic transitions give rise to the bands observed in Figure 3.2 as well as the position of the band envelopes observed in figure 3.1 and is based upon the findings of Makinen *et al.*[119].

University of Cape Town

Table 3.1 Assignment of bands from Figure 3.2

Band	Assignment	λ (nm)	Transition	Band (Figure 3.1)	Position of band envelope maximum (nm)
1	N	359	$b_{2u}(\pi), a'_{2u}(\pi) \rightarrow e_g(\pi^*)$	N	363
2	B(1,0)	390	$a_{2u}(\pi), a_{1u}(\pi) \rightarrow e_g(\pi^*)$ (1^{st} vibrationally excited state)	Soret	shoulder between ~ 380 - 390
3	$B(0,0)_x$*	401	$a_{2u}(\pi), a_{1u}(\pi) \rightarrow e_g(\pi^*)$ x-polarised band	Soret	402
4	$B(0,0)_y$*	405	$a_{2u}(\pi), a_{1u}(\pi) \rightarrow e_g(\pi^*)$ y-polarised band	Soret	402
5	CT III	445	$a'_{2u}(\pi) \rightarrow a_{1g}(d_{z^2})$	shoulder	shoulder around 450
6	Q(1,0)	503	$a_{2u}(\pi), a_{1u}(\pi) \rightarrow e_g(\pi^*)$ (1^{st} vibrationally excited state)	β	500
7	Q(0,0)	535	$a_{2u}(\pi), a_{1u}(\pi) \rightarrow e_g(\pi^*)$	α	530
8	CT II	578	$a_{2u}(\pi) \rightarrow e_g(d_{xz}, d_{yz})$	CT II	575
9	CT I	626	$a_{1u}(\pi) \rightarrow e_g(d_{xz}, d_{yz})$	CT I	624

* x and y arbitrarily assigned as only single crystal spectra can lead to the absolute orientation

University of Cape Town

As Fe(III)PPIX is non-symmetrical, it leads to the x and y components of incidental light being adsorbed differently. This phenomenon results in further broadening of the spectrum as can be seen by the splitting of the B(0,0) band into the $B(0,0)_x$ and $B(0,0)_y$ components.

3.3 Changes in the spectrum of haematin due to interaction with platinum complexes

It is known that when chloroquine interacts with haematin, marked changes are seen in the Soret band, with a strong quenching taking place. Smaller changes can also be observed in the longer wavelength bands. It has been shown that these changes in the spectrum of haematin are

not due to μ-oxo dimer formation, or the formation of low spin Fe(III)PPIX but rather occur due to the formation of a chloroquine-haematin complex[117].

When [Pt(bipy)L]Cl is added to haematin in 40% aqueous DMSO, pH 7.4 and at 25 °C the spectrum of haematin undergoes similar changes (Figure 3.4).

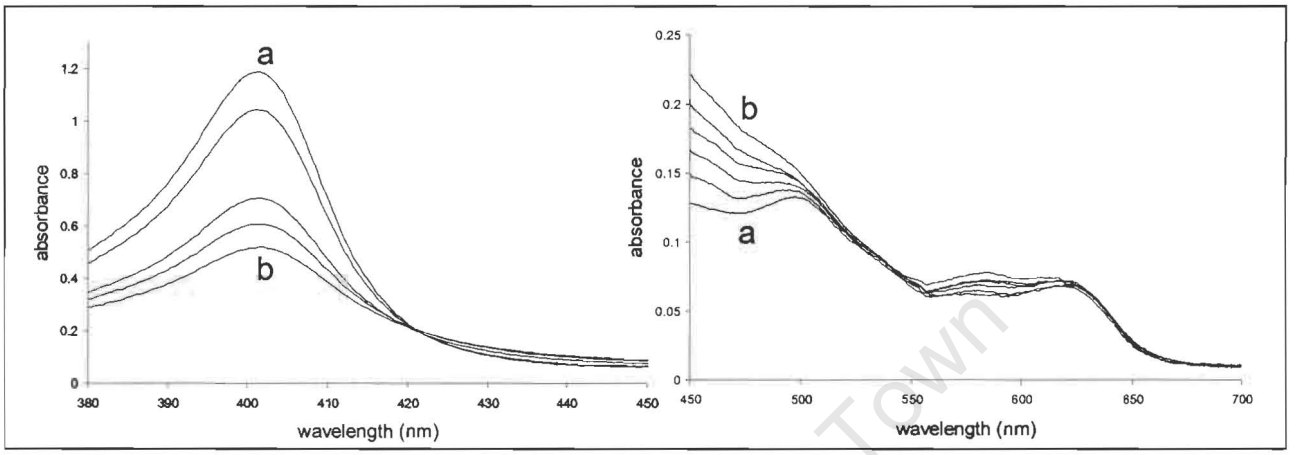

Figure 3.4 Changes in the uv-visible spectrum of haematin with [Pt(bipy)L]Cl in 40% DMSO, pH 7.4, 0.020 M HEPES a) 0 and b) excess [Pt(bipy)L]Cl

The most noticeable change is the quenching and broadening of the Soret band. The cause of this is not fully understood. However, the magnitude of the transition dipole moment of a compound determines its extinction coefficient and it is suggested that the magnitude of the transition dipole moment of haematin could be decreased by interaction with the dipole of the platinum complex. Deconvolution of the Soret band in spectrum b in Figure 3.4 does not show any evidence of an increased splitting of the $B(0,0)_x$ and $B(0,0)_y$ bands indicating that a further loss of symmetry is not the main contributing factor to the decreasing absorptivity of the Soret band. The broadening of the Soret causes an overlap with the Q band, giving rise to increasing absorbance in the 450 – 500 nm region. A blue shift is also observed in the charge transfer bands. These changes in the long wavelength region are almost identical to those observed upon addition of chloroquine to haematin and hence it is argued that [Pt(bipy) L] and chloroquine bind to haematin in an analogous way. These changes are however smaller and not so well suited to quantitation.

Thus, it is the Soret band that is of most interest in the study of the interaction between haematin and the platinum complexes as well as the uncomplexed ligands, as changes in this band are most easily observed. Figure 3.5 shows changes in the Soret band for titrations with

University of Cape Town

2,2'-bipyridine, 3,4,7,8-tetramethyl-1,10-phenanthlroine, 7,8-benzoquinoline, HL', and [Pt(phen)L]Cl using the same conditions as for the haematin – [Pt(bipy)L]Cl interaction.

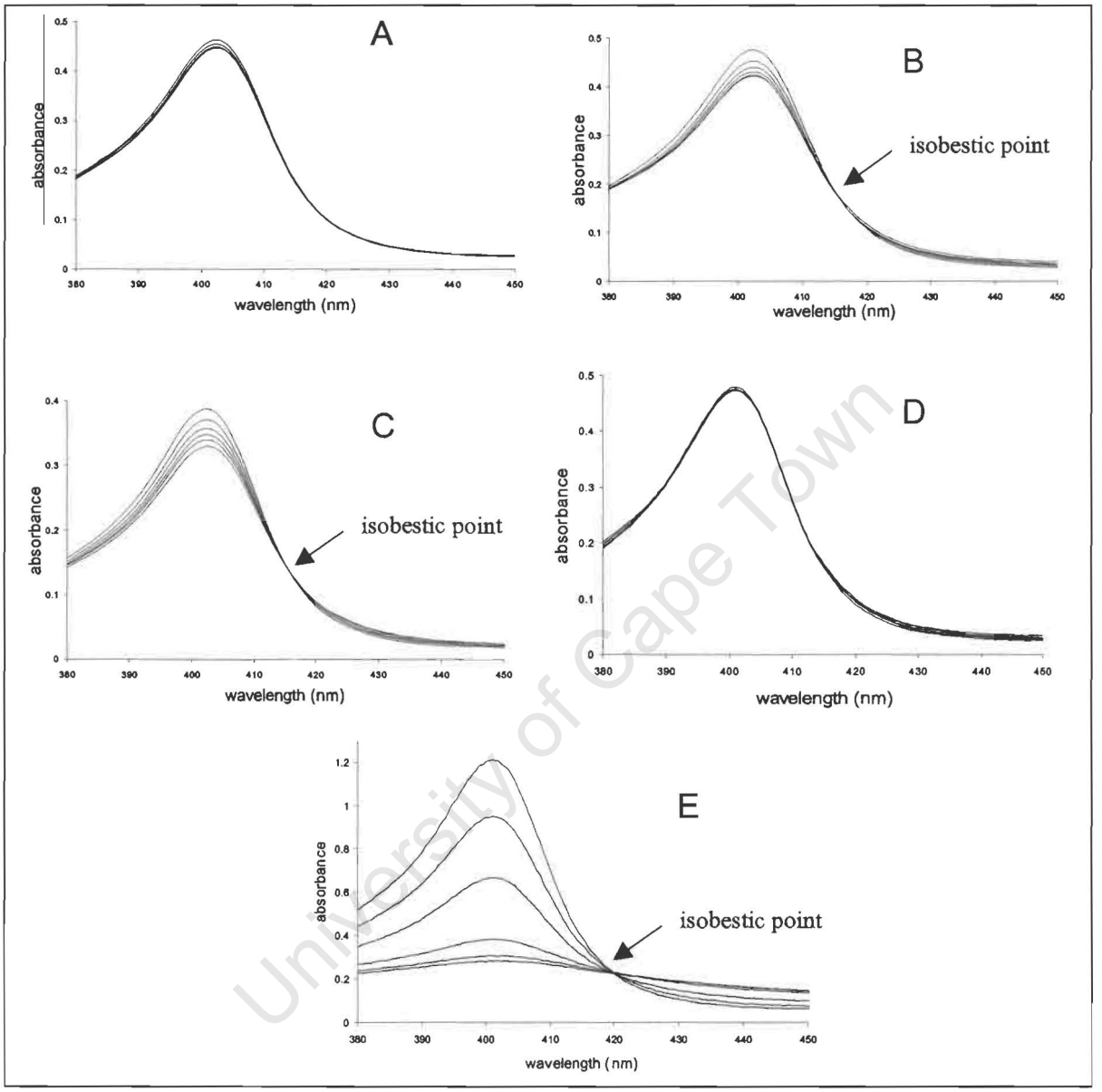

Figure 3.5 Change in the Soret band of haematin in 40% DMSO, pH 7.4, 0.020 M HEPES upon addition A) 2,2'-bipyridine, B) 3,4,7,8-tetramethyl-1,10-phenanthroline, C) 7,8-benzoquinoline, D) HL', E) [Pt(phen) L]Cl

Isobestic points are observed in Figures 3.4(B), 3.4(C) and 3.4 (E) indicating that 3,4,7,8-tetramethyl-1,10-phenanthroline, 7,8-benzoquinoline and [Pt(phen)L]Cl are interacting with haematin and more specifically, resulting in a conversion of one species to another with the two having differing spectra. A strong quenching of the Soret band is observed upon addition of [Pt(phen)L]Cl (Figure 3.5(E)) and this is comparable with changes observed in Figure 3.4 while the rest of the compounds in Figure 3.5 do not show such obvious changes. Figures

University of Cape Town

3.4(A) and 3.4(D) show a very marginal decrease of the whole spectrum and combined with the lack of isobestic points suggests that there is no interaction taking place between 2,2'-bipyridine and HL' with haematin. The slight decrease in the Soret band is possibly attributed to self aggregation of haematin or its adhesion to the cuvette surface, a phenomenon that has frequently been observed during this study.

Thus by monitoring changes in the Soret band (402 nm) it should be possible to quantify the interaction between haematin and [Pt(bipy)L]Cl as well as the other compounds listed in Table 3.2 at the end of section 3.4.

3.4 Titrations

By adding consecutive amounts of titrant to the solution containing haematin and correcting for dilution and the absorbance of the titrant, plots of the absorbance at 402 nm versus the concentration of the titrant could be obtained. Correction for dilution was achieved by multiplying the absorbance by a factor of the actual volume divided by the starting volume. Figure 3.6 shows a representative sample of these plots. The curves in Figure 3.6 have been fitted with a 1:1 binding model using non-linear least squares fitting software and result in a good fit. Other models were investigated (1:2 and 2:1) but were not found to yield a good fit. The 1:1 model can be defined as follows. The interaction of haematin (H) with an interacting molecule (IM) can be represented as:

$$IM + H \overset{K}{\rightleftharpoons} IM \quad H \qquad (3.1)$$

Where K is defined as:

$$K = \frac{[IM \bullet H]}{[IM]_{free} \times [H]} \qquad (3.2)$$

University of Cape Town

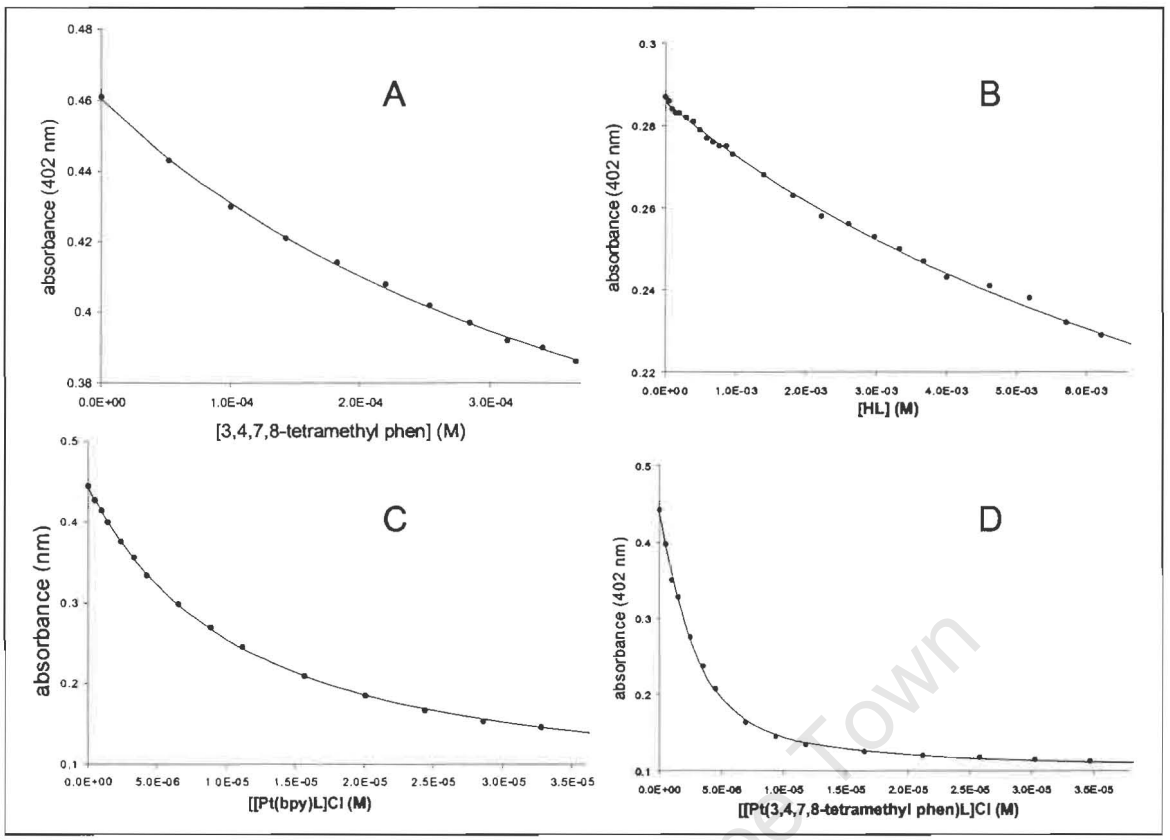

Figure 3.6 Plots showing the absorbance of haematin (402 nm) *vs.* concentration of (A) 3,4,7,8-tetramethyl-1,10-phenanthroline, (B) L, (C) [Pt(bipy)L]Cl, (D) [Pt(3,4,7,8-tetramethyl phen)L]Cl under conditions described in figure 3.5

The absorbance (A) is related to K and the concentration of the interacting molecule which is not associated with haematin, $[IM]_{free}$ by equation 3.3. A_0 is defined as the absorbance of haematin in the absence of the interacting molecule and A_∞ as its absorbance at an infinite concentration of the interacting molecule.

$$A = (A_0 + A_\infty K\ [IM]_{free}) / (1 + K\ [IM]_{free}) \qquad (3.3)$$

The concentration of haematin, the total concentration of the interacting molecule at each stage of the titration and the corresponding corrected absorbance was entered into the non-linear least squares fitting software. The corrected absorbance mathematically rectifies the dilution of the solution in the cuvette due to addition of the interacting molecule solution as well as the absorbance of the solution being added. The software model initially estimates that the free interacting molecule concentration is equal to the total interacting molecule concentration and calculates trial K, A_0 and A_∞ values by substituting the values from the titration into equation 3.3. The solution from the equation yields a more accurate value of the free interacting

University of Cape Town

molecule concentration and this is substituted back into equation 3.3 to obtain more accurate values of K, A_o and A_∞ which in turn results in a more accurate free interacting molecule concentration. A number of these iterations are performed using a Marquard algorithm until the sum of the squares of the errors is minimised.

In this way association constants with haematin were obtained and the results from the titrations are summarised in Table 3.2.

Table 3.2 Association constants of ligands and platinum complexes with haematin

Compound	**Log K (SEM)**
2,2-bipyridine	No binding observed
4,4'-dimethyl-2,2-bipyridine	No binding observed
4,4'-ditertiarybutyl-2,2-bipyridine	No binding observed
1,10-phenanthroline	2.95 ± 0.04
4-methyl-1,10-phenanthroline	3.22 ± 0.03
5-methyl-1,10-phenanthroline	2.93 ± 0.03
3,4,7,8-tetramethyl-1,10-phenanthroline	3.32 ± 0.01
5-chloro-1,10-phenanthroline	3.01 ± 0.03
5-nitro-1,10-phenanthroline	2.88 ± 0.02
7,8-benzoylquinoline	weak binding*
HL	1.93 ± 0.02
HL'	No binding observed
cis-[PtL_2]	No binding observed
[Pt(bipy)L]Cl	5.05 ± 0.02
[Pt(diMebipy)L]Cl	5.13 ± 0.01
[Pt(dtbbipy)L]Cl	4.81 ± 0.01
[Pt(phen)L]Cl	5.75 ± 0.02
[Pt(4-Me phen)L]Cl	5.75 ± 0.01
[Pt(5-Me phen)L]Cl	5.80 ± 0.02
[Pt(3,4,7,8-tetraMe phen)L]Cl	5.96 ± 0.02
[Pt(5-Cl phen)L]Cl	6.03 ± 0.01
[Pt(5-NO_2 phen)L]Cl	6.24 ± 0.02
[Pt(bipy)L']Cl	5.82 ± 0.01
[Pt(ppy)L']	No binding observed

* = not quantifiable

University of Cape Town

3.5 Discussion of titration results

2,2'-Bipyridine, 4,4-dimethyl-2,2'-bipyridine and 4,4'-ditertiarybutyl-2,2'-bipyridine show no evidence of binding to Fe(III)PPIX. This can almost certainly be ascribed to these diimines having twisted structures about the bond linking the pyridine rings which decreases the propensity of these molecules to interact with Fe(III)PPIX via π-π interactions as they are not planar. 1,10-phenanthroline and substituted phenanthrolines show quantifiable interactions with Fe(III)PPIX as the phenanthroline ring system is planar, unlike the bipyridines. This is in agreement with the findings of Shelnutt[98] who reports on phenanthrolines interacting with both Fe(III)uroporphyrin and Cu(II)uroporphyrin. Results from Table 3.2 indicate that substituents on 1,10-phenanthroline do not cause a marked change in association with haematin. Minor differences are evident however, with the strongest association seen with 3,4,7,8-tetramethyl-1,10-phenanthroline. The literature has shown stacking interactions of haem with chloroquine to be driven in part by hydrophobic interactions[51]. The stronger binding of this phenanthroline can thus be attributed to an accentuated hydrophobic effect. Methylation of the 4 position also appears to enhance interaction with Fe(III)PPIX compared with methylation of the 5 position. A possibly related difference in the chemistry of platinum(II) complexes of these ligands was noted in Chapter 2. It was shown that Pt(5-methyl-1,10-phenanthroline)Cl_2 resulted in a racemic mixture of isomers when reacted with an acylthiourea, while the 4 methyl intermediate complex resulted in one isomer being predominately favoured. This probably arose from the 4 methyl group giving rise to unequal electron density on the two phenanthroline nitrogens while with the methyl group in the 5 position was unable to achieve such a differentiation due to its greater distance from the nitrogens. As was noted in Chapter 1.5, the more polarised certain atoms in an aromatic ring are, the stronger the π-π interactions that molecule is capable of achieving. Thus, there is good evidence to indicate that methylation in the 4 position causes greater polarisation of electron density on the ring nitrogens and this could give rise to the stronger π-π interactions. It was expected that electronic effects of the chloro and nitro groups would have a larger effect on association but this is not observed. This may be as a result of the substituents being found in the 5 position rather than the 4 position on the phenanthroline ring.

The interactions of Fe(III)PPIX with both acylthioureas are either very weak or not observable. This is unsurprising as a large aromatic surface is absent in these ligands preventing favourable

University of Cape Town

π-π overlap with the metalloporphyrin[62]. HL has a log K value of 1.93 ± 0.02 while HL' shows no observable interaction with haematin. This difference could result from the steric bulk of the amine substituted acylthiourea or from the participation of the hydroxy group of HL in the association in an analogous way that quinine interacts with haematin (i.e. via weak coordination to the Fe(III) centre).

As was noted from Figure 3.5, the binding of platinum complexes to haematin is stronger than the ligands themselves by several orders of magnitude. With the exception of *cis*-[PtL_2] and [Pt(ppy)L'], all platinum complexes tested show strong association with Fe(III)PPIX. The fact that *cis*-[PtL_2] shows no measurable association with Fe(III)PPIX indicates that it is not the platinum itself nor the acylthiourea that is interacting directly with Fe(III)PPIX to any great extent but rather, association by mixed ligand complexes with haematin is likely to be taking place between the metalloporphyrin and the diimine. Yet the coordination of platinum greatly potentiates the ability of the diimine to bind to haematin. Platinum(II), being electropositive will have a strong electronic withdrawing effect on the diimine ring system and will also affect the electron distribution. This probably gives rise to increased association between the diimine and the electron dense metalloporphyrin ring system. The coordination of platinum to bipyridyl will also force this ligand into adopting a planar configuration[96], making strong association possible.

Of the trends already noted in the phenanthroline ligands tested, only the slight increase in binding constant due to increased hydrophobic interaction appears to carry through to the platinum-phenanthroline complexes. This effect is also probably responsible for the slightly higher association constant of [Pt(diMebipy)L]Cl compared to [Pt(bipy)L]Cl. Several new trends are however apparent. Firstly, the binding strength appears to be dependent on the surface area of the diimine present, with all the phenanthroline complexes showing a binding constant that approaches an order of magnitude larger than that of the bipyridyl complexes. This again reinforces the idea that it is through the diimine that binding to Fe(III)PPIX is taking place. Secondly, the electronic properties of the substituents result in more noticeable changes as compared with trends evident in the uncomplexed 1,10-phenanthrolines. Both chloro and nitro in the 5 position on the phenanthroline ring of the metal complexes result in a marked increase in association with haematin. These groups are both responsible for withdrawing electron density from the ring resulting in a greater interaction with haematin.

University of Cape Town

Thirdly, steric factors appear to have a small but significant influence on the binding, as the bulky ditertiarybutyl groups slightly reduce the binding constant of [Pt(dtbbipy)L]Cl as compared with[Pt(bipy)L]Cl. Finally changing the nature of the acylthiourea results in a marked change in association. Evidence from ^{1}H NMR shows the chemical shifts of the diimine in the complex to be markedly influenced by the acylthiourea. HL' results in down field shifts compared to HL when included in the metal complexes (Figure 3.7). This indicates a lowering of electron density in the diimine ring system of [Pt(bipy)L']Cl compared with that of [Pt(bipy)L]Cl and this is reflected in binding to Fe(III)PPIX with the log K value of the former being 0.77 log units greater.

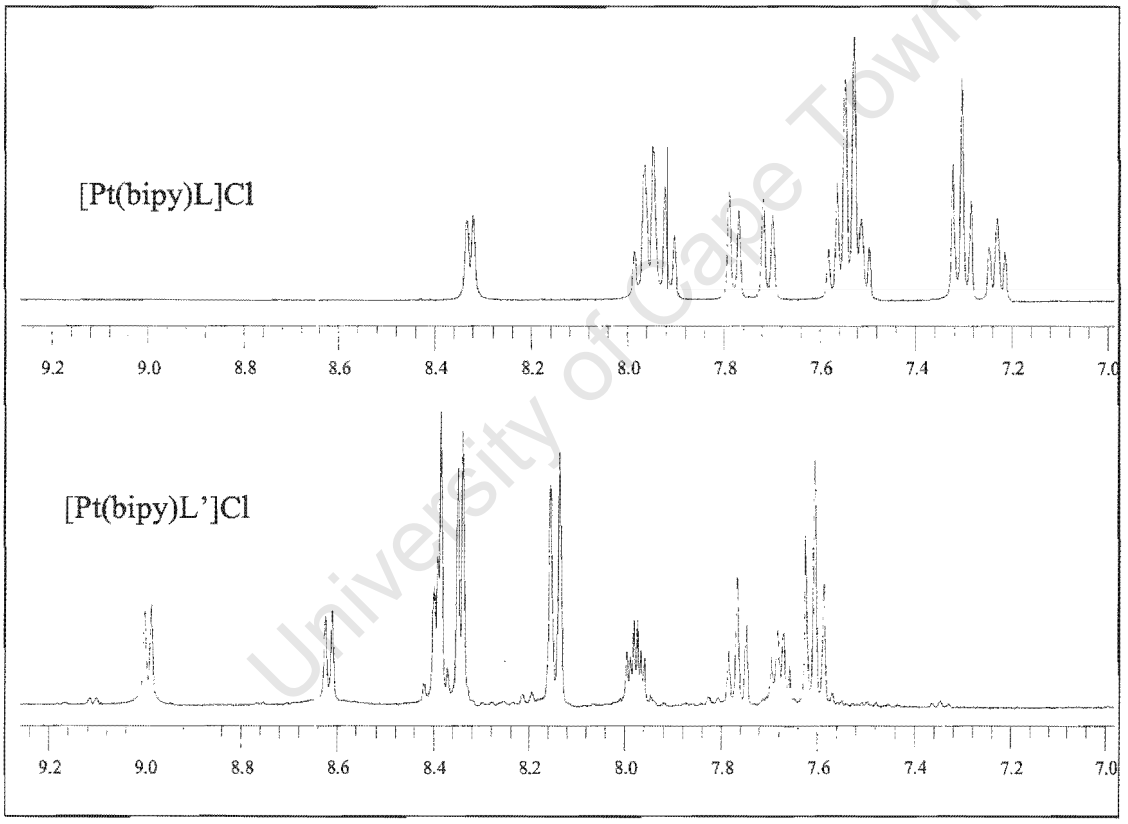

Figure 3.7 Proton NMR spectra of [Pt(bipy)L]Cl and [Pt(bipy)L']Cl showing the aromatic region to illustrate the role of the acylthiourea in effecting electron density in the diimine

The 1,10-phenanthroline analogue 7,8-benzoquinoline which lacks one of the nitrogen atoms, was found to associate very weakly with Fe(III)PPIX as isobestic points were observed in the titration spectra (Figure 2 (C)) but a straight line resulted from plotting Fe(III)PPIX absorbance versus increasing ligand concentration and this does not allow for quantitation of the association. This shows that substitution of a carbon atom for nitrogen in the aromatic ring

University of Cape Town

system can have a marked effect on the ability of a compound to bind to haematin. A similar effect has been observed in quinoline systems where an amino group is required in either the 2 or 4 position to result in strong haematin binding[54]. The finding that 7,8-benzoquinoline interacts with haematin much less strongly than 1,10-phenanthroline gives insights into the inability of [Pt(ppy)L'] to interact with haematin with similar strength as [Pt(bipy)L']Cl . From these findings it would appear that nitrogen is required in both the 1 and 1' (2,2'-bipyridine) or 1 and 10 positions (1,10-phenanthroline) to achieve appreciable interaction with haematin, possibly due to a required electron density distribution pattern.

3.6 Conclusion

UV-visible spectroscopy proved to be an effective tool in establishing association constants of various ligands and platinum complexes with haematin and the findings are summarised in Table 3.3. Several of the uncomplexed ligands did not observably interact with haematin. If such interactions did exist they would be very weak. These complexes were HL', all three 2,2'-bipyridine ligands, *cis*-[PtL_2] and [Pt(ppy)L']. All the 1,10-phenanthroline ligands investigated showed weak interactions with haematin as did 7,8 benzoyl quinoline and HL. The complexes comprising of platinum coordinated to both an acylthiourea and a diimine showed strong interactions with haematin with log K values in the region from 4.8 to 6.2. Thus these complexes show one of the requirements for antimalarial activity as they are capable of strongly binding the suspected drug target with log K values being comparable to known antimalarials[56 and ref. therein].

University of Cape Town

Table 3.3 Summary of results from the association of ligands and platinum complexes with haematin

No quantifiable association	Weak association	Strong association
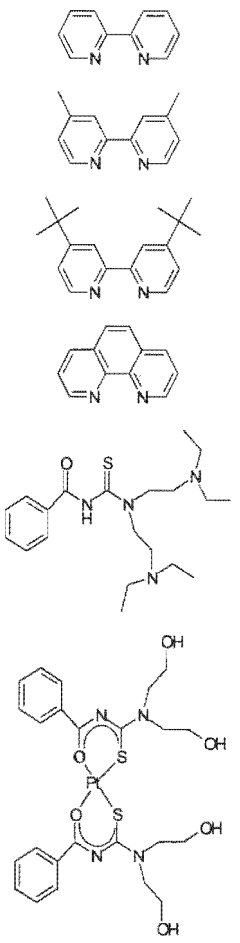	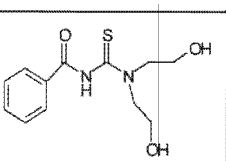 log K =1.93 ± 0.02 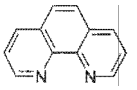 log K =2.95 ± 0.04 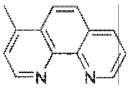 log K =3.22 ± 0.03 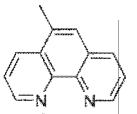 log K =2.93 ± 0.03 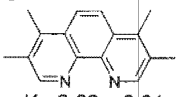 log K =3.32 ± 0.01 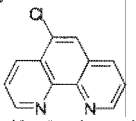 log K =3.01 ± 0.04 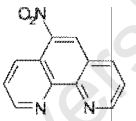 log K =2.88 ± 0.02	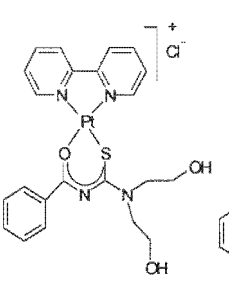 log K =5.05 ± 0.02 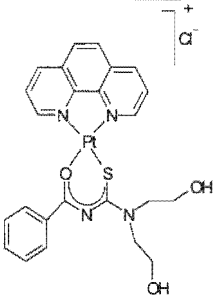 log K =5.75 ± 0.02 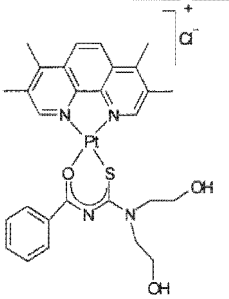 log K =5.96 ± 0.02 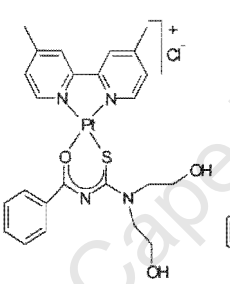 log K =5.13 ± 0.01 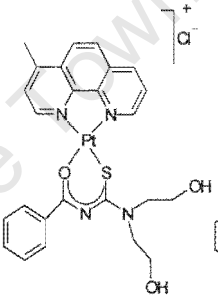 log K =5.75 ± 0.01 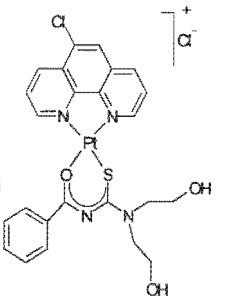 log K =6.03 ± 0.01 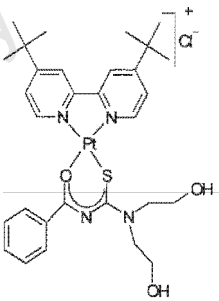 log K =4.81 ± 0.01 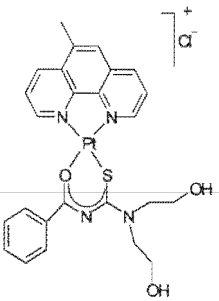 log K =5.80 ± 0.02 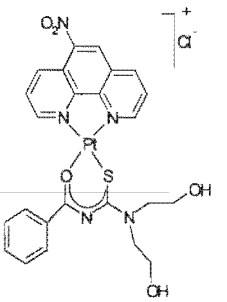 log K =6.24 ± 0.02 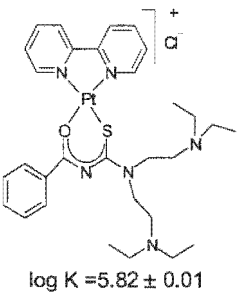 log K =5.82 ± 0.01

University of Cape Town

4 Inhibition of β-Haematin formation and preliminary biological study

4.1 Introduction

The interest in compounds that inhibit the formation of haemozoin is considerable. As Chapter 1.4 has shown, much evidence from the literature exists to support the idea that compounds which bind to haematin in the food vacuole of the parasite and also prevent it from forming haemozoin, have antiplasmodial activity. A synthetic form of haemozoin, β-haematin can be prepared via a number of methods[19] while the equivalence of haemozoin and β-haematin has been proven by x-ray powder diffraction studies[18]. Egan *et al*[120] have developed a convenient method of synthesising β-haematin by dissolving hemin in a sodium hydroxide solution and then adding hydrochloric acid to partially precipitate the haematin that forms. This mixture is then rapidly stirred in a 4.5 M sodium acetate solution buffered at pH 4.5 at 60 °C for 30 minutes. The product consisting predominately of β-haematin with some haematin still present, is filtered then washed extensively with water and dried. The details of this synthesis can be found in Chapter 7.6. This procedure can be carried out in the presence of another compound in order to test its ability to inhibit the formation of β-haematin. Typically three equivalents of the compound being tested are added to the haematin. If the product formed is found not to contain β-haematin then this product is said to inhibit the formation of β-haematin.

University of Cape Town

4.2 Characterisation of β-haematin

As mentioned in the above section, β-haematin can be characterised by means of x-ray powder diffraction. The disadvantage of this method is that the equipment available for this project requires approximately 200 mg of sample. This is not convenient as many of the compounds which would be tested for their ability to inhibit the formation of β-haematin are synthesised in small quantities and the method requires up to gram quantities of these compounds. As β-haematin only exists in the solid state, solution based techniques are not an option for directly detecting it. Thus infrared spectroscopy is the method of choice in discriminating between haematin and β-haematin. Figure 4.1 shows the infrared spectra of these two compounds.

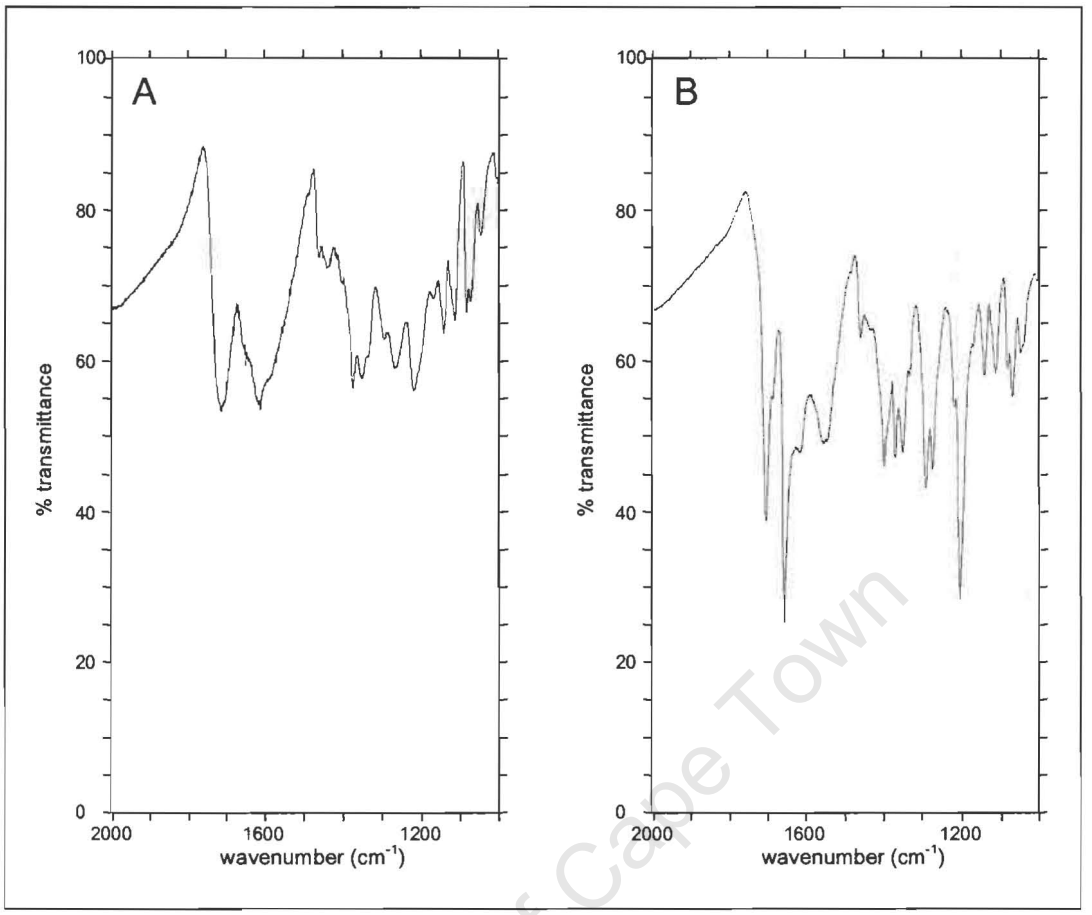

Figure 4.1 Infrared spectra of (A) haematin and (B) β-haematin obtained as KBr discs in the region 2000 cm^{-1} – 1000 cm^{-1} The red dotted lines are at 1662 cm^{-1} and 1210 cm^{-1}

University of Cape Town

Apart from the observation that the peaks in the spectrum of β-haematin are much sharper than in haematin in the 1800 – 1500 cm^{-1} region, two new dominant peaks are found in the β-haematin spectrum at 1662 ± 2 cm^{-1} and 1210 ± 1 cm^{-1}. The band at 1662 cm^{-1} arises due to the C=O stretching frequency while the C-O bond stretching frequency gives rise to the band at 1210 cm^{-1}, both from the iron coordinated carboxylate group[120]. Therefore peaks at both 1662 cm^{-1} and 1210 cm^{-1} provide an excellent fingerprint for β-haematin and will subsequently be used to identify the presence of β-haematin in accordance with the literature[120].

4.3 Results of the inhibition of β-haematin formation experiments

Upon addition of either a ligand or platinum complex prior to addition of the acetate in the synthesis of β-haematin, the β-haematin crystallisation process may continue or it may be inhibited and this is observable using infrared spectroscopy. It is important to note that the platinum complexes themselves give rise to a band in the 1210 ± 5 cm^{-1} region. This makes the 1210 cm^{-1} peak unsuitable for establishing if inhibition of β-haematin has taken place or not and thus the band at 1662 cm^{-1} is used to confirm the presence or absence of β-haematin. In Figure 4.2, representative infrared spectra of the products obtained from the attempted synthesis of β-haematin in the presence of the compounds listed in Table 4.1 at three equivalents relative to haematin are shown.

.

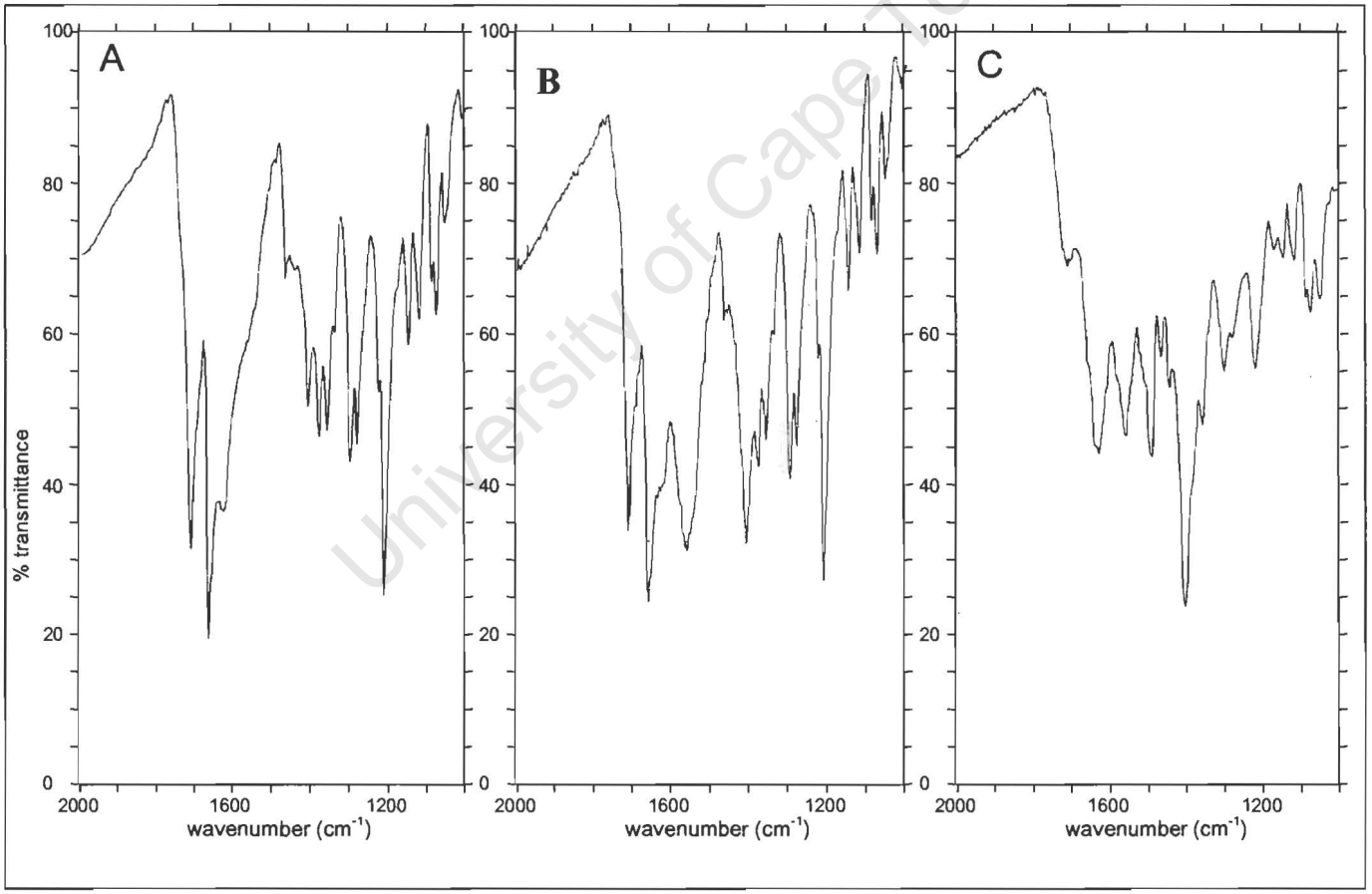

Figure 4.2 Infrared spectra of the product obtained from β haematin inhibition experiments with 3 equivalents of (A) HL, (B) 2,2'-bipyridine and (C) [Pt(bipy)L]Cl present

University of Cape Town

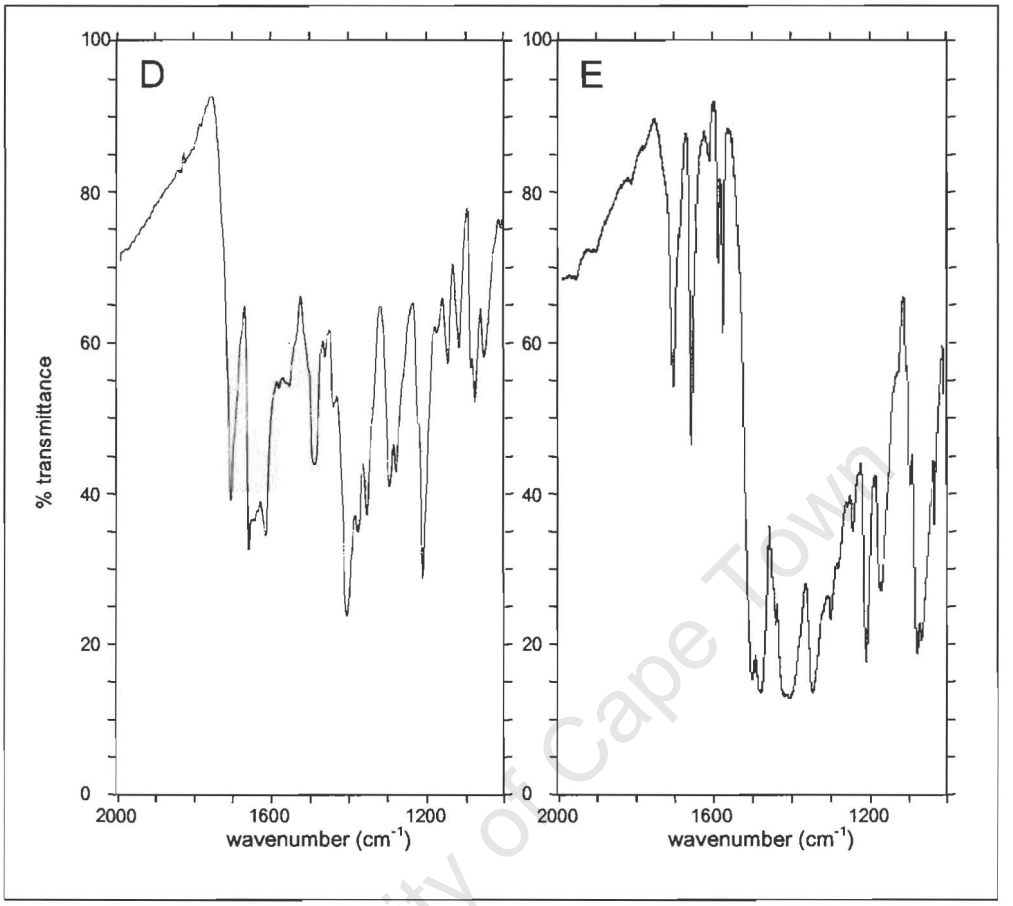

Figure 4.2 (continued) Infrared spectra of the product obtained from β haematin inhibition experiments with 3 equivalents of (D) [Pt(diMebipy)L]Cl and (E) *cis*-[PtL_2]present

University of Cape Town

It can be seen in Figure 4.2 that there are three main categories of products, those where β-haematin has formed without hindrance (strong peaks at 1662 and 1210 cm^{-1} , A and B), those where there no β-haematin formed (no peak at 1662 cm^{-1}, C) and instances where there is partial β-haematin formation with only small peaks observed at 1662 cm^{-1} (D). In (E) there is no inhibition of β-haematin formation as indicated by the strong peak at 1662 cm^{-1}, but a strong spectrum from the insoluble platinum complex can also be seen. The results from Figure 4.2 are summarised according to these three categories in Table 4.1.

Table 4.1 The ability of platinum complexes and associated ligands to inhibit the formation of β-haematin formation

Compound	Inhibition of β-haematin formation
2,2-bipyridine	-
4,4'-dimethyl-2,2-bipyridine	-
4,4'-diteriarybutyl-2,2-bipyridine	-
1,10-phenanthroline	-
4-methyl-1,10-phenanthroline	-
5-methyl-1,10-phenanthroline	-
3,4,7,8-tetramethyl-1,10-phenanthroline	-
5-chloro-1,10-phenanthroline	-
5-nitro-1,10-phenanthroline	-
7,8-benzoylquinoline	-
HL	-
HL'	-
[Pt(bipy)L]Cl	+
[Pt(diMebipy)L]Cl	Partial
[Pt(dtbbipy)L]Cl	Partial
[Pt(phen)L]Cl	+
[Pt(4-Me phen)L]Cl	+
[Pt(5-Me phen)L]Cl	+
[Pt(3,4,7,8-tetraMe phen)L]Cl	+
[Pt(5-Cl phen)L]Cl	+
[Pt(5-NO_2 phen)L]Cl	+
[Pt(bipy)L']Cl	Partial
cis-[PtL_2]	-
Pt(ppy)L'	-

In a further investigation of [Pt(diMebipy)L]Cl that only partially inhibited the formation of β-haematin, it was tested at four, six and eight mol equivalents relative to haematin. These spectra are shown in Figure 4.3 and it is observed that as the concentration of [Pt(diMebipy)L]CL increases, so does the extent of the inhibition of β-haematin formation. As has been mentioned, this platinum complex is water soluble and thus excess complex is washed

University of Cape Town

out during filtering so the disappearance of the 1662cm^{-1} peak is not due to its being obscured by more intense bands arising from the platinum complex. This is observed in Figure 4.3

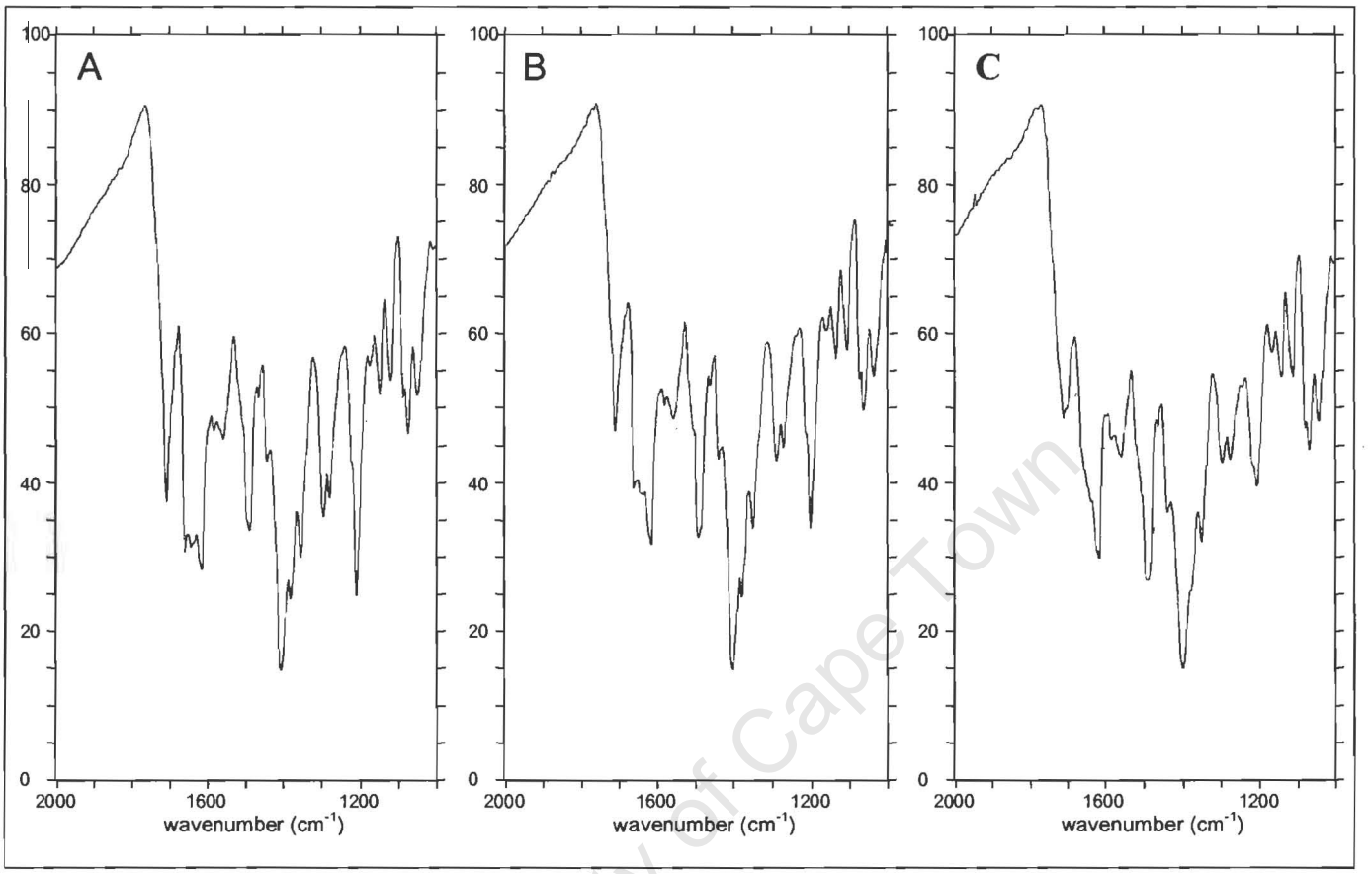

Figure 4.3 Infrared spectra of the product obtained from β-haematin inhibition experiments with (A) 4, (B) 6 and(C) 8 mol equivalents of [Pt(diMebipy)L]Cl present

University of Cape Town

4.4 Discussion of results from the inhibition of β-haematin formation experiments

Table 4.1 shows a clear trend, with none of the ligands alone showing the ability to inhibit β-haematin formation, while those platinum complexes which bind appreciably to Fe(III)PPIX (Table 3.2) all inhibit the formation of β-haematin. A further observation from Figure 4.2 is that the spectra resulting from inhibition with charged platinum complexes have peaks that do not correlate exactly with either the peaks observed in haematin or the platinum complexes or a mixture of haematin and a platinum complex. This is demonstrated in Figure 4.4 for the case of [Pt(bipy)L]Cl and exact peak positions are given in Table 4.2.

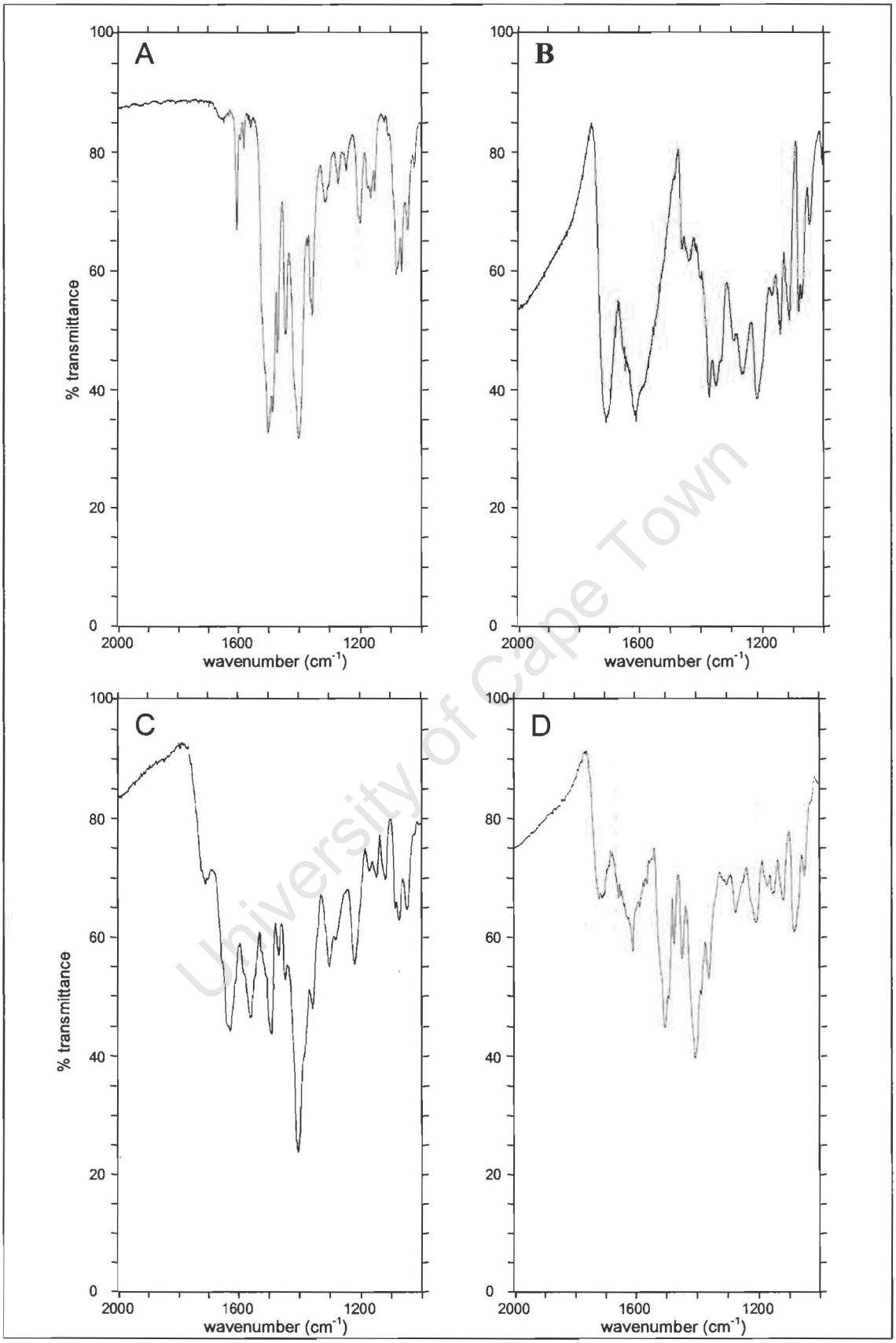

University of Cape Town

Figure 4.4 Infrared spectrum of (A) [Pt(bipy)L]Cl, (B) haematin, (C) product from inhibition experiment with [Pt(bipy)L]Cl and (D) a mixture of 0.5 mg [Pt(bipy)L]Cl and 1.5 mg haematin

Table 4.2 Comparison of the peak positions from the infrared spectra of [Pt(bipy)L]Cl, haematin, a mixture of 0.5 mg [Pt(bipy)L]Cl and 1.5 mg haematin and product from inhibition experiment with [Pt(bipy)L]Cl.

[Pt(bipy)L]Cl (cm^{-1})	haematin (cm^{-1})	[Pt(bipy)L]Cl + haematin (cm^{-1})	inhibition reaction product (cm^{-1})
1712		1706	1707
1613			1629
	1606	1607	
	1502	1501	1559
	1487		1492
	1473	1472	1467
	1443	1444	1447
1435			
	1401	1399	1411
1376			
	1358	1359	1356
1349			
	1312	1300	
1293			1302
	1271	1269	
1263			
	1245		
1218			1219
	1200	1201	
1167		1165	1171
	1165		
	1153		1150
1144		1145	
1115		1114	1118
1085		1078	
	1082		
1073			1075
	1066		
	1050		1049
1048		1047	
	1023		
1001			

University of Cape Town

Thus there is clear evidence that the platinum complexes are not merely contributing peaks characteristic of the complex to the spectrum of haematin (Figure 4.4(C)) but are actually changing the vibrational and stretching energies of the porphyrin. Likewise the porphyrin is also causing a change to the position of the peaks in the spectrum of [Pt(bipy)L]Cl. This would only be possible in the case of the two molecules associating in the solid state and causing some changes to the electronic structure of both compounds. This adds to the finding from Chapter 3 where these platinum complexes were shown to interact in solution and now are also shown to interact in the solid state. In the case of Pt(diMebipy)L]Cl, no β-haematin is seen to form when 8 mol equivalents of the platinum complex is added. Thus, it can be seen that

[Pt(diMebipy)L]Cl does in fact inhibit the formation of β-haematin but does so less effectively than the other platinum complexes which fully inhibit the formation of β-haematin when present in 3 mol equivalents. This is also likely to be the case with [Pt(dtbbipy)L]Cl. Both [Pt(diMebipy)L]Cl and [Pt(dtbbipy)L]Cl have similar binding constants to [Pt(bipy)L]Cl (Chapter 3.4) indicating that association alone is not the only factor in achieving inhibition. This has previously been demonstrated with 9-epiquinine which binds to Fe(III)PPIX with a log K of 4.04 comparable to quinine (log K = 4.10) yet does not inhibit β-haematin formation unlike quinine and also with a variety of aminoquinolines[120]. Thus it is proposed that the methyl or ditertiarybutyl groups substituted onto the bpy ring system cause a changed geometry in the association between Fe(III)PPIX and the platinum complex resulting in less effective blocking of the process of β-haematin formation. This will be investigated in Chapter 5.

The acylthiourea moiety also appears to affect the efficiency of the inhibition of β-haematin formation. HL' causes an increase in association of the platinum complexes with haematin compared with HL yet HL' decreases the ability of the complex to prevent β-haematin formation. The reason for this is not clear at present but it is speculated that either the steric bulk of HL' or the hydroxy groups of HL cause a modification to the geometry of the platinum complex – haematin association resulting in the differentiation observed.

[Pt(ppy)L'] and *cis*-[PtL_2] and which did not measurably bind to Fe(III)PPIX, predictably also do not inhibit the formation of the crystalline dimer. This is consistent with the trends in the literature where such binding is shown to be one of the prerequisites for the inhibition of β-haematin formation[19].

4.5 Preliminary biological study

While the platinum complexes in this thesis were not extensively tested *in vitro* against parasites, a small preliminary study investigated the activities of [Pt(bipy)L]Cl, [Pt(diMebipy)L]Cl, [Pt(phen)L]Cl and [Pt(bipy)L']Cl against *Plasmodium falciparum*. [Pt(bipy)L]Cl was found to have the best activity of these complexes with an IC_{50} of about 1 μM. [Pt(diMebipy)L]Cl was less effective (1.4 μM) while the other two complexes showed less activity with IC_{50} values above 2.8μM. There were problems with the solubility of

University of Cape Town

[Pt(phen)L]Cl which could explain this result as the actual concentration of the solution would have been less than the calculated concentration. Another possibility could be that the larger aromatic surface causes problems in the transport of this complex to the food vacuole of the parasite as these surfaces are hydrophobic and have a greater possibility of being trapped in membranes. The lack of activity of [Pt(bipy)L']Cl could be caused by its lack of efficiency in inhibiting β-haematin formation and secondly, since the amine side chains of this complex are almost certainly protonated outside the food vacuole of the parasite, the triply charged complex may not be able to effectively cross membranes. Furthermore, the arrangement of charge on this molecule would result in the complex having a strongly hydrophilic and hydrophobic portions which could well pose problems in terms of it crossing cell membranes. This is speculative at this stage and the whole series of complexes should be tested against parasites in future work to try to more clearly understand their biological distribution and activity. Thus the attempt to include a weak base into the platinum complex failed to cause greater activity compared to the [Pt(bipy)L]Cl complex.

In a related project in our laboratories, it was found that these platinum complexes exhibit low levels of toxicity against *E.coli* cell lines, in the micromolar concentration range[121]. The mode of action has been shown to be via DNA intercalation. The [Pt(bipy)L]Cl complex was found to be significantly more active against these organisms than [Pt(diMebipy)L]Cl, [Pt(dtbbipy)L]Cl] or [Pt(phen)L]Cl][121]. This again suggests that these three complexes may be less active due to poor membrane crossing potential, exemplified in the case of [Pt(phen)L]Cl, as this should have better intercalation properties than [Pt(bipy)L]Cl. Since the level of toxicity these complexes show against the malaria parasite is several orders of magnitude higher than against *E.coli*, it is almost certain that the complexes are achieving their toxicity by means of the suggested mode of action, the inhibition of formation of malaria pigment. Furthermore this difference in toxicity between malaria parasites and other cell lines suggests that these complexes may have a useful therapeutic index, should complexes which do effectively accumulate in the food vacuole of the parasite, be developed.

University of Cape Town

4.6 Conclusion

It has been shown that none of the uncomplexed ligands are able to inhibit the formation of β-haematin which was predictable as they all demonstrated weak or no association with haematin (Chapter 3). However when diimines were complexed to platinum opposite an acylthiourea, inhibition of β-haematin formation was found to occur. The platinum complexes were found to have varying abilities to inhibit the β-haematin crystallisation process when present at three equivalents with all the 1,10-phenantholine complexes allowing full inhibition compared to only one of the 2,2'-bipyridine complexes. While only one complex was made using the acylthiourea ligand HL, [Pt(bipy)L']Cl, was found to be less effective in inhibiting β-haematin formation than the complex, [Pt(bipy)L]Cl. These findings are summarised in Table 4.3. Thus it has been shown that it is critical for platinum to be bound to diimines for these aromatic ligands to be able to inhibit the formation of β-haematin. This is probably due to the electronic withdrawing properties of the metal. In the case of 2,2'-bipyridyl complexes the platinum also results in the untwisting of 2,2'-bipyridine allowing for strong association with haematin.

It has also been shown that [Pt(bipy)L]Cl and [Pt(diMebipy)L]Cl show moderate activity against *Plasmodium falciparum* in the micromolar concentration range despite their apparent lack of ability of being able to accumulate within the food vacuole of the parasite. This is an encouraging result as it shows that as templates for novel antimalarial drugs, these complexes do have potential.

University of Cape Town

Table 4.3 Summary of the abilities of ligands and platinum complexes which measurably bind to haematin to inhibit the formation of β-haematin

No inhibition of β formation	Partial inhibition of β formation	Strong inhibition of β formation
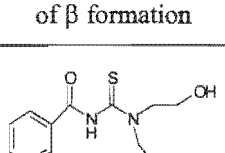	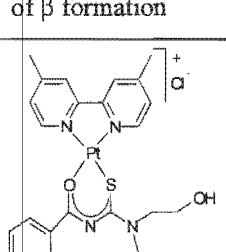	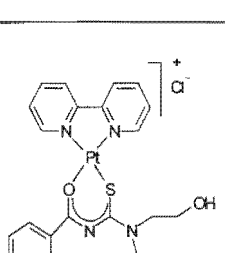 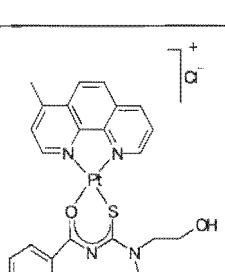 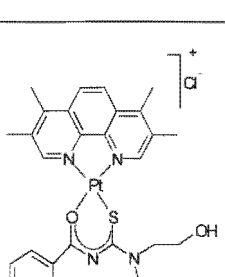
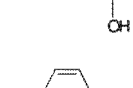	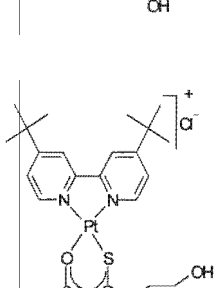	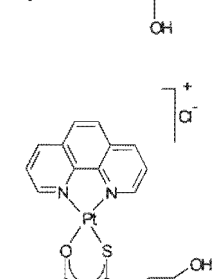 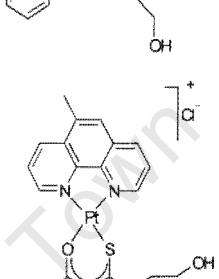 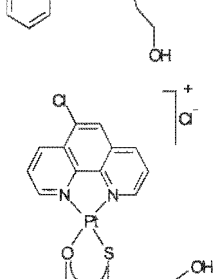
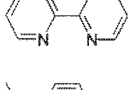	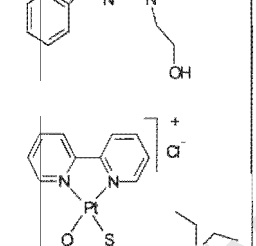	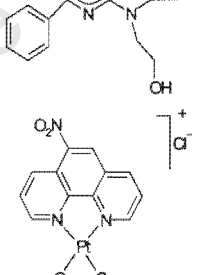
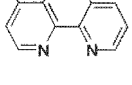		
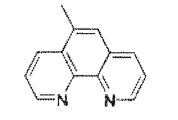		
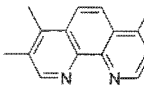		
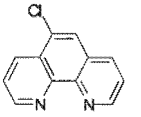		

University of Cape Town

5 Structure and geometry of platinum complex – Zn(II)PPIX interactions

5.1 Objectives

Changes in chemical shifts are observed in the ^{1}H NMR spectra of molecules that associate in solution. Koch *et al.*[97] have done such a study looking at the self-association of platinum complexes similar to those in this dissertation in a mixed deutero-acetonitrile, D_2O solvent system. As the concentration of complexes was increased so the peaks corresponding to protons involved in overlap of the molecules were seen to move up-field in the proton spectrum. Another study by Abraham *et al.*[67] has involved studying the self association of zinc(II) protoporphyrin IX dimethyl ester in deutero-chloroform using both ^{1}H and ^{13}C spectroscopy. Again, up-field shifts were observed in peaks arising from protons involved in intermolecular interactions.

It should therefore be possible to gain insights into the geometries involved in the association of platinum complexes with metalloporphyrins by observing shifts of peaks in the proton NMR spectrum upon mixing of the two compounds. It is of considerable interest to elucidate the geometry of association between [Pt(diimine)L]Cl complexes and Fe(III)PPIX. Chapter 3 has shown [Pt(bipy)L]Cl and [Pt(diMebipy)L]Cl to have similar association constants with Fe(III)PPIX. However Chapter 4 has shown these two platinum complexes to exhibit differing properties regarding the inhibition of β-haematin. This difference suggests that the two complexes may adopt a differing geometry with the metalloporphyrin with important consequences for β-haematin inhibition activity and insight may thus be obtained regarding the mechanism of inhibition of β-haematin formation.

5.2 Methodology

NMR serves as a good diagnostic tool, but Fe(III)PPIX is not ideal for use in an NMR study since it is paramagnetic which results in very broad peaks in the NMR spectrum. Ga(III)PPIX was synthesised (Chapter 2.8) as a diamagnetic model for Fe(III)PPIX since Ga(III) is of similar size to Fe(III) and both have the same charge. However as reported in Chapter 2.8, it does not yield a ^{1}H NMR spectrum that would be of use in such a study due to extensive

University of Cape Town

aggregation. Thus it was decided to use Zn(II)PPIX as a model for Fe(III)PPIX the Zn(II)PPIX behaviour is well understood, it is commercially available and it gives a satisfactory proton NMR spectrum.

A solvent system of 80% deutero-DMSO, 20% D_2O has been used in this study to achieve adequate solubilities of both the Zn(II)PPIX and platinum complexes. It has previously been reported that interactions with Fe(III)PPIX are strongly dependant on water being present[51, 19, 69] and thus the 20% D_2O present not only facilitates the solvation of platinum complexes but also increases interaction between the platinum complexes and Zn(II)PPIX relative to pure DMSO. On the other hand, using much more than 20% water (D_2O) would cause problems in maintaining Zn(II)PPIX in solution at the concentrations required for NMR.

After establishing a suitable solvent system, the peaks in the proton spectrum of Zn(II)PPIX, [Pt(bipy)L]Cl and [Pt(diMebipy)L]Cl were assigned. The platinum complexes had been previously assigned in a 50% deutero-acetonitrile / D_2O solvent system (Chapter 6.3.5) and the ^1H NMR spectra in the 80% deutero-DMSO solvent system were essentially the same, with minor differences in the chemical shifts of the acylthiourea side chain protons. The Zn(II)PPIX ^1H NMR spectrum was assigned using NOESY, a two dimensional technique showing through space interactions of protons, and double quantum filtered COSY spectroscopy as detailed in Chapter 5.3. All three compounds are likely to self associate at concentrations required for NMR and this was quantitatively investigated by successive dilution of samples of Zn(II)PPIX, [Pt(bipy)L]Cl and [Pt(diMebipy)L]Cl. It was found that while the two platinum complexes showed significant shifts in the proton peaks, particularly peaks arising from the diimines, Zn(II)PPIX showed only very small concentration dependant changes in chemical shifts. This suggests that the metalloporphyrin is either essentially monomeric or fully aggregated. Evidence from the study by Abraham *et al.*[67] shows that in Zn(II)PPIX dimethyl ester, the monomeric state is characterised by meso protons giving a shift in the 10 ppm region compared with aggregated states of around 8 ppm. Thus one can conclude that Zn(II)PPIX in this work is essentially monomeric as the meso proton peaks are located in the 10 ppm region (see Figure 5.1).

With all the peaks assigned, a third order polynomial equation was fitted to the chemical shift of each proton at each concentration encountered during the dilution of samples. By interpolation, this allowed calculation of the chemical shift of every proton at any

University of Cape Town

concentration in the range used in titrations of the platinum complexes with Zn(II)PPIX. This is necessary as the titrations result in changing concentrations of both the compounds involved in the interaction as a result of dilution. As has been alluded to above, this change in concentration results in shifts, particularly of the platinum complexes and thus it is important to differentiate the shifts caused by changes in self association from those interactions between the platinum complexes and haematin.

Titrations were carried out by titrating the platinum complexes with Zn(II)PPIX and also in reverse by titrating Zn(II)PPIX with the platinum complexes according to the description given in Chapter 7.6. Peaks in each titration were assigned and then were corrected for the effects of dilution during the titration. Finally the change of shift for each proton was calculated for each point in the titration.

5.3 Assignment of the Zn(II)PPIX proton NMR spectrum

Four types of protons are found in Zn(II)PPIX and these systems are easily differentiated in the proton NMR spectrum (Figure 5.1) based on the assignments of Abraham *et al.*[67].

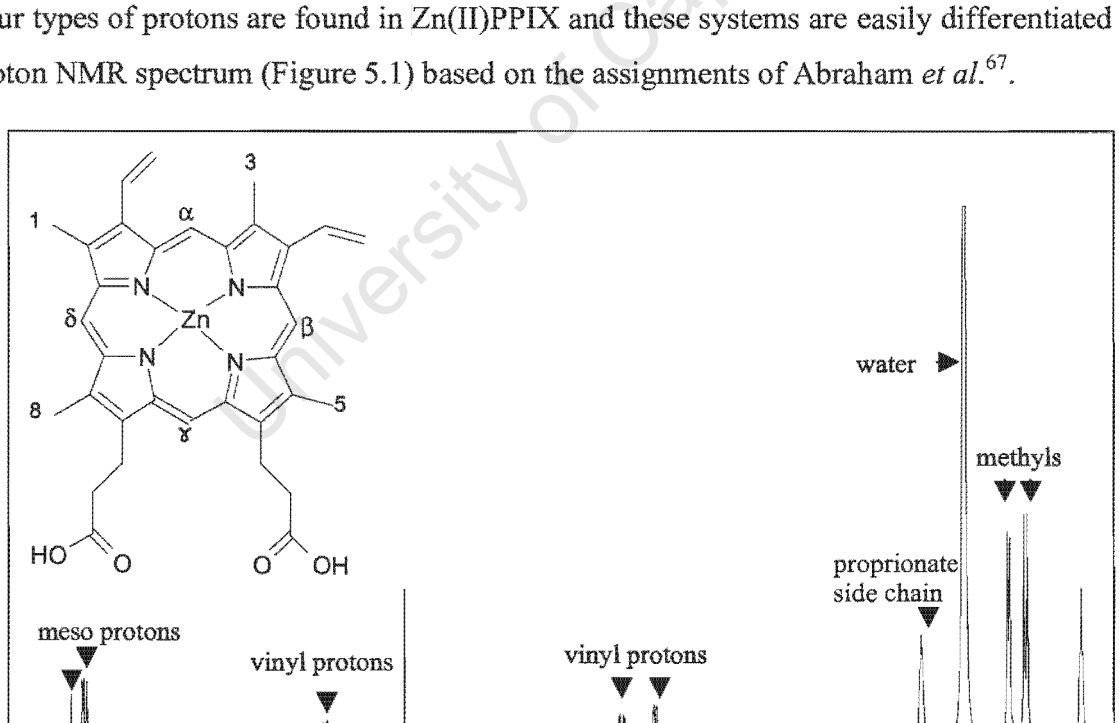

Figure 5.1 ^{1}H NMR spectrum of Zn(II)PPIX in 80% d6-DMSO, 20% D_2O including the numbering system of Zn(II)PPIX

University of Cape Town

There are four methyl groups attached to the ring and these give rise to four singlets, with peaks at 3.54 and 3.66 ppm which have the appearance of two doublets. The protons in the proprionate side chains give rise to two triplets, one at 4.3 ppm and the other at 3.2 ppm. These are both poorly defined due to their broadness. The vinyl protons give rise to three peaks. Two doublets of doublets arise from the protons of the carbon furthest from the aromatic ring at around 6 ppm. The vinyl proton closest to the ring gives rise to a multiplet at 8.4 ppm. Lastly, four singlet peaks arise from the meso protons and these are found at around 10 ppm. Solvent peaks at 2.5 ppm (DMSO) and 4.0 (H_2O) are prominent due to the rather low concentrations of Zn(II)PPIX. The three singlets at 2.71, 2.86 and 7.87 ppm are most likely due to DMF.

For the purposes of this chapter, a general assignment of Zn(II)PPIX is not sufficient and each of the meso and methyl proton peaks must be unambiguously assigned. This has been previously achieved in the literature[67] by using isotope labelling of Zn(II)PPIX dimethyl ester. This is very time consuming and extremely expensive. The sample reported in the literature was recorded in deutero-chloroform while in this study, a deutero-DMSO/ D_2O solvent system is being used and as a result the proton spectrum must be re-assigned since the change of solvent system could well affect the assignment of the closely spaced meso peaks and methyl peaks.

Using NOESY, it is theoretically possible to unambiguously assign all these peaks. The two sets of methyl singlets can be assigned based on their proximity to the proprionate side chains and with this assignment in place, the meso protons would each give rise to a unique coupling pattern to the vinyl, proprionate and methyl protons. Once the meso protons have been assigned, the methyl protons can then be fully assigned. Unambiguous assignment thus requires being able to detect NOE effects between the meso, vinyl, proprionate and methyl protons. The NOESY spectrum of Zn(II)PPIX is shown in Figure 5.2. There is considerable interference from water present in the sample as well as DMSO but what is of interest are the NOE effects detected between the meso, vinyl, proprionate and methyl protons which are more clearly shown in the expansions in Figure 5.3.

University of Cape Town

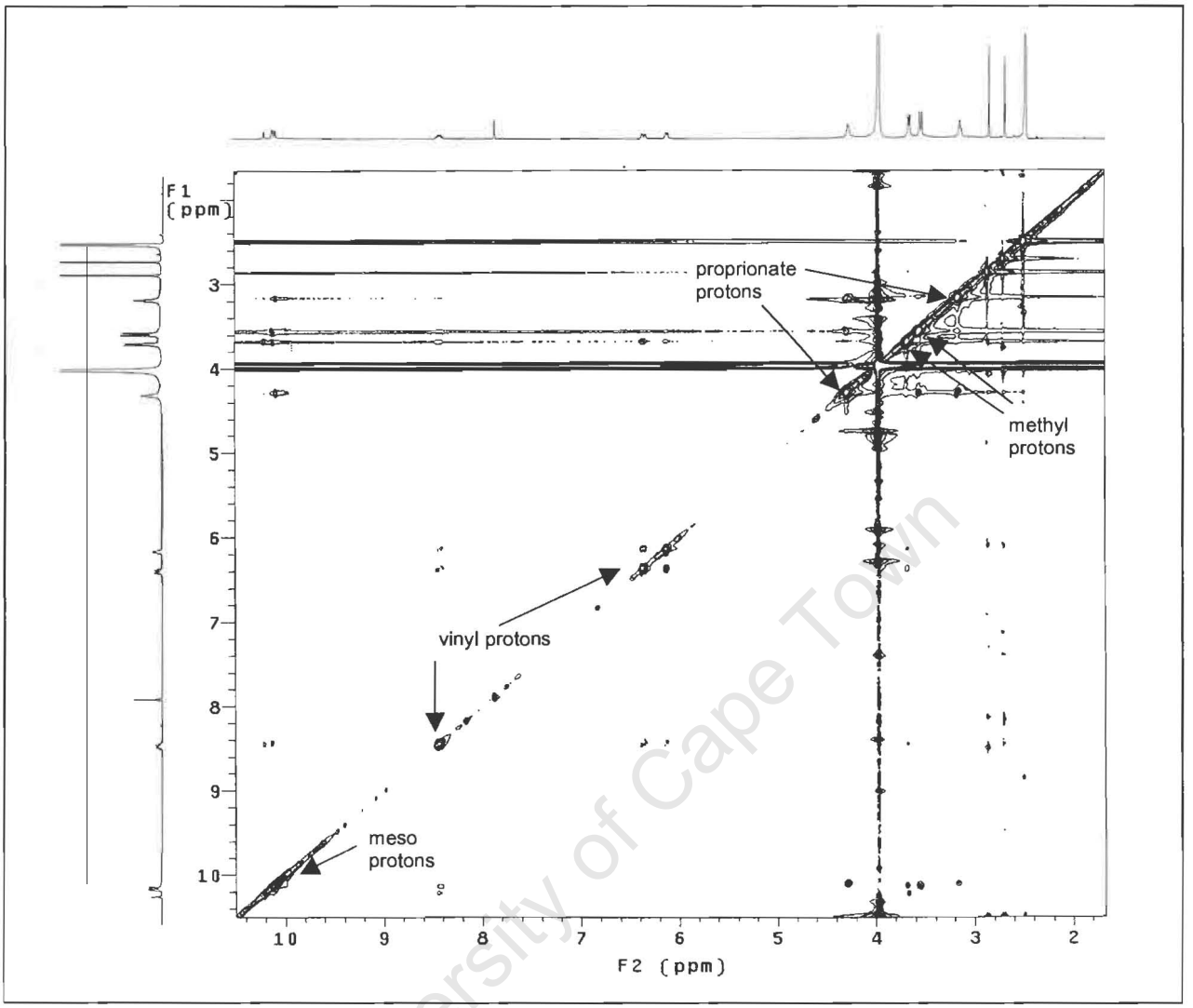

Figure 5.2 NOESY spectrum of Zn(II)PPIX in 80% deutero-DMSO, 20% D_2O

University of Cape Town

Correlation between two methyl peaks at 3.54 ppm and a proprionate peak is observed in Figure 5.3(A) while correlation is seen between the other pair of methyls and the vinyl protons. Thus the methyls at 3.54 ppm can be assigned as 5, 8 and those at 3.66 ppm can be assigned as the 1, 3 methyls (Figure 5.1). The meso protons in the NOESY spectrum can now be assigned and are observed as three contoured areas on the main diagonal of the spectrum between 10.08 and 10.21 ppm with the middle contoured region being broader than the other two regions and accounting for two protons. This is most clearly illustrated in the bottom left hand corner of Figure 5.3(B). The four peaks have been assigned *i* – *iv* in Figure 5.2(C) to clarify the process of their assignment.

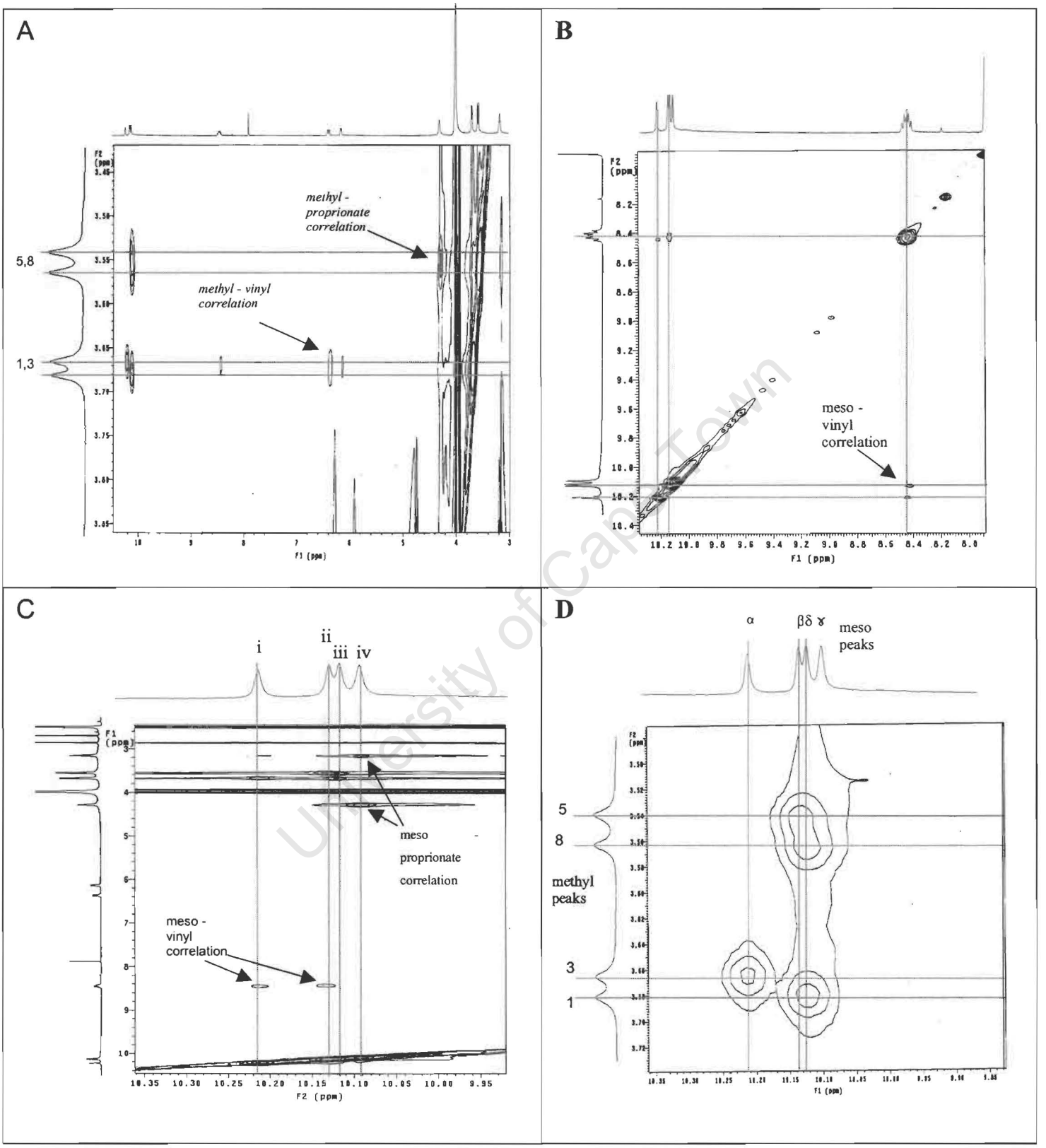

University of Cape Town

Figure 5.2 NOESY spectrum of Zn(II)PPIX showing various expansions and correlation peaks

Peak *iv* in Figure 5.2(C) can clearly be seen coupling to both propionate peaks and thus must be assigned as the ɤ proton. Peak *iii* shows no observable correlation with either the vinyl groups or the propionate chains and thus must be assigned as the δ proton. Finally peaks *i* and *ii* (Figure 5.2(C)) can be seen to couple to the inner vinyl proton and this is further illustrated in Figure 5.2(B). Due to their proximity to the vinyls, these peaks must correlate to the α and β protons. Figure 5.2(D) shows coupling between methyl and meso peaks. The α proton can now be assigned as the most down-field peak as it can be seen correlating to one of the 1,3 methyl peaks while the β meso proton is observed coupling to one of the 5,8 methyl peaks. Figure 5.4 shows the complete assignment of the meso protons.

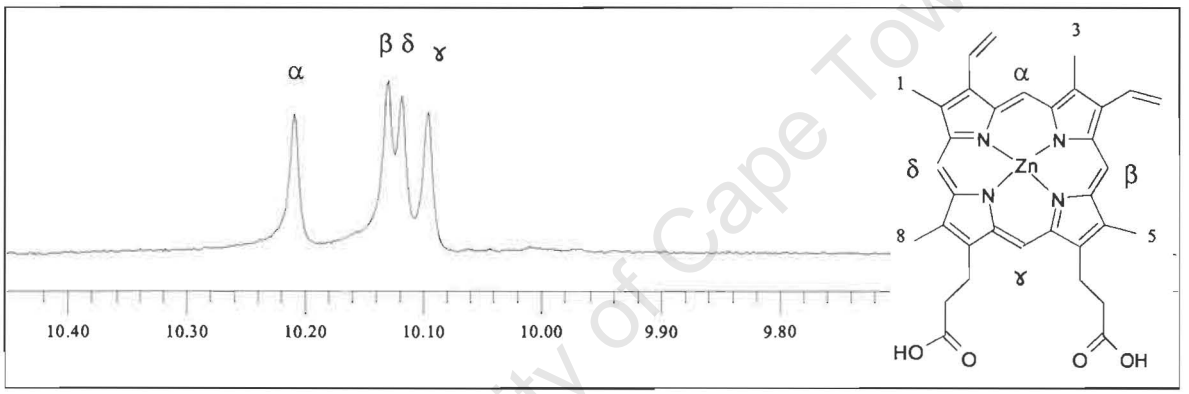

Figure 5.4 Assignment of meso protons in ^{1}H NMR spectrum of Zn(II)PPIX

University of Cape Town

Figure 5.3(D) shows the α proton correlating to a single methyl peak which must be assigned as methyl 3. Likewise, the β meso peak couples to a single methyl which is now assigned as 5. Finally, as it has been shown methyls 1 and 3 will be found in close proximity as will 5 and 8. As a result the remaining peaks, 1 and 8 can be assigned. The δ meso peak can also be seen coupling to methyls 1 and 8 which agrees with the assignments already made.

5.4 Interaction of platinum complexes with Zn(II)PPIX

Much information is available from the NMR spectra obtained during the titrations. These data includes the broadening of peaks upon interaction of the two compounds during the titration as well as possible changes in coupling constants. However, this study will concentrate upon the change of chemical shift. When molecules associate with each other, atoms experience a

change in their electronic environment which causes a change in their chemical shift. The greater the shift that occurs to a particular peak, the greater the change in the chemical environment of the proton giving rise to that resonance and hence that proton is experiencing a closer interaction with another molecule. When aromatic molecules interact, so do their ring currents which leads to a decreased induced magnetic field in the aromatic ring and thus protons in the plane of the one ring become less deshielded and more up-field as the second ring approaches above the first. As a result, in this chapter, a shift up-field will be defined as a positive shift to signify a "positive" interaction.

The effect of Zn(II)PPIX on Pt(bipy)L]Cl and Pt(diMebipy)L]Cl

Certain peaks arising from protons of the platinum complexes show large changes in chemical shifts when these complexes are titrated with Zn(II)PPIX. Figures 5.5 and 5.6 show the total changes in chemical shift of protons of [Pt(bipy)L]Cl and [Pt(diMebipy)L]Cl respectively. Due to extensive broadening of peaks, assignment was not always possible, particularly in the case of [Pt(diMebipy)L]Cl.

The titration curves can be found in the appendix and are not reproduced here as they do not add significantly to the understanding of the geometry of interaction between the platinum complexes and Zn(II)PPIX but they do show that the trends observed in Figures 5.5 and 5.6 are continued at different concentrations.

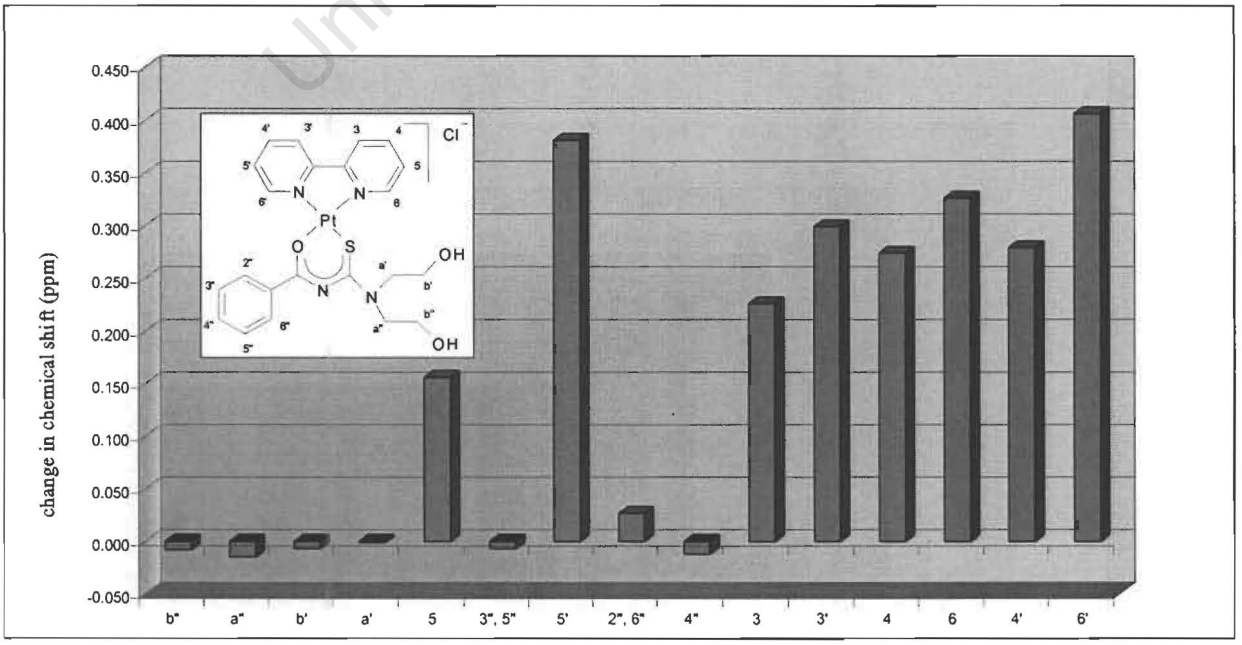

Figure 5.5 Shifts of ^{1}H NMR peaks of [Pt(bipy)L]Cl after 0.45 mol equivalents of Zn(II)PPIX was added

University of Cape Town

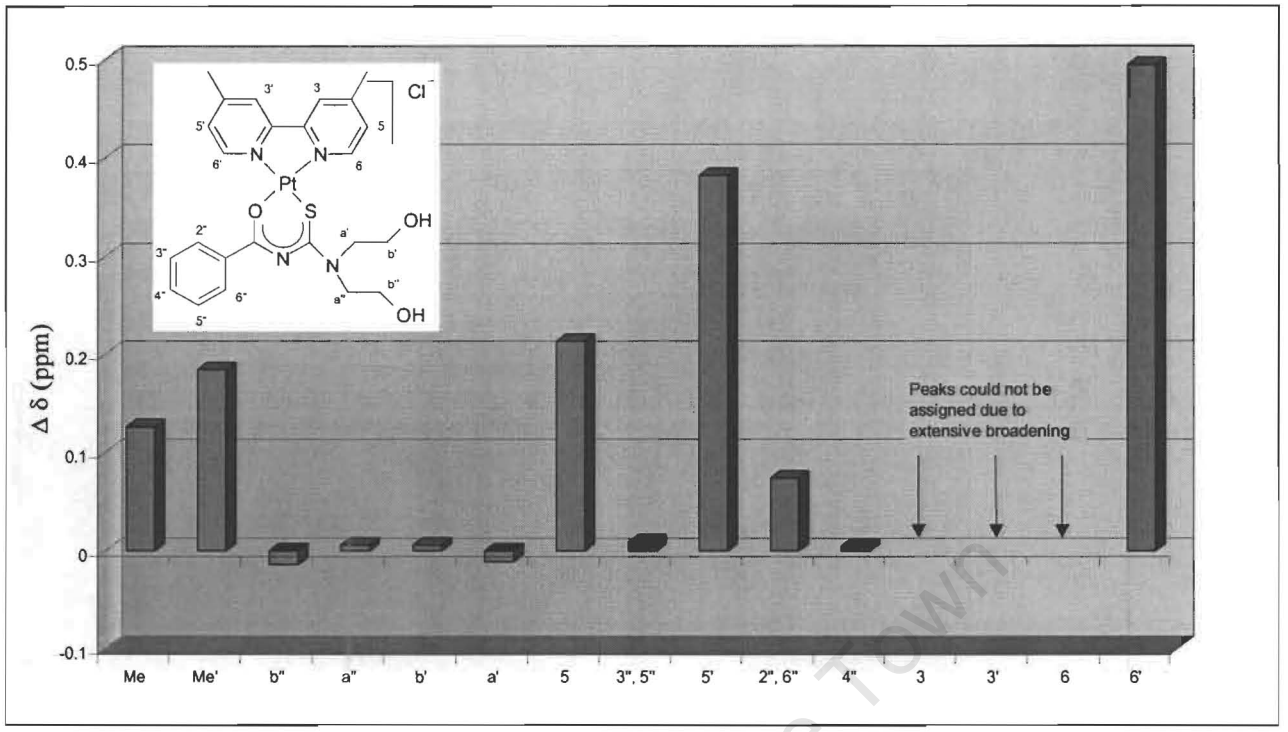

Figure 5.6 Shifts of ^{1}H NMR peaks of [Pt(diMebipy)L]Cl after 0.62 mol equivalents of Zn(II)PPIX was added

University of Cape Town

What is immediately apparent from Figures 5.5 and 5.6 is that the protons attached to bipyridyl ring system as well as methyl protons of [Pt(diMebipy)L]Cl are the most affected. This clearly supports the proposition made in Chapter 3, that it is the diimine portions of the platinum complexes which most strongly interact with the metalloporphyrin. Furthermore, the acyl protons, 2" and 6" of the benzene ring, also demonstrate involvement in the interaction albeit to a much lesser extent than the diimine protons while the other acyl protons, 3", 4" and 5", do not show a change in chemical shift.

A further trend which is apparent in both platinum complexes is that the side of the diimine that is *trans* to the sulphur donor atom of the acylthiourea (ring A), shows greater interaction with Zn(II)PPIX than the side *cis* to the sulphur (ring B). This is reflected in [Pt(diMebipy)L]Cl with the proton 5' showing a much greater change in chemical shift than the 5 proton and Me' also more affected than Me. In [Pt(bipy)L]Cl it can be noted that the change chemical shift of 5' is larger than 5 by an amount greater than in the case of [Pt(diMebipy)L]Cl. This trend continues, but to a lesser, extent in the other bipyridyl protons. The differentiation between the two rings of the bipyridyl probably results from the sulphur

atom withdrawing relatively more electron density away from the nitrogen *trans* to it (ring A) as discussed in Chapter 2.5. This would result in ring A, being more electropositive than ring B. As has already been shown in Chapter 3, electron withdrawal from the diimine causes a greater strength of interaction with metalloporphyrins. It may be speculated that ring A, which is less electron dense than ring B, is likely to interact more strongly with the aromatic ring system of Zn(II)PPIX, hence causing greater changes in chemical shift. This would be consistent with ring A lying over the porphyrin ring while ring B of the diimine is offset toward the metal in Zn(II)PPIX, or away from the porphyrin ring.

If dilution effects are not taken into account (Figure 5.7), the emerging trends are essentially the same as those already described which do correct for dilution. This confirms that the major interaction taking place is indeed between the platinum complexes and Zn(II)PPIX rather than a change in the extent of self association due to dilution effects dominating the interaction.

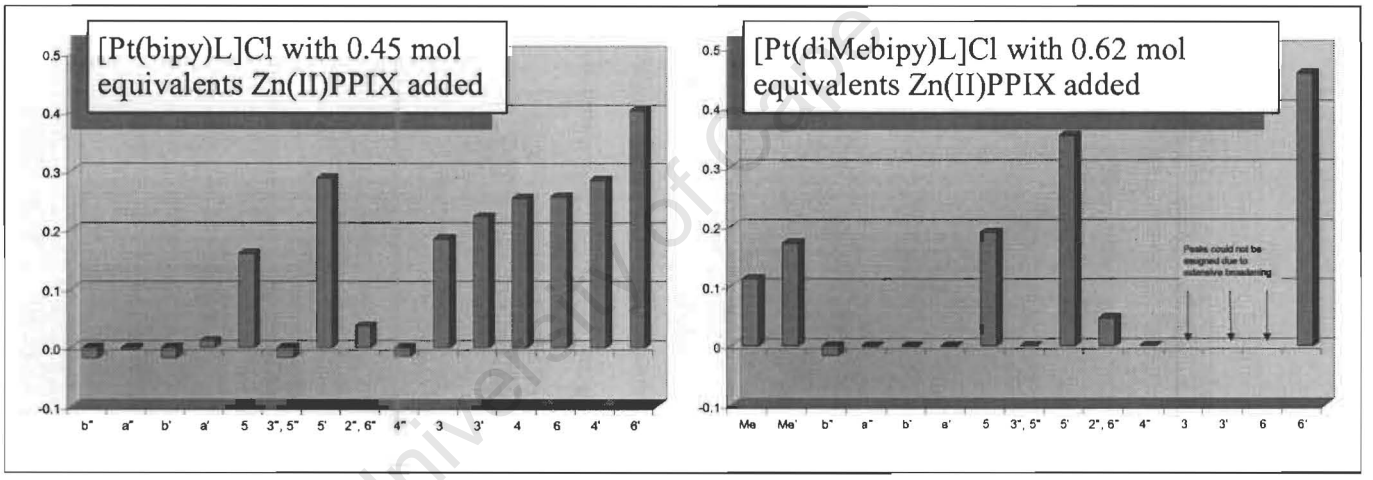

Figure 5.7 Chemical shifts of the platinum complexes' protons upon addition of Zn(II))PPIX without adjustment of the chemical shift due to changing concentration of the platinum complexes

University of Cape Town

The effect of [Pt(bipy)L]Cl and [Pt(diMebipy)L]Cl on Zn(II)PPIX

When comparing the change in chemical shifts of Zn(II)PPIX upon the addition of the two platinum complexes, [Pt(bipy)L]Cl and [Pt(diMebipy)L]Cl, trends emerge which have both similarities and some differences. The changes in shifts in the proton resonances of Zn(II)PPIX can be seen in Figure 5.8. The overall trends are the same regardless of whether [Pt(bipy)L]Cl or [Pt(diMebipy)L]Cl is added with the meso protons that undergo the largest changes in

chemical shift. The next most affected groups are the vinyl and methyl protons, as well as the methylene protons closest to the porphyrin aromatic ring system. The methylene protons furthest from the ring are affected to a negligible extent. A trend emerges for both platinum complexes where both the meso and methyl protons furthest from the proprionate chains show greater interaction than those closest to the side chains. Furthermore in each graph in Figure 5.8 it can be seen that the δ proton is more affected than the β proton and that the 3 methyl peak shifts more than the 1 methyl peak.

Apart from the similar trends observed for the resonances of Zn(II)PPIX with addition of the two platinum complexes, some differences are also observable in these spectra. Figure 5.8(A) shows that the meso protons α, β and δ are all shifted significantly more than ɤ by [Pt(bipy)L]Cl which contrasts with what is observed in Figure 5.8(C). Here the α proton shows a slightly greater interaction with [Pt(diMebipy)L)Cl than the rest of the meso protons, all of which are shifted by similar values. This pattern is partially carried through at higher concentrations of platinum complexes (Figures 5.8(B) and 5.8(D)). The only difference is that at higher [Pt(diMebipy)L]Cl concentrations, the meso proton ɤ, shows slightly smaller shifts than protons, α, β and δ. It is also observed that both sets of methylene protons (CH_2' and CH_2") undergo larger shifts with addition of [Pt(diMebipy)L]Cl than with [Pt(bipy)L]Cl.

Considering all these changes in the chemical shifts on titrating Zn(II)PPIX with [Pt(bipy)L]Cl and [Pt(diMebipy)L]Cl and *visa versa* it now becomes possible to qualitatively and tentatively propose geometries of interaction between the platinum complexes and Zn(II)PPIX. Because of the relatively long NMR time scale, the chemical shift changes that have been described are due to an average of a number of possible geometries between Zn(II)PPIX and the platinum complex. Thus it is not appropriate to assign a single geometry but rather a range of favoured geometries.

University of Cape Town

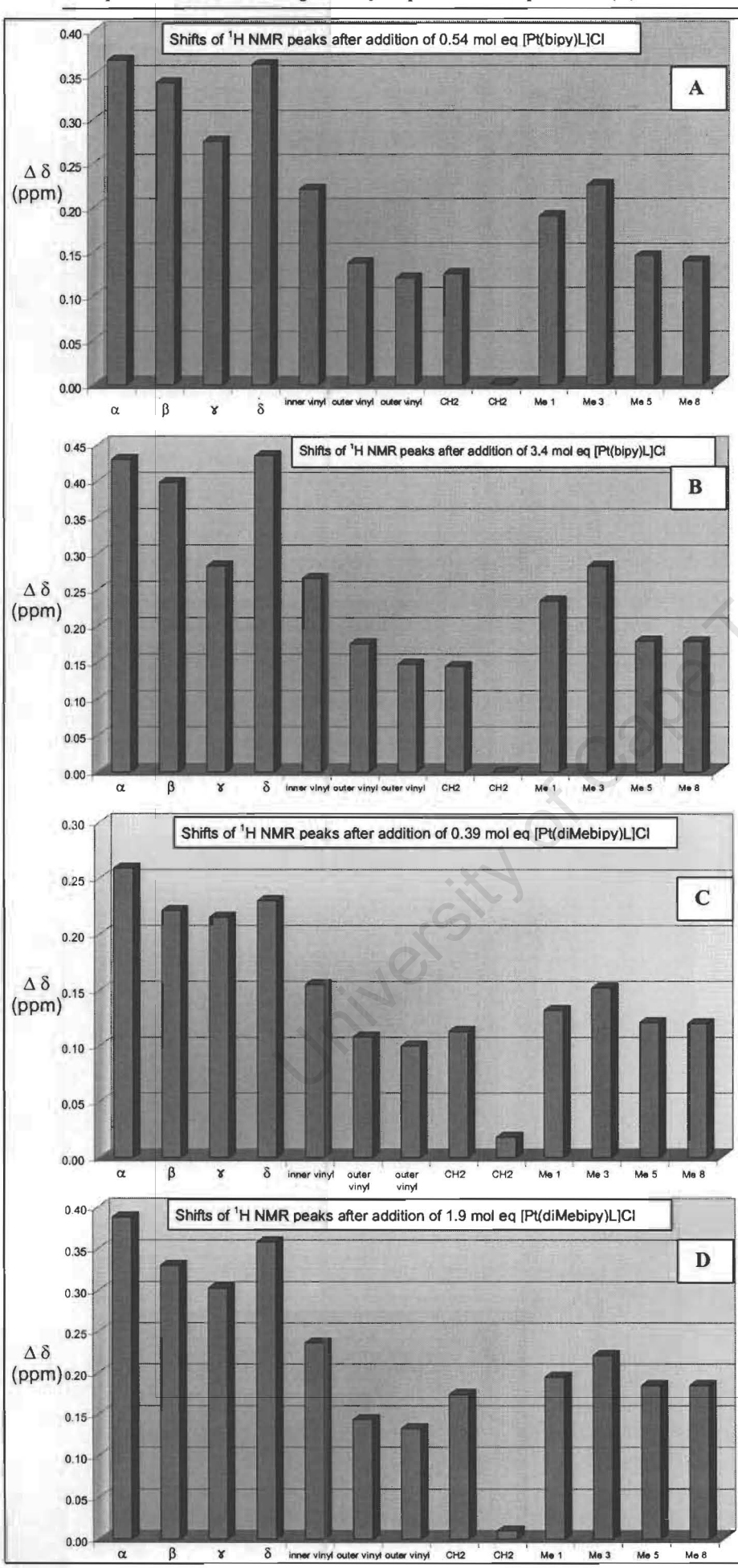

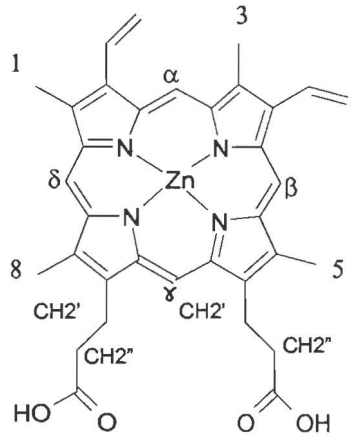

Figure 5.8 Changes in chemical shift of Zn(II)PPIX proton peaks observed upon addition of [Pt(bipy)L]Cl and [Pt(diMebipy)L]Cl

University of Cape Town

The overall structure of the aggregate between [Pt(bipy)L]Cl and Zn(II)PPIX should be consistent with the following observations:

- Dominant interactions existing between the diimine of the platinum complex and the aromatic pyrrole rings
- The relatively larger changes in shifts of the protons of the A ring of the bipyridyl trans to the sulphur donor of the acylthiourea moiety interacting with the porphyrin pyrrole ring system rather than interacting with the metal in the porphyrin or offset from the porphyrin ring system.
- Some interaction existing between the 2" and 6" protons of the acylthiourea and Zn(II)PPIX but not between the other protons of the acyl group of the acylthiourea and the porphyrin
- Very little or no interaction between the pendant side chains of the acylthiourea and the porphyrin
- A preference of the α, β and δ meso protons of Zn(II)PPIX in the interaction with the diimine of [Pt(bipy)L]Cl compared to the ɤ meso proton of the porphyrin
- A slightly greater interaction of the platinum complex with the δ proton compared with the β proton
- Greater interaction of the platinum complex with the 1 and 3 methyls rather than the 5 and 8 methyls with 3 methyl being favoured
- Some interaction of [Pt(bipy)L]Cl with the porphyrin vinyl group
- Some interaction of [Pt(bipy)L]Cl with the methylene group closest to the porphyrin ring and virtually none with methylene group further away from the porphyrin ring
- Minimised overall steric interactions

In order to develop a plausible structure for the Zn(II)PPIX – platinum complex aggregate, it is highly likely that areas of low electron density of [Pt(bipy)L]Cl interact most strongly with the most negatively charged areas of the metalloporphyrin as this would be most energetically favourable. This also correlates to the model studies of Hunter and Saunders[62] which show that

University of Cape Town

when two porphyrins interact, the pyrrole ring (electron dense) of one porphyrin is located over the central cavity or metal of another porphyrin where the electron density is lower. Therefore the positively charged platinum ion is likely to be found interacting with the electron dense pyrrole rings in Zn(II)PPIX. Hunter and Saunders[62] have also shown π-π interactions to result in molecules being off-set. Figure 5.9 graphically represents 4 possible structures representing the interaction between [Pt(bipy)L]Cl and Zn(II)PPIX that takes into account all of these requirements. In solution, the best model is likely to be an average of these possible structures, as well as additional structures which are likely to occur.

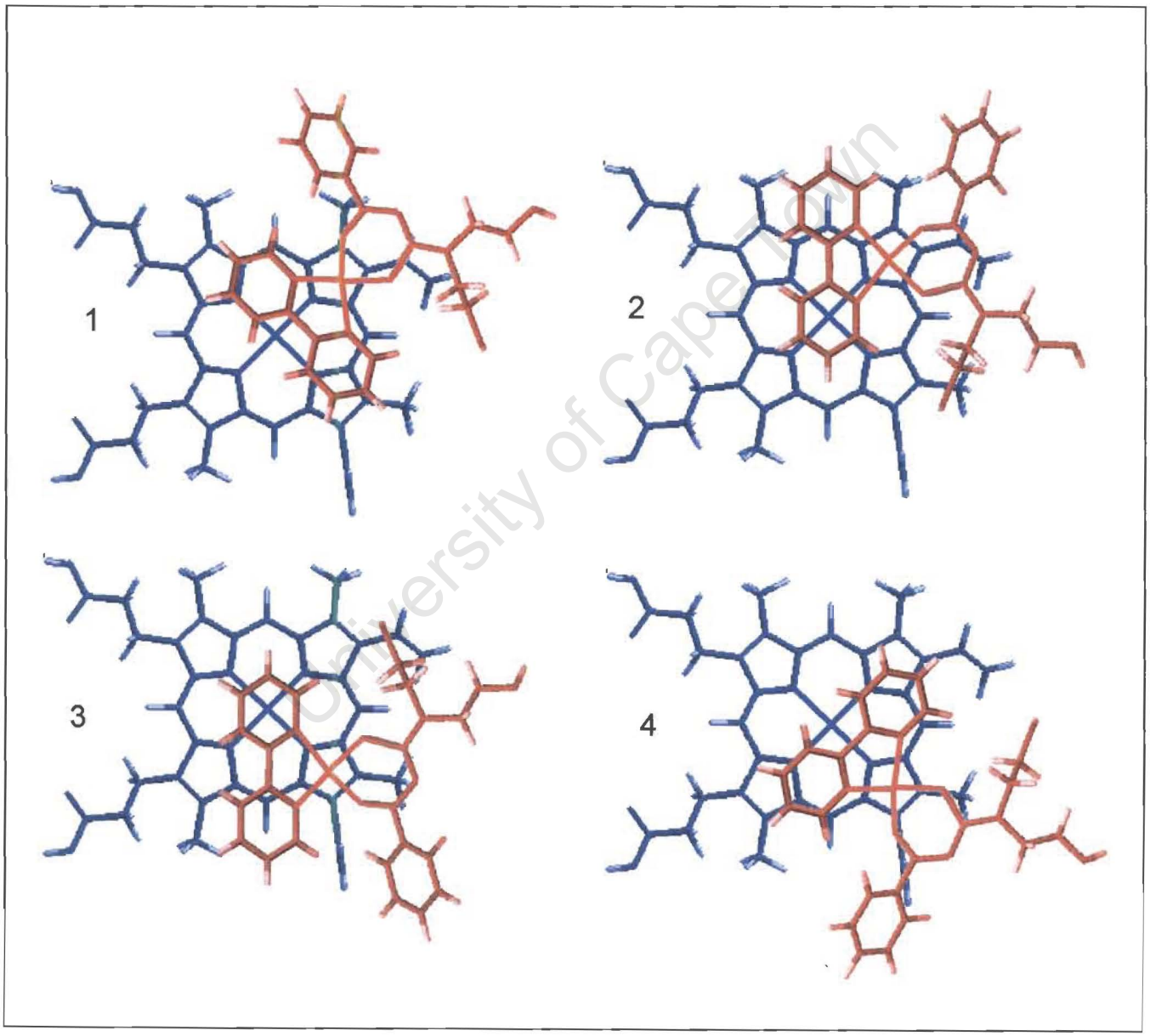

University of Cape Town

Figure 5.9 Several likely structures adopted when [Pt(bipy)L]Cl interacts with Zn(II)PPIX

In structure 1 in the Figure 5.9, ring A of the diimine is likely to cause a greater shift in the δ meso proton compared to the effect of ring B on the β-proton. The α proton also is in close proximity to the diimine ring and will be strongly affected. The diimine is also closer to the 3 methyl than the 1 methyl of the porphyrin. Interaction of the 2" and 6" acyl protons with the vinyl is also possible. The respective side chains of the molecules are also seen not to be near the area of overlap. In structure 2, it can be seen that ring A of the diimine is able to interact with the porphyrin ring while ring B is found over the metal of the porphyrin. The α proton is once again in close proximity to the diimine and this time the 1 methyl is favoured over the 3 methyl. In structure 3 the 3 methyl is favoured over the 1 methyl but the β proton will experience a changed chemical environment while the δ proton will not. In structure 4, similar trends emerge as for conformation 3 except that the α meso proton once again has closer proximity to the diimine. Thus it can be seen that a dynamic equilibrium of all four of these conformations and to a lesser extent those described in Figure 5.10 could lead to the observed changes in the NMR spectra of both [Pt(bipy)L]Cl and Zn(II)PPIX.

As has already been shown, [Pt(diMebipy)L]Cl results in somewhat different trends in shifts of the Zn(II)PPIX protons as compared to [Pt(bipy)L]Cl. Thus the range of geometries of the overall complex formed between [Pt(diMebipy)L]Cl and Zn(II)PPIX should reflect the following changes as compared to the interaction [Pt(bipy)L]Cl and Zn(II)PIIX.

- Slightly less differentiation between rings A and B of the diimine in the interaction with the porphyrin ring
- Greater interaction of the 2" and 6" acyl protons with Zn(II)PPIX
- Greater involvement of the ɤ proton of Zn(II)PPIX in the interaction with [Pt(diMebipy)L]Cl
- Greater involvement of the proprionate side chains of Zn(II)PPIX in the interaction

University of Cape Town

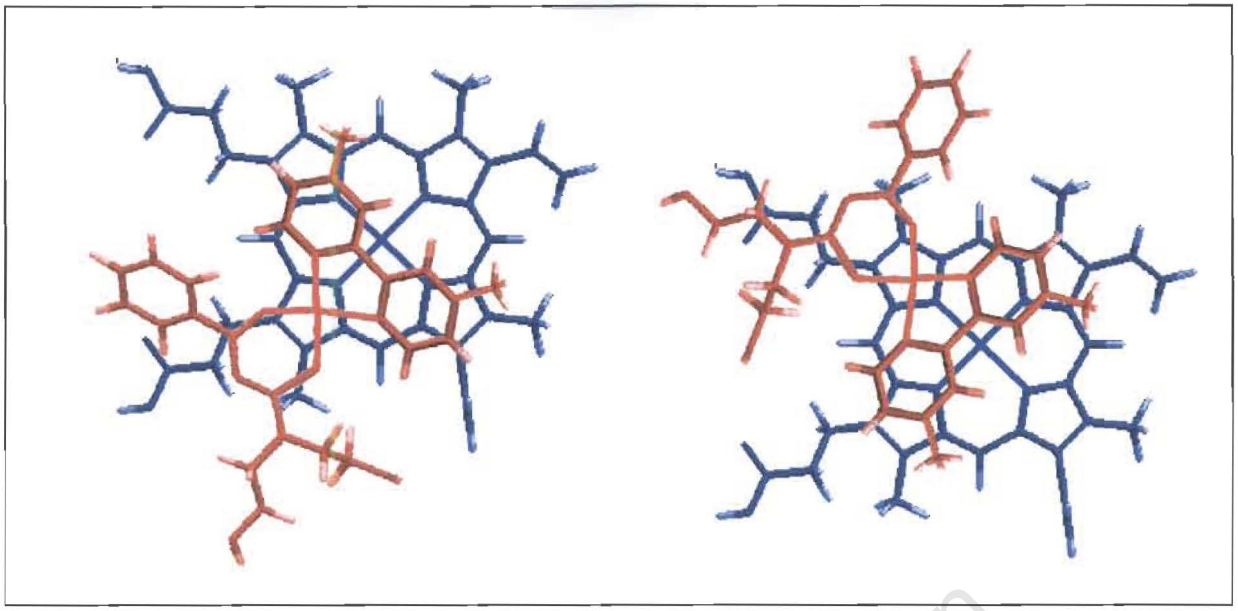

Figure 5.10 Possible additional geometries favoured in the interaction between [Pt(diMebipy)L]Cl and Zn(II)PPIX

In the two structures shown in Figure 5.10, it can be seen that both the A and B rings are involved in a similar way leading to a lessening of the differentiation of their shifts. The two structures also may result in some increased interaction between the methylene protons, the 5 and 8 methyl protons and the ɤ proton, with the platinum complex. If the geometries suggested in Figure 5.10 in addition to those depicted in Figure 5.9 are more prominent in the interaction between [Pt(diMebipy)L]Cl and Zn(II)PPIX, then the points mentioned on the previous page would be satisfied.

5.5 Conclusion

It has clearly been demonstrated that it is the diimine portion of the platinum complexes which interact with the porphyrin ring. Convincing evidence from the NMR study suggests π-π or π-cation stacking interactions dominating the aggregation formation. In addition it has been found that the aggregation of [Pt(diMebipy)L]Cl with Zn(II)PPIX, appears to form a wider range of structures compared aggregation of [Pt(bipy)L]Cl and Zn(II)PPIX. This might result in the difference in the ability of the two platinum complexes to inhibit the formation of β-haematin, despite statistically equivalent association constants. If the same effect persists in the complexes with Fe(III)PPIX, the greater mobility of the [Pt(diMebipy)L]Cl – Fe(III)PPIX complex may permit the attack of the propionate side chain of a second Fe(III)PPIX molecule

University of Cape Town

and thus this platinum complex is not an efficient inhibitor of β-haematin formation. This indicates that the phenomenon of β-haematin inhibition may originate in the dynamic properties of the Fe(III)PPIX complexes formed and not in their thermodynamic properties.

While this NMR study has brought greater insight into the nature of the interactions between metalloporphyrins and platinum complexes of the type described here, it is clear that the results obtained give at best a broad understanding rather than a detailed description of the geometries adopted. To gain greater clarity, this system could possibly be modelled computationally. What is more, computational modelling would allow both the study of Fe(III)PPIX instead of Zn(II)PPIX and the modelling of a pure aqueous solvent system which is not experimentally available using NMR.

University of Cape Town

6 Overall conclusions

A range of platinum complexes was successfully synthesised using acylthiourea, various diimine and 2-phenylpyridine ligands. The association constants of these complexes with haematin was investigated and their ability to inhibit the formation of β-haematin was determined.

Association with haematin was determined using spectrophotometric titrations and a 1:1 binding model was found to be most suitable in describing this association. The following trends emerged from this study.

No observable association

2,2'-bipyridine ligands

HL'

cis-[PtL_2]

[Pt(ppy)L']

7,8-benzoquinoline

HL

1,10-phenanthroline ligands

[Pt(dtbbipy)L]Cl, [Pt(bipy)L]Cl, [Pt(diMebipy)L]Cl

[Pt(bipy)L']Cl

[Pt(phen)L]Cl, [Pt(4-Me phen)L]Cl, [Pt(5-Me phen)L]Cl

[Pt(3,4,7,8-tetraMe phen)L]Cl, [Pt(5-Cl phen)L]Cl, [Pt(5-NO_2 phen)L]Cl

Strong association

University of Cape Town

The most likely interactions between the platinum complexes and haematin were found to be taking place through π-π or π-cation stacking interactions between the diimine moiety of the platinum complex and the porphyrin ring. It was found that platinum enhances the association of the diimine with haematin. A larger diimine surface area results in stronger association with haematin as do electronic withdrawing groups on the diimine but the introduction of these groups result in greater difficulties in the synthesis of these complexes.

The complexes which associate strongly with haematin were also found to inhibit the formation of β-haematin to some extent which none of the unbound ligands themselves were able to achieve. In the case of [Pt(bipy)L]Cl, association with haematin in the solid state takes

place, which complements the finding in Chapter 3 in which solution based interactions are shown to occur, and it is expected that the other charged platinum complexes would also interact with haematin in the solid state.

An interesting result is that while [Pt(diMebipy)L]Cl has a marginally greater association with haematin than [Pt(bipy)L]Cl, the former complex is less efficient in the inhibition of β-haematin formation. This result was investigated in Chapter 5 where the geometries of the interaction between these two platinum complexes with zinc(II) protoporphyrin IX was described. It was found that the two complexes interact differently with the porphyrin and that [Pt(bipy)L]Cl almost certainly adopts a smaller range of favoured geometries with Zn(II)PPIX. These observations may be important in building a deeper understanding of the factors that influence the ability of a compound to inhibit the formation of β-haematin. Previous work[19 and ref. within] has shown that while binding of a compound to haematin is required to inhibit β-haematin formation, some complexes which associate strongly with haematin do not inhibit β-haematin formation. It has also been shown that for quinoline systems, substitution of a strongly electron withdrawing group on the 7 position of the ring causes 4-aminoquinolines to inhibit the formation of β-haematin without markedly changing the strength of association with haematin[54]. These observations indicate that the electronic distribution in the aromatic ring is likely to be an important factor. The current work builds on these findings and gives greater insights into how the geometry of the overall complex between haematin and an interacting molecule influences the compound's ability to inhibit the formation of haemozoin and hence impact upon its potential antimalarial activity. Future work investigating the interaction of Zn(II)PPIX with a number of known antimalarial drugs and closely related compounds which do not show activity against the parasite should prove very useful in gaining further insights into the processes involved in the inhibition of β-haematin.

The findings of the preliminary biological study in Chapter 4.5 vindicate the suggestion that the platinum complexes in this study do have potential as templates for novel antimalarial drugs as the complexes are toxic to malaria parasites albeit at a concentration 30 greater than that of chloroquine. As all the charged platinum complexes in this study associate strongly with haematin and inhibit the formation of β-haematin, their lesser activity, as contrasted to chloroquine, is most likely due to their poorer biological distribution. As has been mentioned in Chapter 1, pH trapping markedly increases the concentration of chloroquine and other weak

University of Cape Town

base containing drugs in the food vacuole of the parasite. Neutral platinum complexes would appear to be the best option as the are likely to cross cell membranes with greater ease than their charged counterparts. However, it must be noted that these neutral complexes generally have low solubilities in aqueous systems. A feasible option however, involves the synthesis of zwitterions which are overall formally neutral yet should remain in solution in an aqueous medium. An example of such a complex is seen in top left hand corner of Figure 6.1. As charged complexes which have good antiplasmodial activity are known (Chapter 1.6), it is also suggested that future work proceed with remaining complexes in Figure 6.1. Therefore these complexes should be synthesised, investigated for their interaction with haematin, ability to inhibit the formation of β-haematin formation and be tested for activity against *Plasmodium falciparum*. These compounds would all be expected to bind to haematin and since they include weak bases, they may have good potential to accumulate by means of pH trapping in the food vacuole of the parasite. Incorporating the amine onto the diimine should limit the polarisation of the molecule into hydrophilic and hydrophobic halves. Exchanging an acyl group for ditertiarybutyl group on the acylthiourea may further improve the bio-availability of the compound.

In conclusion, this work has shown that strong interactions occur between platinum complexes of the type [Pt(diimine)acylthiourea]Cl and haematin and that these complexes are able to inhibit the formation of β-haematin with some of these complexes showing moderate activity against malaria parasites. Thus future work suggested in this chapter should be pursued as this class of compounds does appear to have potential antimalarial activity.

University of Cape Town

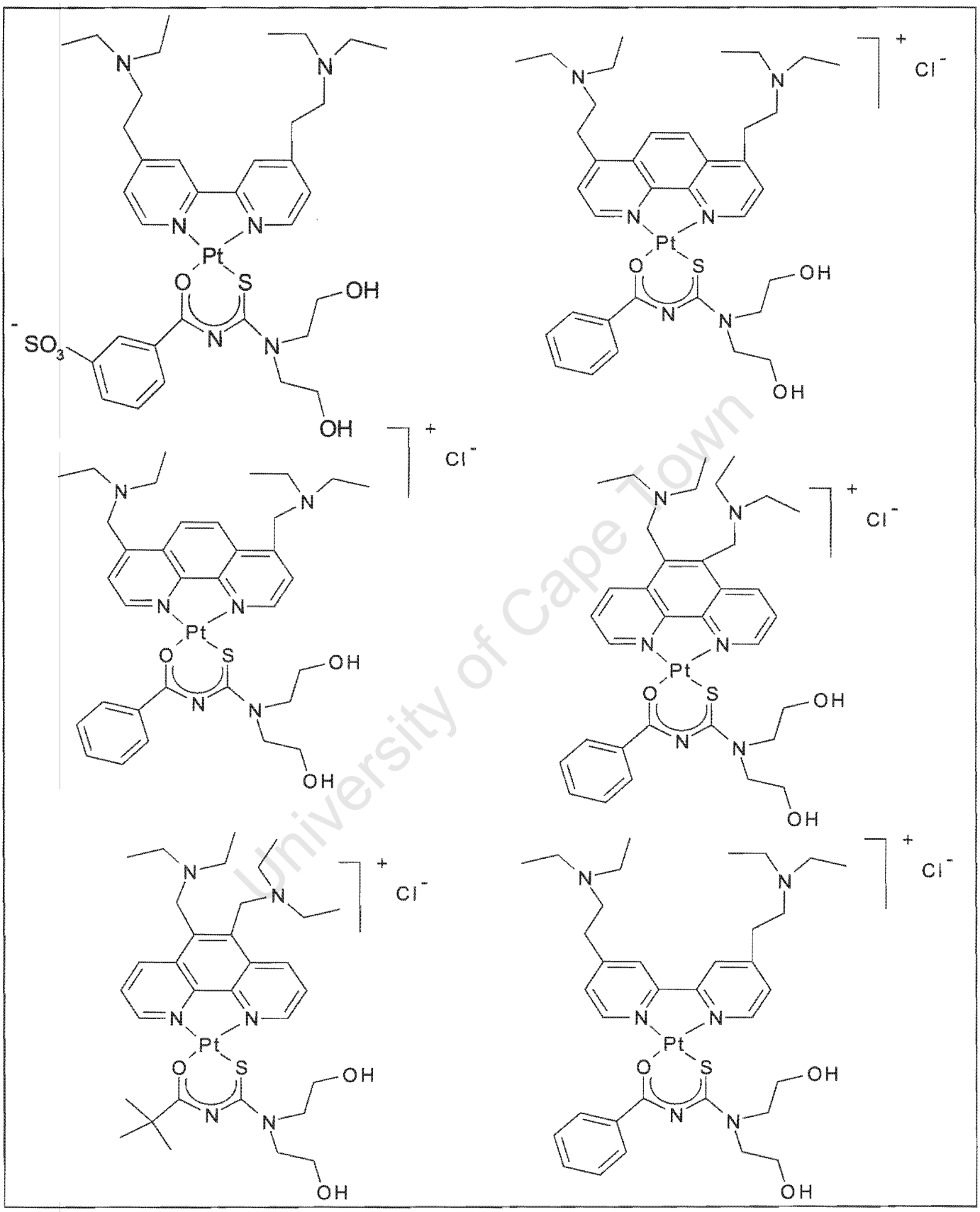

University of Cape Town

Figure 6.1 Proposed structures of complexes to be synthesised as part of future possible work

7 Experimental

7.1 Materials for synthesis

All reagents used in the synthesis of acylthioureas were commercially available through Sigma-Aldrich Chemicals and were used without further purification. Acetone was distilled and dried over 4Å molecular sieves. The diimines used in the synthesis of Pt(diimine)Cl_2 were commercially available through Alfa Aesar or Sigma-Aldrich except 4,4'-di-*tert*-butyl-2,2'-bipyridine which was synthesised from 4-*tert*-butyl-2,2'-pyridine obtained from Sigma-Aldrich. Potassium tetrachloroplatinate was obtained on loan from Johnson Matthey plc.

7.2 Instrumentation for synthetic characterisation

Elemental analyses for %C, H, N and S were was run on a Fissions EA 1108 elemental analyser by Mr Piero Benincasa of the Department of Chemistry, University of Cape Town. Mass spectra were recorded on a VG Quattro Fissions electrospray mass spectrometer courtesy of Dr. Thinus van der Merwe of the Department of Biochemistry, University of Stellenbosch. Sixty percent methanol water solutions were used for all compounds except for *N*-benzoyl-*N'N'*-di-2-hydroxyethylthiourea (L) (acetonitrile), $Pt(L)_2$ (50% acetonitrile water + trace DMSO), Pt(2-phenylpyridine)(*N*-benzoyl-*N',N'*-bisdiethyl-aminoethylthiourea) (50% acetonitrile water) and Ga(III)protoporphyrin IX (methanol + trace DMSO). Melting points were measured on a Reichert-Jung Thermovar attached to a DP-4 digital thermometer and are uncorrected. ^{1}H and ^{13}C nuclear magnetic resonance spectra were recorded on Varian Mercury 300 MHz FT-NMR, Varian Unity 400 MHz FT-NMR or Varian INOVA 600 MHz spectrometers using 5mm tubes at 30 °C unless otherwise stated. All shifts were referenced relative to tetramethylsilane. UV-visible spectra were recorded on a HP-8452A UV-Visible diode array spectrophotometer using quartz cuvetts. Infrared spectra were run on a Perkin Elmer 983 spectrometer using KBr discs pressed under 10 tons of pressure.

University of Cape Town

7.3 Preparation of Compounds

7.3.1 Preparation of 4,4'-ditertiarybutyl-2,2'bipyridine[110]

1.0 g of palladium on charcoal (10% palladium) was degassed at 180 °C for 8 hours and added to a Schlenck tube under a nitrogen atmosphere. To this was added 25 ml of 4-tert-butyl-pyridine and the mixture was heated at approximately 200 °C for 6 days. After cooling, 75 ml

dry THF was added to the Schlenck tube. The mixture was filtered trough celite to remove the catalyst and then the total volume was reduced to 75 ml under vacuum. Following this, 30 g of neutral alumina was added, then all solvent was removed. Unreacted 4-tert-butyl-pyridine was removed by heating at 120 °C under vacuum. The desired product was collected by sublimation under vacuum at 180 – 190 °C. The product was then dissolved in THF and filtered twice to remove alumina. Finally the solvent was removed under vacuum yielding 4.14 g (18%) of pure 4,4'-di-tert-butyl-bipyridine as white crystals. Melting point 159 °C (lit., [110] 156 °C). *Anal.* Calc. for $C_{18}H_{24}N_2$: C, 80.55; H, 9.01; N, 10.44; M^+ 269. Found: C, 80.63; H, 8.76; N, 10.22%; M^+ 268.88; δ_H (399.95 MHz; solvent $CDCl_3$; reference $SiMe_4$) 8.59 (2H, dd, J=5.2 and 0.8 Hz, H_6, $H_{6'}$), 8.41 (2H, dd, J=1.8 and 0.6 Hz, H_3, $H_{3'}$) 7.29 (2H, dd, J=5.2 and 0.8 Hz, H_5, $H_{5'}$), 1.38 (18H, s, CH_3); δ_C (100.58 MHz; solvent $CDCl_3$; reference $SiMe_4$) 160.96 (C_2, $C_{2'}$), 156.56 (C_4, $C_{4'}$), 149.03 (C_6, $C_{6'}$), 120.68 (C_5, $C_{5'}$), 118.29 (C_3, $C_{3'}$), 34.97 (C_7, $C_{7'}$), 30.62 (CH_3)

7.3.2a Preparation of *N*-benzoyl-*N'*,*N'*-di-2-hydroxyethylthiourea[109]

Acetone was distilled over 4 Å Linde molecular sieves and K_2CO_3 and added to dry potassium thiocyanate (0.04 mol) in a two necked round bottom flask under a nitrogen atmosphere. Heating under reflux caused the potassium thiocyanate to dissolve, and to this solution benzoyl chloride (0.04 mol) was added dropwise with constant stirring. Immediate formation of a potassium chloride precipitate was noted. After the mixture was refluxed for 1 hour, diethanolamine (0.04 mol) dissolved in acetone was added dropwise and the mixture was refluxed for a further 5 hours. Upon cooling, a minimum volume of water was added to dissolve all the potassium chloride. Further cooling to 10 °C resulted in crystallisation of the product. This was filtered off and further product was precipitated from the supernatant by removal of acetone under vacuum. Recrystallisation from an ethanol water mixture gave 8.00 g (75%) of a white crystalline material. Melting point 120-121 °C (lit., [109] 120-122 °C). *Anal.* Calc. for $C_{12}H_{16}N_2O_3S$: C, 53.73; H, 6.01; N, 10.45; S, 11.90 M^+ 269. Found: C, 53.84; H, 6.00; N, 10.46; S, 11.83%; M^+ 268.93; δ_H (399.95 MHz; solvent CD_3CN; reference $SiMe_4$) 10.42 (1H, s, NH) 7.88 (2H, d, J=8.0 Hz, H_2, H_6), 7.62 (1H, t, J=7.3 Hz, H_4) 7.52 (2H, t, J=7.5 Hz, H_3, H_5), 4.04 (2H, unres. m, $H_{a'}$), 3.92 (2H, unres. m, $H_{a''}$), 3.85 (4H, unres. m, $H_{b'}$, $H_{b''}$), 3.17 (1H, broad, OH'), 2.16 (1H, s, OH''); δ_C (100.58 MHz; solvent CD_3CN; reference $SiMe_4$) 181.81 (C=S), 165.86 (C=O), 134.38 (C_1), 132.66 (C_4), 128.92 (C_3, C_5), 127.99 (C_2, C_6), 60.26 ($C_{b'}$), 59.14 ($C_{b''}$), 54.99 ($C_{a'}$), 54.71 ($C_{a''}$)

University of Cape Town

7.3.2b Preparation of *N*-benzoyl-*N'*,*N'*-bisdiethylaminoethylthiourea

This acylthiourea was prepared according to the general method reported by Douglass and Dains[102]. Acetone was distilled over 4 Å Linde molecular sieves and K_2CO_3 and added to dry potassium thiocyanate (3.78 mmol) in a two necked round bottom flask under a nitrogen atmosphere. Refluxing caused the potassium thiocyanate to dissolve and to this, benzoyl chloride (3.78 mmol) was added dropwise with constant stirring with immediate formation of a potassium chloride precipitate. After the mixture was refluxed for 40 minutes, tetraethyldiethylenetriamine (3.78 mmol) dissolved in acetone was added dropwise and the mixture was refluxed for a further 3 hours. The solution was filtered to remove potassium chloride and then acetone was removed under vacuum to yield an oil. This was purified by column chromatography using 40 g silica gel (60 mesh) with an eluting solvent of 2% concentrated ammonia solution in methanol. The product fraction was reduced in volume and then diethyl ether was added, resulting in a crystalline product which was further recrystallised from diethyl ether and dried yielding a mass of 0.79 g (57%). Melting point 98-99 °C. *Anal.* Calc. for $C_{20}H_{34}N_4OS$: C, 63.51; H, 9.05; N, 14.80; M^+ 379. Found: C, 63.63; H, 9.31; N, 14.64; M^+ 378.60; δ_H (300.077 MHz; solvent acetone-d_6; reference $SiMe_4$) 7.76 (2H, d, J=7.6 Hz, H_2, H_6), 7.54 (1H, t, J=7.2 Hz, H_4) 7.46 (2H, t, J=7.5 Hz, H_3, H_5), 3.92 (2H, t, 6.8 $H_{a'}$), 3.87 (2H, unres. m, $H_{a''}$), 2.82-2.87 (4H, unres. m, $H_{b'}$, $H_{b''}$), 2.60 (4H, q, J=7.2 Hz, $H_{c'}$, $H_{e'}$), 2.57 (4H, q, J=7.2 Hz, $H_{c''}$, $H_{e''}$), 1.04 (6H, t, J=7.2 Hz, $H_{d'}$, $H_{f'}$), 099 (6H, t, J=7.0 Hz, $H_{d''}$, $H_{f''}$); δ_C (75.462 MHz; solvent acetone-d_6; reference $SiMe_4$) 184.02 (C=S), 169.48 (C=O), 137.47 (C_1), 133.13 (C_4), 129.80, 129.78 (C_3, C_5, C_2, C_6), 54.40 ($C_{a'}$), 53.73 ($C_{b'}$), 52.55 ($C_{a''}$), 51.54 ($C_{b''}$), 50.38 ($C_{c'}$, $C_{e'}$), 48.97 ($C_{c''}$, $C_{e''}$), 13.51 ($C_{d'}$, $C_{f'}$), 12.36 ($C_{d''}$, $C_{f''}$).

University of Cape Town

7.3.3 Preparation of *cis*-bis(*N*-benzoyl-*N'*,*N'*-di-2-hydroxyethylthioureato) platinum(II)[109]

N-benzoyl-*N'*,*N'*-di-2-hydroxyethylthiourea (1.0 mmol) was dissolved in acetonitrile (30 ml) in a two necked round bottom flask and sodium acetate (1.0 mmol) dissolved in acetonitrile (6 ml) was added. K_2PtCl_4 (0.5 mmol) dissolved in water (20 ml) was added dropwise while stirring at 35 °C. After 3 hours the volume of acetonitrile was reduced causing the product to precipitate which was centrifuged and washed thoroughly twice and then dried under vacuum at room temperature yielding 0.283 g (78%) of yellow powder. Melting point 158-159 °C (lit.[109] 144-146 °C) *Anal.* Calc. For $C_{24}H_{30}N_4O_6PtS_2$: C, 39.50; H, 4.14; N, 7.68; M^- 807

($C_{24}H_{30}N_4O_6PtS_2$ DMSO). Found: C, 39.24; H, 3.92; N, 7.69%; M^- 807.34; δ_H (399.95 MHz; solvent CD_3CN; reference $SiMe_4$) 8.22 (4H, d, J=7.7 Hz, H_2, H_6), 7.64 (2H, t, J=7.3 Hz, H_4) 7.51 (4H, t, J=7.7 Hz, H_3, H_5), 4.04 (4H, unres. m., $H_{b'}$), 3.96-3.82 (12H, unres. m., $H_{b''}$, $H_{a'}$, $H_{a''}$)

7.3.4 Preparation of Pt(diimine)Cl_2 Complexes[111]

K_2PtCl_4 (0.5 mmol) was dissolved in 15 ml of water and to this was added the appropriate diimine (0.5 mmol). The mixture was acidified with 1.0 ml 4M HCl and stirred and refluxed for 2 hours. The yellow precipitate that formed was filtered and washed extensively with water followed by a small volume of methanol and then diethyl ether. The product was dried at room temperature under vacuum for 24 hours. Yields and elemental analyses were as follows:

7.3.4a 2,2'-bipyridyldichloroplatinum(II) (96%) Melting point >330 °C. *Anal.* Calc. for $C_{10}H_8Cl_2N_2Pt$: C, 28.44; H, 1.90; N, 6.64. Found: C, 28.37; H, 1.70; N, 6.39%

7.3.4b 4,4'-dimethyl-2,2'-bipyridyldichloroplatinum(II) (96%) Melting point >330 °C. *Anal.* Calc. for $C_{12}H_{12}Cl_2N_2Pt$: C, 32.00; H, 2.69; N, 6.22. Found: C, 32.36; H, 2.59; N, 6.11%

7.3.4c 4,4'-di-*tert*-butyl-2,2'-bipyridyldichloroplatinum(II) (91%) Melting point >330 °C. *Anal.* Calc. for $C_{18}H_{24}Cl_2N_2Pt$: C, 40.46; H, 4.53; N, 5.24. Found: C, 40.76; H, 4.31; N, 4.93%

7.3.4d 1,10-phenanthrolinedichloroplatinum(II) (97%) Melting point >330 °C. *Anal.* Calc. for $C_{12}H_8Cl_2N_2Pt$: C, 32.29; H, 1.81; N, 6.29. Found: C, 32.34; H, 1.56; N, 6.05%

7.3.4e 4-methyl-1,10-phenanthrolinedichloroplatinum(II) (93%) Melting point >330 °C. *Anal.* Calc. for $C_{13}H_{10}Cl_2N_2Pt$: C, 33.93; H, 2.19; N, 6.09. Found: C, 34.07; H, 1.97; N, 6.05%

7.3.4f 5-methyl-1,10-phenanthrolinedichloroplatinum(II) (81%) Melting point >330 °C. *Anal.* Calc. for $C_{13}H_{10}Cl_2N_2Pt$: C, 33.93; H, 2.19; N, 6.09. Found: C, 34.30; H, 1.98; N, 6.00%

7.3.4g 3,4,7,8-tetramethyl-1,10-phenanthrolinedichloroplatinum(II) (94%) Melting point >330 °C. *Anal.* Calc. for $C_{16}H_{16}Cl_2N_2Pt$: C, 38.26; H, 3.21; N, 5.58. Found: C, 38.25; H, 3.11; N, 5.41%

University of Cape Town

7.3.4h 5-chloro-1,10-phenanthrolinedichloroplatinum(II) (81%) Melting point >330 °C. *Anal.* Calc. for $C_{12}H_7Cl_2N_2Pt$: C, 29.99; H, 1.47; N, 5.83. Found: C, 30.31; H, 1.27; N, 5.83%

7.3.4i 5-nitro-1,10-phenanthrolinedichloroplatinum(II) (86%) Melting point >330 °C. *Anal.* Calc. for $C_{12}H_7Cl_2N_3O_2Pt$: C, 29.34; H, 1.44; N, 8.55. Found: C, 29.82; H, 1.16; N, 8.33%

7.3.5a Preparation of (*N*-benzoyl-*N'*,*N'*-di-2-hydroxyethylthioureato-*S*,*O*)(2,2'-bipyridyl) platinum(II) chloride

2,2'-bipyridyldichloroplatinum(II) (0.237 mmol) was dissolved in warm DMF (14 ml) to which a solution of *N*-benzoyl-*N'*,*N'*-di-2-hydroxyethylthiourea (0.261 mmol) and triethylamine (0.26 mmol) in DMF (4 ml) was added dropwise. The mixture was heated at 80 °C and stirred for 4 hours, then acetonitrile (50 ml) was added and the flask was cooled. The resulting precipitate was filtered and washed with DMF then diethyl ether and dried at room temperature under vacuum yielding 0.132 g (85%) of bright yellow powder. Melting point (product decomposes) 206-207 °C. *Anal.* Calc. for $C_{22}H_{23}ClN_4O_3PtS$: C, 40.40; H, 3.54; N, 8.56; M^+ 618. Found: C, 40.24; H, 3.44; N, 8.15%; M^+ 617.84; δ_H (399.95 MHz; solvent 50% CD_3CN, 50% D_2O; reference $SiMe_4$, sample concentration, 0.02M) 8.33 (1H, d, J=5.5 Hz, $H_{6'}$), 7.96 (1H, t, J=8.1 Hz, $H_{4'}$) 7.95 (1H, d, J=8.4 Hz, H_6), 7.92 (1H, t, J=8.1 Hz, H_4), 7.78 (1H, d, J=7.7 Hz, $H_{3'}$), 7.71 (1H, d, J=7.7 Hz H_3), 7.56 (1H, t, J=7.4, $H_{4''}$), 7.54 (2H, d, J=7.0 Hz, $H_{2''}$, $H_{6''}$), 7.51 (1H, t, J=6.0 Hz, $H_{5'}$), 7.30 (2H, t, J=7.7 Hz, $H_{3''}$, $H_{5''}$), 7.23 (1H, t, J=6.6 Hz, H_5), 3.83 (2H, t, J=6.3 Hz, $H_{a'}$), 3.71 (2H, t, J=5.9 Hz, $H_{b'}$) 3.67 (4H, unres. m, $H_{a''}$, $H_{b''}$).

7.3.5b Preparation of (*N*-benzoyl-*N'*,*N'*-di-2-hydroxyethylthioureato-*S*,*O*)(4,4'-dimethyl-2,2'-bipyridyl) platinum(II) chloride

4,4'dimethyl-2,2'-bipyridyldichloroplatinum(II) (0.178 mmol) was dissolved in warm dry DMF (10 ml). To this, a solution of *N*-benzoyl-*N'*,*N'*-di-2-hydroxyethylthiourea (0.196 mmol) and triethylamine (0.20 mmol) in DMF (3 ml) was added dropwise. The mixture was heated at 80 °C and stirred for 4 hours. After cooling to room temperature, acetonitrile (40 ml) was added and the flask cooled further to –10 °C. The resulting precipitate was filtered and washed with DMF then diethyl ether and dried at room temperature under vacuum yielding 0.104 g (85%) of yellow powder. Melting point (product decomposes) 223-225 °C. *Anal.* Calc. for

University of Cape Town

$C_{24}H_{27}ClN_4O_3PtS$: C, 42.26; H, 3.99; N, 8.21; M^+ 646. Found: C, 41.77; H, 3.87; N, 8.03%; M^+ 645.96; δ_H (399.95 MHz; solvent 50% CD_3CN, 50% D_2O; reference $SiMe_4$, sample concentration, 0.02M) 7.91 (1H, d, J=5.5 Hz, $H_{6'}$), 7.74 (1H, t, J=5.9 Hz, H_6) 7.62 (1H, t, J=7.3 Hz, $H_{4''}$), 7.48 (1H, s, $H_{3'}$), 7.47 (2H, d, J=8.1 Hz, $H_{2''}$, $H_{6''}$), 7.37 (1H, s, H_3), 7.36 (2H, t, J=8.1, $H_{3''}$, $H_{5''}$), 7.19 (1H, d, J=5.5 Hz, $H_{5'}$), 6.99 (1H, d, J=5.9 Hz, H_5), 3.83 (2H, t, J=6.3 Hz, $H_{a'}$), 3.69 (2H, t, J=5.9 Hz, $H_{b'}$) 3.69 (4H, t, J=5.1 Hz, $H_{a''}$, $H_{b''}$), 2.19 (3H, s, CH_3), 2.11 (3H, s, CH_3')

7.3.5c Preparation of (*N*-benzoyl-*N*',*N*'-di-2-hydroxyethylthioureato-*S*,*O*)(4,4'-di-*tert*-butyl-2,2'-bipyridyl)platinum(II) chloride

4,4'di-*tert*-butyl-2,2'-bipyridyldichloroplatinum(II) (0.374 mmol) was dissolved in warm dry acetone (60 ml). To this a solution of *N*-benzoyl-*N*',*N*'-di-2-hydroxyethylthiourea (0.411 mmol) and triethylamine (0.41 mmol) in acetone (15 ml) was added dropwise. The mixture was refluxed and stirred for 4 hours. After cooling at –10 °C the resulting precipitate was filtered and washed with methanol and then diethyl ether and dried at room temperature under vacuum yielding 0.185 g (72%) of bright yellow powder. Melting point (product decomposes) 206-208 °C. *Anal.* Calc. for $C_{30}H_{39}ClN_4O_3PtS$: C, 47.02; H, 5.13; N, 7.31; M^+ 730. Found: C, 47.22; H, 5.51; N, 7.21%; M^+ 730.11; δ_H (399.95 MHz; solvent 50% CD_3CN, 50% D_2O; reference $SiMe_4$, sample concentration, 0.02M) 8.46 (1H, d, J=6.2 Hz, $H_{6'}$), 8.26 (1H, t, J=6.2 Hz, H_6) 8.09 (1H, d, J=2.2 Hz, $H_{3'}$), 7.93 (1H, d, J=2.2 Hz, H_3), 7.70 (2H, d, J=7.0 Hz, $H_{2''}$, $H_{6''}$), 7.68 (1H, d, J=5.9 Hz, $H_{5'}$), 7.58 (1H, t, J=7.3 Hz, $H_{4''}$), 7.48 (1H, dd, J=6.2 Hz and 2.2 Hz, H_5), 7.32 (2H, t, J=7.9 Hz, $H_{3''}$, $H_{5''}$), 4.02 (4H, unres. m, $H_{a'}$, $H_{b'}$), 3.84 (2H, t, J=5.7 Hz, $H_{a''}$) 3.76 (2H, t, J=6.3 Hz, $H_{b''}$), 1.47 (9H, s, CH_3), 1.35 (9H, s, CH_3')

7.3.5d Preparation of (*N*-benzoyl-*N*',*N*'-di-2-hydroxyethylthioureato-*S*,*O*)(1,10-phenanthroline) platinum(II) chloride

1,10-phenanthrolinedichloroplatinum(II) (0.4 mmol) was suspended in refluxing acetonitrile (220 ml). To this a solution of *N*-benzoyl-*N*',*N*'-di-2-hydroxyethylthiourea (0.44 mmol) in acetonitrile (20 ml) was added dropwise. The mixture was gently refluxed and stirred for 4 hours. Triethylamine (0.44 mmol) in acetonitrile was added dropwise and the mixture was refluxed for a further hour. After cooling overnight the mixture was filtered and washed with acetonitrile and then diethyl ether. This crude product was dissolved in hot methanol and the insoluble starting material was filtered off. The volume of methanol was then reduced and

University of Cape Town

acetonitrile was added. Again the solvent volume was reduced and more acetonitrile added with this being repeated until the product precipitated from solution. After cooling the precipitate was filtered and washed with acetonitrile then diethyl ether and dried at room temperature under vacuum yielding 0.158 g (58%) of yellow powder. Melting point (product decomposes) 209-210 °C. *Anal.* Calc. for $C_{24}H_{23}ClN_4O_3PtS$ ½H_2O: C, 41.95; H, 3.52; N, 8.15; M^+ 642. Found: C, 41.76; H, 3.39; N, 8.01%; M^+ 642.33; δ_H (399.95 MHz; solvent 50% CD_3CN, 50% D_2O; reference $SiMe_4$, sample concentration, 0.02M) 8.16 (1H, d, J=8.1 Hz, H_2), 8.07 (1H, d, J=7.7 Hz, H_9) 7.82 (1H, d, J=4.8 Hz, H_4), 7.74 (1H, d, J=5.1 Hz, H_7), 7.53 (1H, dd, J=7.7 and 2.9 Hz, H_3), 7.46 (1H, t, J=7.0 Hz $H_{4'}$), 7.30 (1H, d, J=8.8, H_5) *, 7.24 (1H, d, J=9.2 Hz, H_6)*, 7.21 (1H, dd, J=8.1 and 2.9 Hz, H_8), 7.14 (2H, t, J=7.5 Hz, $H_{3'}$, $H_{5'}$), 7.06 (2H, t, J=7.3 Hz, $H_{2'}$, $H_{6'}$), 3.73 (2H, t, J=6.0 Hz, $H_{a'}$), 3.57 (2H, t, J=6.2 Hz, $H_{a''}$) 3.54 (2H, t, J=6.2 Hz, $H_{b'}$), 3.46 (2H, t, J=5.5 Hz, $H_{b''}$).

7.3.5e Preparation of (*N*-benzoyl-*N'*,*N'*-di-2-hydroxyethylthioureato-*S*,*O*)(4-methyl-1,10-phenanthroline) platinum(II) chloride

The same method as for (*N*-benzoyl-*N'*,*N'*-di-2-hydroxyethylthioureato-*S*,*O*)(1,10-phenanthroline) platinum(II) chloride was used with 4-methyl-1,10-phenanthrolinedichloroplatinum(II) being used as the starting material. Two isomers formed, anti (89%) and syn (11%) which were determined by ^1H NMR, and these could not be separated. 60% overall isolated yield. Melting point (product decomposes) 196-197 °C. *Anal.* Calc. for $C_{25}H_{25}ClN_4O_3PtS$ H_2O: C, 42.29; H, 3.83; N, 7.89; M^+ 656. Found: C, 42.13; H, 3.66; N, 7.99%; M^+ 656.17; δ_H (399.95 MHz; solvent 50% CD_3CN, 50% D_2O; reference $SiMe_4$, sample concentration, 0.02M) Anti isomer 8.29 (1H, d, J=8.4 Hz, H_9), 7.66 (1H, m, H_8), 7.53 (1H, m, H_2), 7.45 (1H, t, J=7.0 Hz, $H_{4'}$), 7.38 (1H, d, J=8.8 Hz, H_6), 7.18-7.11 (3H, m, H_7, $H_{2'}$, $H_{6'}$), 7.11 (1H, d, J=7.3 Hz, H_5), 6.95 (3H, unres. m, H_3, $H_{3'}$, $H_{5'}$), 3.76 (2H, t, J=5.5 Hz, $H_{a'}$), 3.58 (2H, t, J=5.5 Hz, $H_{a''}$), 3.56 (2H, t, J=5.5 Hz, $H_{b'}$), 3.43 (2H, t, J=5.9 Hz, $H_{b''}$), 2.03 (3H, s, CH_3)

7.3.5f Preparation of (*N*-benzoyl-*N'*,*N'*-di-2-hydroxyethylthioureato-*S*,*O*)(5-methyl-1,10-phenanthroline) platinum(II) chloride

The same method as for (*N*-benzoyl-*N'*,*N'*-di-2-hydroxyethylthioureato-*S*,*O*)(1,10-phenanthroline) platinum(II) chloride was used with 5-methyl-1,10-phenanthrolinedichloroplatinum(II) being used as the starting material. Two isomers formed,

* = assignment uncertain

University of Cape Town

syn and anti, in approximately equal amounts and these could not be separated. Overall isolated yield 41%. Melting point (product decomposes) 194-196 °C. *Anal.* Calc. for $C_{25}H_{25}ClN_4O_3PtS$ ½H_2O: C, 42.29; H, 3.83; N, 7.89; M^+ 656. Found: C, 42.13; H, 3.66; N, 7.99%; M^+ 656.17; δ_H (399.95 MHz; solvent 50% CD_3CN, 50% D_2O; reference $SiMe_4$, sample concentration, 0.02M) Syn isomer 8.09 (1H, d, J=7.7 Hz, H_2), 8.03 (1H, d, J=8.1 Hz, H_9) 7.87 (1H, d, J=4.8 Hz, H_7), 7.53-7.43 (2H, m, H_3, H_4'), 7.26-7.19 (2H, m, H_4, H_8), 7.16-7.09 (2H, m, $H_{3'}$, $H_{5'}$), 6.96-6.87 (3H, m, H_6, $H_{2'}$, $H_{6'}$), 3.76 (2H, m, $H_{a'}$), 3.56 (4H, m, $H_{b'}$, $H_{a''}$), 3.46 (2H, m, $H_{b''}$), 1.99 (3H, s, CH_3); Anti isomer 8.18 (1H, d, J=7.7 Hz, H_9), 7.93 (1H, d, J=8.1 Hz, H_2) 7.77 (1H, d, J=4.8 Hz, H_4), 7.53-7.43 (2H, m, H_8, $H_{4'}$), 7.16-7.09 (4H, m, H_7, H_3, $H_{3'}$, $H_{5'}$), 6.96-6.87 (3H, m, H_6, $H_{2'}$, $H_{6'}$), 3.76 (2H, m, $H_{b'}$), 3.56 (4H, m, $H_{a'}$, $H_{b''}$), 3.46 (2H, m, $H_{a''}$), 1.93 (3H, s, CH_3)

7.3.5g Preparation of (*N*-benzoyl-*N'*,*N'*-di-2-hydroxyethylthioureato-*S*,*O*) (3,4,7,8-tetramethyl-1,10-phenanthroline) platinum(II) chloride

The same method as (*N*-benzoyl-*N'*,*N'*-di-2-hydroxyethylthioureato-*S*,*O*)(1,10-phenanthroline) platinum(II) chloride was used with 3,4,7,8-tetramethyl-1,10-phenanthroline-dichloroplatinum(II) being used, as the starting material. Overall isolated yield 50%. Melting point (product decomposes) 203-205 °C. *Anal.* Calc. for $C_{28}H_{31}ClN_4O_3PtS$ H_2O: C, 44.71; H, 4.42; N, 7.44; M^+ 698. Found: C, 44.61; H, 4.14; N, 7.48%; M^+ 698.42; δ_H (399.95 MHz; solvent 50% CD_3CN, 50% D_2O; reference $SiMe_4$, sample concentration, 0.02M) 7.59 (1H, s, H_2), 7.57 (1H, s, H_9) 7.55 (1H, d, J=9.0 Hz, H_6)*, 7.50 (1H, d, J=9.3 Hz, H_5)*, 7.42 (1H, unres. m, $H_{4'}$), 7.29 (2H, d, J=7.5 Hz, $H_{2'}$, $H_{6'}$), 7.28 (2H, d, J=7.5 Hz, $H_{3'}$, $H_{5'}$), 3.84 (2H, t, J=5.9 Hz, $H_{a'}$), 3.77 (2H, t, J=5.7 Hz, $H_{b'}$), 3.69 (2H, t, J=5.7 Hz, $H_{a''}$) 3.64 (2H, t, J=5.9 Hz, $H_{b''}$), 2.13 (6H, s, CH_3-4, CH_3-7), 2.04 (3H, s, CH_3-8) 1.99 (3H, s, CH_3-3)

7.3.5h Preparation of (*N*-benzoyl-*N'*,*N'*-di-2-hydroxyethylthioureato-*S*,*O*)(5-chloro-1,10-phenanthroline) platinum(II) chloride

The same method as for (*N*-benzoyl-*N'*,*N'*-di-2-hydroxyethylthioureato-*S*,*O*)(1,10-phenanthroline) platinum(II) chloride was used, with 5-chloro-1,10-phenanthroline-dichloroplatinum(II) being used as the starting material. Two isomers formed, anti (85%) and syn (15%), and these could not be separated. Yield 68%. Melting point (product decomposes) 192-194 °C. *Anal.* Calc. for $C_{24}H_{22}Cl_2N_4O_3PtS$ H_2O: C, 39.46; H, 3.31; N, 7.66; M^+ 676/677. Found: C, 39.07; H, 3.19; N, 7.61%; M^+ 676.31/677.29; δ_H (399.95 MHz; solvent 50%

* = assignment uncertain

University of Cape Town

CD_3CN, 50% D_2O; reference $SiMe_4$, sample concentration, 0.02M) E Isomer 8.31 (1H, d, J=7.2 Hz, H_9^*), 8.25 (1H, d, J=7.8 Hz, H_2^*), 8.11 (2H, unres. m, H_7, H_8^*) 7.46-7.41 (3H, unres. m, H_3^*, H_4^*, $H_{4'}$), 7.39 (1H, s, H_6), 7.08 (2H, t, J=7.3, $H_{3'}$, $H_{5'}$) 6.87 (2H, d, J=7.7 Hz, $H_{2'}$, $H_{6'}$), 3.83 (2H, t, J=5.9 Hz, $H_{a'}$), 3.66 (2H, t, J=5.1 Hz, $H_{b'}$) 3.60 (2H, t, J=5.1 Hz, $H_{a''}$), 3.53 (2H, t, J=4.8 Hz, $H_{b''}$)

7.3.5i Preparation of (*N*-benzoyl-*N'*,*N'*-di-2-hydroxyethylthioureato-*S*,*O*)(5-nitro-1,10-phenanthroline) platinum(II) chloride

5-Nitro-1,10-phenanthrolinedichloroplatinum(II) (0.204 mmol) was dissolved in warm DMF (20 ml). To this a solution of *N*-benzoyl-*N'*,*N'*-di-2-hydroxyethylthiourea (0.224 mmol) and triethylamine (0.23mmol) in DMF (5 ml) was added dropwise. The mixture was heated at 60 °C and stirred for 8 hours then cooled. Diethyl ether was added to aid the precipitation of the product and then evaporated again, promoting solvation of impurities. The precipitate was filtered and washed with DMF then diethyl ether and dried at room temperature. Further addition of diethyl ether to the filtrate yielded more product which was filtered and washed. The two crops were combined and dissolved in hot methanol with the insoluble starting material being filtered off. The volume of methanol was then reduced under vacuum and acetonitrile was added. Again the solvent volume was reduced and more acetonitrile added with this being repeated until the product precipitated from solution. After cooling the precipitate was filtered and washed with acetonitrile and then diethyl ether and dried at room temperature under vacuum yielding 0.070 g (47%) of orange powder representing two isomers anti (20%) and syn (80%), and these could not be separated. Melting point (product decomposes) 182-183 °C. *Anal.* Calc. for $C_{24}H_{22}ClN_5O_5PtS$ $1.5H_2O$: C, 38.40; H, 3.36; N, 9.33; M^+ 687. Found: C, 38.11; H, 2.94; N, 9.31%; M^+ 687.30; δ_H (399.95 MHz; solvent 50% CD_3CN, 50% D_2O; reference $SiMe_4$, sample concentration, 0.02M) syn Isomer 8.88 (1H, d, J=8.4 Hz, H_2^*), 8.76 (1H, d,J=7.7 Hz, H_9^*) 8.54 (1H, d, J=4.8 Hz, H_4^*), 8.48 (1H, s, H_6), 8.11 (1H, unres., H_7^*) 8.01 (1H, t, J=6.2 Hz, H_8^*), 7.70 (1H, dd, J=8.7 and 3.3 Hz, H_3^*), 7.36 (1H, t, J=7.0 Hz, $H_{4'}$), 7.00 (2H, t, J=7.3, $H_{3'}$, $H_{5'}$), 6.88 (2H, t, J=7.3 Hz, $H_{2'}$, $H_{6'}$) 3.94 (2H, t, J=5.5 Hz, $H_{a'}$), 3.83 (2H, t, J=5.1 Hz, $H_{b'}$), 3.63 (4H, unres., $H_{a''}$, $H_{b''}$)

* = assignment uncertain

University of Cape Town

7.3.5j Preparation of (*N*-benzoyl-*N'*,*N'*-bisdiethylaminoethylthioureato-*S*,*O*)(2,2'-bipyridyl) platinum(II) chloride

2,2'-bipyridyldichloroplatinum(II) (0.237 mmol) was partially dissolved in hot acetonitrile, to which *N*-benzoyl-*N'*,*N'*-bisdiethylaminoethylthiourea (0.261 mmol) dissolved in acetonitrile, was added dropwise. The mixture was continuously stirred at 70 °C for 2 hours. The volume of solvent was reduced under vacuum, then diethyl ether (100 ml) was added to precipitate the product which was filtered. The yellow powder was dissolved in dry hot methanol and any residual insoluble starting material was filtered off. After the volume of methanol was reduced under vacuum, diethyl ether was added to precipitate the product, which was filtered and washed extensively with acetonitrile to remove triethylamine hydrochloride. Drying under vacuum at room temperature yielded 0.122 g (67%) of yellow-orange powder. Melting point (product decomposes) 169-171 °C. *Anal.* Calc. for $C_{30}H_{41}ClN_6OPtS\ 2½H_2O\ 2HCl$: C, 40.84; H, 5.48; N, 9.53; M^+ ($C_{30}H_{41}ClN_6OPtS$) 728. Found: C, 40.54; H, 5.48; N, 9.40; M^+ 728.69; δ_H (399.95 MHz; solvent 50% CD_3CN, 50% D_2O; reference $SiMe_4$) 8.99 (1H, d, J=5.5 Hz, $H_{6'}$), 8.62 (1H, d, J=5.9 Hz, H_6) 8.39 (2H, m, $H_{3'}$, $H_{4'}$), 8.34 (2H, d, J=4.0 Hz, H_3, H_4), 8.14 (2H, d, J=9.2 Hz, $H_{2''}$, $H_{6''}$), 7.98 (1H, m, $H_{5'}$), 7.76 (1H, t, J=7.7 Hz, $H_{4''}$), 7.68 (1H, dd, J=9.9 and 5.0 Hz, H_5), 7.60 (2H, t, J=8.1Hz, $H_{3''}$, $H_{5''}$), 4.23-4.16 (4H, m, $H_{a'}$, $H_{a''}$) 5.52 (2H, t, J=8.0 Hz, $H_{b'}$), 3.35 (6H, m, $H_{b''}$, $H_{c'}$, $H_{e'}$), 3.21 (4H, q, J=7.3 Hz, $H_{c''}$, $H_{e''}$), 1.40 (6H, t, J=7.3 Hz, $H_{d'}$, $H_{f'}$), 1.18 (6H, t, J=7.3 Hz, $H_{d''}$, $H_{f''}$)

7.3.6 Preparation of di-μ-chlorobis[2-(2-pyridinyl)phenyl-(*C*,*N*)]di-platinum[114]

Kvam *et al.*[114] have previously published a synthesis of di-μ-chlorobis[2-(2-pyridinyl)phenyl-(*C*,*N*)]di-platinum but this was not followed due to unavailability of starting materials. Instead the following synthesis was used. Potassium tetrachloroplatinate (0.481 mmol) was dissolved in 20 ml water in a round bottom flask. Acetone (20 ml) was added to the solution. 2-phenyl pyridine (0.481mmol) was dissolved in 60 ml acetone and added over a period of an hour to the platinum containing solution which was heated at 60 °C and stirred. After 2½ hours the reaction was cooled and water (30 ml) was added. The acetone was removed under vacuum resulting in the precipitation of the product which was filtered and washed with water then diethyl ether. After drying under vacuum at room temperature 0.127g (69%) of yellow powder was recovered. Melting point: product decomposes *Anal.* Calc. For $C_{22}H_{16}Cl_2N_2Pt_2$: C, 34.34; H, 2.09; N, 3.64. Found: C, 35.10; H, 2.17; N, 3.54%

* = assignment uncertain

University of Cape Town

7.3.7 Preparation of (*N*-benzoyl-*N'*,*N'*-bisdiethylaminoethylthioureato-*O*,*S*)(2-phenyl pyridine) platinum(II)

Di-μ-chlorobis[2-(2-pyridinyl)phenyl-(*C*,*N*)]di-platinum (0.078 mmol) was dissolved in acetonitrile (60 °C) in a two necked round bottom flask. While stirring the solution, *N*-benzoyl-*N'*,*N'*-bisdiethylaminoethylthiourea (0.172 mmol) dissolved in acetonitrile was added dropwise and the reaction monitored by TLC with a spot to spot conversion taking place after 1 hour. After evaporation of the solvent under vacuum, diethyl ether and 1 mol equivalent of HCl was added to precipitate the product, which was filtered and washed with diethyl ether. Drying the product under vacuum yielded 0.108 g (75%). Melting point 217–219 °C. *Anal.* Calc. for $C_{31}H_{41}N_5OPtS{\cdot}H_2O$ 2HCl : C, 45.54; H, 5.55; N, 8.56; M^+ ($C_{31}H_{41}N_5OPtS$) 727. Found: C, 45.19; H, 5.63; N, 8.48; M^+ 727.49; δ_H (399.95 MHz; solvent CD_3CN, reference $SiMe_4$) 9.16 (1H, d, J=5.8 Hz, $H_{6'}$), 8.33 (2H, m, H_4, H_6) 8.04 (1H, t, J=8.0 Hz, $H_{4'}$), 7.91 (1H, d, J=8.4 Hz, $H_{3'}$), 7.62 (2H, d, J=7.3 Hz, $H_{2''}$, $H_{6''}$), 7.55-7.43 (4H, m, H_3, $H_{4''}$, H_5, $H_{5'}$), 7.08 (2H, m, $H_{3''}$, $H_{5''}$), 4.46 (4H, broad, $H_{a'}$,$H_{a''}$) 3.52 (2H, broad, $H_{b'}$), 3.31 (2H, broad, H_b), 3.15 (8H, m, $H_{c'}$, $H_{c''}$, $H_{e'}$ $H_{e''}$), 1.40 (6H, broad, $H_{d'}$, $H_{f'}$), 1.27 (6H, broad, $H_{d''}$, $H_{f''}$)

7.3.8 Preparation of gallium(III)protoporphyrin IX chloride

Protoporphyrin IX (0.355 mmol) was dissolved in acetic acid (40 ml) in a two necked flask under nitrogen. Gallium chloride (0.521 mmol) dissolved in hydrochloric acid (1M, 1.83 ml) was added, followed by sodium acetate (4.9 mmol) dissolved in acetic acid (10 ml) and sodium hydroxide (1.83 mmol) dissolved in water (0.366 ml). The mixture was heated under reflux for 6 hours with the reaction being monitored by quenching of the band at 508 nm in the visible spectrum. After cooling, the product was precipitated with the addition of diethyl ether and filtered then washed with water followed by diethyl ether. Drying under vacuum and phosphorus pentoxide for 48 hours yielded 0.170g (76%) of powder. Melting point > 330 °C. *Anal.* Calc. for $C_{34}H_{32}ClGaN_4O_4{\cdot}H_2O$: C, 59.72; H, 5.01; N, 8.19; M^+ 630. Found: C, 59.42; H, 4.91; N, 7.79; M^+ 630.24 , 1313.55 (dimer); δ_H (399.95 MHz; solvent DMSO-d_6; reference $SiMe_4$) 10.60-10.50 (broad m, meso protons), 8.63 (m, -CH=CH_2) 6.53 (m, -CH=CH_2), 6.31 (m, -CH=CH_2), 4.48 (t, J=7.4 Hz, -CH_2-), 3.87 (s, CH_3), 3.85 (s, CH_3) 3.77 (s, CH_3), 3.74 (s, CH_3), 3.24 (t, J=7.4 Hz, -CH_2)

University of Cape Town

7.4 Spectrophotometric titrations[51]

Spectrophotometric titrations of haematin with various platinum complexes and ligands were performed on a Beckman DU 68 UV-visible spectrometer using quartz cuvettes in a thermostated cell holder regulated at 25 °C. All glassware was thoroughly cleaned in a sodium hydroxide bath followed by extensive washing with deionised and finally distilled water. All aqueous solutions were made up with glass distilled water. A fresh stock solution of ferriprotoporphyrin IX (Fe(III)PPIX) was made by dissolving 8.0 mg hemin chloride (Sigma) in 10.0 ml DMSO and was kept in the dark. 1.0 ml of this solution was made up to 10.0 ml again with DMSO. A working solution was obtained by adding 50 µl of the diluted stock solution to a cuvette containing 38% aqueous DMSO (1.95 ml) to achieve a 40% v/v aqueous DMSO solution containing 0.020M *N*-[2-hydroxyethyl]piperazine-*N*'-[2-ethane sulphonate] (HEPES) with an apparent pH of 7.5. Known volumes of solutions containing a platinum complex or ligand (40% aqueous DMSO, 0.020 M HEPES, pH 7.4) were added and the absorbances at 402 nm recorded. Titrations were done in triplicate and a blank titration containing no Fe(III)PPIX was also performed. Values of the blank titration were subtracted from the absorbances of the haematin titration and the difference absorbance values corrected for dilution. Data was analysed using a non-linear least squares fitting software package "Fit" with a 1:1 binding model. Equation 7.1 was used to obtain K values.

$$A = (A_0 + A_\infty K [IM]_{free}) / (1 + [IM]_{free}) \quad (7.1)^{51}$$

A_0 is the initial absorbance of Fe(III)PPIX. A_∞ is the absorbance of Fe(III)PPIX as the concentration of the substance interacting with Fe(III)PPIX approaches infinity. $[IM]_{free}$ (interacting molecule) is the concentration of the substance whose association constant is being investigated which is not bound to Fe(III)PPIX. The absorbance and $[IM]_{total}$ is known for each point in the titration and iterations are performed to obtain fitted values for A_0, A_∞, and K. Details of the model are described elsewhere (Mavuso, W.M. PhD thesis[117]).

7.5 β-Haematin synthesis and inhibition [120]

University of Cape Town

Haematin was obtained in-situ by dissolving 5.0 mg hemin chloride (Sigma) in sodium hyrdoxide solution (0.10 M, 1.00 ml) in a thermostated and stirred reaction vessel at 60 °C. Hydrochloric acid (1.0 M, 0.10ml) was added, resulting in precipitation of some haematin. Sodium acetate (12.9 M, 0.58 ml, pH 5) pre-incubated at 60 °C was added to the vessel which then was covered to maintain solution concentrations. If haematin was required the reaction mixture was cooled in ice at this point, the solution diluted with distilled water and filtered on 0.2 μm cellulose nitrate filters (Millipore). The product was washed extensively with water and dried over phosphorus pentoxide for 48 hours. If β-haematin was required the mixture was heated for 30 minutes at 60 °C with rapid stirring and the product was collected in the same way as for haematin. Product characterisation was by infrared spectroscopy. Two milligrams of product were ground together finely with 200 mg dry KBr and pressed into a disc using a hydraulic press exerting 10 tons of force. The spectra were recorded on a Perkin Elmer 983 infrared spectrometer scanning from 2000 cm^{-1} to 1000 cm^{-1}.

Where the inhibition of β-haematin formation by various substances was being investigated, 3 mol equivalents of compound was added prior to addition of acetate.

7.6 NMR investigation of Zn(II)PPIX – platinum complex interactions

Titrations were performed predominately on a Varian INOVA 600 MHz FT-NMR spectrometer with Varian Mercury 300 MHz FT-NMR and Varian Unity 400 MHz FT-NMR also being used. A solvent system of 80% d_6-DMSO, 20% D_2O at 25 °C in 5 mm tubes was used. Titrations were carried out by titrating the platinum complexes with Zn(II)PPIX and also in reverse by titrating Zn(II)PPIX with the platinum complexes. This was to establish which of the protons were interacting in both the platinum complex and Zn(II)PPIX. In the first titration, 5 mg of Zn(II)PPIX was dissolved in 0.56 ml deutero-DMSO and then 0.14 ml of D_2O was added to give a Zn(II)PPIX concentration of 11.4 mM. A solution of [Pt(bipy)L]Cl was prepared by adding 0.14 ml D_2O to 10 mg of the platinum complex and dissolving it as far as possible. Deutero-DMSO (0.56 ml) was then added and the mixture was warmed until the complex was dissolved with a concentration of 10.9 mM. This was added in small aliquots to the Zn(II)PPIX sample and the proton NMR spectrum was measured after each addition.

University of Cape Town

The same procedure was used in the titration with [Pt(diMebipy)L]Cl but as this complex is less soluble than the unsubstituted bipy complex, a 5.2 mM solution was added to the metalloporphyrin.

Titrations involving the addition of Zn(II)PPIX to platinum complexes were also conducted in the same manner, starting with 10.9 mM [Pt(bipy)L]Cl and 5.2 mM [Pt(diMebipy)L]Cl solutions and adding Zn(II)PPIX (11.4 mM) in 100 µl aliquots.

University of Cape Town

8 References

1) World Health Organisation Report on Infectious Diseases, Removing Obstacles to Healthy Development, WHO, Geneva, 1999

2) P.I. Trigg, A.V. Kondrachine, In Malaria. Parasite biology, pathogenesis and protection ,Ed. I.W. Sherman,; ASM Press: Washington DC, 1998, pp 11-22

3) Malaria: Principles and Practice of Malariology, W.H. Wernsdorfer, I. McGregor, Churchill-Livingstone, Edinburgh, 1988

4) www.wooster.edu/biology/Ciliates/disease/Student%20Web%20pages/Nelson,%20L.%20/Nelson_Life%20Cycle.html

5) D.J. Krogstad, P.H. Schlesinger, I.Y. Gluzman, *J. Cell. Biol.*, 1985, **101**, 2302-2309

6) S.M. Dzekunov, L.M.B. Ursos, P.D. Roepe, *Mol. Biochem. Parasitol.*, 2000, **110**, 107-124

7) D.E. Goldberg, A.F.G. Slater, R Beavis, B. Chait, A Cerami, G.B. Henderson, *J. Exp. Medicine*, 1991, **173**, 961-969

8) I.Y. Gluzman, S.E. Francis, A. Oksman, C.E. Smith, K.L. Duffin, D.E. Goldberg, *J. Clin. Invest.*, 1994, **93**, 1602-1608

9) K.K. Eggleson, K.L. Duffin, D.E. Goldberg, *J. Biol. Chem.*, 1999, **274**, 32411-32417

10) S.E. Francis, I.Y. Gluzman, A. Oksman, D. Banerjee, D.E. Goldberg, *Mol. Biochem. Parasitol.*, 1996, **83**, 189-200

11) S. Pagola, P.W. Stevens, D.S. Bohle, A.D. Kosar, S.K. Madsen, *Nature*, 2000, **404**, 307-310

12) A.U. Orjih, H.S. Banyal, R. Chevli, C.D. Fitch, *Science*, 1981, **214**, 667-669

University of Cape Town

13) H. Ladan, Y. Nitzan, Z. Malik, *FEMS Microbiol. Lett.*, 1993, **112**, 173-177

14) J. van der Zee, D.P. Barr, R.P. Mason, *Free Radical Bio. &Med.*, 1996, **20**, 199-206

15) Y. Sugioka, M. Suzuki, K. Sugioka, M. Nakano, *FEBS Lett.*, 1987, **223**, 251-254

16) Y. Sugioka, M. Suzuki, *Biochim. Biophys. Acta*, 1991, **1074**, 19-24

17) B.A. Schacter, *Semin. Hematol.*, 1988, **25**, 349-369

18) D.S. Bohle, R.E. Dinnebier, S.K. Madsen, P.W. Stevens, *J. Biol. Chem.*, 1997, **272**, 713-716

19) T.J. Egan, H.M. Marques, *Coord. Chem. Rev.*, 1999 **190-192**, 493-517

20) A.F.G. Slater, A Cerami, *Nature*, 1992, **355**, 167-169

21) A.F.G. Slater, W.J. Swiggard, B.R. Orton, W.D. Flitter, D.E. Goldberg, A. Cerami, G.B. Henderson, *Proc Natl. Acad. Sci. USA*, 1991, **88**, 325-329

22) A. Dorn, R, Stoffel, H. Matile, A. Bubendorf, R.D. Ridley, *Nature*, 1995, **374**, 269-271

23) K. Bendrat, B.J. Berger, A. Cerami, *Nature*, 1995, **378**, 138-139

24) A.Dorn, S.R. Vippagunta, H. Matile, A. Bubendorf, J.L. Venneerstrom, R.G. Ridley, *Biochem. Pharmacol.*, 1998, **55**, 737-747

25) R.G. Ridley, A. Dorn, H. Matile, M. Kansy, *Nature*, 1995, **378**, 138-139

26) D.J. Sullivan, I.Y. Gluzman, D.E. Goldberg, *Science*, 1996, **271**, 219-222

27) J. Ziegler, R.T. Chang, D.W. Wright, *J. Am. Chem. Soc.*, 1999, **121**, 2395-2400

28) T.J. Egan, W.W. Mavuso, K.K. Ncokazi, *Biochemistry* 2001, **40**, 204-213

29) D.W. Wright, J. Ziegler, *Mater. Res. Soc. Symp. Proc.*, 2000, **599**, 293-298.

30) F.S. Parker, J.L. Irvin, *J. Biol. Chem.*,1952, **199**, 897-909

31) S.N. Cohen, K.L. Yielding, *Proc. Natl. Acad. Sci. USA*, 1965, **54**, 521-527

32) J. Ciak, F.E. Hahn, *Science*, 1966, **151**, 347-349

University of Cape Town

33) K. Van Dyke, C. Lantz, C. Szustkiewicz, *Science*, 1970, **169**, 492-493

34) A.F.G. Slater, *Pharamac. Ther.*, 1993, **57**, 203-235

35) M.W. Davidson, B.G. Griggs, D.W. Boykin, W.D. Wilson, *J. Med. Chem.*, 1977, **20**, 1117-1122

36) N. Surolia, G Padmanaban, *Proc. Natl. Acad. Sci. USA*, 1991, **88**, 4786-4790

37) C.A. Homewood, D.C. Warhurst, V.C. Baggaley, *Trans. Royal. Soc. Trop. Med. Hyg.*, 1971, **65**, 10

38) I.W. Sherman, Comp. *Biochem. Physiol.*, 1976, **53**, 447-450

39) G.C. Kirby, M.J. O'Neill, J.D. Phillipson, D.C. Warhurst, *Biochem. Pharm.*, 1989, **38**, 4367-4374

40) E. Koenigk, S. Mirtsch, B Pukfarken, S. Abdel-Rasoul, *Trop. Parasitol.*, 1981, **32**, 73-76

41) P.H. Schlesinger, D.J. Krogstad, B.L. Herwaldt, *Antimicr. Agents Chemother.*, 1988, **32**, 793-798

42) C.A. Homeward, D.C. Warhurst, W. Peters, V.C. Baggaley, *Nature*, 1972, **235**, 50-52

43) A. Yayon, Z.I. Cabantchik, H. Ginsburg, *Proc. Natl. Acad. Sci. USA*, 1985, **82**, 2784-2788

44) H. Ginsburg, E. Nissani, M. Krugliak, *Biochem. Pharm.*, 1989, **38**, 2645-2654

45) D.J. Krogstad, P.H. Schlesinger, I.Y. Gluzman, *J. Cell. Biol.*, 1985, **101**, 2302-2309

46) A. Yayon, R. Timberg, S Friedman, H. Ginsburg, *J. Protozool.*, 1984, **31**, 367-372

47) H. Ginsburg, T.G. Geary, *Biochem. Pharm.*, 1987, **36**, 1567-1576

48) F.N. Gyang, B. Poole, W. Trager, *Mol. Biochem. Prasitol.*, 1982, **5**, 263-273

49) H.Ginsburg, O. Famin, J Zhang, M Krugliak, *Biochem. Pharm.*, 1998, **56**, 1305-1313

50) P. Loria, S. Miller, M. Foley, L. Tilley, *Biochem.*, 1999, **339**, 363-370

University of Cape Town

51) T.J. Egan, W.W. Mavuso, D.C. Ross, H.M. Marques, *J. Inorg. Biochem.*, 1997, **68,** 137-145

52) P.G. Bray, M. Mungthin, R.G. Ridley, S.A. Ward, *Mol. Pharm.*, 1998, **54**, 170-179

53) P.G. Bray, O. Janneh, K.J. Raynes, M. Mungthin, H. Ginsburg, S.A. Ward, *J. Cell Biol.*, 1999, **145**, 363-376

53a) M. Mungthin, P.G. Bray, R.G. Ridley, S.A.Ward, *Antimicr. Agents Chemother.*, 1998, **42**, 2973-2977

54) T.J. Egan, R. Hunter, C.H. Kaschula, H.M. Marques, A Misplon, J. Walden, *J. Med. Chem.*, 2000, **43**, 283-291

55) D. De, F.M. Krogstad, F.B. Cogswell, D.J. Krogstad, *Am. J. Trop. Med. Hyg.*, 1996, **55**, 579-583

56) T.J. Egan, *Exp. Opin. Ther. Patents*, 2001, **11**, 185-209

57) S. Moreau, B. Perly, C. Chachaty, C. Deleuze, *Biochim Biophys Acta*, 1985, **840**, 107-116

58) I. Constantinidis, J.D. Satterlee, *J. Am. Chem. Soc.*, 1988, **110**, 927-932

59) S.K. Burley, G.Petsko, *Science*, 1985, **229**, 23-28

60) S.K. Burley, G. Petsko, *J. Am. Chem. Soc.*, 1986,**108**, 7995-8001

61) W.L. Jorgensen, D.L. Severance, *J. Am. Chem. Soc.*, 1990, **112**, 4768-4774

62) C.A. Hunter, J.K.M. Sanders, *J. Am. Chem. Soc.*, 1990, **112**, 5525-5534

63) J. Caillet, P Claverie, *Acta Crystallogr., Sect. A*, 1975, **31**, 448-461

64) S.L. Price, A.J. Stone, *Chem. Phys.*, 1987, **86**, 2859-2868

65) M.S. Searle, M.S. Westwell, D.H. Williams, *J. Chem. Soc. Perkin Trans. 2*, 1995, 141-151

66) J.A. Shelnutt, *J. Am. Chem. Soc.*, 1981, **103**, 4275-4277

67) R.J. Abraham, S.C.M. Fell, H. Pearson, K.M. Smith, *Tetrahedron*, 1979, **35**, 1759-1766

University of Cape Town

68) K.A. Cole, J. Ziegler, C.A. Evans, D.W. Wright, *J. Inorg. Biochem.*, 2000, **78**, 109-115

69) D.C. Warhurst, *Ann. Trop. Med. Parasitol.*, 1987, **81**, 65-67

70) C.H. Kaschula, Unpublished results, University of Cape Town

71) H.E. Howard-Lock, C.J.L. Lock, In Comprehensive Co-ordination Chemistry; Ed. G. Wilkinson, R.D. Gillard, J.A. McCleverty, Pergamon, Oxford, 1987, Vol 6, 755-778

72) P.J. Sadler, J. *Adv. Inorg. Chem.*, 1991, **36**, 1-48

73) C. Orvig, M.J. Abrams, *Chem. Rev.*, 1999, **99**, 2201-2203

74) R. Sanches-Delgado, M. Navarro, H. Perez, J. Urbina, *J. Med. Chem.*, 1996, **39**, 1095-1099

75) M. Navarro, H. Perez, R.A. Sanchez-Delgado, *J. Med. Chem.*, 1997, **40**, 1937-1939

76) C. Biot, G. Glorian, L.A. Maciejewski, J.S. Brocard, O. Domarle, G. Blampain, P. Millet, A.J. Georges, H. Abessolo, D. Dive, J. Lebibi, *J. Med. Chem.*, 1997, **40**, 3715-3718

77) D.E.Goldberg, V. Sharma, A. Oksman, I.Y. Gluzman, T.E. Wellems, D. Piwnica-Worms, *J. Biol. Chem.*, 1997, **272**, 6567-6572

78) M.S. Wysor, US Patent 4020150, 1977

79) V. Sharma, D. Piwnica-Worms, A. Beatty, D.E. Goldberg, *Chem. Comm.*, 1997, 2223-2224

80) J. Reedijk, *Chem. Comm.*, 1996, 801-806

81) J. Swiatek, J. *Coord. Chem.*, 1994, **33**, 191-217

82) P.M. Takahara, A.C. Rosenzweig, C.A. Frederick, S.J. Lippard, *Nature*, 1995, **377**, 649-652

83) L. Nair, V.K. Bhasin, *Jap. J. Med. Sci. Biol.*, 1994, **47**, 241-252

84) S.L. Lippard, *Acc. Chem. Res.*, 1978, **11**, 211-217

85) A.H. Wang, J. Nathans, G. van der Marel, J.H. van Boom, A. Rich, *Nature*, 1978, **276**, 471-474

University of Cape Town

86) Y.S. Wong, S.J. Lippard, *Chem. Comm.*, 1977, 824-825

87) R.B. Silverman, The Organic Chemistry of Drug Designed Drug Action, Academic Press Inc., New York, 1992 ch. 6

88) O. Kennard, W.N. Hunter, *Angew. Chem. Int. Ed. Engl.*, 1991, **30**, 1254-1272

89) K.W. Jennette, S.J. Lippard, G.A.Vassiliades, W.R. Bauer, *Proc. Nat. Acad. Sci. USA*, 1974, **71**, 3839-3843

90) G.M. Intille, C.E. Pflunger, W.A. Baker Jr., *Cryst. Struct. Commun.*, 1973, **2**, 217-20

91) M. Cusumano, M.L. Di-Pietro, A. Giannetto, *Chem. Comm.*, 1996, 2527-2528

92) S.A. Tysoe, R.J. Morgan. A.D. Baker, T.C. Strekas, C. Thomas *J. Phys. Chem.*, 1993, **97**, 1707-1711

93) F.A. Cotton, G. Wilkinson, Advanced Inorganic Chemistry, 4th Ed.,Wiley, New York, 1980, p1188

94) L. Helm, L.I. Elding, A.E. Merbach, *Inorg. Chem.*, 1985, **24**, 1719-1721

95) L. Helm, L.I. Elding, A.E. Merbach, *Helv. Chim. Acta.*, 1984, **67**, 1453-1460

96) S. Achar, V.J. Catalano, *Polyhedron*, 1997, **16**, 1555-1561

97) K.R. Koch, C. Sacht, C.L. Lawrence, *J.Chem. Soc. Dalton Trans.*, 1998, 689-695

98) J. Shelnutt, *Inorg. Chem.*, 1983 **22**, 2535-2544

99) M. Schuster, *Fresenius J. Anal. Chem.*, 1992, **342**, 791-794

100) P. Vest, M. Schuster, K.H. König, *Fresenius J. Anal. Chem.*, 1991, **341**, 566-568

101) A. Irving, K.R. Koch, M. Matoetoe, *Inorg Chim Acta.*, 1993, **206**, 193-199

102) I.B. Douglass, F.B. Dains, *J. Am. Chem. Soc.*, 1934, **56**, 719-721

103) L. Bayer, E. Hoyer, H. Henning, R Kimse, H Hartmann, J. Liebscher, *Journal f. Prakt. Chemie*, 1975, **317**, 829-839

University of Cape Town

104) K.R. Koch, Y Wang, A Coetzee, *J. Chem. Soc. Dalton Trans.*, 1999, 1013-1016

105) B.A. Jansen, J. van der Zwan, H. den Dulk, J. Brouwer, J. Reedijk, *J. Med. Chem.*, 2001, **44**, 245-249

106) A. Takamizawa, K, Hira, K. Matsui, *Bull. Chem Soc. Japan*, 1963, **36**, 1214

107) D.T. Elmore, R.J. Ogle, *J. Chem. Soc*, 1958, 1141

108) C.L. Lawrence, Masters dissertation, 1997, UCT

109) K.R. Koch, C. Sacht, S. Bourne, *Inorg. Chim. Acta.*, 1995, **232**, 109-115

110) T. Ben Hadda, H. Le Bozec, *Inorg. Chim. Acta.*, 1993, **204**, 103-107

111) G.T. Morgan, F.H. Burnstall, *J. Chem. Soc.*, 1934, 965-971

112) NMR spectra from the Integrated Spectral Data Base System for Organic Compounds http://www.aist.go.jp/RIODB/SDBS/sdbs/owa/sdbs_sea.cre_frame_sea

113) K.R. Koch, A. Irving, M. Matoetoe, *Inorg. Chim. Acta.*, 1993, **206**, 193-199

114) P.I. Kvam, J. Songstad, *Acta Chem. Scand.*, 1995, **49**, 313-324

115) A. Coutsolelos, R. Guilard, D. Bayeul, C. Lecomte, *Polyhedron*, 1986, **5**, 1157-1164

116) D.H. O'Keefe, C.H. Barlow, G.A. Smythe, W.H. Fuchsman, T.H. Moss, H.R. Lilienthal, W.S Caughey, *Bioinorg. Chem.*, 1975, **5**, 125-147

117) W.M. Mavuso, PhD Thesis, 2001, UCT

118) O.Q. Munro, H.M Marques, *Inorg. Chem.*, 1996, **35**, 3768-3779

119) M.W. Makinen, A.K. Churg, Iron Porphyrins Part 1, Ed. H.B. Gary, A.B.P. Lever, Addison-Wesley, New York, pp.141-235

120) T.J. Egan, D.C. Ross, P.A. Adams, *FEBS Lett.*, 1994, **352**, 54-57

121) Y. Wu, PhD Thesis, 2002, University of Cape Town

University of Cape Town

Appendix 1

Tables of data from spectrophotometric titrations. All titrations were performed at 25 °C at pH 7.4 (0.020 M HEPES buffer) in 40% aqueous DMSO and measure the association of various compounds with haematin. The absorbances listed in triplicate (Abs1, Abs 2 and Abs 3) are those of haematin and have been corrected for dilution as well as the absorbance of the compounds being added. The concentrations listed are those of the compound which is named in the top left hand corner of each table.

H_3L Conc [M]	Abs 1	Abs 2	Abs 3
0.00E+00	0.297	0.287	0.282
4.99E-05	0.294	0.286	0.281
9.95E-05	0.293	0.284	0.279
1.49E-04	0.291	0.283	0.278
1.98E-04	0.291	0.283	0.278
2.96E-04	0.289	0.282	0.277
3.92E-04	0.289	0.281	0.275
4.88E-04	0.287	0.279	0.274
5.83E-04	0.284	0.277	0.272
6.76E-04	0.283	0.276	0.271
7.69E-04	0.282	0.275	0.269
8.61E-04	0.281	0.275	0.269
9.52E-04	0.280	0.273	0.268
1.40E-03	0.275	0.268	0.263
1.82E-03	0.271	0.263	0.259
2.22E-03	0.264	0.258	0.254
2.61E-03	0.262	0.256	0.252
2.98E-03	0.260	0.253	0.248
3.33E-03	0.256	0.250	0.246
3.67E-03	0.252	0.247	0.241
4.00E-03	0.249	0.243	0.238
4.62E-03	0.244	0.241	0.234
5.19E-03	0.242	0.238	0.231
5.71E-03	0.238	0.232	0.227
6.21E-03	0.233	0.229	0.223
6.67E-03	0.230	0.225	0.221
Log K:	**1.93 SEM 0.02**		

1,10 Phenanthroline Conc [M]	Abs 1	Abs 2	Abs 3
0.00E+00	0.465	0.466	0.436
2.43E-04	0.452	0.458	0.422
4.65E-04	0.446	0.452	0.416
6.67E-04	0.437	0.446	0.409
8.52E-04	0.431	0.444	0.406
1.02E-03	0.428	0.439	0.404
1.18E-03	0.424	0.437	0.402
1.32E-03	0.421	0.435	0.4
1.46E-03	0.417	0.434	0.398
1.59E-03	0.419	0.434	0.396
1.70E-03	0.417	0.432	0.395
Log K:	**2.95 SEM 0.04**		

4-Methyl-1,10-phenanthroline Conc [M]	Abs 1	Abs 2	Abs 3
0.00E+00	0.461	0.464	0.440
2.03E-04	0.444	0.456	0.422
3.87E-04	0.436	0.449	0.413
5.56E-04	0.429	0.445	0.408
7.10E-04	0.424	0.442	0.406
8.52E-04	0.421	0.440	0.403
9.83E-04		0.438	0.400
1.10E-03		0.436	0.398
1.22E-03		0.435	0.398
1.32E-03		0.436	0.394
1.42E-03		0.438	0.395
Log K:		**3.23 SEM 0.03**	

University of Cape Town

5-methyl-1,10-phenanthroline Conc [M]	Abs 1	Abs 2	Conc [M]	Abs 3
0.00E+00	0.473	0.474	0.00E+00	0.437
1.10E-04	0.463	0.459	2.52E-04	0.425
2.11E-04	0.451	0.448	4.81E-04	0.418
3.03E-04	0.442	0.442	6.90E-04	0.414
3.87E-04	0.433	0.436	8.82E-04	0.410
4.64E-04	0.426	0.430	1.06E-03	0.409
5.35E-04	0.424	0.426	1.22E-03	0.406
6.01E-04	0.420	0.423	1.37E-03	0.402
6.63E-04	0.414	0.417	1.51E-03	0.403
7.20E-04	0.412	0.415	1.64E-03	0.402
7.73E-04	0.405	0.413	1.76E-03	0.398
Log K:		**2.93 SEM 0.03**		

5-chloro-1,10-phenanthroline Conc [M]	Abs 1	Abs 2	Abs 3
0.00E+00	0.477	0.477	0.469
1.00E-04	0.459	0.456	0.450
1.91E-04	0.447	0.442	0.438
2.74E-04	0.439	0.432	0.428
3.50E-04	0.433	0.424	0.418
4.20E-04	0.424	0.418	0.410
4.85E-04	0.419	0.411	0.403
5.44E-04	0.414	0.405	0.400
6.00E-04	0.409	0.400	0.396
6.52E-04	0.406	0.397	0.390
7.00E-04	0.405	0.392	0.387
Log K:		**3.01 SEM 0.03**	

[Pt(bipy)L]Cl Conc [M]	Abs 1	Abs 2	Abs 3
0.00E+00	0.445	0.437	0.446
4.76E-07	0.427	0.427	0.433
9.50E-07	0.414	0.412	0.421
1.42E-06	0.400	0.397	0.407
2.37E-06	0.376	0.373	0.386
3.31E-06	0.356	0.349	0.364
4.25E-06	0.334	0.317	0.344
6.57E-06	0.298	0.290	0.307
8.88E-06	0.269	0.261	0.279
1.12E-05	0.245	0.237	0.253
1.57E-05	0.209	0.201	0.217
2.01E-05	0.185	0.175	0.189
2.44E-05	0.167	0.157	0.175
2.86E-05	0.153	0.145	0.156
3.28E-05	0.146	0.137	0.147
3.69E-05	0.141	0.131	0.140
5.62E-05	0.135	0.125	0.133
Log K:		**5.05 SEM 0.02**	

3,4,7,8-tetramethyl-1,10-phenanthroline Conc [M]	Abs 1	Abs 2	Abs 3
0.00E+00	0.461	0.474	0.470
5.24E-05	0.443	0.455	0.452
1.00E-04	0.430	0.442	0.442
1.43E-04	0.421	0.432	0.432
1.83E-04	0.414	0.425	0.425
2.20E-04	0.408	0.418	0.419
2.54E-04	0.402	0.412	0.412
2.85E-04	0.397	0.406	0.408
3.14E-04	0.392	0.403	0.405
3.41E-04	0.390	0.399	0.402
3.67E-04	0.386	0.395	0.399
Log K:		**3.32 SEM 0.01**	

5-nitro-1,10-phenanthroline Conc [M]	Abs 1	Abs 2	Abs 3
0.00E+00	0.473	0.468	0.475
1.05E-04	0.455	0.448	0.458
2.01E-04	0.437	0.436	0.446
2.88E-04	0.428	0.426	0.431
3.68E-04	0.418	0.415	0.424
4.42E-04	0.411	0.406	0.418
5.10E-04	0.403	0.402	0.408
5.73E-04	0.398	0.396	0.402
6.31E-04	0.393	0.391	0.398
6.86E-04	0.387	0.386	0.390
7.37E-04	0.381	0.380	0.387
Log K:		**2.82 SEM 0.06**	

University of Cape Town

5-methyl-1,10-phenanthroline Conc [M]	Abs 1	Abs 2	Conc [M]	Abs 3
0.00E+00	0.473	0.474	0.00E+00	0.437
1.10E-04	0.463	0.459	2.52E-04	0.425
2.11E-04	0.451	0.448	4.81E-04	0.418
3.03E-04	0.442	0.442	6.90E-04	0.414
3.87E-04	0.433	0.436	8.82E-04	0.410
4.64E-04	0.426	0.430	1.06E-03	0.409
5.35E-04	0.424	0.426	1.22E-03	0.406
6.01E-04	0.420	0.423	1.37E-03	0.402
6.63E-04	0.414	0.417	1.51E-03	0.403
7.20E-04	0.412	0.415	1.64E-03	0.402
7.73E-04	0.405	0.413	1.76E-03	0.398
Log K:		**2.93 SEM 0.03**		

5-chloro-1,10-phenanthroline Conc [M]	Abs 1	Abs 2	Abs 3
0.00E+00	0.477	0.477	0.469
1.00E-04	0.459	0.456	0.450
1.91E-04	0.447	0.442	0.438
2.74E-04	0.439	0.432	0.428
3.50E-04	0.433	0.424	0.418
4.20E-04	0.424	0.418	0.410
4.85E-04	0.419	0.411	0.403
5.44E-04	0.414	0.405	0.400
6.00E-04	0.409	0.400	0.396
6.52E-04	0.406	0.397	0.390
7.00E-04	0.405	0.392	0.387
Log K:		**3.01 SEM 0.03**	

[Pt(bipy)L]Cl Conc [M]	Abs 1	Abs 2	Abs 3
0.00E+00	0.445	0.437	0.446
4.76E-07	0.427	0.427	0.433
9.50E-07	0.414	0.412	0.421
1.42E-06	0.400	0.397	0.407
2.37E-06	0.376	0.373	0.386
3.31E-06	0.356	0.349	0.364
4.25E-06	0.334	0.317	0.344
6.57E-06	0.298	0.290	0.307
8.88E-06	0.269	0.261	0.279
1.12E-05	0.245	0.237	0.253
1.57E-05	0.209	0.201	0.217
2.01E-05	0.185	0.175	0.189
2.44E-05	0.167	0.157	0.175
2.86E-05	0.153	0.145	0.156
3.28E-05	0.146	0.137	0.147
3.69E-05	0.141	0.131	0.140
5.62E-05	0.135	0.125	0.133
Log K:		**5.05 SEM 0.02**	

3,4,7,8-tetramethyl-1,10-phenanthroline Conc [M]	Abs 1	Abs 2	Abs 3
0.00E+00	0.461	0.474	0.470
5.24E-05	0.443	0.455	0.452
1.00E-04	0.430	0.442	0.442
1.43E-04	0.421	0.432	0.432
1.83E-04	0.414	0.425	0.425
2.20E-04	0.408	0.418	0.419
2.54E-04	0.402	0.412	0.412
2.85E-04	0.397	0.406	0.408
3.14E-04	0.392	0.403	0.405
3.41E-04	0.390	0.399	0.402
3.67E-04	0.386	0.395	0.399
Log K:		**3.32 SEM 0.01**	

5-nitro-1,10-phenanthroline Conc [M]	Abs 1	Abs 2	Abs 3
0.00E+00	0.473	0.468	0.475
1.05E-04	0.455	0.448	0.458
2.01E-04	0.437	0.436	0.446
2.88E-04	0.428	0.426	0.431
3.68E-04	0.418	0.415	0.424
4.42E-04	0.411	0.406	0.418
5.10E-04	0.403	0.402	0.408
5.73E-04	0.398	0.396	0.402
6.31E-04	0.393	0.391	0.398
6.86E-04	0.387	0.386	0.390
7.37E-04	0.381	0.380	0.387
Log K:		**2.82 SEM 0.06**	

University of Cape Town

[Pt(diMebipy)L]Cl Conc [M]	Abs 1	Abs 2	Abs 3
0.00E+00	0.446	0.438	0.441
8.80E-07	0.415	0.411	0.417
1.76E-06	0.391	0.389	0.393
2.64E-06	0.371	0.365	0.370
4.38E-06	0.338	0.333	0.337
6.12E-06	0.311	0.304	0.311
7.86E-06	0.288	0.281	0.288
1.22E-05	0.249	0.242	0.249
1.64E-05	0.224	0.217	0.224
2.06E-05	0.206	0.198	0.206
2.90E-05	0.184	0.176	0.184
3.71E-05	0.172	0.162	0.171
4.51E-05	0.163	0.152	0.162
5.30E-05	0.156	0.145	0.154
6.07E-05	0.151	0.139	0.150
6.83E-05	0.147	0.134	0.144
Log K:		**5.13 SEM 0.01**	

[Pt(dtbbipy)L]Cl Conc [M]	Abs 1	Abs 2	Abs 3
0.00E+00	0.513	0.556	0.557
5.15E-07	0.504	0.547	0.547
1.03E-06	0.493	0.539	0.539
1.54E-06	0.485	0.532	0.532
2.06E-06	0.476	0.523	0.523
2.57E-06	0.469	0.519	0.517
3.59E-06	0.460	0.505	0.505
4.60E-06	0.448	0.494	0.491
5.61E-06	0.440	0.483	0.479
6.62E-06	0.430	0.473	0.469
7.63E-06	0.421	0.464	0.461
1.01E-05	0.405	0.447	0.448
1.26E-05	0.388	0.434	0.434
1.74E-05	0.369	0.413	0.410
2.22E-05	0.351	0.397	0.392
3.38E-05	0.323	0.365	0.363
4.48E-05	0.302	0.344	0.343
5.53E-05	0.289	0.332	0.330
6.53E-05	0.277	0.321	0.319
Log K:		**4.82 SEM 0.01**	

[Pt(dtbbipy)L]Cl Conc [M]	Abs 1	Abs 2	Abs 3
0.00E+00	0.513	0.556	0.557
5.15E-07	0.504	0.547	0.547
1.03E-06	0.493	0.539	0.539
1.54E-06	0.485	0.532	0.532
2.06E-06	0.476	0.523	0.523
2.57E-06	0.469	0.519	0.517
3.59E-06	0.460	0.505	0.505
4.60E-06	0.448	0.494	0.491
5.61E-06	0.440	0.483	0.479
6.62E-06	0.430	0.473	0.469
7.63E-06	0.421	0.464	0.461
1.01E-05	0.405	0.447	0.448
1.26E-05	0.388	0.434	0.434
1.74E-05	0.369	0.413	0.410
2.22E-05	0.351	0.397	0.392
3.38E-05	0.323	0.365	0.363
4.48E-05	0.302	0.344	0.343
5.53E-05	0.289	0.332	0.330
6.53E-05	0.277	0.321	0.319
Log K:		**4.82 SEM 0.01**	

University of Cape Town

[Pt(bipy)L']Cl Conc [M]	Abs 1	Abs 2	Abs 3
0.00E+00	0.392	0.398	0.394
9.80E-07	0.329	0.342	0.337
1.96E-06	0.284	0.293	0.291
2.93E-06	0.245	0.250	0.250
3.91E-06	0.215	0.216	0.216
4.88E-06	0.195	0.193	0.194
7.30E-06	0.163	0.159	0.162
9.71E-06	0.145	0.138	0.143
1.21E-05	0.135	0.129	0.132
1.45E-05	0.127	0.120	0.125
1.92E-05	0.119	0.112	0.115
2.39E-05	0.114	0.105	0.111
2.86E-05	0.110	0.101	0.108
3.77E-05	0.107	0.098	0.104
4.67E-05	0.105	0.096	0.102
6.84E-05	0.102	0.092	0.101
8.92E-05	0.098	0.094	0.101
1.09E-04	0.098	0.092	0.101
1.28E-04	0.098	0.090	0.099
1.64E-04	0.097	0.086	0.100
1.96E-04	0.097	0.090	0.104
Log K:		**5.82 SEM 0.01**	

[Pt(phen)L]Cl Conc [M]	Abs 1	Abs 2	Abs 3
0.00E+00	0.443	0.444	0.444
5.24E-07	0.406	0.405	0.411
1.05E-06	0.372	0.373	0.379
1.57E-06	0.341	0.342	0.346
2.61E-06	0.291	0.293	0.296
3.65E-06	0.256	0.256	0.261
4.68E-06	0.225	0.227	0.231
7.25E-06	0.157	0.163	0.173
9.79E-06	0.129	0.140	0.146
1.23E-05	0.116	0.125	0.130
1.73E-05	0.112	0.117	0.117
2.21E-05	0.109	0.112	0.112
2.69E-05	0.104	0.108	0.108
3.16E-05	0.102	0.107	0.104
3.62E-05	0.104	0.107	0.104
4.07E-05	0.105	0.105	0.104
Log K:		**5.75 SEM 0.02**	

[Pt(4-Me phen)L]Cl Conc [M]	Abs 1	Abs 2	Abs 3
0.00E+00	0.447	0.446	0.421
5.67E-07	0.403	0.402	0.374
1.13E-06	0.370	0.366	0.338
1.70E-06	0.335	0.332	0.303
2.83E-06	0.283	0.279	0.253
3.95E-06	0.246	0.242	0.217
5.07E-06	0.216	0.213	0.190
7.84E-06	0.169	0.167	0.146
1.06E-05	0.145	0.144	0.123
1.33E-05	0.130	0.129	0.111
1.87E-05	0.119	0.118	0.098
2.39E-05	0.113	0.112	0.092
2.91E-05	0.110	0.109	0.087
3.42E-05	0.107	0.106	0.084
3.91E-05	0.106	0.104	0.083
4.40E-05	0.107	0.104	0.079
Log K:		**5.75 SEM 0.01**	

University of Cape Town

[Pt(5-Me phen)L]Cl Conc [M]	Abs 1	Abs 2	Abs 3
0.00E+00	0.447	0.443	0.444
4.97E-07	0.407	0.400	0.405
9.92E-07	0.370	0.371	0.370
1.49E-06	0.338	0.338	0.338
2.47E-06	0.287	0.290	0.290
3.45E-06	0.249	0.249	0.252
4.43E-06	0.215	0.214	0.215
6.86E-06	0.148	0.158	0.163
9.27E-06	0.126	0.128	0.138
1.16E-05	0.118	0.115	0.123
1.63E-05	0.110	0.105	0.112
2.09E-05	0.104	0.098	0.105
2.55E-05	0.101	0.095	0.103
2.99E-05	0.101	0.090	0.101
3.42E-05	0.102	0.090	0.101
3.85E-05	0.100	0.091	0.101
Log K:		**5.80 SEM 0.02**	

[Pt(3,4,7,8-tetraMe phen)L]Cl Conc [M]	Abs 1	Abs 2	Abs 3
0.00E+00	0.440	0.442	0.442
5.02E-07	0.394	0.397	0.396
1.00E-06	0.355	0.350	0.356
1.50E-06	0.229	0.327	0.321
2.50E-06	0.266	0.275	0.266
3.50E-06	0.228	0.237	0.228
4.49E-06	0.197	0.207	0.197
6.94E-06	0.155	0.163	0.155
9.38E-06	0.136	0.145	0.136
1.18E-05	0.126	0.134	0.125
1.65E-05	0.117	0.125	0.115
2.12E-05	0.112	0.120	0.108
2.58E-05	0.111	0.118	0.104
3.03E-05	0.106	0.115	0.093
3.47E-05	0.093	0.113	0.102
3.90E-05	0.102	0.112	0.102
Log K:		**5.96 SEM 0.01**	

[Pt(5-Cl phen)L]Cl Conc [M]	Abs 1	Abs 2	Abs 3
0.00E+00	0.447	0.440	0.446
3.31E-07	0.416	0.405	0.412
6.61E-07	0.386	0.378	0.383
9.90E-07	0.356	0.352	0.353
1.65E-06	0.310	0.304	0.308
2.30E-06	0.271	0.266	0.270
2.95E-06	0.237	0.228	0.236
4.57E-06	0.174	0.161	0.185
6.17E-06	0.138	0.131	0.143
7.76E-06	0.123	0.114	0.125
1.09E-05	0.111	0.100	0.113
1.40E-05	0.102	0.095	0.108
1.70E-05	0.101	0.092	0.105
1.99E-05	0.098	0.090	0.103
2.28E-05	0.097	0.088	0.102
2.56E-05	0.096	0.088	0.102
Log K:		**6.03 SEM 0.01**	

University of Cape Town

[Pt(5-NO_2 phen)L]Cl Conc [M]	Abs 1	Abs 2	Abs 3
0.00E+00	0.438	0.440	0.446
4.71E-07	0.396	0.395	0.405
9.40E-07	0.358	0.355	0.361
1.41E-06	0.320	0.318	0.320
2.34E-06	0.261	0.255	0.257
3.27E-06	0.212	0.206	0.211
4.20E-06	0.178	0.171	0.174
6.50E-06	0.141	0.131	0.136
8.78E-06	0.125	0.116	0.119
1.10E-05	0.117	0.106	0.113
1.55E-05	0.114	0.108	0.113
1.99E-05	0.113	0.106	0.113
2.41E-05	0.113	0.105	0.114
2.83E-05	0.113	0.105	0.114
3.25E-05	0.112	0.106	0.113
3.65E-05	0.115	0.107	0.115
Log K:		**6.24 SEM 0.02**	

University of Cape Town

Appendix 2

Infrared spectra of the products obtained from the inhibition of β-haematin experiments where 3 equivalents of (A) 4,4'-dimethyl-2,2'-bipyridyl, (B) 4,4'-ditertiarybutyl-2,2'-bipyridyl, (C) 1,10-phenanthroline, (D) 4-methyl-1,10-phenanthroline, (E) 5-methyl-1,10-phenanthroline, (F) 3,4,7,8-tetramethyl-1,10-phenanthroline (G) 5-chloro-1,10-phenanthroline and (H) 5-nitro-1,10-phenanthroline, (I) 7,8-benzoquinoline, (J) HL', (K) [Pt(dtbbipy)L]Cl, (L) [Pt(phen)L]Cl, (M) [Pt(4-Me phen)L]Cl, (N) [Pt(5-Me phen)L]Cl, (O) [Pt(3,4,7,8-tetraMe phen)L]Cl, (P) [Pt(5-Cl phen)L]Cl, (Q) [Pt(5-NO_2 phen)L]Cl, (R) [Pt(bipy)L']Cl and (S) Pt(ppy)L' present. All Y axes represent % transmittance.

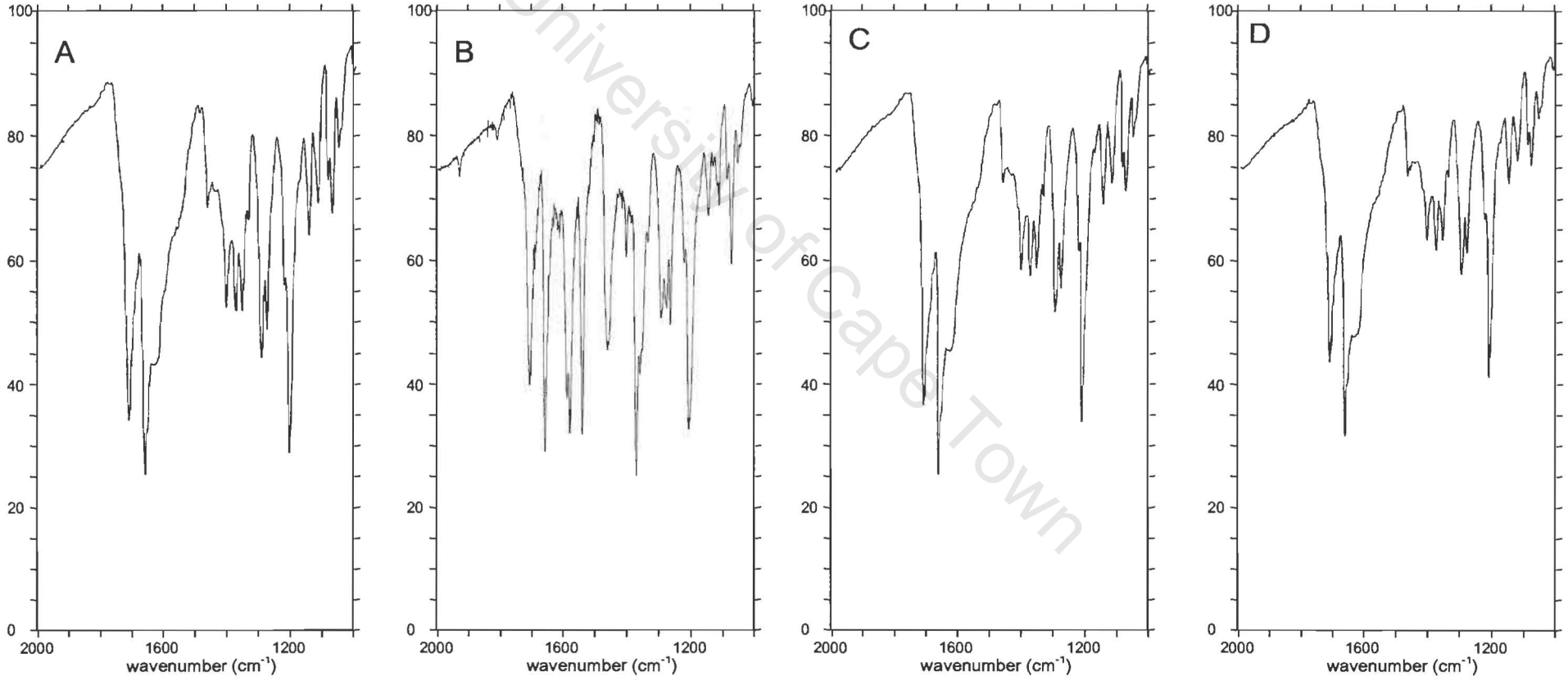

University of Cape Town

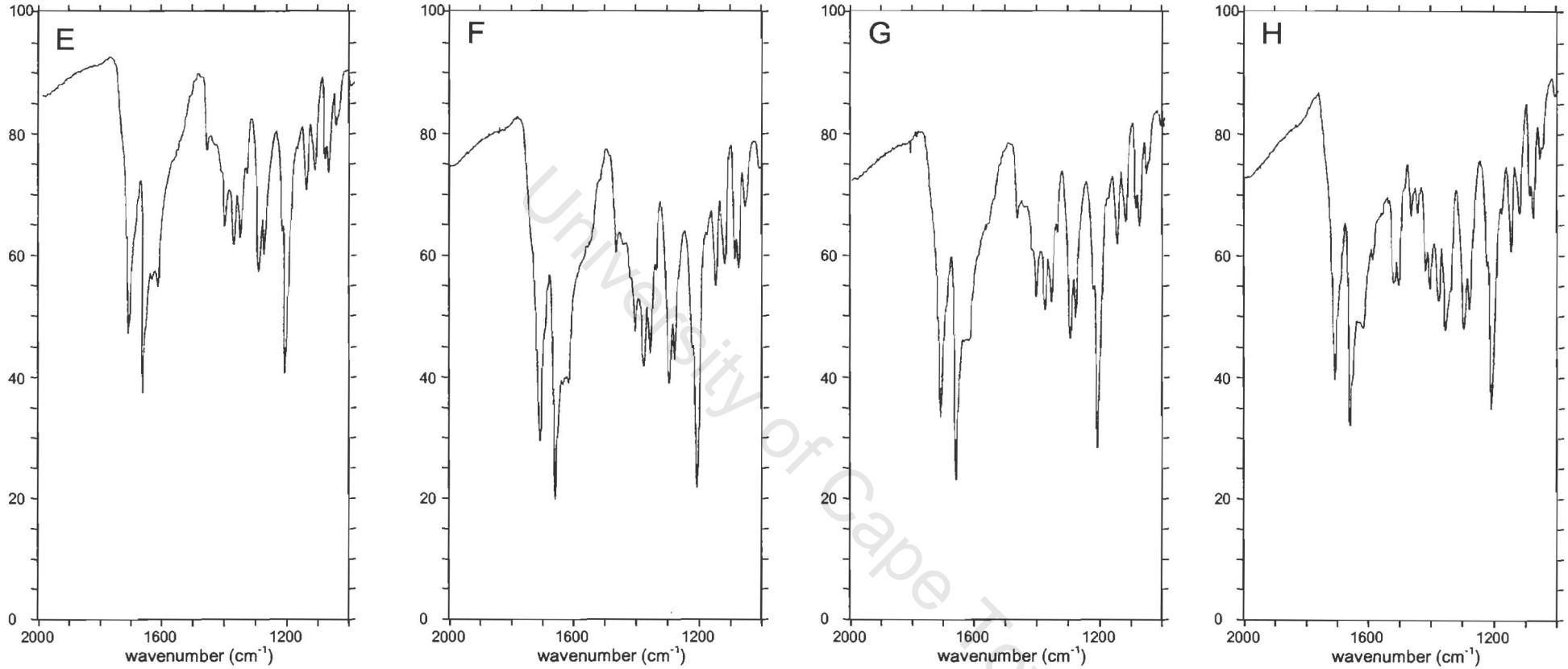

University of Cape Town

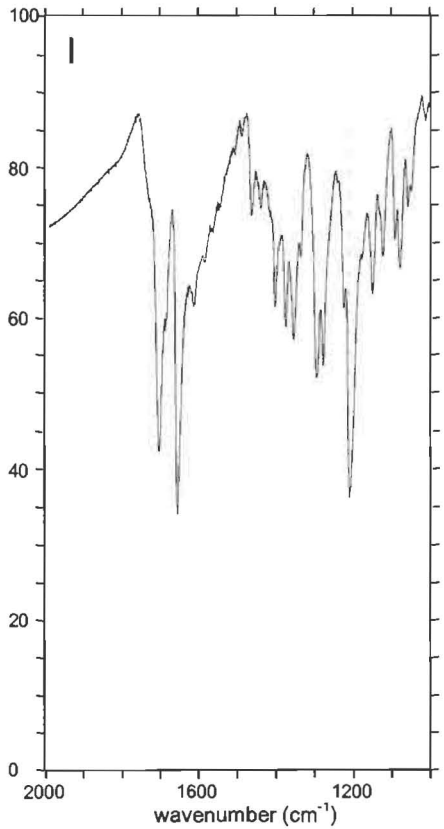

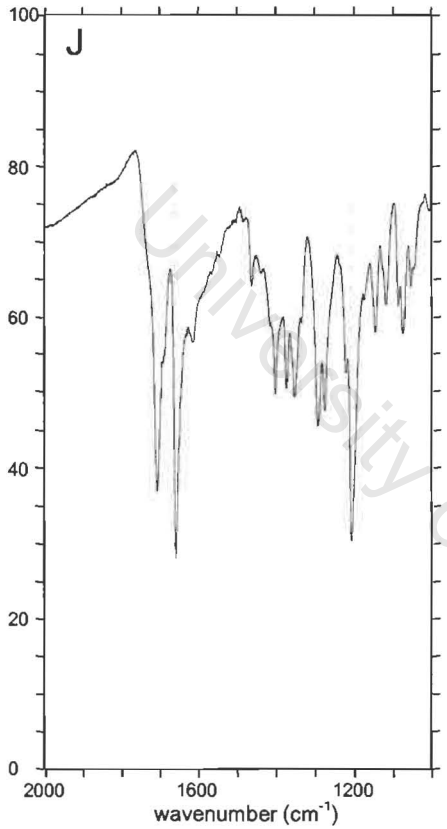

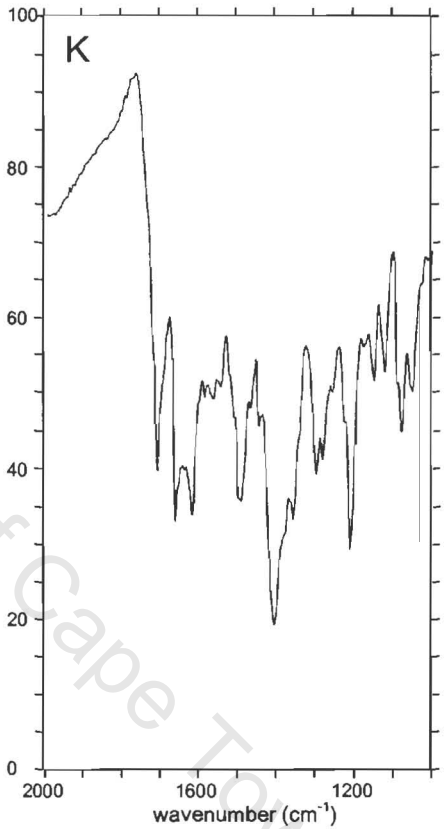

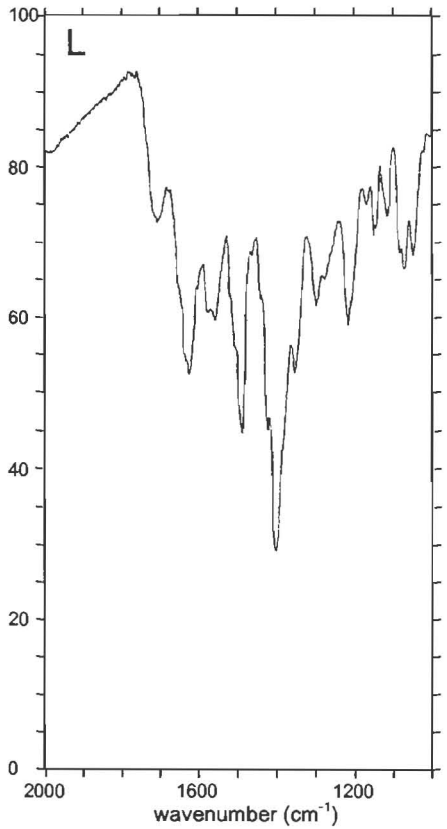

University of Cape Town

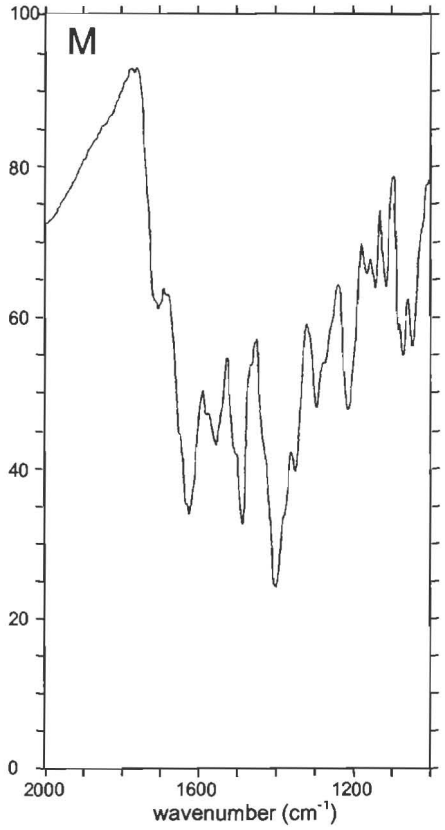

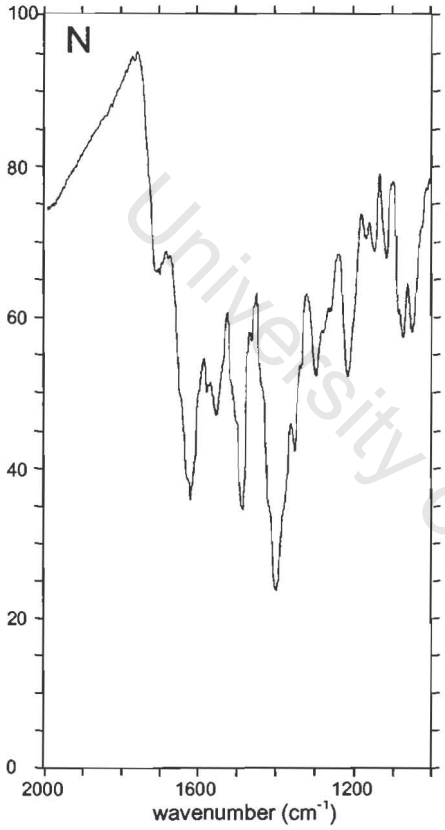

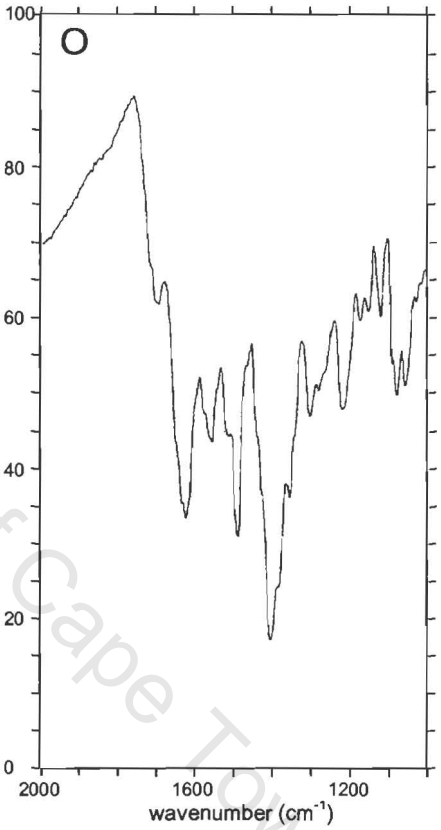

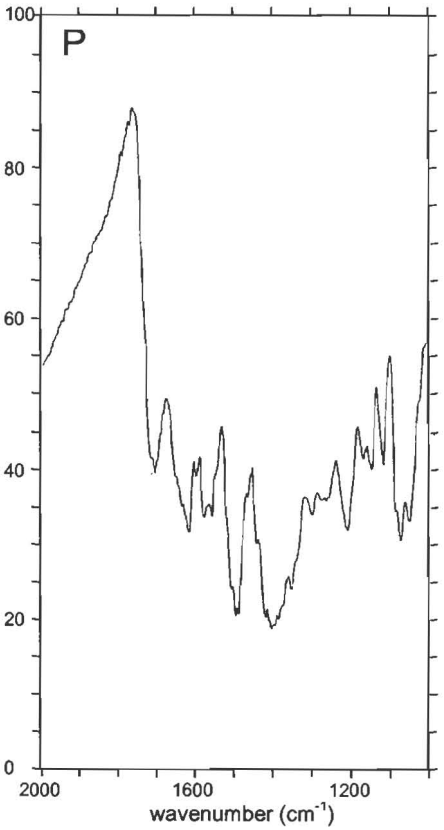

University of Cape Town

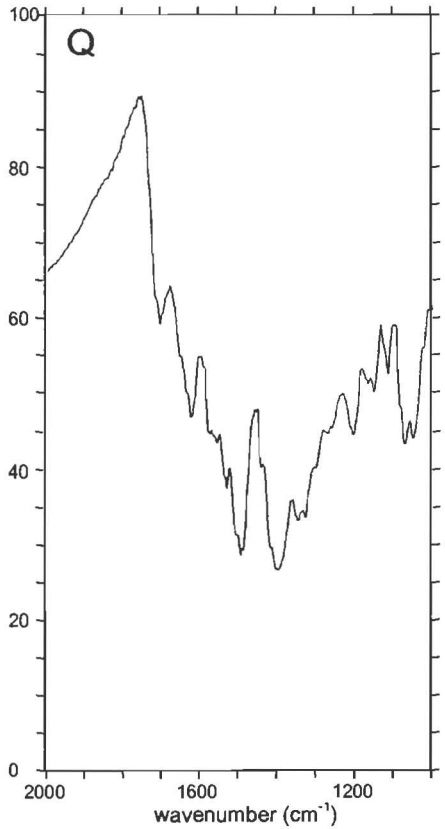

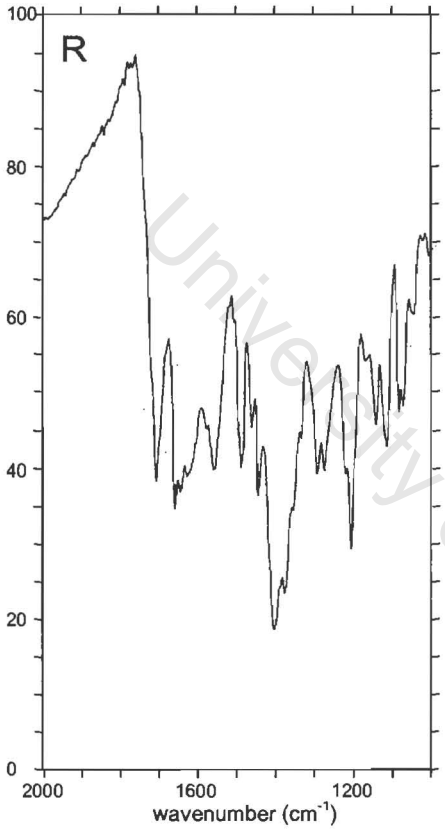

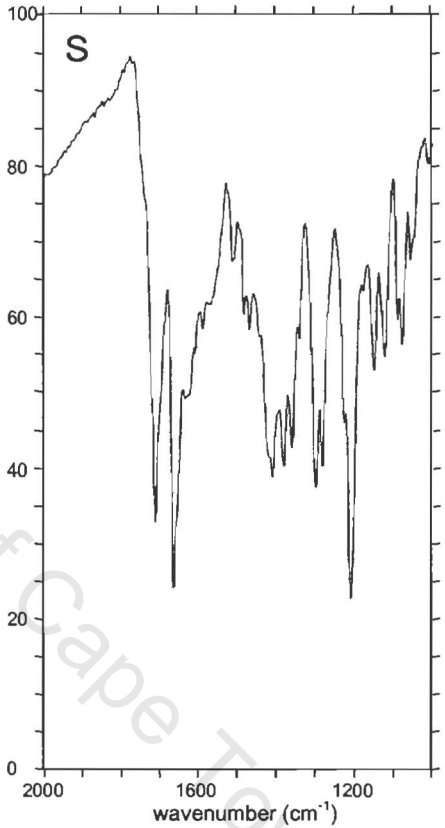

University of Cape Town

Appendix 3

Graphs showing changes in chemical shift of protons in the NMR spectrum of platinum complexes upon addition of Zn(II)PPIX and changes in chemical shift of protons in the NMR spectrum of Zn(II)PPIX upon addition of platinum complexes

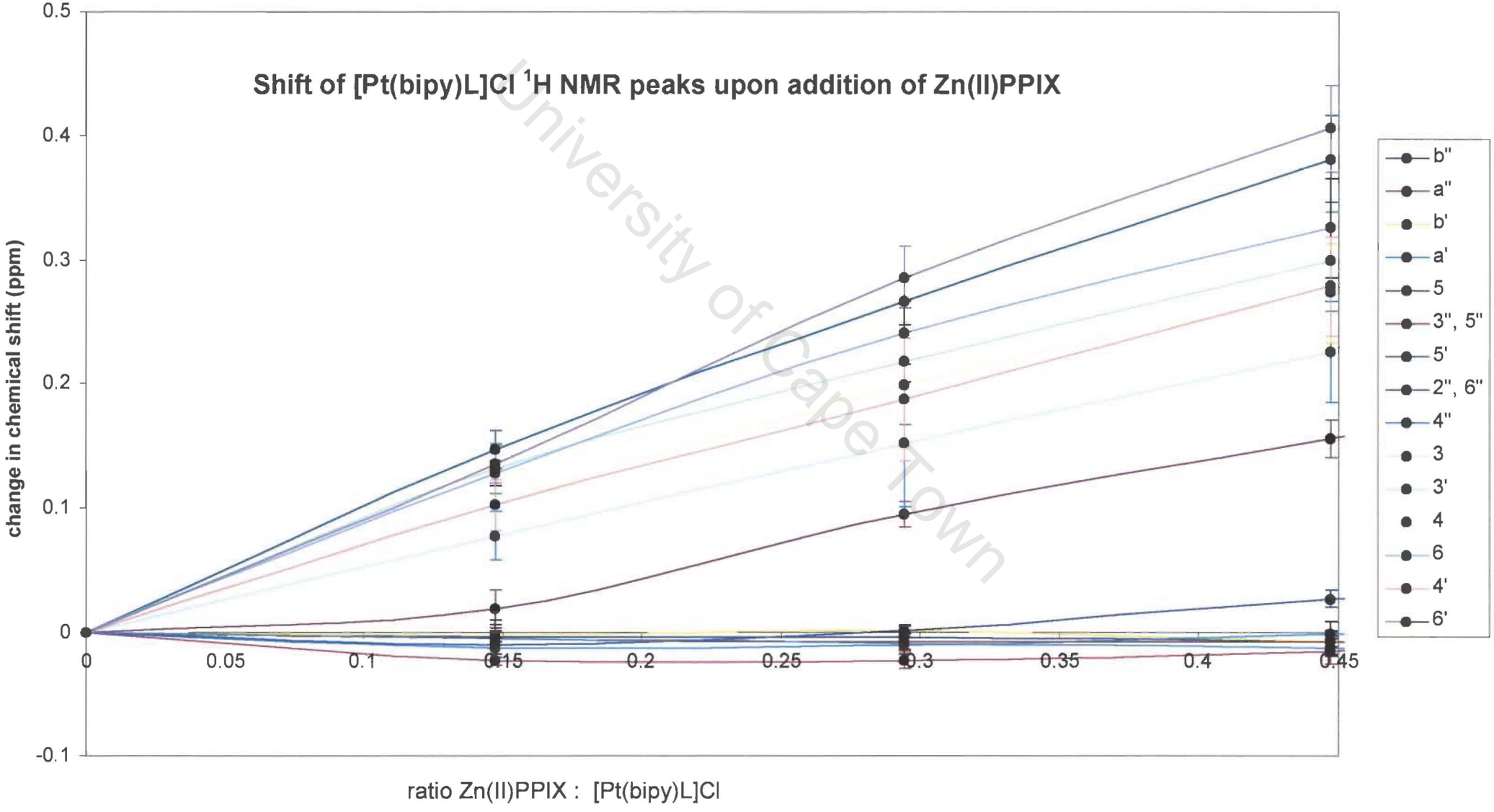

University of Cape Town

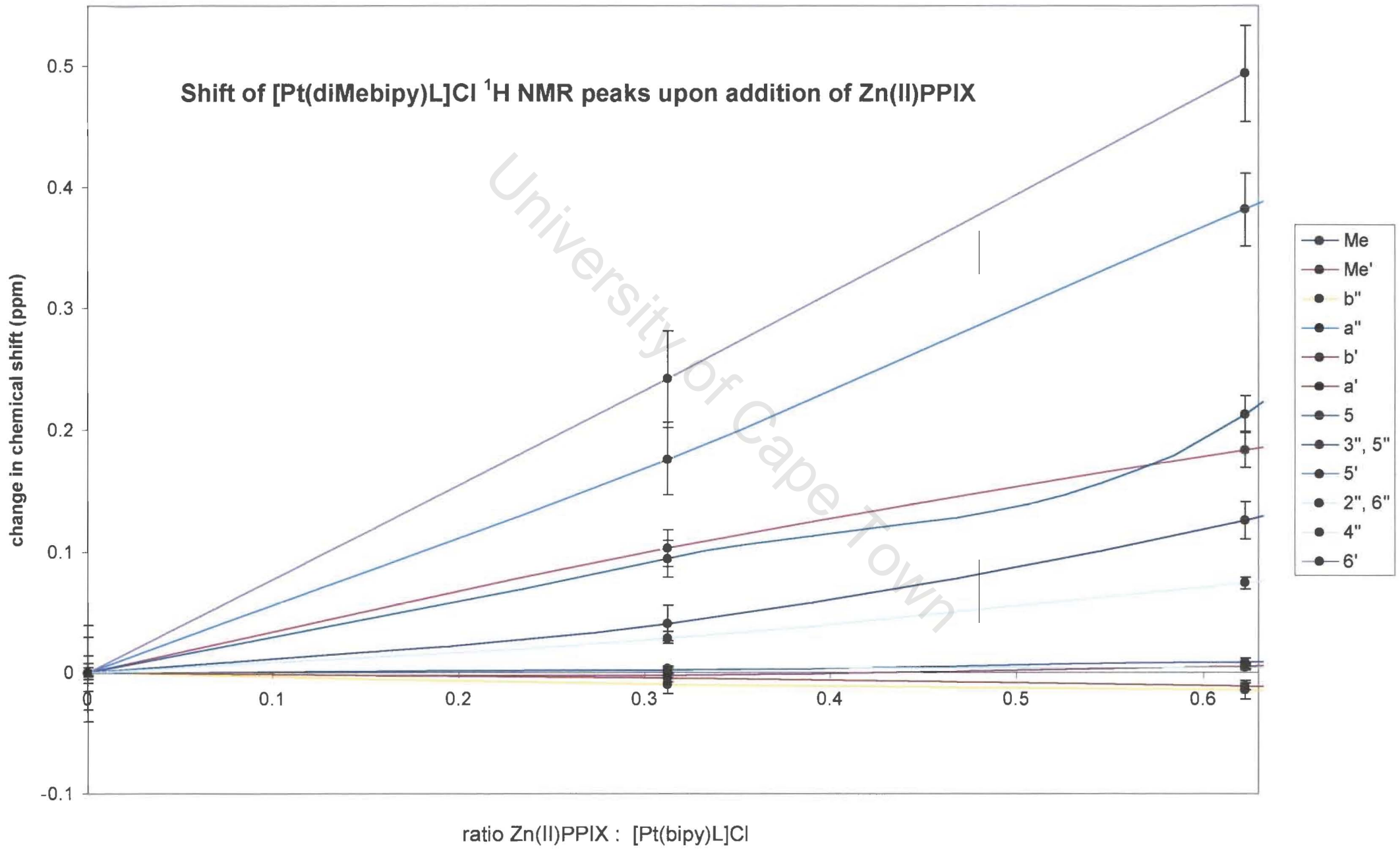

University of Cape Town

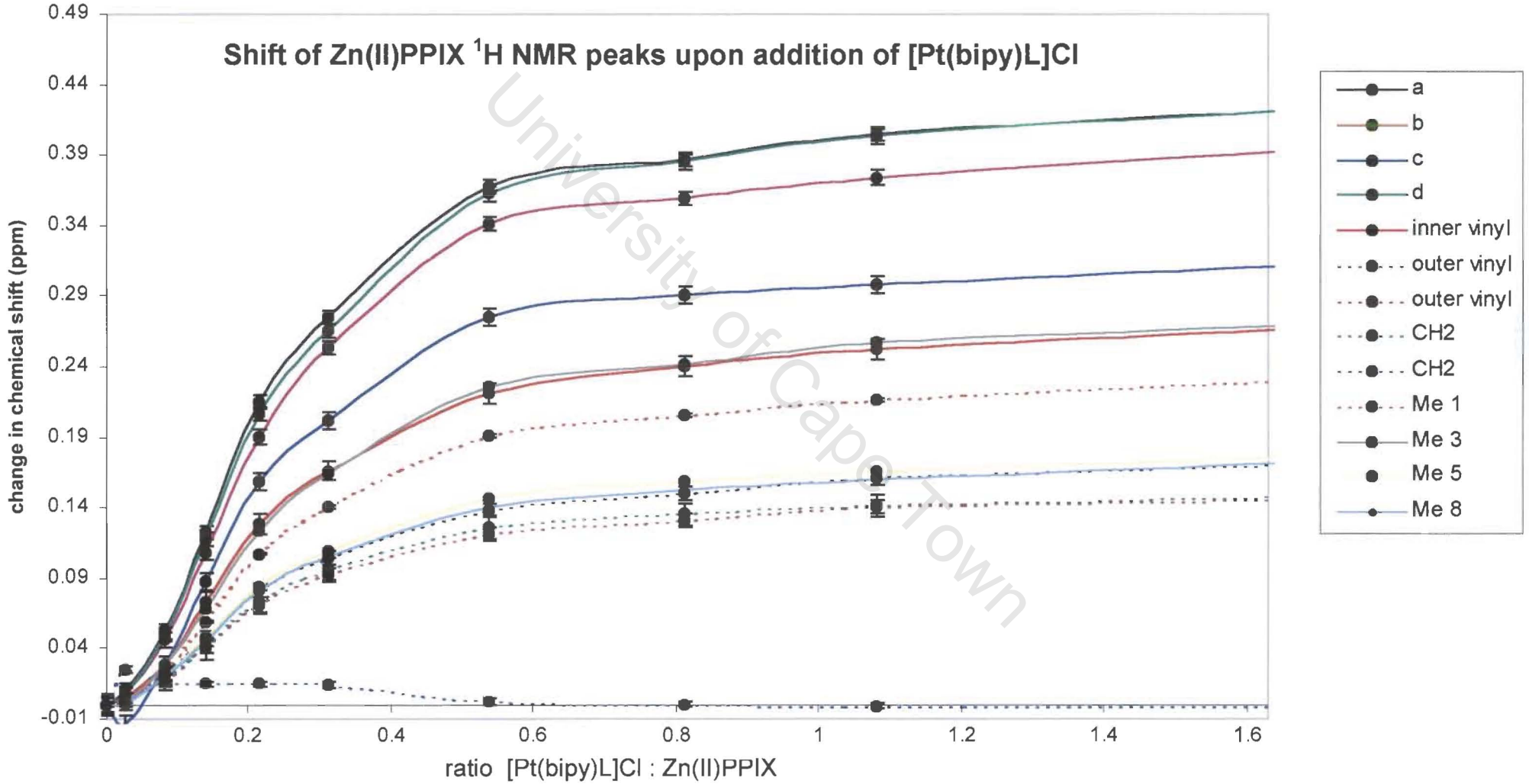

University of Cape Town

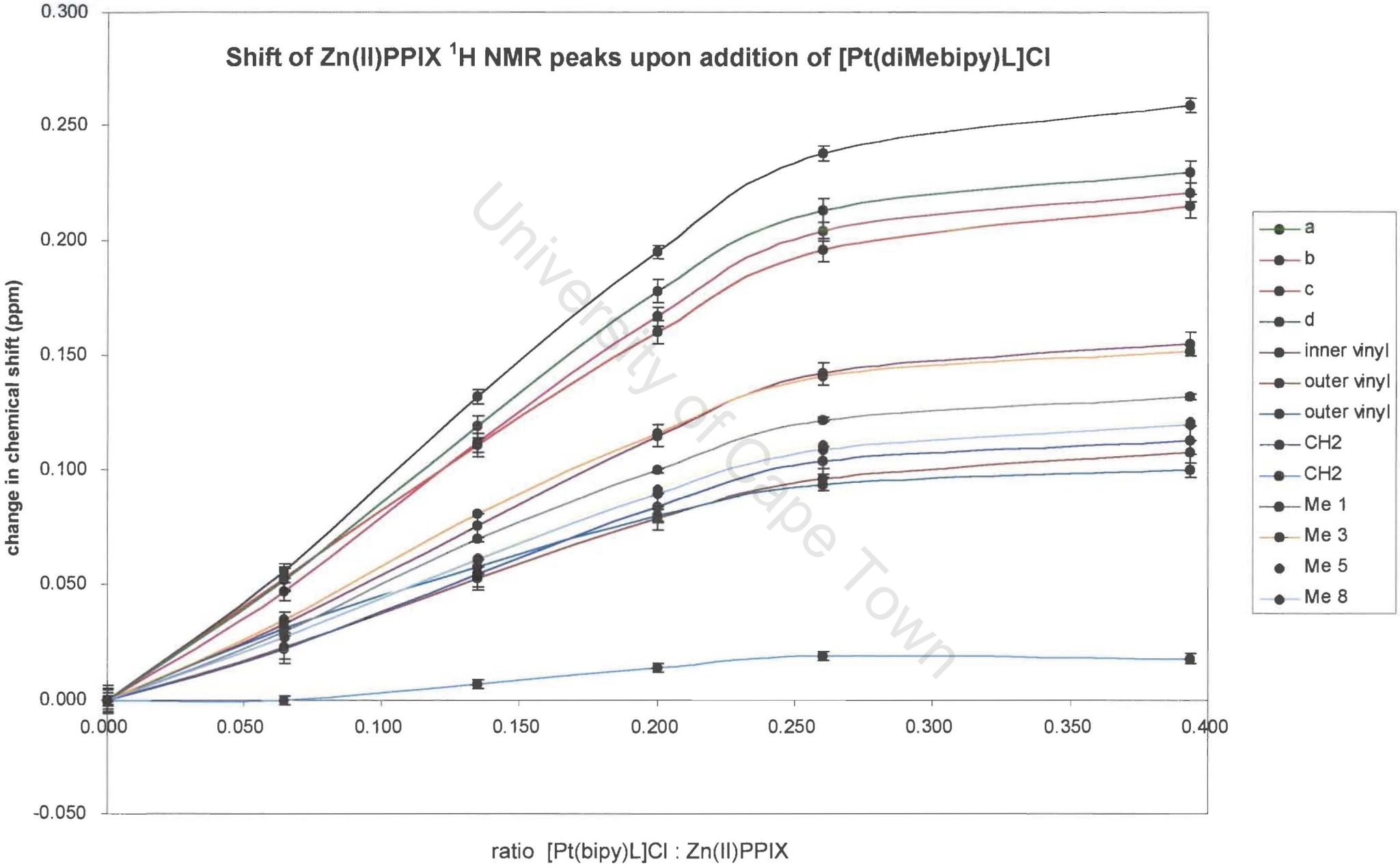

University of Cape Town